Modelling Deficit Irrigation of Wheat in Zimbabwe

by

John Findlay MacRobert
B.Sc. Agric. (Natal), M.Sc. Agric. (Sask.)

Submitted in partial fulfilment
of the requirements for
the degree of

DOCTOR OF PHILOSOPHY

in the
Department of Agronomy
University of Natal
Pietermaritzburg
NATAL
SOUTH AFRICA

DECEMBER, 1993

DECLARATION

I declare that the results contained in this thesis are from my own original work except where acknowledged.

John F MacRobert
December 1993

ACKNOWLEDGEMENTS

I acknowledge and thank the Lord God Almighty, without Whom I would not have been able to embark on or complete this work. If there be any glory arising from this thesis, let it be directed to the Him, the Creator and Sustainer of all things.

I thank my wife, Amy, and children, Charles and Nicola, for supporting me in this work.

I thank the Beit Trust for providing the funding to cover academic fees for the first three years.

Sincere appreciation is extended to the Trustees and Board of Management of the Agricultural Research Trust for supporting and funding this research. In particular, I thank the Director, Richard Winkfield, for his enthusiasm and encouragement. I thank the following staff members of ART who contributed significantly to the day to day managment and data collection involved in this research: Langton Mutemeri, Morris Chidamoyo, Ernest Chiwara, Charles Nyandoro, Stephen Nyandoro (deceased), Doesnotmatter Dungwe, Simeon Mutovo, Joseph Sixpence, Thomas Sibau, Erinado Mgweteza, Phillip Tilowakuti, and many others.

I thank all the farmers who assisted with this work: Duncan Cramp and Mr N Browne (Wooler Farm), Jeremy and Janet Selby (Zanadu Farm), Mark and Trish Hook (Doonside Farm), Keith Brooke-Jackson (Lions Den Estate), Angus and April Thompson (Gunn Estate) and Dave Hannay (Victory Estate).

Professor M J Savage is gratefully acknowledged for his interest, advice and assistance. Also, his wife, Meryl, is thanked for her encouragement and hospitality.

I thank Mr Baillie of Foothills Farm, Bindura, for his continuous encouragement.

Dr D Hall, Dr P Nyamagafata and Ms D T Nyazenga of the Soil and Chemistry Research Institute, Department of Research and Specialist Services, performed the soil profile descriptions and soil water retention analyses. The Department of Meteorological Services kindly supplied weather data.

John F MacRobert

TABLE OF CONTENTS

LIST OF TABLES

LIST OF FIGURES

Figure Page

Figure Page

ABSTRACT

Wheat is grown in Zimbabwe during the relatively dry, cool winter with irrigation. On most large-scale farms, land resources exceed irrigation water resources. Consequently, the efficient use of water is of prime concern. This has led to the development and adoption of deficit irrigation techniques, with the aim of maximizing net financial returns per unit of applied water rather than per unit land area. This often requires that less water be applied than that required for maximum yields, which implies that water deficits are allowed to develop in the crop. Although the basic principles of deficit irrigation are known, there exists no systematic procedure for advising farmers on whether or not to, or how to, employ such a management option in Zimbabwe. This research was therefore undertaken to develop an interactive computer programme that would assist farmers in determining optimum irrigation strategies for wheat.

The CERES-Wheat version 2.10 crop simulation model (WHV21) was chosen as the basis for this programme. In order to validate and modify, where necessary, WHV21, a series of field experiments were conducted at a number of wide-ranging locations in Zimbabwe during the period 1986 to 1992. These included sowing date x cultivar, sowing date x seeding rate, growth analysis and irrigation experiments. In all, 122 data sets were collected, of which 47 were used for model validation and 75 used for calibration and modification of WHV21.

The initial validation of WHV21 showed that the model gave biased and imprecise predictions of phenological development, particularly under deficit-irrigated conditions. The simulation of tillering was poor and the model tended to over-predict dry matter accumulation and under-predict leaf area indices. The yield component and grain yield predictions were also generally imprecise. On the other hand, for most data sets, the simulated soil water contents were similar to measured soil water contents. These inconsistencies prompted a revision of the phenological and growth subroutines of the model.

In the phenological subroutine, new thermal time durations and base temperatures (T_b) for all growth phases were determined from regressions of the rate of phasic development on mean air

temperatures. For growth phases one, two and three, a T_b of 4 °C was established, whereas for growth phases four and five, a T_b of 3 °C was used. The revised model included the prediction of leaf emergence (as apposed to leaf appearance) and first node appearance (Zadoks growth stage 31). In order to hasten plant development under conditions of soil water deficit stress, daily thermal time was made to increase whenever the actual root water uptake declined below 1.5 times the potential plant evaporation. These changes improved the prediction of crop phasic development: for example, the Index of Agreement for the prediction of physiological maturity was improved from 0.643 with WHV21 to 0.909 with the revised version.

Many changes were made to the growth subroutine, *inter alia*: 1. the extinction coefficient in the exponential photosynthetically active radiation (PAR) interception equation was reduced from 0.85 to 0.45; 2. an allowance was made for the interception of PAR by the wheat ears during growth phases four and five, with the statement *IPAR=1-EXP(-0.004*TPSM)*, where IPAR is the proportion of PAR intercepted and TPSM is the number of tillers m^{-2}; 3. the area to mass ratio of leaves was increased from 115 cm^2 g^{-1} to 125 cm^2 g^{-1} during growth phase two and this was allowed to decrease under conditions of water deficit stress; 4. tiller production during growth phase one was made a function of daily thermal time, total daily solar radiant density and plant density, moderated by high air temperatures and a new soil water deficit factor that takes the dryness of the surface soil layer into account; 5. a cold temperature routine was added to reduce kernel numbers whenever the exposed minimum air temperature decreased below 0 °C during the period ear emergence to the start of the linear kernel growth phase (cold temperatures during anthesis occasionally cause reductions to kernel numbers in Zimbabwe); and 6. the kernel growth rate was gradually increased during growth phase four, and the rate of kernel growth was increased under conditions of water deficit stress during growth phase five. The modifications made to the growth subroutine of WHV21 improved predictions of tillering, ear density, yield components and yield on the independent validation data set.

The modified model (WHVZIM22) was used to evaluate wheat sowing date and irrigation strategies on ten-year sets of

weather data from representative locations in Zimbabwe. The results indicated that the highest yields were obtained with sowings during the latter half of April and the early part of May at all tested locations. Yields were greater for each sowing date and irrigation regime at the high altitude (1480 m) location than at warmer, lower altitude locations. The response of wheat yield to irrigation application was typically curvilinear, particularly on the soil with a high water holding capacity. Maximum yields were attained with the application of 400 to 500 mm (net) water. Soils with low water holding capacities produced lower mean yields than soils with a high water holding capacity. Maximum financial returns tended to occur with the application of less water than that required for maximum yields, particularly on the soil with a high water holding capacity. However, the variance of financial returns increased with reductions in the amount of water applied.

These simulation results corroborated field observations and, taken together with the improved predictive ability of WHVZIM22 over WHV21, provided sufficient justification to use the revised model as a basis for the development of a pre-season irrigation optimization computer programme. This programme seeks the intraseasonal irrigation regime that maximizes the total gross margin for a particular soil, cultural and weather scenario, within the constraints of land and water availability. The programme is written in Microsoft QuickBASIC 4.00 and can generate an optimized irrigation regime within 4 to 5 minutes when executed on an IBM AT-compatible 80486 computer running at 25 MHz.

It is envisaged that the programme would be used as a pre-season management tool, but the literal application of the results in the field is not recommended in view of the fact that the WHVZIM22 model has a number of inherent limitations and is therefore not a perfect predictor of crop growth and yield. The optimum irrigation solution generated by the programme simply provides a basis from which a farmer can plan irrigation management strategies. The actual intraseasonal irrigation schedule would necessarily depend on the real-time crop, soil and weather conditions.

PREFACE

"A bag of wheat per inch of water" was a common phrase amongst wheat farmers in Zimbabwe in the early 1970's (Wilson, 1974). If this were true, then irrigation management would be simple. However, most farmers would agree that although tantalizing, such a statement is not true, and so irrigation management requires some pre-planning and intraseasonal management. Simply put, the farmer's problem is, "how should wheat be irrigated to best advantage?" Obviously, the answer is not so simple and requires much information about the soil, crop, climate, water availability, and capital and management resources.

The aim of this research was therefore to provide the farmer with guidelines for economically optimizing his wheat irrigation management. This whole project was conducted with the farmers interests very much at the forefront, and most of the basic information obtained from the research has already been passed onto them through popular articles in the farming press and the Agricultural Research Trust Winter Reports (1987 to 1992). This thesis, then, has attempted to assimilate this information into a useable pre-season irrigation management computer programme, based on the crop simulation model CERES-Wheat, that would help a farmer decide what area of wheat to grow with the available water resources, and give an indication on scheduling the intraseasonal allocation of water.

INTRODUCTION

Wheat was one of the first crops to be grown on a commercial scale in Zimbabwe (Edwards, 1971). However, it was not until 1966 that it assumed national importance. During the period 1920 to 1965 national annual production never exceeded 5000 t, with average yields of 2,0 t ha^{-1} or less (Edwards, 1971). Since 1965 though, national production and yields have steadily increased, such that by 1990, 325454 t were produced at an average yield of 5,92 t ha^{-1} (Mashiringwani, 1990a; Smith and Gasela, 1991).

This increase in production was brought about by positive government policies related to the producer price and irrigation development (Morris, 1988) and the adoption of improved wheat cultivars (Edwards, 1974; Mashiringwani, 1990a). However, Zimbabwe is not self-sufficient in wheat, and the gap between local production and demand is widening (Morris, 1989). Consequently, the government relies on controlled wheat imports and rationing to limit consumption.

Presently, about 94% of the wheat is produced by large scale commercial farmers (Longmire, Ngobese and Tembo, 1986) during the relatively dry, cool winter under irrigation. Within this sector, about 70% is produced on the high- and middleveld (altitude > 900 m), and the remainder in the lowveld (mean altitude 443 m) (P.D. Wells, 1991, Personal Communication). Semi-dwarf soft spring wheat cultivars with high yield potential and rust (*Puccinia graminis* f. sp. *tritici* and *P. recondita* f. sp. *tritici*) resistance are sown in May and harvested in September and October. The crop is grown in double-crop rotations with soyabeans, maize, cotton, tobacco and groundnuts.

The dependance of wheat production on irrigation in a semi-arid environment implies that water resources and their efficient use is of prime concern. In 1990, there was a total of about 191169 ha of irrigated commercial farming land in Zimbabwe (Central Statistical Office, 1991, Personal Communication), but wheat was grown on only 55000 ha (Smith and Gasela, 1991). Although this indicates that the wheat area could increase within the current irrigation infrastructure,

irrigated land is used for a variety of crops (many of which are perennial) and the expansion of the wheat area would require a reduction in the area of other crops. Any shift in the relative areas of irrigated crops would be dictated by the relative profitabilities of the various crops and the abundance of water carried over from the summer rainy season. Morris (1988) concluded from a macro-economic study on wheat production that when water was abundant, wheat production represented an efficient use of Zimbabwe's resources. However, in times of drought, both farmers and the nation were better off if water was used to irrigate other crops, principally because many farmers applied water inefficiently to wheat. Longmire, Ngobese and Tembo (1987), Ngobese (1988) and Tembo and Senzanje (1988) all reached similar conclusions by stating that the adoption of more efficient irrigation methods would be one of the main factors contributing to higher wheat production in Zimbabwe.

With a limited water supply, the adoption of efficient irrigation systems implies the use of 'deficit irrigation' (James, 1988). This is an irrigation management method that involves the deliberate application of less water than that required for maximum grain production per unit area, with the aim of maximizing grain production or, perhaps more importantly from the farmers' perspective, net financial return per unit of water applied per unit area produced (Heermann, Martin, Jackson and Stegman, 1990) and to maximize profit with respect to the total area under production (English and Orlob, 1978). However, most irrigation systems are limited logistically in the area of land that can be irrigated. Therefore, deficit irrigation must seek to maximize net returns both per unit of applied water and per unit land area.

The problems of deficit irrigation management lie firstly in deciding the area to be irrigated and the minimum return interval that can be employed with the current irrigation infrastructure, secondly, in determining the intraseasonal sequence and amounts of irrigation to apply, and thirdly, in evaluating the financial returns and risk associated with allowing the development of soil water deficits. Thus, analyses beyond conventional irrigation management decisions are

required for deficit irrigation, and Heermann *et al.* (1990) concluded that one cannot give general recommendations for deficit irrigation because each situation was unique and depended on a number of factors. Stegman, Musick and Stewart (1983) advocated the use of computer simulation to evaluate deficit irrigation options, and some attempts have been made in this direction (e.g., Howell and Hiler, 1975; Martin, 1984; Martin, Gilley and Supalla, 1989).

A number of crop simulation models are available for wheat (Singels, 1989, identified 13), of which the most notable are CERES-Wheat (Ritchie and Otter, 1984; Godwin, Ritchie, Singh and Hunt, 1989), PUTU (de Jager, van Zyl, Kelbe and Singels, 1987; Singels, 1990), TAMW (Maas and Arkin, 1980) and SWHEAT (van Keulen and Seligman, 1987). These models are based on rational empiricisms and they all simulate crop growth, development and grain yield as a function of the soil type, the soil water balance, solar radiation, air temperature, plant (cultivar) characteristics and a range of management factors. They are micro-computer based models, operate on a daily time step and require inputs of weather variables, crop and management information and soil pedon data. CERES-Wheat and SWHEAT also simulate the nitrogen dynamics of the crop. These models share common philosophies in the physiological and physical processes but they differ in the approaches taken to describe them and they differ in the level of hierarchy. CERES-Wheat simulates the growth of a single 'average' plant, whereas PUTU and SWHEAT simulate the growth of the whole crop.

In a comparison of three wheat crop models (CERES-Wheat, SWHEAT, and ARCWHEAT2 (Porter, 1984; Weir *et al.*, 1984)), Porter, Jamieson and Wilson (1993) concluded that although the three models made reasonable predictions of yield for the cultivars examined, they all needed improvement. Similarly, Booysen (1987) found that by comparison with other models, CERES-Wheat estimated leaf area index well, but was unsatisfactory in estimating tiller numbers.

CERES-Wheat is a well documented model and it comprises one of a suite of crop simulation models in the Decision Support System for Agrotechnology Transfer developed by the International Benchmark Sites Network for Agrotechnology

Transfer (IBSNAT, 1989). It has been validated for a range of environments (Otter and Ritchie, 1985; French and Hodges, 1984), and used in a number of diverse applications (e.g., Bacsi, Thornton and Dent, 1991; Booysen, 1987; McGregor and Thornton, 1990; Rodrigues *et al.*, 1990; Savdie *et al.*, 1991). For this reason, it was decided to use CERES-Wheat version 2.10 as the basis of this research.

The objectives of this work were to 1. conduct field experiments to evaluate and refine where necessary CERES-Wheat for application to deficit irrigated wheat in Zimbabwe, 2. apply the model to evaluate deficit irrigation strategies and determine under what conditions deficit irrigation is suited in Zimbabwe, 3. evaluate the risks of deficit-irrigated wheat, and 4. develop a simple interactive computer model to assist farmers with wheat irrigation management decisions.

1 LITERATURE REVIEW

1.1 Irrigated wheat in Zimbabwe

Wheat was one of the first crops introduced to Zimbabwe by the European settlers at the turn of the nineteenth century (Edwards, 1971). It was initially confined mostly to winter crops grown on water retaining bottomlands (Whitlow, 1991). Summer production of wheat constituted an insignificant proportion of total production. From 1920 to 1965, total annual production was low (< 5000 t), but since 1965 production has steadily increased (Figure 1.1) due to government support prices (Edwards, 1974), government subsidised irrigation development loans (Smith and Gasela, 1991) and improved production practices, notably the use of improved cultivars (Mashiringwani, 1990a). The majority of the wheat is now produced as an irrigated crop during the relatively cool, dry winter season. Summer rainfed wheat is not economic because of low yields, disease problems and competition with traditional summer crops (Smith and Gasela, 1991).

Irrigation is applied predominantly with hand-moved, overhead sprinkler systems, with water derived from underground reserves, river storage dams and river flow. Only some 20% of all irrigated land in Zimbabwe is surface irrigated (Central Statistical Office, 1991, Personal Communication). The dependance of production on stored water makes it vulnerable to summer droughts, such as occurred in 1983, 1984 and 1992 (Figure 1.1). Furthermore, because water is usually less available than land, issues related to irrigation management and water use efficiency are of prime importance. Surprisingly, however, scant attention has been devoted to these aspects of wheat production, particularly on the highveld (Longmire, Ngobese and Tembo, 1986). Much of the early wheat irrigation studies were conducted in the lowveld (mean altitude of 443 m) during the 1960's and early 1970's (Cackett, 1968, 1970; McGugan, 1972), possibly because a number of large scale irrigation projects were developed in that area (Cackett, 1972) and the majority of wheat (60%) was grown there (Edwards,

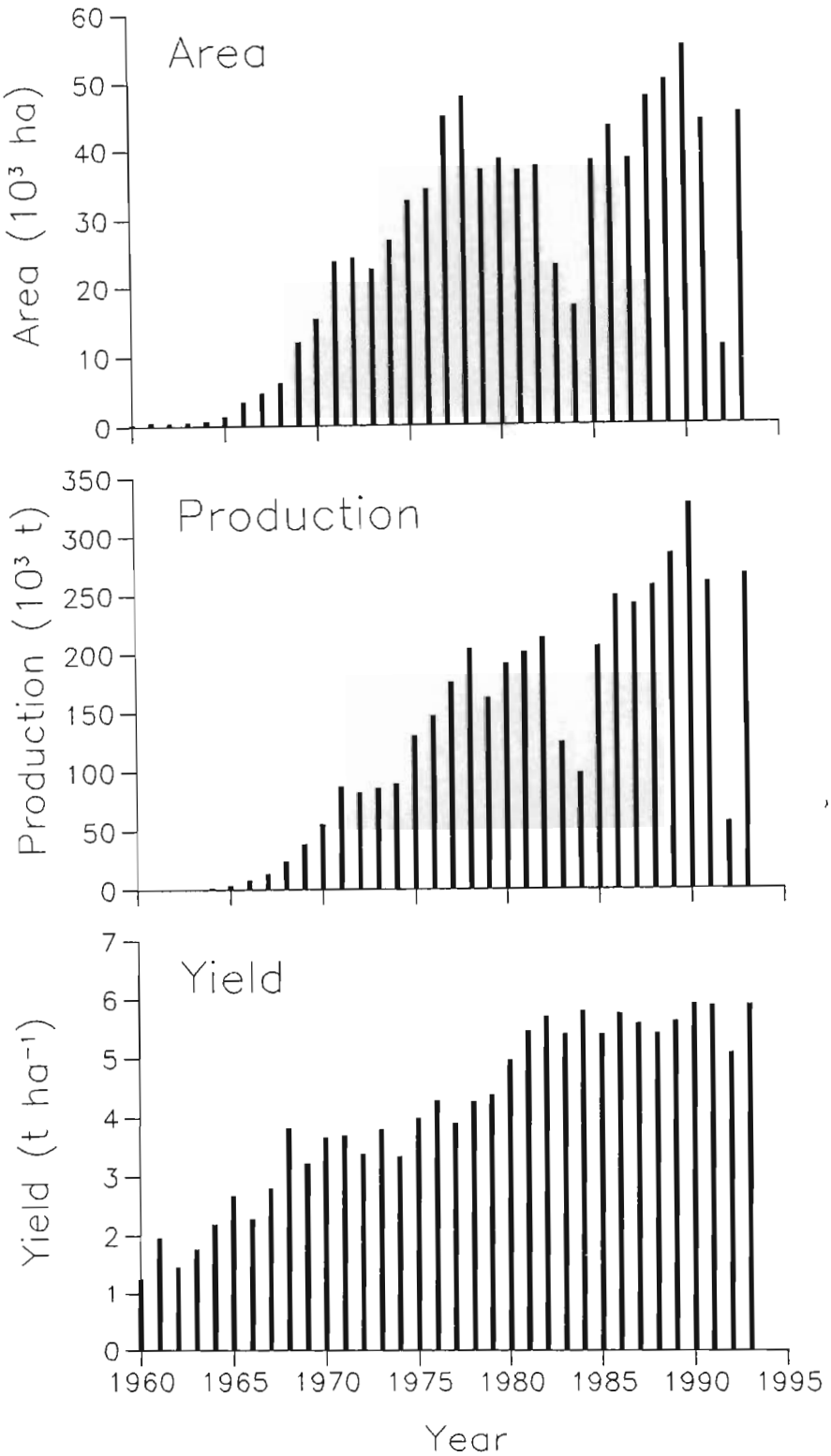

Figure 1.1: The annual area, production and average yield of wheat in Zimbabwe, 1960 to 1990 (data from from Edwards, 1974, and Smith and Gasela, 1991).

1974). The geographical distribution of wheat production has, however, changed since then, with the majority (>65%) now produced on the middle and highvelds (altitudes > 900 m) (Longmire, Ngobese and Tembo, 1986; Tembo and Senzanje, 1988).

Wheat farmers have generally been generous and inefficient with the amount of water applied to wheat (Morris, 1988). A survey of 41 commercial wheat farms by Longmire, Ngobese and Tembo (1986) indicated that the average total water applied was 570 mm (range 360 to 800 mm) and they found no satisfactory relationships between water application amount and yield, soil type, location, water source or pumping costs. Many farmers apply the summer rainfed crop philosophy of maximum yield per unit area to the wheat crop, and therefore believe that the wheat crop should never be stressed (Tembo and Senzanje, 1988). There is also an apparent lack of understanding of the need for efficient water use. Tembo and Senzanje (1988) noted that most Zimbabwean farmers make little effort to schedule wheat irrigation, and cited the following reasons for such behaviour:

- Water costs were too low for farmers to be concerned about conserving it.
- Pumping and energy costs are low.
- Farmers lack the know-how to implement scientific scheduling.
- Farmers do not want to be bothered with a management practice that appears academic.
- There has been inadequate research carried out in Zimbabwe to show farmers the benefits of improved water management.
- The marginal benefits from improved scheduling appear minimal and are not obvious, compared to the extra effort required.

These farmer attitudes may have been brought about by the government programmes to promote wheat production during the 1960's and early 1970's (Edwards, 1974) and the good financial returns that could be expected from the crop (Garvin, 1976). Also, this apparent trend to over-irrigate wheat may be considered as a type of "insurance" by farmers to protect themselves against the vagaries of climate (Vaux and Pruitt, 1983) and the detrimental effects of possible equipment

breakdowns (Stegman, 1982).

However, during the period 1983/84 to 1990/91 there was an erosion in the profitability of wheat production, principally because of increased production costs (Smith and Gasela, 1991), notably irrigation application costs (Table 1.1). Irrigation costs, together with fertiliser costs comprise at least 50% of the total variable costs of wheat production (P.D. Wells, 1993, Zimbabwe Cereal Producers' Association, Personal Communication). Concurrent with these cost increases, the country experienced a number of droughts. Water resources became scarce and farmers were made more aware of the needs to improve water use efficiency.

Table 1.1: Irrigation application costs for wheat, 1986 to 1992. (Data derived from the Agricultural Research Trust 1987 to 1992. Depreciation and labour costs are not included. Note, as at August 1993, ZW$1 ≈ SAR0.50.)

Cost Component	1986	1987	1988	1989	1990	1991	1992
	ZW$ $(mm.ha)^{-1}$						
Electricity	0.24	0.28	0.26	0.47	0.50	0.52	1.15
Repairs and maintenance	0.07	0.18	0.15	0.21	0.25	0.26	0.35
Total	0.31	0.46	0.41	0.68	0.75	0.78	1.50

The overhead sprinkler schemes used for wheat have generally been designed with the objectives of fully irrigating a wheat crop in winter and supplimentary irrigating a summer crop (J. Pitt, 1986, Personal Communication). The average area of irrigated land under wheat per farm ranges between 90 and 110 ha following reasonable summer rainy seasons (Central Statistical Office, 1991, Personal Communication). However, in the Zimbabwe Cereal Producers' Association registry of farmers for 1985, 70% of farmers grew less than 100 ha, but this group of small operations represented only 32% of the total area planted (Ngobese, 1987, 1988). By contrast, the 30% of farmers with large operations, accounted for 68% of the total wheat area and 70% of total production. Of the total arable area

under crops and fruit in 1987, 64% was unirrigated and 36% irrigated (Central Statistical Office, 1991, Personal Communication), indicating that most large scale commercial farms have more arable land than potential fully irrigated land (i.e., water resources are more limiting than land). Because of this, and the fact that irrigation schemes also often cater for summer supplementary irrigation, the schemes are reasonably flexible but usually over-designed.

1.2 Crop-water production functions and the implications for irrigation management

An irrigation manager's task is essentially one of maximizing net financial returns from a crop with the aid of irrigation. Irrigation is only one of many inputs of crop production and so an irrigation manager is faced with numerous long and short term decisions which will impact on his economic success (Heermann *et al.*, 1990). Yet, in the context of current wheat production methods in Zimbabwe, irrigation is an essential input, and therefore decisions related to the total quantity of water applied and the intraseasonal allocation of the water are likely to have an overriding influence on yield and economic success. This is simply because the winters of Zimbabwe are dry and wheat cannot be grown successfully in the absence of irrigation. Nevertheless, this is not to say that irrigation management does not interact with the other production variables, such as climate, fertiliser management, cultivar choice, sowing date, etc.

Production functions, or the relationship between yield and the quantity of a variable input, e.g., fertilizer or irrigation, often form the basis for economic analysis of crop production (Hexem and Heady, 1978; Yaron and Bresler, 1983). In the case of irrigation management, the functional relationship between yield (Y) and water use (WU) is of principle concern. Water use has been expressed (Stewart and Hagan, 1973) as: total evaporation (E_T = plant evaporation [E_p] + soil evaporation [E_s]) (e.g., Singh, Wolkewitz and Kumar, 1987); the depth of irrigation water applied (e.g., MacRobert and Mutemeri, 1988; Machado, 1992); or the total field water supply

(i.e., effective rainfall + irrigation + soil water storage).

Hanks and Rasmussen (1982) and Vaux and Pruit (1983), in reviews of literature, suggest that the relationship between Y and E_T is linear, particularly when E_T deficits (i.e., when E_T is less than potential evaporation, E_o) are optimally sequenced through the season, and when Y and E_T are expressed as proportions of maximum Y (Y_{max}) and E_o, respectively. This has been corroborated for wheat by the works of Hunsaker and Bucks (1987), Steiner *et al.* (1985) and Singh, Wolkewitz and Kumar (1987). No such relationships pertaining to wheat in Zimbabwe could be found in the literature. Although functions of this type have been used to predict yield (e.g., Rasmussen and Hanks, 1978), their use *per se*, in economic analysis, is limited because they do not explicitly account for the amount or timing of irrigation applied.

Of greater interest economically, is the Y *vs* irrigation (I) function, because irrigation is the variable over which the farmer has direct control (Vaux and Pruitt, 1983). This function is usually curvilinear (Stewart and Hagan, 1973) but can be related to, and derived from, the Y *vs* E_T function (Figure 1.2). The linear [$Y = f(E_T)$] and curvilinear [$Y = f(I)$]

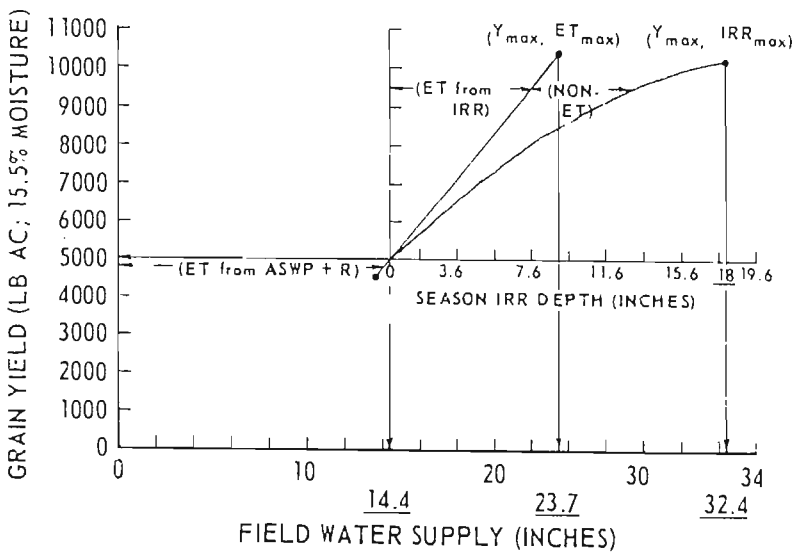

Figure 1.2: Water production function from Stewart and Hagan (1973). Note, the position of the "30" tick mark on the x-axis is incorrectly positioned. It should be one position to the right. This was an error in Stewart and Hagan (1973).

functions are coincident up to a point and then depart from one another as applied water increases. The difference between the two curves is in the proportion of applied water that does not contribute to E_T but which contributes to other terms of the water balance equation (drainage below the root system, runoff, etc.), and in the inexactness of irrigation scheduling and inefficiencies inherent in the water application methods (Stegman *et al.*, 1981).

The economic interpretation of the Y *vs* I function depends on the relative magnitudes of water and land availability. Yaron and Bresler (1983) presented three situations that irrigators may face, each of which requires a different irrigation strategy:

1. Land area is the only limiting factor; water can be purchased and applied at a constant cost per unit (P_{Irr}). In this case the agroeconomic optimization rule requires that water be allocated to the crop so that the marginal net return per unit water be equal to its price. Or in another form, maximum profit is achieved when water is applied in a quantity defined when the slope of the Y *vs* I curve (dY/dI) equals the price ratio (P_{Irr}/P_{Yield}), where P_{Yield} is the unit crop price (Stegman *et al.*, 1980). Applying irrigation using this criteria will achieve the maximum net return per unit land area.

   The optimal irrigation depth for land-limited irrigation is often near that required for Y_{max} because the price ratio is inherently flat (Stegman *et al.*, 1980). However, the maximum yield physically achievable is not the most profitable, unless the cost of water application is zero (Yaron and Bresler, 1983). Hargreaves and Samani (1984) indicated that irrigating for Y_{max} would be more likely to produce maximum benefits when: a. Land is limited and water is abundant; b. Crop values and yields are high; c. Rainfall makes little contribution to the crop water supply; and d. The irrigation costs are low.

2. Water is the only restricting factor; land area is relatively abundant and unlimiting. Limited water relative to land may be defined as a quantity inadequate for a farmer to irrigate all of his irrigable land at a level which will

maximize net returns per unit area (Stegman, Musik and Stewart, 1983).

In this case, water allocation should aim at maximizing the average net return per water unit. This implies the "spreading out" of water over the available land area in a way that equalizes the marginal net return of water on all land units (Yaron and Bresler, 1983), and maximizes profit over the total land area (Stegman *et al.*, 1980). Yaron and Bresler (1983) do state, however, that the "spreading out" process depends on the ability to pay for the fixed cost per unit land area, and so some land area may need to be left unirrigated. Additionally, with this analysis, the "spreading out" of water can only be done in the absence of additional capital expenditure on extra irrigation equipment (Pilbrough and MacRobert, 1988). This situation usually requires that irrigation be applied at a level below that required to achieve maximum net return per unit land area. This is often termed deficit irrigation (James, 1988), because the irrigator deliberately under-irrigates the crop.

3. Both land and water limiting. In this case, irrigation is applied to maximize returns per unit land and water, with all land units irrigated.

Some Zimbabwean wheat research has been directed at establishing the relationship between Y and I (Wilson, 1969; McGugan, 1972; MacRobert and Mutemeri, 1988; Machado, 1992). Published wheat crop-water production functions (MacRobert and Mutemeri, 1988; Machado, 1992) indicate that they are site specific, but curvilinear in nature. MacRobert and Mutemeri (1988), working at one site, obtained a two year average Y_{max} with the application of 570 mm and maximum irrigation water use efficiency (i.e., yield per unit water applied) with the application of 370 mm. Machado (1992) found different yield maxima at two sites, and accounted for the difference in irrigation application required for Y_M by the dissimilarities in E_o of the two sites. Because of this seasonal and site variability in the Y *vs* I functions, Stegman, Musik and Stewart (1983) recommend that they can only form the basis for broad guidelines to irrigation policy.

Pilbrough and MacRobert (1988) made an ecomomic analysis of the data of MacRobert and Mutemeri (1987), and showed that the amount of irrigation required for situations 1 and 2 (from above) differed substantially. MacRobert (1993) re-worded this data with updated prices (Figure 1.3) and showed that for the particular production function, maximum profit per unit area (appropriate to situation 1, above) occurred with the application of 530 mm irrigation. Conversely, maximum profit per unit water applied (appropriate to situation 2, above) was achieved with 330 mm water application.

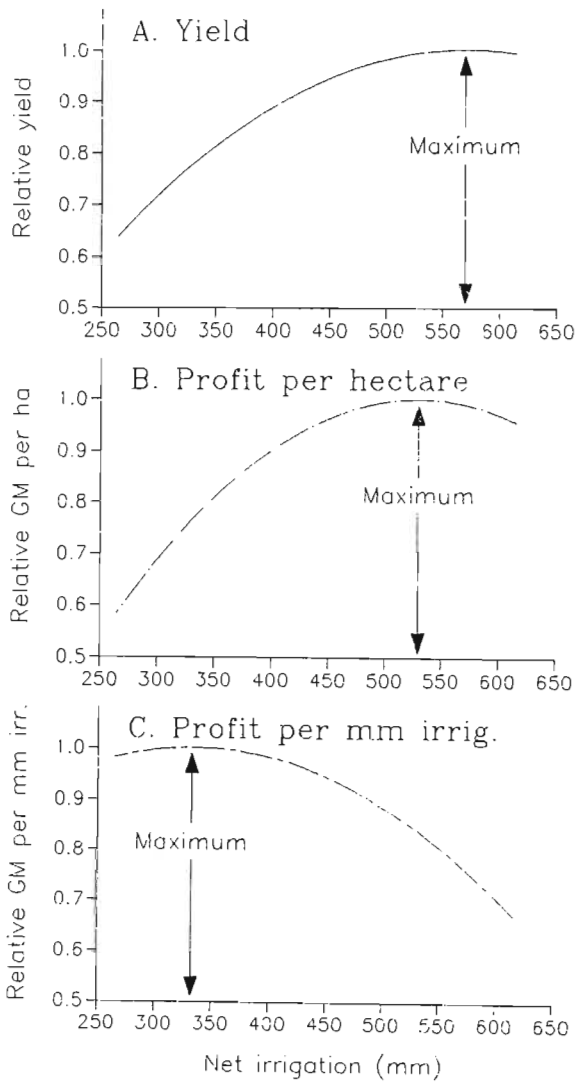

Figure 1.3: Estimated yield (A), gross margin per hectare (B) and gross margin per mm applied irrigation (C) of wheat as a function of net irrigation application at Harare (from MacRobert, 1993).

These two optimal levels of irrigation may provide a guideline to the boundaries within which farmers should irrigate their crop (English, 1990). If the range is wide, the risk of moving toward the lower irrigation level may be regarded as small. On the other hand, a narrow range would imply greater risk and a need for careful consideration and management. A decision to practice deficit irrigation implies a willingness to accept lower yields in exchange for increased total net income (English and Nakamura, 1989), and it also increases the risk of an economic loss (Martin, van Brocklin and Wilmes, 1989). Because of lower yields under deficit irrigation and the observation that yields decline more rapidly on the side of too little water than too much water (relative to Y_{max}), Stegman (1983) concluded that it is safer to err on the side of applying too much water than on the side of applying too little. This observation of Stegman may be right, but a study by English, James and Chen (1990) indicated that deficit irrigation has been a profitable long-term strategy for farmers with limited water supplies.

Simple Y *vs* I production functions give indications of the total quantity of water to apply for a given situation, but they do not lend any information on the intra-seasonal allocation of water (Vaux and Pruitt, 1983). A number of attempts have been made to overcome this deficiency with the use of multi-stage or dated water production functions (e.g., for wheat: Minhas, Parikh and Srinivasan, 1974; Singh, Wolkewitz and Kumar, 1987). These dated water production functions divide the growing season into a number of time or crop growth stage dependent periods and apply additive (Singh, Wolkewitz and Kumar, 1987) or multiplicative (Minhas, Parikh and Srinivasan, 1974) Y/Y_{max} *vs* E_T/E_o functions, modified by estimated stress-sensitivity parameters, to each period.

These dated water production functions have been widely adopted in optimal irrigation studies on many crops (e.g., Baird *et al.*, 1987; Furniss, 1988; Schulze and George, 1987; Hargreaves and Samani, 1984; Rao, Sarma and Chander, 1988). Consequently, they may be considered as being widely applicable. However, Vaux and Pruitt (1983) caution that the greatest problem with crop-water produciton functions is the

extent to which they can be generalized from site to site. There are a number of other limitations to the use of dated water production functions:

1. They should only be applied to situations where the proposed irrigation regimes are similar to those applied in the experiments used to establish the functions.
2. The stress sensitive parameters need to be locally established, both for the edaphic conditions and the crop (cultivar).
3. The dated functions are discontinuous in that they divide the crop season into distinct periods (usually three or four), whereas crop growth is continuous. Yield is dependant in interactions between stages, and the dated water production functions do not adequately deal with this aspect.
4. Yield is predicted as a function of a single index (E_T/E_o or, in some cases, soil water deficit), whereas in reality, yield is the product of a multiplicity of functions (Townley-Smith and Hurd, 1979). For one example, high temperature effects on grain growth (Wiegand and Cuellar, 1981) imposed, say, by altered sowing dates, would not be accounted for in a dated water production function based soley on an E_p/E_T index.

In light of these caveats to the use of crop water production functions, it is not suprising that Vaux and Pruitt (1983) suggested that a physiological approach may hold the most promise to understanding crop response to the environment.

1.3 The physiology of soil-plant water relations of wheat

The growth, function, yield and water use of a plant are intimately related to its water status (Hsiao, 1990). The plant attempts to regulate its water status to survive, for example, by controlling stomata aperture, osmoregulation and root growth. However, its capacity to maintain an adequate water status is limited, since it is subject to the atmospheric demand (E_o) for water and the water supply capacity of the soil,

both of which vary in time and magnitude, and over which the plant has no direct control (Monteith, 1986).

Plant water deficits arise when the flux of water through the plant is insufficient to meet E_o. The dessication of plant tissue can have detrimental effects on tissue function and ultimately yield depending on the magnitude and duration of, and the sensitivity of the processes to, dessication. The timing of plant water deficits in relation to ontogeny also plays a role in the extent to which plant growth is reduced. Generally, a plant organ is most sensitive to stress during its period of rapid development (Begg and Turner, 1976).

Hsiao (1990) presented a schematic diagram to qualitatively summarise the effects of water stress on plant function and yield (Figure 1.4). The diagram indicates that source size (i.e., leaf growth and size) is more sensitive to water stress than source intensity or sink size (i.e., fruit set and growth). It also shows how stress can influence a number of interacting plant functions, all of which can reduce yield.

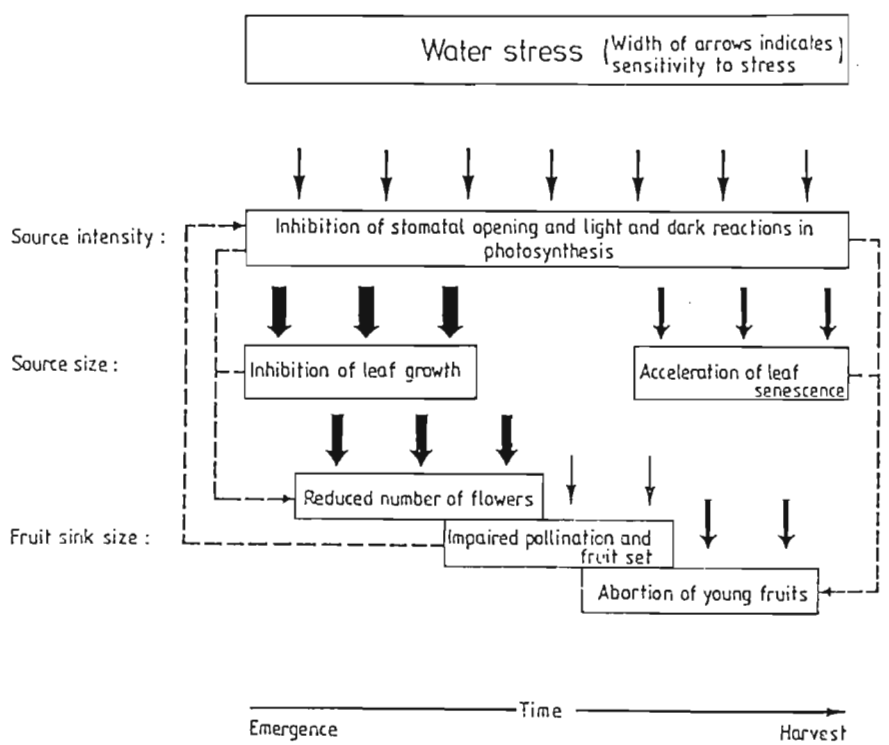

Figure 1.4: Schematic representaion of the possible effects of water stress on plant growth (from Hsiao, 1990).

Interestingly, though, Hsiao did not include the effects of drought on root growth, possibly because roots may respond either positively or negatively to water deficits depending on the severity of stress and genotype (Blum, Mayer and Gozland, 1983). Turner (1986) emphasised the importance of understanding root- as well as shoot-water relations.

The literature on the subject of plant water relations is vast and contains a number of reviews, some appropriate to wheat (Boyer and McPherson, 1974; Gusta and Chen, 1987; Kirkham and Kanemasu, 1983). The aim of this section, therefore, is to highlight the important issues, particularly in relation to irrigation management of wheat.

1.3.1 Growth

1.3.1.1 Photosynthesis and plant evaporation

Photosynthesis, respiration and plant evaporation (E_p) are inextricably linked with one another. As plants dessicate, their leaf water potential (Ψ_{leaf}) decreases, and this is associated with a concomitant decline in photosynthesis, E_p and, in some cases, respiration (both light and dark respiration) (Boyer and McPherson, 1974; Johnson, Frey and Moss, 1974).

The decline in photosynthesis under water deficit may be due to stomatal inhibition of CO_2 conductance, nonstomatal inhibition of photosynthesis, or both (Johnson *et al.*, 1987). Frank, Power and Willis (1973) showed that photosynthesis declined linearly with a decline in Ψ_{leaf} and the decline in photosynthesis began before an appreciable increase in stomatal diffusion resistance was observed. Stomatal closure of stressed plants was affected by leaf position and age, and by ambient temperature. Johnson, Frey and Moss (1974) obtained a high linear correlation between photosynthesis and transpiration (E_p) for flag leaf leaves in a pot experiment.

Decreases in E_p with plant water stress may be due to stomatal closure (Hsiao, 1973) or increased soil-root resistance (Meyer and Green, 1980a). In the field, probably both factors play a role. The relationship between leaf stomatal resistance and Ψ_{leaf} of wheat was shown to have three

phases (Morgan, 1977): 1. no apparent effect until Ψ_{leaf} reached about -1.8 MPa; 2. increasing resistance as Ψ_{leaf} decreased to about -3 MPa; and 3. complete failure of stomatal opening at lower Ψ_{leaf}. There were, however, growth stage effects, with leaf resistances during phase 1 and 2 always greater pre-anthesis than post-anthesis.

The close association between photosynthesis and E_p is not only due to plant control over the processes, principally through stomatal control, but also due to the fact that both processes are tightly coupled to the amount of radiant energy received per unit area and the proportion of this energy absorbed by the foliage as photosynthetically active radiation (Monteith, 1986). The ratio of dry matter production to water use is generally conservative (Vaux and Pruitt, 1983), especially in a temperate environment (de Wit, 1958, cited by Monteith, 1986).

Monteith (1986) suggested that plants attempt to balance the gain in carbon against the corresponding loss of water in order to maximize dry matter production. Plants do this through a complex of controls, moderated by stomatal conductance, governing shoot growth (which affects demand for water) and root growth (which affects supply of water). He demonstrated that through a basic understanding of this water supply and demand balance in crops, optimal irrigation strategies could be formulated. He proposed that 1. irrigation water should be applied at the critical point where the demand, as determined by the photosynthesis of foliage, exceeds the supply, as determined by the extension of the root system, and 2. to minimize the direct loss of water from the soil surface as well as minimizing labour costs, the number of irrigations should be kept to a minimum. He also showed that at times, particularly as the crop approaches maturity, it is not necessary to apply irrigation sufficient to re-fill the soil profile for the amount previously consumed, because any irrigation will enable growth to continue at a maximum rate through to either the next irrigation or maturity. This latter point is supported in a discussion by Ritchie (1981a), in which he stated that when water is applied to a dry soil condition, the added water remains near the surface where root density is greatest and

provides a soil water status which is satisfactory for good plant turgor and hence growth.

1.3.1.2 Vegetative shoot growth

Vegetative shoot growth is highly sensitive to water deficit stress (cf. Figure 1.4; Hsiao, 1973, 1990). Leaf initiation and elongation may be retarded or cease under conditions of water stress (Barlow *et al.*, 1977; Husain and Aspinall, 1970; Munns and Weir, 1981). Leaf elongation is generally affected well before photosynthesis (Hsiao, 1973). If the water stress is mild and short, and osmotic adjustment takes place, leaf elongation rates may recover before release of stress (Munns and Weir, 1981), or return to pre-stress levels on release of stress (e.g., for maize leaves: Acevedo, Hsiao and Henderson, 1971). However, with enduring water deficits during leaf area expansion, final leaf area is reduced (Quarrie and Jones 1977). Leaf area accumulation was decreased in wheat when more than 55% of the plant available water had been extracted from the soil profile (Meyer and Green, 1980a). Although these leaf area reductions reduce water use, they also reduce source size and may consequently decrease sink size and yield (Hsiao, 1990). Since the leaf area of wheat is fixed at about ear emergence, reduction in source size during vegetative growth is irreversible. After ear emergence, water deficit stress can hasten leaf senescence (Wilson, 1969) and thereby decrease leaf area duration (Fischer and Kohn, 1966). Yield has been shown to be positively correlated with leaf area duration (Evans, Wardlaw and Fischer, 1975; Fischer and Kohn, 1966).

Tillering is an important aspect of wheat development because the number of tillers per unit area is a determinant of yield. Tiller emergence of spring wheat begins when the plant has two to three leaves and proceeds as a function of phyllochron interval (Klepper, Rickman and Peterson, 1982), plant density (Puckridge and Donald, 1967), air temperature and solar irradiance (Friend, 1965; Evans, Wardlaw and Fischer, 1975), nutrition (Power and Alessi, 1978) and soil water content (Blum *et al.*, 1990; Chaturvedi *et al.*, 1981; Talukder, Mogensen and Jensen, 1987).

The withholding of water from pot-grown wheat inhibited tiller production and growth when applied during early tillering but not when applied during late tillering (Blum *et al.*, 1990). When stress was relieved in the early stress treatment, tillering resumed at an accelerated rate. At harvest, ear numbers were equal to or greater than the well watered control, depending on the severity of the applied stress, and the tillers that developed after stress relief made significant contributions to yield. When the stress was relieved in the late tillering treatment, few new tillers were produced, especially when the stress was severe. This phenomenon was also observed to occur in the field by Talukder, Mogensen and Jensen (1987). Wheat that was subjected to water deficit stress prior to the completion of heading developed late tillers which contributed up to 39% of the final grain yield, but they ripened two weeks later than the normal tillers. Stark and Longley (1986) noted that the rate of appearance of main stem tillers was decreased by soil water deficits applied in early growth stages. When stressed plants were irrigated, the appearance rate of affected tillers frequently increased 40 to 70 °C d (base 0°C) after irrigation.

Water deficits may also increase senescence of tillers, which will not only reduce leaf area but also sink size (Begg and Turner, 1976). Keim and Kronstad (1981), working with winter wheat, reported a large reduction in tiller number following the imposition of water-stress after maximum tiller number attainment. Davidson and Chevalier (1990) compared the tillering patterns of irrigated and unirrigated spring wheat. In both treatments, the majority of tiller death occurred during main stem extension, but greater numbers of tillers died in the stressed (unirrigated) wheat than in the irrigated wheat. Those tillers that emerged late during plant development were most likely to senesce prematurely. The loss of tillers may, however, not be entirely detrimental, for it has been noted that senescing tillers remobilize nitrogenous and other organic substances to surviving shoots (Lupton and Pinthus, 1969; Rawson and Donald, 1969), and the abortion of tillers will reduce the water use of the plant.

This discussion indicates that tillering is an important yield component of wheat, and although tillering may recover from early water deficit stress, these tillers are later maturing and will interfere with the smooth harvesting of the crop (Mogensen, Jensen and Rab, 1985). From an irrigators point of view, therefore, the avoidance of early stress is important, in order to unify tiller ontogeny and ensure maximum tiller survival.

1.3.1.3 Root growth

On germination, the primary root is the first plant part to pierce through the seed coat and penetrate the surrounding environment (Lersten, 1987). Root axes are thereafter produced at predictable times in relation to shoot development, and the total number of roots formed is associated with the number of leaves on the main stem and the extent of tillering (Klepper, Belford and Rickman, 1984). The root system of wheat consists of the seminal root system that arises from the embryo and the crown or nodal root system that arises from the main shoot and tiller nodes (Musick and Porter, 1990). An extensive, deep root system is associated with drought resistance in wheat (Hurd, 1974).

The seminal root system is important in the early stages of growth, but if conditions are conducive to nodal root growth, they become increasingly less important. Nevertheless, Belford, Klepper and Rickman (1987) noted that, in winter wheat, seminal roots remain active throughout the season and provide the greater fraction of roots in the lower profile than nodal roots. These deep seminal roots may, therefore, be important to the plant under conditions of soil water deficits.

Nodal roots begin to grow 25 to 30 d after plant emergence (Muxick and Porter, 1990). Their development may be retarded or halted by dry soil surface conditions (Musick and Porter, 1990), but Portas and Taylor (1976), working with maize, noted that root tips, whose growth had been inhibited by dry soil, will elongate rapidly if the soil around them becomes wetted. The early deep development of nodal roots of wheat is considered by Musick and Porter (1990) to be important for

irrigated wheat so as to enable depletion of soil water from the lower profile. Irrigation at crown root initiation may enhance rooting and yield, due to both increased tillering and enhanced profile water utilization (Gajri and Prihar, 1983; Gajri *et al.*, 1991).

In field trials in South Africa with spring wheat, high frequency irrigation resulted in a shallower rooting system than low-frequency irrigation (Proffitt, Berliner and Oosterhuis, 1985). The deep rooted plants under low frequency irrigation were able to extract more water from greater depths within the soil profile during a soil drying-out period. Deep roots of winter wheat have also been shown to take up considerable quantities of water when upper profile roots were in dry soil (Gregory, McGowan and Biscoe, 1978). Rooting depths of over 0.9 m are common for irrigated wheat in Zimbabwe (MacRobert, Wells and Savage, 1991).

Wardlaw (1971) noted that wheat roots were sensitive to water stress during grain development and that their consequent impaired functional ability may be an important factor in premature senescence of grains.

1.3.1.4 Reproductive growth

Reproductive growth in wheat spans a long period of the total growth of the plant. The initiation of reproductive growth is identified by the elongation of the apical dome (Stern and Kirby, 1979) and the formation of "double ridges" on the shoot apex (Oosterhuis, 1977). This occurs in spring wheat when the main shoot has about three full leaves (Simmons, 1987). Floral formation continues through to anthesis. Following anthesis, pollination and fertilization, grain growth begins. Grain growth goes through an initial lag phase of one to two weeks, when cell numbers increase, followed by a period of rapid dry matter accumulation until maximum dry weight is reached and kernel water content declines.

Water deficit stress can adversely affect growth in all phases of reproductive growth in wheat. Apex elongation and spikelet growth is sensitive to water stress (Barlow *et al.*, 1977; Husain and Aspinall, 1970), but the apical meristem can

withstand severe dessication and resume growth following stress relief (Barlow *et al.*, 1977). The developing wheat spike is extremely sensitive to water stress during the transition phase from vegetative to reproductive differentiation and during late internode elongation immediately prior to spike emergence (Oosterhuise and Cartwright, 1983). Water stress at these critical times generally caused floret and sometimes whole spikelet death at the terminal ends of the spike. Abortion of florets and spikelets in response to stress causes reduced grain numbers but makes little impact on total plant dry weight.

Water deficit stress applied during meiosis in the pollen mother cells (which occurs at approximately the same time as meiosis in the egg-mother-cells and about ten days prior to anthesis (Bennet *et al.*, 1973, cited by Saini and Aspinall, 1981)), significantly reduced grain set as a result of reduced male fertility but not female fertility (Saini and Aspinall, 1981, 1982). This effect was found to be the result not of dessication of the sporogenous tissue, but rather an indirect outcome of the decrease in water potential elsewhere in the plant, probably mediated by abscisic acid.

The duration and rate of grain growth is affected by water deficits. Mogensen and Talukder (1987) reported higher grain growth rates during the linear phase of grain growth for stressed wheat compared to a well-watered wheat. However, grain-fill duration was shorter and final kernel masses lower in the stressed wheat. Similar observations were made by Gallagher, Biscoe and Hunter (1976). Kobata, Palta and Turner (1992) noted that the rate of development of post-anthesis water deficits markedly affected kernel mass but not kernel number. Faster rates of stress development and a greater degree of stress (i.e., lower Ψ_{leaf}) reduced grain yield per plant by 33%, compared to a mild stress that developed slower.

Pre-anthesis non-structural dry matter stored in stems and translocated to kernels during drought may account for this observed increase in grain growth rate (Gallagher, Biscoe and Hunter, 1976; Mogensen and Talukder, 1987; Pheloung and Siddique, 1991), although Bidinger, Musgrave and Fischer (1977) note that this may account for less than a third of the final

yield. The proportion of current assimilates translocated to kernels may also increase during water stress (Johnson and Moss, 1976).

Increased grain growth rates under drought conditions may be an indirect effect of increased plant temperature. Grain growth rates have been noted to increase with increased ambient temperature (Sofield *et al.*, 1977), while wheat canopy temperatures increase with decreases in plant water potential induced by water deficit stress (Ehrler *et al.*, 1978). Similarly, higher canopy temperatures due to drought may hasten maturity, since the duration of grain fill has been shown to be negatively correlated with average ambient temperature (Wiegand and Cuellar, 1981). In a summary of pertinent literature, Wiegand and Cuellar estimated that the average shortening of the grain fill duration was 3.3 d $°C^{-1}$ increase in ambient temperature. Ehrler *et al.* (1978) noted that midday wheat canopy temperature exceeded air temperature when leaf water potentials declined below -1.9 MPa.

Late grain filling is less sensitive to water stress (Musick and Porter, 1990). Consequently, major depletion of soil water after milk stage is commonly practiced in the USA, as this contributes to efficient water use.

1.3.2 Phasic development

The phasic development and the duration of growth are important determinants of potential yields (Ritchie, 1991). Wheat phasic development is affected primarily by genetic and environmental factors (e.g., air temperature, photoperiod, nutrition and water). The effects of water deficit stress on growth and growth duration have been discussed in the previous section. The aim here is to look specifically at phasic development, i.e., the timing of identifiable growth stages, such as leaf appearance, anthesis and physiological maturity.

A number of schemes have been devised to describe wheat phasic development. For example, the Feeks scale (Large, 1954) and the Zadoks decimal scale (Zadoks, Chang and Konzak, 1974; Tottman and Broad, 1987) are in common use. These scales are more useful in describing growth stages and for advising

farmers on the timing of management inputs than a time scale because development, especially across environments, is not well correlated with time *per se*.

Leaf appearance on wheat follows an ordered pattern (Klepper, Rickman and Peterson, 1982) which is closely related to accumulated thermal time (Gallagher, 1979). The thermal time interval between the appearance of successive leaves is called the phyllochron interval (Ritchie, 1991). Unirrigated wheat had shorter phyllochron intervals compared to irrigated wheat (Baker *et al.*, 1986). This was attributed to warmer plant temperatures as a consequence of drought. In contrast, Krenzer, Nipp and McNew (1991) noted greater phyllochron intervals in stressed wheat compared to well watered wheat in a controlled environment experiment. They concluded that the slower leaf appearance rate under stress may have been associated with the smaller rooting volume and faster change in plant water status of their container-grown wheat compared to the field grown wheat of Baker *et al.* (1986).

Spring wheat cultivars either have no vernalization requirement or a low sensitivity to vernalization (Ritchie, 1991). Photoperiod sensitivity also varies among wheat cultivars, with the rate of infloresence development of sensitive cultivars increasing with longer photoperiods (Riddell, Gries and Stearns, 1958). Air temperature, however, plays a dominant role in determining the rate of wheat development in Zimbabwe (Cackett and Wall, 1971).

Water deficit stress may either lengthen or shorten the duration of pre-anthesis growth of wheat. Jones (1977) observed that a drought treatment hastened anthesis of 12 spring wheat cultivars by an average of four days. Angus and Moncur (1977) and Meyer and Green (1980b) found that mild stress (Ψ_{leaf} about -1.5 MPa) between floral initiation and anthesis hastened the onset of anthesis, whereas severe stress (Ψ_{leaf} from about -2.5 to -4.0 MPa) during the same period delayed anthesis compared to well-watered controls. Angus and Moncur suggested that the delay in anthesis under severe water stress was due to cessation of development of the shoot apex. The hastening of development under mild stress may have been due to increased plant temperature or a drought avoidance mechanism of the plant

itself or both. The Ψ_{leaf} of wheat in Jones' study were mostly above -2.5 MPa, and so the stress was probably not severe enough to cause a delay in anthesis as observed in the studies of Angus and Moncur (1977) and Meyer and Green (1980 b).

Cutford *et al.* (1988) working with spring wheat in Canada noted that dryland wheat matured 30 d or more earlier than irrigated wheat. Although the time from sowing to flag leaf emergence and anthesis was extended by irrigation, the duration from anthesis to maturity was most affected. They attributed the extended growth of irrigated wheat to cooler plant temperatures induced by frequent irrigation and better plant water status. Davidson and Chevalier (1990) also observed that heading and anthesis occurred earlier in unirrigated wheat than in irrigated wheat.

The duration of grain filling is shortened under conditions of drought (Mogensen and Talukder, 1987). Fischer, Lindt and Glave (1977), in a field study with spring wheat, noted that a delay of irrigation led to plant water stress and significant acceleration of development. This topic was also discussed in section 1.3.1.

1.3.3 Yield and yield components

Yield is of principle concern to the farmer. The sensitivity of yield to water deficit stress is a function of the timing and duration of the deficit. This implies that crops are more sensitive to drought at some stages than others and these stages are often termed critical growth stages (Musick and Porter, 1990).

An early study in Zimbabwe (Wilson, 1969) using potted wheat plants showed that an isolated period of severe soil water stress applied prior to ear emergence had no depressing effect on grain yield. The sensitivity of plants to stress increased after ear emergence and was most acute during the early grain-fill period. Water deficit stresses during grain-filling reduced the magnitude of all yield components compared to unstressed plants. These results, however, seem anomolous compared to other reports. Salter and Goode (1967, cited by Carter, 1987) concluded that the shooting and heading stages

are particularly sensitive to water stress and that irrigations after soft dough stage do not increase yields.

Fischer, Lindt and Glave (1977), working in Mexico, established that the most sensitive stage appeared to last from 25 d before until 20 d after spike emergence. Stress prior to anthesis reduced the number of grains m^{-2}, stress after flowering reduced kernel weight, while stress before and after flowering reduced both yield components. Early stress, or moderate grain-filling stress had no effect on yield. These results of Fischer and co-workers are similar to those summarized by McGugan (1972) working in the lowveld of Zimbabwe. In Denmark, Mogensen, Jensen and Rab (1985) determined that the tillering and jointing stage was the most critical if late developing stress-recovery tillers were excluded. If, however, these late tillers were included, then the critical stage was around booting and heading. Stark and Longley (1986) observed that if the first irrigation after emergence was delayed from the third to the seventh leaf stage, yield declined, mainly because of reduced tiller numbers. Cooper (1980) found that increasing the frequency of irrigation on wheat increased yield by increasing kernels m^{-2}, with little effect on kernel weight. He therefore suggested that, because kernel numbers are set at anthesis, the period prior to anthesis was most responsive to applied irrigation.

1.3.4 Summary

Severe water deficit stress at any time in the life of wheat is likely to reduce yield to some extent. However, there does not appear to be a distinct critical stage, as for example flowering in maize (Musick and Dusek, 1980). Water stress in the early vegetative stages will reduce root, leaf and tiller growth, which may be permanently impaired if stress relief is delayed. Stress spanning ear emergence and early grain development will likely cause an irreversible decline in kernel numbers, while stress during grain filling may decrease kernel weight. The late grain fill period is probably the least sensitive to water deficits.

1.4 Deficit irrigation and irrigation scheduling

Deficit irrigation is the deliberate under-irrigation of a crop with the objective of maximizing net returns per unit water applied. In Section 1.2 the economic justification for deficit irrigation was discussed. Here, the emphasis is on translating the economically determined optima into field practice. Farmers have certain contraints in the form of edaphic conditions, field layouts, irrigation infrastructure, labour availability, and so on. The question, therefore, is, "How can they transform a gross amount of water into a manageable seasonal allocation schedule that will maximize profits with an acceptable level of risk?"

The application frequency of irrigation (equivalent to the return interval, and defined as the minimum time between irrigations (English and Nuss, 1982)) is largely determined by the method of irrigation. Centre pivots are normally designed for frequent irrigation (return interval < 7 d) with small amounts of water (< 30 mm) (Heermann *et al.*, 1990). This is often termed "high frequency" irrigation, especially if irrigation is applied on a daily basis (Miller and Hang, 1982). Hand-moved sprinkler irrigation, on the other hand, usually applies water on a low frequency (return intervals > 6 d) with large amounts of water (> 30 mm) per application. In the absence of water deficit stress, Proffitt, Berliner and Oosterhuis (1984) noted that wheat yield was greater from high-frequency irrigation than from low frequency irrigation. However, water stress imposed on the high frequency regime reduced grain yields more than when imposed on the low frequency regime.

Irrigations at high frequency and full E_T replacement maintain high soil water potentials in the upper root zone, thereby ensuring maximum yield (Stegman, 1983; Rawlins and Raats, 1975). Deficit, high frequency irrigation is based on the concept of partial replacement of daily potential E_T (Stegman, 1983), which results in a gradual decrease in the profile soil water content through the season (English and Nuss, 1982; English and Nakamura, 1989). For this reason, high-frequency deficit irrigation has been termed "planned soil

water depletion" (Woodruff *et al.*, 1972, cited by Stegman, Musick and Stewart, 1983). The problem is that optimal E_T replacement fractions are not easily determined (Stegman, 1983) and profile soil water content may reach a level beyond which the crop experiences progressively more stress.

Proponents of high-frequency deficit irrigation maintain that frequent irrigation sustains relatively high soil water potentials in the upper root zone (Stegman, 1983) that may mitigate the effects of profile water deficits (Miller, 1977, cited by English and Nuss, 1982). Maintaining high water contents in the upper root zone may also be beneficial since this is the zone where nutrients are mostly concentrated (Stegman, 1983). However, high-frequency irrigation may result in greater evaporation of soil water and greater evaporative loss of plant-intercepted water than lower frequency irrigation (Faci and Fereres, 1980).

Miller and Hang (1982), working with winter wheat, found that with a loam soil near the upper limit of available water at the time of near full ground cover, daily irrigations thereafter could be reduced to 0.4 potential E_T without reducing yield below Y_M. Conversely, on a sandy soil, any level of deficit high frequency irrigation reduced yields. Musick (1989) reworked some of the data of English and Nakamura (1989) and concluded that high frequency deficit irrigation that reduced water application to one-half or two-thirds of potential E_T could be a very efficient means of deficit irrigation management.

The success of irrigation application as a percent of potential E_T is dependant on the extractable soil water content (Miller and Hang, 1982) and is influenced by seasonal rainfall (Furniss, 1988). Fischbach and Somerholder (1974) suggest that the concept works well when it is applied to deep soils with available water capacities greater than 0.13 $m^3\ m^{-3}$. It also requires that the crop season is started on a soil profile that is at or near the upper limit of plant available water, and the irrigation system must operate without down time during the high use period (Fonken, Steele and Fischbach, 1974).

High frequency irrigation is inappropriate to hand moved sprinkler systems, because more piping would be required to

cover the field, implying higher capital costs, and within season labour and maintenance costs would increase (English and Nuss, 1982). English and Nakamura (1989) concluded from a study comparing high- and low-frequency deficit irrigation on wheat that highest yields and the highest water use efficiencies were consistently realized with relatively low frequency irrigation. Similarly, Faci and Fereres (1980), working with sorghum, concluded that yields were lower under high irrigation frequencies. English, James and Chen (1990) studied farm deficit irrigation practices in the Columbia Basin, USA, and observed that both high- and low-frequency irrigation was used. They did not give any yields associated with the two methods, but indicated that the different methods were more a function of available irrigation equipment (centre pivots *vs* set-move systems) than yield or other advantages or disadvantages.

Low frequency deficit irrigation causes profile soil water content to fluctuate within a wide range (English and Nuss, 1982). A large application will be followed by a long period of extraction, during which the stress experienced by the crop will range from none to severe. The severity of the stress at the end of each irrigation cycle will depend on the amount of water applied, the other components of the water balance (i.e., the initial soil water content, E_p, E_s, and drainage), and the return interval. Since deficit irrigation implies under-irrigation, with each irrigation cycle, the severity of each cyclical stress will increase, and the irrigation managers job, then, is to allow some, pre-defined, gradual increase in plant stress, or cummulative E_T deficit, through the season.

Stewart *et al.* (1977, cited by Stegman, 1983) suggested that a maximum yield for a given seasonal E_T deficit will tend to occur when deficits are spread as evenly as possible over the growing season. Singh (1981) concluded that where irrigation water supplies are limited, irrigation application should be managed in such a way that unavoidable water deficits coincide with growth stages that influence grain yield the least. He further stated that although irrigation at the critical stage is important in its own right, wheat yield was sensitive to deficits at the critical stage only when the crop was not preconditioned to some water stress in previous growth stages.

Thus, he concluded that if water is limited, irrigations should be timed so that deficits are spread nearly evenly over the previous growth stages and the critical stage. Fischer and Hagan (1965) stated that whenever it is anticipated that a water deficiency may arise, a water management programme which allows imposition of some degree of early stress may be an advantage. This implies that early mild stresses may be allowable and enables the plant to cope with later more severe stresses.

Such studies and conclusions are useful, but they still do not provide a farmer with an explicit irrigation schedule. Stewart *et al.* (1975) presented guidelines on the approximate upper limits of E_T deficits by growth stage (pre- and post-anthesis) for maize. These would be used in conjunction with a water balance model to indicate irrigation requirements and provide a reasonably practical means for farmers or advisors to schedule irrigations. More sophisticated attempts to schedule deficit irrigation have also been made, usually with the use of dated water production functions and dynamic linear programming (e.g., Bras and Cordova, 1981; Howell, Hiler and Reddell, 1975; Martin *et al.*, 1983; Martin and Heermann, 1984; Yaron and Strateener, 1973). Hood, McClendon and Hook (1987) used the soyabean crop simulation model, SOYGRO, to evaluate irrigation strategies, while Epperson, Hook and Mustafa (1993) combined the CERES-Maize crop simulation model with dynamic programming to determine optimal irrigation thresholds for maize.

In none of these reports did the authors give any indication of their schedules being used by farmers for pre-season water allocation decisions or for day to day management decisions. Pleban and Israeli (1989) pointed out that although several computer programmes for irrigation scheduling were available, farmer acceptance had been low. They attributed this to the programmes being oriented to researchers and professionals and were therefore not farmer-friendly.

There is a need in Zimbabwe to develop a farmer oriented wheat deficit irrigation management programme that will assist with planning wheat areas and intraseasonal water allocations appropriate to his situation. Farmers currently use their own experience and that of their advisors to develop irrigation

policies. However, as outlined above, the determination of optimal deficit irrigation strategies are not as simple as those required when irrigating for maximum yield. Stegman, Musick and Stewart (1983) recommended the use of computer simulation to evaluate deficit irrigation options.

Crop growth simulation models enable rapid estimates of yield over many seasons and production conditions and they may be linked to economic routines to evaluate financial returns and risk (Epperson, Hook and Mustafa, 1993; Singels and de Jager, 1991). Their use in forecasting optimum production strategies may result in moderate economic benefits over the long term (Thornton and MacRobert, 1993). Unfortunately, though, crop simulation models are not perfect predictors of yield and they are often based on many assumptions. Therefore, their use in irrigation optimization problems will be associated with a degree of uncertainty (English, 1981). Consequently, effort needs to be made to quantify this uncertainty in order to provide a better basis on which to make irrigation decisions. This requires that the model be locally calibrated and verified, and the mean and variance of multi-replicate simulation runs be calculated to characterise the error involved (Thornton, Blair-Fish and Wilson, 1991).

When using computer simulation modelling to evaluate management options, literally hundreds of treatments may be assessed in a very short space of time. For example, Thornton and MacRobert (1993) evaluated 400 treatments using CERES-Maize within ten minutes on an IBM AT-compatible 80486 (50 MHz) computer. The problem comes in choosing the optimum treatment out of such an array. The literature indicates that a number of methods have been used; for example, mean-variance diagrams (Thornton, Blair-Fish and Wilson, 1991; Thornton and MacRobert, 1993), stochastic dominance techniques (Epperson, Hook and Mustafa, 1992; McGregor and Thornton, 1990; Pandey, 1990; Singels, 1992; Thornton, Blair-Fish and Wilson, 1991) and Pareto optimization techniques (Alocilja and Ritchie, 1990; MacRobert and Savage, 1991) have been employed. Such methods still need to be interfaced with the farmer, otherwise they will remain research tools and farmers will not reap the potential benefits.

1.5 An overview of CERES-Wheat

The CERES-Wheat model has evolved over many years through the work of many people (the July, 1988, version (Ritchie *et al.*, 1988) names 12 authors plus other unnamed workers). The 1983 version (Ritchie and Otter, 1984) simulated plant growth and yield in response to daily weather, soil water and plant factors. The 1989 version (version 2.10: Godwin *et al.*, 1989) included nitrogen dynamics, while more recently phosphorus movement in the soil and plant was added (Thornton, Blair-Fish and Wilson, 1991). Work is also proceeding to incorporate the effects of pests and diseases, and plant competition, with respect to weeds and intercropping (McGregor and Thornton, 1990).

For the purposes of this thesis, the CERES-Wheat standard version 2.10 (WHV21) was used. The nitrogen routines were ignored because the focus was on using the model for irrigation management, and farmers in Zimbabwe generally apply sufficient quantities of N (and P) fertilizer to wheat (Whingwiri, Mataruka and Ntungakwa, 1984). This section summarizes the principle components of WHV21 in relation to the objectives of this thesis. There is more detailed documentation available on the model (Godwin *et al.*, 1989; Ritchie and Otter, 1984; Ritchie, 1991).

The core of WHV21 is comprised of three subroutines, which simulate the soil-plant-atmosphere continuum, crop phenological stages and crop growth. A number of other subroutines are included to read in treatment, soil and weather data, and output simulated results. Each of the essential subroutines are summarized (Table 1.2) and a simplified flow diagram of the model is given (Figure 1.5). The input and output files used by the Standard Version are listed (Table 1.3), as are the input data necessary to execute the model (Table 1.4). The appropriate form in which these files and data should be arranged are given in IBSNAT (1986) and Godwin *et al.* (1989).

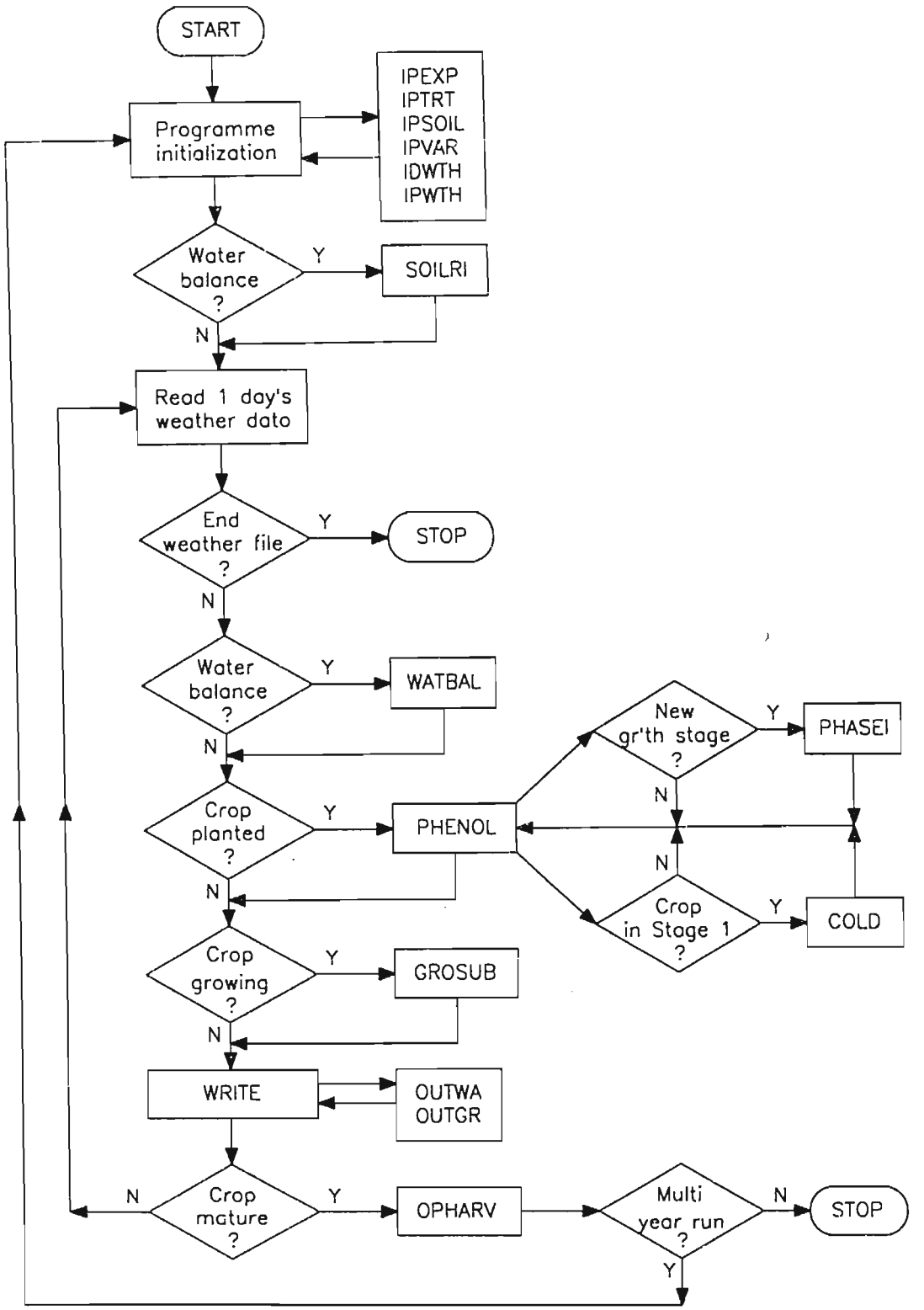

Figure 1.5: Flow diagramme of the CERES-Wheat crop simulation model (adapted from Godwin *et al.*, 1989).

1.5.1 Water balance subroutine (WATBAL)

The water balance section of WHV21 was described in detail by Ritchie and Otter (1984). The procedures are used in similar formats in the other models in the IBSNAT suite (e.g., CERES-Maize and SOYGRO), and they are also used in part in the wheat model of O'Leary, Connor and White (1985).

The upper-most soil layer receives additions of water from rain, melted snow and/or irrigation. The proportion of rainfall that runs-off the soil is calculated from the USDA SCS curve number technique. The balance plus any irrigation infiltrates the soil surface. The distribution of infiltrated water through the profile is based on a cascading layer model, with drainage calculated as a function of the water content above the drained upper limit. Upperward flow of water from one layer to another is allowed in the top four soil layers if the volumetric soil water content in the upper layer is less than that in the lower layer.

Evaporation is separated into soil evaporation (ES[§]) and plant evaporation (EP), based on Ritchie (1972). The potential evaporation (EO) calculation is based on the Priestly-Taylor method. The equilibrium evaporation rate (EEQ) is calculated from daily solar radiation (SOLRAD), the combined crop and soil reflection coefficient (ALBEDO = f(SALB, LAI)) and the weighted mean daily air temperature. Potential evaporation is then calculated from EEQ from the maximum air temperature (TEMPMX).

Potential ES (EOS) is calculated as a function of EO and leaf area index (LAI). Actual ES is a two stage process, whereby during stage 1, evaporation proceeds at a maximum rate (energy limited) when there is sufficient soil water to meet the demand. Stage 1 evaporation continues until a soil-dependent upper limit of evaporation (U, Table 1.4) is reached. Thereafter, stage 2 evaporation begins and is calculated as a function of time. Potential EP (EP1) is calculated as a function of EO and LAI for LAI $\leq$ 3, or is set equal to EO for LAI > 3. If EP1 + ES > Eo, then EP1 is equal to EO - ES.

[§] The uppercase terms ES, EO, EP, etc. are those used in the Fortran code of CERES-Wheat (Ritchie *et al.*, 1988)

Table 1.2: List of subroutines and their principle functions in CERES-Wheat v. 2.10 (adapted from Ritchie *et al.*, 1988). (For an explanation of file names, refer Table 1.3.)

Subroutine	Description of function
IPEXPT	Reads WHEXP.DIR file, enables selection of experiment Reads FILE 8, enables selection of treatment, after treatment choice, reads in treatment details.
IPTRT	Reads FILE 6, finds treatment and reads in irrigation management data (day of irrigation and amount).
IPSOIL	Reads SPROFILE.WH2, selects appropriate profile and reads in profile characteristics.
IPVAR	Reads GENETICS.WH9, selects appropriate cultivar and reads in cultivar genetic coefficients.
IDWTH	Reads WTH.DIR, locates weather file (FILE 1).
IPWTH	Reads first weather record, checks that start of simulation date and sowing date are greater or equal to first weather record date.
PROGRI	Initializes all state variables.
SOILRI	Reads and initializes soil information.
CALDAT	Converts day of year to month and date.
WATBAL	Water balance subroutine. Includes irrigation application, runoff calculation, drainange and soil water redistribution, potential evaporation calculation, root growth and depth accumulation and calculates water uptake and soil water deficit factors.
PHENOL	Subroutine to calculate phenological stage PHASEI and COLD called from within PHENOL. At the end of each growth stage, summary output data written to file OUT1.WH. At physiological maturity, calls OPHARV.
PHASEI	Initializes phenological variables at the change of each growth stage.
COLD	Calculates vernalization factors, leaf senescence and tiller and plant death due to cold in vegetative growth stages.
GROSUB	Growth subroutine; controls leaf area development and senescence, tillering, and root, stem, leaf and grain dry weight accumulation. Grain yield is determined.
WRITE	Accumulates weather and soil outputs and calls OUTWA and OUTGR.
OUTWA	Writes evaporation, radiation and soil water information to OUT3.WH
OUTGR	Writes plant growth information to OUT2.WH
OPHARV	Writes predicted and observed (if available) output to summary file OUT1.WH.

Table 1.3: Input and output files used by Standard CERES-Wheat v. 2.10 (adapted from IBSNAT, 1986 and Godwin *et al.*, 1989).

File Name	Description of contents
WHEXP.DIR	Lists experiments together with the associated input and output file names.
WTH.DIR	Lists weather files along with information on location, beginning and ending dates of weather data in each file.
FILE 1	Weather file. The name of each file identifies the location, months and year of weather in file (e.g., ARTF0112.W89 identifies ART Farm, starting month 01, with 12 months data for 1989). Contains latitude, longitude and daily listing of minimum data set.
SPROFILE.WH2	Contains a list of soil pedons together with basic data such as soil reflection coefficient, stage 1 soil evaporation, and soil water characteristics for each layer.
FILE 5	Soil profile initial conditions. The file name identifies the experiment. For each treatment within the experiment, the initial values of soil water content are given for each soil layer, corresponding to the chosen soil pedon in SPROFILE.WH2.
FILE 6	Irrigation management data file. The file name identifies the experiment. For each treatment within the experiment, the day and amount of irrigation are specified.
FILE 8	Treatment management data. The file name identifies the experiment. Contains a brief description of each treatment, together with necessary input data, such as sowing date, cultivar, etc.
GENETICS.WH9	Genetic coefficient data. Contains a list of cultivars and their associated genetic coefficients.
OUT1.WH	Summary output file for simulation results
OUT2.WH	Detailed output file for growth characteristics
OUT3.WH	Detailed output file for soil water and plant water use characteristics

Table 1.4: Input data required for the Standard CERES-Wheat simulation model (from Ritchie *et al.*, 1988 and IBSNAT, 1986).

Parameter or Variable	Acronym	Units[1]
Location data		
Latitude (Note, Southern Latitudes prefixed with a -ve sign)	LAT	degrees
Longitude	XLONG	degrees
Weather data		
Year	IYR	Two digit year
Day of year	DOY	day number
Daily total solar radiation	SOLRAD	MJ m^{-2}
Daily maximum air temperature	TEMPMX	°C
Daily minimum air temperature	TEMPMN	°C
Daily total rainfall	RAIN	mm
Sowing data		
Sowing date	ISOW	day of year
Plant density	PLANTS	plants m^{-2}
Row width	ROWSPC	m
Seeding depth	SDEPTH	cm
Irrigation data		
Irrigation date	IDAY	day of year
Gross irrigation amount	AIRR	mm
Irrigation efficiency	EFFIRR	decimal fraction
Irrigation soil depth	DSOIL	m
Available soil water triggering irrigation	THETAC	percent
Genetic data		
Cultivar number	IVAR	-
Cultivar name	VARTY	-
Phyllochron	PHINT	°C d
Vernalization coefficient	P1V	scaled 0 to 8
Photoperiod sensitivity coefficient	P1D	scaled 0 to 3
Thermal time for grain filling	P5	scaled 0 to 8
Kernel number per stem dry weight	G1	scaled 1 to 6
Potential grain-fill rate	G2	scaled 1 to 6
Optimum tiller growth rate factor	G3	scaled 1 to 6
Soil data		
Soil reflection coefficient	SALB	decimal fraction
Stage 1 soil evaporation coefficient	U	mm
Soil water drainage constant (fraction drained per day)	SWCON	decimal fraction
USDA SCS Runoff curve number	CN2	-
Thickness of soil layer, L	DLAYR(L)	cm
Lower limit of extractable soil water for soil layer L	LL(L)	cm^3 cm^{-3}
Drained upper limit of extractable soil water for layer L	DUL(L)	cm^3 cm^{-3}
Saturated water content for soil layer L	SAT(L)	cm^3 cm^{-3}
Root-distribution weighting factor for soil layer l	WR(L)	-
Initial soil water content for soil layer L	SW(L)	cm^3 cm^{-3}

[1] Some of the units are in non-SI units; these are in the units required by the model input files.

Roots grow down into the profile as a function of daily thermal time and soil water content. The root length density in each soil layer is calculated as a function of root dry weight accumulation and a root weighting function (WR(L), Table 1.4). This is used in determining root water uptake from each layer as a function of soil water content. If the total root water uptake (TRWU) is less than EP1, then EP = TRWU, else the water uptake in each layer is scaled down so that TRWU equals EP1, and so EP = EP1. Soil water deficit factors, which are used to decrease growth, are calculated as functions of EP1 and TRWU. Whenever TRWU < EP1, SWDF1 = TRWU/EP1, and if TRWU/EP1 < 1.5, then SWDF2 = 0.67*TRWU/EP1. The soil water deficit factor, SWDF1, is used for reducing photosynthesis and transpiration; SWDF2 is used to reduce leaf and stem extension growth and tillering. The total evaporation ET is calculated as ES + EP.

1.5.2 Phenology subroutine (PHENOL)

The phenological subroutine of WHV21 was fully described by Ritchie (1991). Essentially, plant development from sowing to physiological maturity is divided into seven stages (Table 1.5). Two extra stages in the model allow for pre-sowing simulation of the soil water balance and grain dry-down to harvest. From sowing to physiological maturity, the main driving force is temperature, but during stage 1 (emergence to terminal spikelet), vernalization, photoperiod and phyllochron also influence the rate of development. Leaves are accumulated in stages 1 and 2, as a function of air temperature and a cultivar specific phyllochron interval.

Zimbabwe winters are mild (average screened-air temperature for May through September at Harare = 16.1°C and at Mid-Save = 18.8°C (Department of Meteorological Services, 1981)), and photoperiod changes minimally during the normal period from sowing to terminal spikelet formation (Figure 1.6). The wheat grown in Zimbabwe is considered typical spring wheat. Therefore, the vernalization subroutines are redundant. Arguably, the photoperiod subroutines are also redundant for the main growing season, because of the small change in photoperiod during typical stage 1 growth, and the latitude

change across the main wheat producing areas of Zimbabwe is only about 3.5°. However, since there may be a need to use the model for assessing wheat production in other seasons, they should remain.

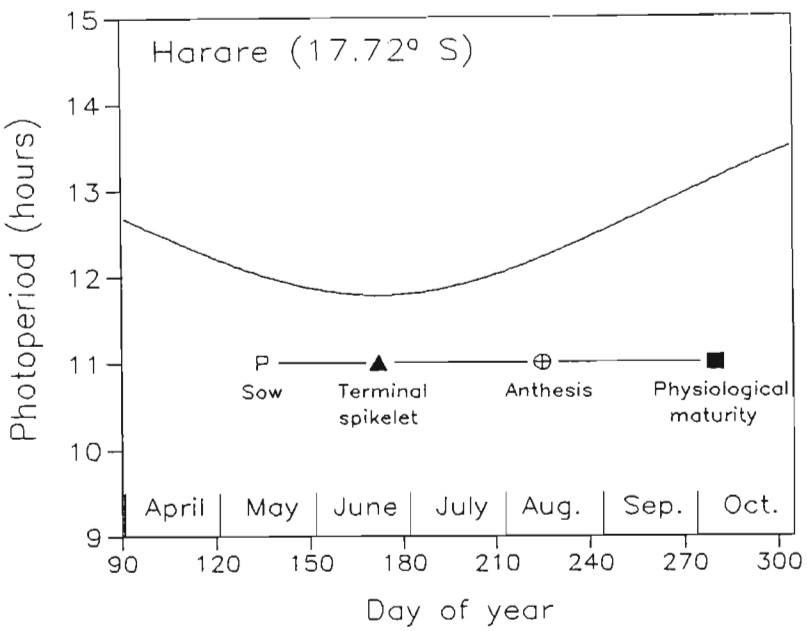

Figure 1.6: Change in photoperiod at Harare, Zimbabwe, during the winter months, and the approximate normal times of sowing, terminal spikelet, anthesis and physiological maturity of wheat.

Table 1.5: Growth stages of wheat as used in WHV21 (from Ritchie, 1991), the equivalent Zadoks growth period (Zadoks, Chang and Konzak, 1974), and the associated thermal time duration and base temperatures (T_b) (from Ritchie, 1991).

CERES Stage	Zadoks Period	Thermal time duration (°C d)	T_b
7	-	Nil	
8	00 - 05	One day, if adequate soil water	
9	05 - 10	40 + 10.2 * SDEPTH	2
1	10 - TS[1]	400 * PHINT / 95	0
2	TS - 39	PHINT * 3	0
3	39 - 59	PHINT * 2	0
4	59 - 61	80	0
	59 - 71	200	0
5	71 - 87	430 + 20 * P5 P5 scaled 1 to 8	1
6	87 - 90	250	1

[1] Terminal spikelet (TS) is not accounted for in Zadoks, Chang and Konzak (1974).

From a farmer's or advisor's point of view, two changes to the phenology subroutine of WHV21 would be beneficial:

1. Leaves in WHV21 are counted at leaf tip appearance. Many herbicides, particularly the hormone type herbicides, are recommended for application between the *emergence* of leaves three and five. Also, in order to determine a leaf tip number, one has to count the number of emerged leaves, anyway. Therefore, the inclusion leaf emergence prediction was considered desirable.
2. Terminal spikelet is not easy for farmers to determine, as it requires the use of a low powered microscope for detection. However, terminal spikelet occurs near the time of first node appearance (Zadoks growth stage 31). This stage is used in Zimbabwe for timing the nitrogen topdressing, and so its prediction, if different in timing from terminal spikelet, would also be useful.

Finally, the duration of growth stages are not influenced by soil water deficits, which may be important in a model for deficit irrigation (see section 1.3.2).

1.5.3 Growth subroutine (GROSUB)

The growth subroutines of the 1983 version of WHV21 were described by Ritchie and Otter (1984). A number of changes in the source code were made for version 2.1, but in essence the processes are the same.

Potential dry matter is calculated as a function of intercepted photosynthetically active radiation (PAR), where PAR is set equal to 0.5 x SOLRAD. The daily potential dry matter production (PCARB, g plant^{-1}) is

$$PCARB = \frac{7.5 \times PAR^{0.6} \times (1 - EXP(-0.85 \times LAI))}{PLANTS} \qquad 1.1$$

The actual rate of dry matter production (CARBO) is usually less than PCARB due to the effects of non-optimal temperature and water stress. CARBO is apportioned between shoots and roots with a growth stage dependent partioning coefficient (PTF) (Table 1.6). In growth stages 2 to 4, the proportion of CARBO

partioned to roots increases slightly under water deficits. Plant biomass is comprised of root dry weight (ROOTWT), leaf dry weight (LFWT), stem dry weight (STMWT) and grain dry weight (GRNWT).

Table 1.6: The proportion of CARBO partitioned to shoot growth (PTF) as a function the soil water deficit factor (SWDF1) prior to grain filling, or as a function of the ratio of the stem weight at anthesis (SWMIN) and current stem weight (STMWT) during grain filling.

CERES stage	PTF
1	0.65
2	0.70 + 0.1 x SWDF1
3	0.75 + 0.1 x SWDF1
4	0.80 + 0.1 x SWDF1
5	0.65 + 0.35 x SWMIN/STMWT

During stage 1, plant leaf area is calculated from the expansion of leaves on the main stem and tillers, as a function of leaf and tiller number, moderated by SWDF2. During growth stage 2, leaf area is accumulated as a function of the proportion of CARBO assigned to leaf growth and the specific leaf area (115 cm^2 g^{-1}). During this latter stage, CARBO is preferentially partitioned to stem and root growth, with the residual partioned to leaf growth. Leaf senescence is coupled with crop phasic development, and is increased by plant water deficits.

In growth stage 1, tillering is an empirical function of leaf number > 2.5 (i.e., essentially dependent on thermal time). During growth stages 2 and 3, tillering (both number and dry weight) is a function of dry matter accumulation, thermal time and a genetic coefficient (G3), moderated by SWDF1. Tiller death may occur in growth stage 1 as a result of cold air temperatures, while tiller senescence due to competition for assimilates and plant water deficits occurs in growth stages 2 and 3. Ritchie and Otter (1984) admit that this section of the model is not reliable in predicting tiller numbers (corroborated by Booysen, 1987), but they state that it does

not cause a serious error in the grain number calculations because the number of tillers growing is controlled by a source-sink balance.

The number of kernels per plant is a linear function of STMWT and a genetic coefficient (G1) at the start of grain filling. The kernel weight is a function of air temperature and the potential grain fill rate (genetic coefficient G2). Plant water deficit has no effect on grain filling except indirectly through a reduction in the assimilate supply during grain filling. Kernel growth rate has been shown to increase under water deficits (see Section 1.3.1.4), but this is not specifically accounted for in CERES-Wheat. Grain yield is the product of plant density, kernels per plant and kernel weight.

1.5.4 Summary

The CERES-Wheat model covers most of the important factors governing plant growth in response to solar radiation, air temperature and soil water, although it certainly is not complete. In the context of its proposed use in deficit irrigation management in Zimbabwe, the model has a number of routines that can be discarded (e.g., COLD, vernalization, snow management), and some areas that may need improvement, such as the modification of phenological development in response to plant water deficits, an improvement in the tillering routines to more accurately match field observations, a more exact relationship between kernel numbers and plant dry weight, and the incorporation of soil water deficit effects on kernel growth rate. The main advantage of the model is that it is widely known and accepted, and the input requirements are readily available. The accuracy, precision and limitations of the output data also needs to be assessed.

2 MATERIALS AND METHODS

Two types of experiments were conducted, viz., sowing date trials and irrigation trials. The sowing date trials consisted of sowing date x cultivar experiments and sowing date x seed rate experiments. These had the basic aim of evaluating wheat response to temperature and, in the case of the seed rate treatments, plant competition. The irrigation trials had the aim of establishing the effects of irrigation timing and soil water dynamics on crop growth and yield. Together, the experiments provided a set of data that could be used for model calibration, modification, and validation. This section describes the general experimental procedures; specific details, additions or variations from these are described in the following chapters. Unless otherwise stated, the following experimental procedures were employed.

2.1 Experimental sites

Experiments were conducted in Zimbabwe over the five year period, 1988 to 1992. The locations of the experimental sites in each year were as follows:

1988 Agricultural Research Trust Farm, Harare (ART)
Rattray Arnold Research Station, Arcturus (RARS)
1989 ART
RARS
Wooler Farm, Glendale (GLEN)
1990 ART
GLEN
Lions Den Estate, Shamva (SHAM)
1991 ART
Doonside Farm, Mutorashanga (BANK)
Victory Estate, Doma (DOMA)
Gunn Estate, Middle Save (SAVE)
1992 ART

Details of these locations are provided in Table 2.1 and Figure 2.1. The ART and RARS locations represented the highveld (altitude > 1200 m), while BANK, DOMA, GLEN and SHAM were

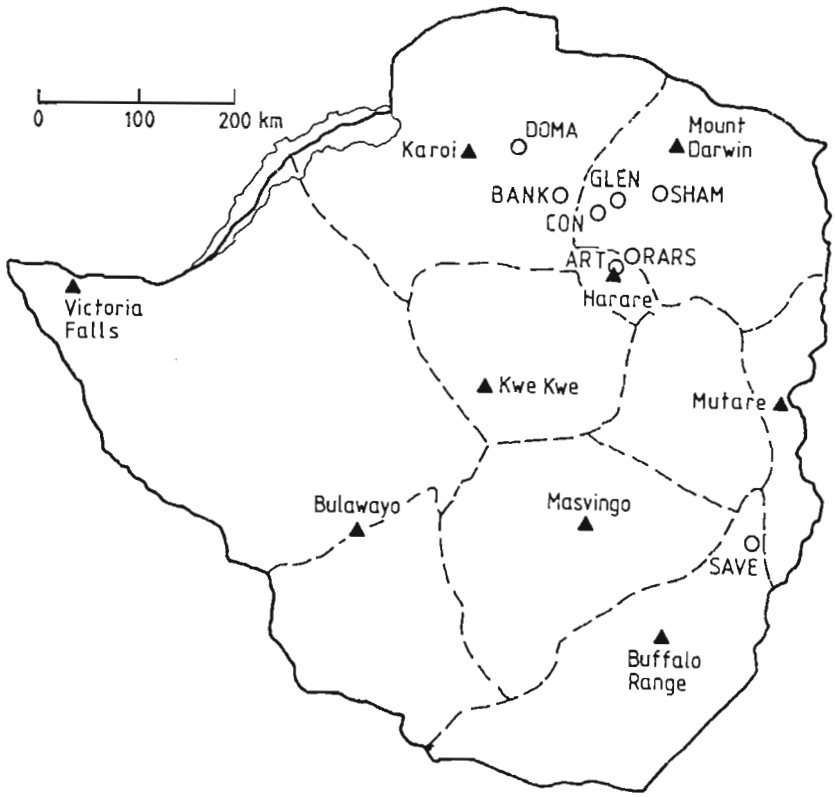

Figure 2.1: Map of Zimbabwe showing the location of experimental sites and Weather Forecast Zones of the Department od Meteorological Services, Government of Zimbabwe (Department of Meteorological Services, 1981).

typical middleveld sites (altitude = 900 to 1250 m), and SAVE was a lowveld site (altitude = 490 m). Air temperatures decrease with increasing altitude, so the cooler sites were ART and RARS and the warmest site was SAVE. At ART and GLEN, different fields were used in each year, due to rotational requirements, but the fields at both sites had similar edaphic characteristics.

Table 2.1: Location, altitude and soil type of sites used for the field experiments.

	ART	BANK	DOMA	GLEN	RARS	SAVE	SHAM
Latitude (S)	17°42′	17°12′	16°49′	17°18′	17°41′	20°10′	17°15′
Longitude (E)	31°03′	30°33′	30°08′	31°03′	31°13′	32°21′	31°33′
Altitude (m)	1500	1200	1100	1150	1360	490	950
Soil family§	5E.2	5G.2	5S.2	5S.2	5E.2	4U.2	5E.2
Soil depth (m)	>1.5	1.5	>1.2	>1.5	>1.5	>1.5	1.5
Soil texture: A	SaC	LSa	SaCL	SaCL	SaCL	SaCL	CL
B	C	SaL	SaC	SaCL	SaC	SaCL	C

§ From Thompson and Purves (1978)

2.2 Meteorological measurements

2.2.1 Air temperature

At each site the daily maximum and minimum screened air temperatures were recorded with mercury thermometers (G.H. Zeal, London). Screens were constructed according to Anon. (1974). The base of the screen was 1.2 m above ground level. The thermometers were read at 08.00 h each day, with the maximum booked back to the previous day and the minimum booked to the day of reading.

At ART Farm, ground-level exposed and screened air temperatures were recorded with Li-COR thermistors connected to a Li-COR LI-1000 data logger during the period 1 October 1989 to 3 September 1991. Hourly mean temperatures and daily maximum, minimum and mean temperatures were recorded.

2.2.2 Solar radiation

Daily solar radiation was measured at ART for the period 1 April, 1986 to 31 March, 1988 with a Li-COR LI-200SA pyranometer connected to a Li-COR LI-1000 data logger. However, instrument problems in later years required the use of radiation data collected by the Department of Meteorological Services at the Harare Kutsaga Experiment Station (25 km from ART). For the period when the datalogger was working at ART, there was close agreement between radiation measured at ART and Kutsaga (ART = 0.974 x Kutsaga, r^2 = 0.983). No radiation data was collected at the other sites. For the ART, GLEN and RARS sites, Kutsaga measured radiation was used, since all these sites are within a radius of 70 km from Kutsaga.

For the SHAM and DOMA sites, the Department of Meteorological Services radiation data from Mount Darwin and Karoi, respectively, were used, as these sites are in close proximity to those weather stations. For the BANK and SAVE sites, the closest Department of Meteorological Services weather stations (Banket and Buffalo Range, respectively) only measured sunshine hours. These data were converted to radiation using the Angström equation (Angström, 1924, cited by Savage,

1980). The *a* and *b* coefficients used were 0.267 and 0.486, respectively, for Banket (BANK) and 0.256 and 0.534, respectively, for Buffalo Range (SAVE). These coefficients were established for the Banket sunshine records from Kutsaga daily sunshine and radiation records for the period 1984 to 1988 (r^2 = 0.829), and for the Buffalo Range sunshine data from Buffalo Range daily sunshine and radiation data for the period 1974 to 1978 (r^2 = 0.900).

The extrapolation of radiation data from point of measurement to nearby sites (< 100 km) within the Department of Meteorological Services Forecast Areas (Figure 2.1; Department of Meteorological Services, 1981) is feasible because these areas have been defined primarily on the basis of similarities in weather conditions, notably, cloud type and frequency, rainfall and air temperature. Furthermore, during the winter months, cloud cover is minimal over large areas of the country.

2.2.3 Weather files

Weather data files for each of the sites were created to conform to the CERES-Wheat v. 2.10 format (IBSNAT, 1986). These files are given on the accompanying diskette, with the file names and period of data given in Table 2.2 (also summarized in the file *WTH.DIR* in sub-directory WEATHER).

2.3 Experimental procedures

2.3.1 Sowing date x cultivar experiments

The sowing date x cultivar experiments consisted of a factorial of five sowing dates x four cultivars at ART 1988 to 1991, RARS 1989, GLEN 1989 and 1990, SHAM 1990, DOMA 1991 and SAVE 1991. Due to land limitations at RARS in 1988, the experiment there consisted of four sowing dates x four cultivars. The treatments were layed out in a split plot design, with sowing dates as main plots and cultivars as sub-plots. This facilitated the sowing and establishment of each sowing date, with little

Table 2.2: Weather files of the sites used in the experiments.

Site	File name	Period of weather data	Source of solar irradiance data
ART	ARTF0112.W86	01/01/1986 to 31/12/1986	Kutsaga and ART
ART	ARTF0112.W87	01/01/1987 to 31/12/1987	ART
ART	ARTF0112.W88	01/01/1988 to 31/12/1988	ART and Kutsaga
ART	ARTF0112.W89	01/01/1989 to 31/12/1989	Kutsaga
ART	ARTF0112.W90	01/01/1990 to 31/12/1990	Kutsaga
ART	ARTF0112.W91	01/01/1991 to 31/12/1991	Kutsaga
ART	ARTF0112.W92	01/01/1992 to 31/12/1992	Kutsaga
BANK	BANK0505.W91	08/05/1991 to 30/09/1991	Banket sun
DOMA	DOMA0506.W91	24/01/1991 to 16/10/1991	Karoi
GLEN	GLEN0506.W89	27/04/1989 to 27/10/1989	Kutsaga
GLEN	GLEN0506.W90	27/04/1990 to 24/10/1990	Kutsaga
RARS	RARS0506.W88	25/04/1988 to 19/10/1988	Kutsaga
RARS	RARS0506.W89	24/04/1989 to 25/10/1989	Kutsaga
SAVE	SAVE0505.W91	27/04/1991 to 04/10/1991	Buffalo Range sun
SHAM	SHAM0506.W90	28/04/1990 to 18/10/1990	Mount Darwin

interference with other sowings. The main plot treatments were arranged in randomised complete blocks with four replicates at ART 1988 to 1991, RARS 1989 and GLEN 1990, and three replicates at other sites. At each site, the treatments were re-randomised.

The sowing dates were nine to 11 days apart starting in late April and ending in early June at each site (Table 2.3). The cultivars were standard adapted Zimbabwean spring wheat cultivars. During 1988 to 1990, the four cultivars were W170/84, Sengwa, Rusape and Angwa. In 1991, Angwa was replaced by a newly released cultivar, Nata, because Angwa was no longer publicly available, and the practical nature of this research required testing the newly available cultivar in response to sowing date. Nata will not be discussed in this thesis. A list of the data sets within the planting x cultivar trials used for calibration and validation of CERES-Wheat is given (Table 2.3). Thirty four data sets were used for modification of the model and 20 for verification.

The sub-plot gross size was eleven rows at 0.3 m spacing by 11 m. In order to estimate field scale yield (FYIELD), the centre three rows by five m (4.5 m^2) was reaped, threshed by hand, winnowed and weighed. The grain water content was determined with a Burrows Digital Moisture Meter on a sample of grain from each plot at the time of weighing and yields were adjusted to 12.5 % water content. Also at the time of harvest,

the number of ears in a 2.0-m length of row (0.6 m^2), sampled from the centre of the plot, was counted. From this a sub-sample of 30 ears was taken and the number of kernels and kernel dry mass (PGRNWT) determined. The kernel number m^{-2} (GPSM) was calculated from the product of the number of kernels per ear and the ear density. The observed yield component-yield (YCYIELD) was calculated as the product of GPSM and PGRNWT.

Two additional rows were sown on the outer edges of each main plot, as border rows. In each sub-plot of 11 rows, the outer single rows were border rows, while rows 2, 4, 8 and 10 were used for sampling plants for leaf area and plant part dry matter determination. For these measurements, above-ground plant samples were harvested at Zadoks growth stage (Tottman and Broad, 1987) 22 at ART 1988, and at growth stages 31, 39, 61, 75 and 87 at ART 1988 and 1989. The date of each growth stage-sample differed for each cultivar and sowing date because of different rates of development. The above-ground plant samples were harvested at ground-level from randomly selected one-m lengths of row (0.3 m^2) from sub-plots within each of the first three replicates. The samples were placed in labelled plastic bags and stored under refrigeration until processed. Usually, the period of storage was less than two days. The plants were divided into leaf blade, leaf sheath, stem, ear and kernel sub-samples. The leaf blade area was measured with an electro-optical system similar to that described by Clarke and McCaig (1985). The sub-samples were dried in a forced-air oven at approximately 80°C for 24 hours and weighed to 0.1 g.

Additional samples were removed from the trials at ART 1989 and 1990, GLEN 1989 and SHAM 1990 for kernel dry mass determination. Ear samples were harvested from randomly selected 0.5-m lengths of row (0.15 m^2) taken from within rows 2, 4, 8 and 10 in each of the first three replicates. Beginning seven to 10 d after GS61, and continuing every five to 10 d through to GS87, the ear samples were removed from the plants, placed in labelled plastic bags, returned to the laboratory, and stored under refrigeration until processing. Usually, the period of storage was less than two days. The total number of kernels in each sample was counted manually. The kernel dry mass was established by drying the kernels in a forced-air oven

at approximately 80°C for 24 hours and weighing the dried sample to within 0.1 g accuracy.

A 2-m length of row in the centre of the plot was selected for taking stem counts at regular intervals through the season. Zadoks growth stages (GS 31, 39, 61, 75 and 87) were recorded on each plot when the majority of plants were considered to be at the specified stage. At all sites in 1988, 1989 and 1990, growth stages double ridge (DR) and terminal spikelet (TS) were determined. Two to three plants from each plot of one replicate were collected at daily to two-daily intervals and examined under a low-powered dissecting microscope to determine the DR and TS growth stages. This was not done at any site in 1991 because the large distance between sites prevented the frequent visits required to collect, dissect and examine plants.

Immediately prior to sowing each main plot, the soil was fertilized (Appendix 1), the fertilizer incorporated with hand hoes, and the planting furrows (20 to 40 mm deep) drawn with hand tools. The seed was sown along the furrows by hand at a seed rate of 100 kg ha^{-1}, and the furrows closed. Irrigation was applied on the same day of sowing and the seasonal schedule of irrigation was fixed to cater for the different sowing dates and site conditions (Appendix 1). In general, the trials were well irrigated, with all sites receiving at least 600 mm irrigation plus rain. At the three to four leaf stage, the plants were topdressed with ammonium nitrate, so that the total amount of N applied was adequate for good growth (Appendix 1).

Table 2.3: List of the sowing date x cultivar trials, their data set number, trial code, calendar date and day of year (DOY) of sowing and use as calibration and revision or validation data sets.

Data set	Site	Year	Trial code	Sowing date Date	DOY	Calibration data set	Independent data set
1	ART	1988	WPDA8810	25 April	116	+	
2			WPDA8820	5 May	126	+	
3			WPDA8830	14 May	135	+	
4			WPDA8840	22 May	143	+	
5			WPDA8850	3 June	155	+	
6	RARS	1988	WPDR8810	26 April	117	+	
7			WPDR8820	9 May	130	+	
8			WPDR8830	22 May	143	+	
9			WPDR8840	3 June	155	+	
10	ART	1989	WPDA8910	24 April	114	+	
11			WPDA8920	5 May	125	+	
12			WPDA8930	15 May	135	+	
13			WPDA8940	24 May	144	+	
14			WPDA8950	3 June	154	+	
15	RARS	1989	WPDR8910	25 April	115		+
16			WPDR8920	5 May	125		+
17			WPDR8930	15 May	135		+
18			WPDR8940	24 May	144		+
19			WPDR8950	3 June	154		+
20	GLEN	1989	WPDG8910	26 April	116	+	
21			WPDG8920	6 May	126	+	
22			WPDG8930	16 May	136	+	
23			WPDG8940	26 May	146	+	
24			WPDG8950	6 June	157	+	
25	ART	1990	WPDA9010	24 April	114	+	
26			WPDA9020	4 May	124	+	
27			WPDA9030	14 May	134	+	
28			WPDA9040	24 May	144	+	
29			WPDA9050	4 June	155	+	
30	GLEN	1990	WPDG9010	26 April	116		+
31			WPDG9020	6 May	126		+
32			WPDG9030	17 May	137		+
33			WPDG9040	26 May	146		+
34			WPDG9050	6 June	157		+
35	SHAM	1990	WPDS9010	27 April	117	+	
36			WPDS9020	6 May	126	+	
37			WPDS9030	16 May	136	+	
38			WPDS9040	26 May	146	+	
39			WPDS9050	6 June	157	+	
40	ART	1991	WPDA9110	25 April	115		+
41			WPDA9120	4 May	124		+
42			WPDA9130	15 May	135		+
43			WPDA9140	25 May	145		+
44			WPDA9150	5 June	156		+
45	DOMA	1991	WPDD9110	25 April	115		+
46			WPDD9120	3 May	123		+
47			WPDD9130	14 May	134		+
48			WPDD9140	24 May	144		+
49			WPDD9150	4 June	155		+
50	SAVE	1991	WPDM9110	26 April	116	+	
51			WPDM9120	6 May	126	+	
52			WPDM9130	18 May	138	+	
53			WPDM9140	27 May	147	+	
54			WPDM9150	6 June	157	+	

2.3.2 Sowing date x seeding rate experiments

The sowing date x seeding rate experiments consisted of a factorial of three sowing dates x four seeding rates at ART 1989 and 1990, GLEN 1989 and 1990 and SHAM 1990. The treatments were layed out in a split plot design, with sowing dates as main plots and seeding rates as sub-plots. The main plot treatments were arranged in randomised complete blocks with four replicates at ART and three replicates at GLEN and SHAM. At each site, the treatments were re-randomised. The cv. Sengwa was used throughout.

The sowing dates were approximately 20 d apart, with the first in late April, the second in mid-May and the last in early June (Table 2.4). The seeding rates were 30, 75, 120 and 165 kg seed ha^{-1} in each trial. These were chosen to give a range in plant densities from 50 to 350 plants m^{-2}. The actual emerged plant densities (Table 2.4) varied from site to site, primarily due to differences in seeding conditions influencing stand establishment. All the data sets in Table 2.4 (fifteen in total) were used for calibration and verification of CERES-Wheat.

The sub-plot gross size was eleven rows at 0.3 m spacing by 11 m. For field yield determination, the centre three rows by five m (4.5 m^2) was reaped, threshed by hand, winnowed and weighed. Yields were standardized to 12.5 % grain water content. To estimate yield components, the same sampling procedure as described in section 2.3.1 was employed. Two additional rows were sown on the outer edges of each main plot, as border strips. In each sub-plot, the outer two rows were discard rows, while rows 3 and 9 were used for sampling plants for dry matter determination. A 2-m length of row in the centre of each plot was used for counting the number of stems at regular intervals through the season.

Immediately prior to sowing each main plot, the soil was fertilized (Appendix 1), the fertilizer incorporated with hand hoes, and the planting furrows (20 to 40 mm deep) drawn with hand tools. The seed was sown along the furrows by hand at the appropriate seed rate and the furrows closed. Irrigation was applied on the same day of sowing and the seasonal schedule of

irrigation was fixed to cater for the different sowing dates and site conditions (Appendix 1). The sowing date x cultivar and sowing date x seeding rate trials were adjacent to one another and so they received the same irrigation regimes. At the three to four leaf stage, the plants were topdressed with ammonium nitrate, so that the total amount of applied N was adequate for good growth (Appendix 1).

Table 2.4: List of the sowing date x seeding rate trials, their data set number, trial code, date of sowing and the emerged plant density relative to each seeding rate.

Data set	Site	Year	Trial code	Sowing date		Seeding rate (kg ha^{-1})			
				Date	DOY	30	75	120	165
						plants m^{-2}			
55	ART	1989	WSRA8910	24 April	114	66	132	208	295
56			WSRA8920	15 May	135	68	127	206	255
57			WSRA8930	3 June	154	47	136	207	248
58	GLEN	1989	WSRG8910	26 April	116	56	122	206	277
59			WSRG8920	16 May	136	51	95	172	262
60			WSRG8930	5 June	156	52	106	200	213
61	ART	1990	WSRA9010	24 April	114	85	169	274	363
62			WSRA9020	14 May	134	70	146	231	367
63			WSRA9030	4 June	155	96	198	277	353
64	GLEN	1990	WSRG9010	26 April	116	74	184	277	332
65			WSRG9020	17 May	137	87	171	229	304
66			WSRG9030	6 June	157	76	185	283	391
67	SHAM	1990	WSRS9010	27 April	117	57	157	234	326
68			WSRS9020	16 May	136	67	154	207	214
69			WSRS9030	6 June	157	65	186	254	341

2.3.3 Irrigation experiments

2.3.3.1 Wheat irrigation timing experiments

These experiments were conducted at ART from 1989 to 1992, GLEN in 1989 and 1990, and BANK in 1991. The trials in 1989 and 1990 all had the same basic five treatment structure, viz., frequent (8 to 10 d interval) irrigations of either 30 or 50 mm, medium frequency (13 to 15 d intervals) irrigations of either 30 or 50 mm, and infrequent (18 to 21 d intervals) irrigations of 50 mm. The BANK 1991 trial also had a similar set of five treatments, but because the soil was sandier than all the other sites, the irrigation intervals were shorter. The trials at ART in 1991 and 1992 included three frequencies of irrigation, but all irrigations after 20 days after sowing (das) were 50 mm. Within each of these irrigation frequencies there were two (1991) or three (1992) times of irrigation termination. The actual dates and amounts of irrigations of each treatment for each site is given (Table 2.5). Detailed site and cultural data is also given (Appendix 1). The allocation of the sites to calibration or validation data sets is given in Table 2.7.

All treatments within a trial site were uniformly irrigated at sowing, emergence, 20 das and 40 das. This was because earlier research by the author had shown the importance of stimulating tillering and nodal root development with the 20 d irrigation. The irrigation treatments described above were imposed after the 40 d irrigation.

The uniform irrigations prior to treatment imposition were applied with overhead sprinklers. The amounts of these irrigations were measured using four rain gauges positioned within the experimental area. The irrigation treatments were applied to 6.0 m x 7.0 m gross plots arranged in randomized complete blocks replicated three times at GLEN in 1989 and 1990, and four times at the other locations. Irrigation treatments were applied with small plot irrigation apparatus (Figure 2.2). These consisted of 4 L h^{-1} drip emitters spaced on a 0.5 m x 0.5 m grid and suspended 1.0 m above the soil over the central 4.0 m x 5.5 m of the plot. Water was delivered to each apparatus via an irrigation line and hose pipe fitted with

a 0.1 MPa pressure regulator and filter. The theoretical water application rate was 16.0 mm h^{-1}, but the actual measured rate averaged 14.5 mm h^{-1}. The close spacing of emmitters enabled complete soil surface wetting. The border of wheat around the irrigated area of each plot served as a boundary between plots and ensured no lateral movement of soil water from one plot to another occurred. This was visually apparent in the field, as the wheat outside the irrigated area showed marked water stress features (short, wilted and dry) in contrast to the wheat in the irrigated area.

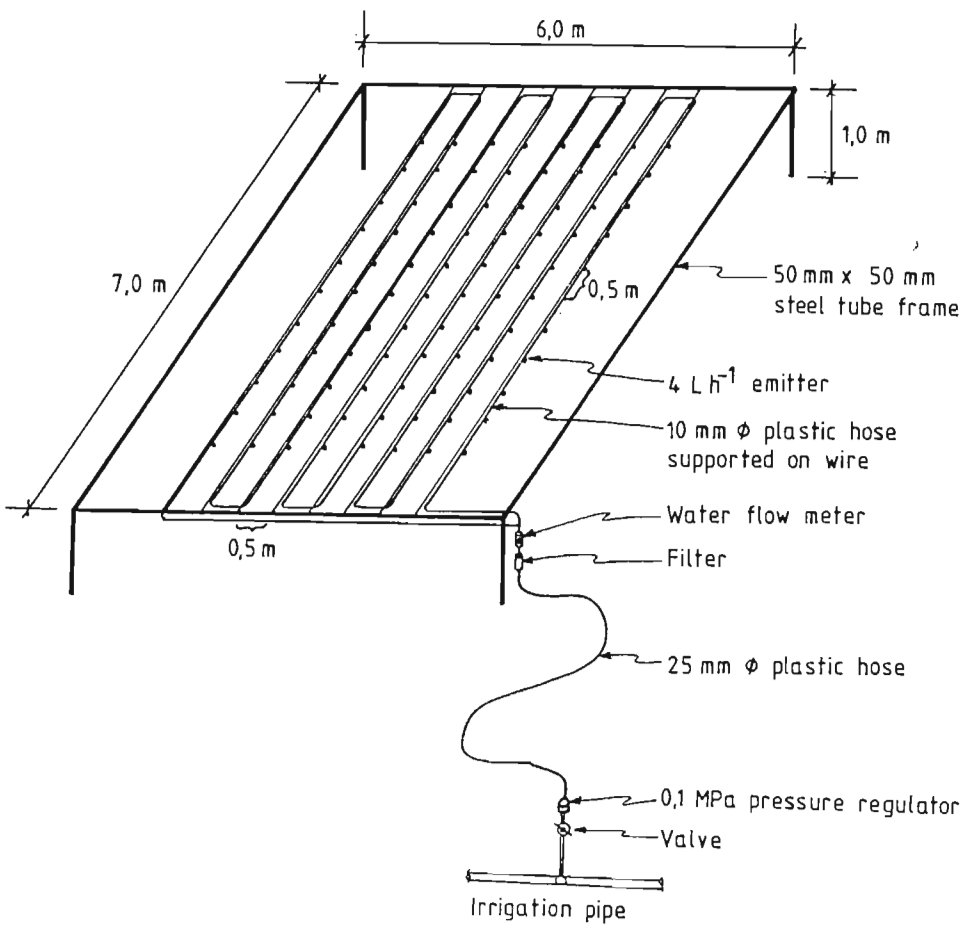

Figure 2.2: Illustration of the small plot irrigation apparatus.

Table 2.5: List of the wheat irrigation timing trials, their data set number, treatment code and associated irrigation dates and amounts.

Data set	Trial code	Treatment															
ART 1989		Irrigation date (das)															
		0	4	20	40	59	70	75	80	90	100	105	110				
		Irrigation amount (mm)															
70	WITA8921	30	16	30	30	30	-	30	-	30	-	30	-				
71	WITA8922	30	16	30	30	50	-	50	-	50	-	50	-				
72	WITA8923	30	16	30	30	30	30	-	30	30	30	-	30				
73	WITA8924	30	16	30	30	50	50	-	50	50	50	-	50				
74	WITA8925	30	16	30	30	50	-	-	50	-	50	-	-				
GLEN 1989		Irrigation date (das)															
		0	5	21	39	52	63	67	73	81	91	95	101				
		Irrigation amount (mm)															
75	WITG8921	57	32	34	30	30	-	30	-	30	-	30	-				
76	WITG8922	57	32	34	30	50	-	50	-	50	-	50	-				
77	WITG8923	57	32	34	30	30	30	-	30	30	30	-	30				
78	WITG8924	57	32	34	30	50	50	-	50	50	50	-	50				
79	WITG8925	57	32	34	30	50	-	-	50	-	50	-	-				
ART 1990		Irrigation date (das)															
		0	5	21	42	58	70	74	80	90	100	105	111				
		Irrigation amount (mm)															
80	WITA9021	31	38	29	31	29	-	30	-	30	-	30	-				
81	WITA9022	31	38	29	30	50	-	50	-	50	-	50	-				
82	WITA9023	31	38	29	30	32	30	-	30	30	30	-	30				
83	WITA9024	31	38	29	30	50	50	-	50	50	50	-	50				
84	WITA9025	31	38	29	30	50	-	-	50	-	50	-	-				
GLEN 1990		Irrigation date (das)															
		0	5	22	42	57	68	72	78	86	97	101	107				
		Irrigation amount (mm)															
85	WITG9021	26	12	31	30	30	-	30	-	30	-	30	-				
86	WITG9022	26	12	31	30	50	-	50	-	50	-	50	-				
87	WITG9023	26	12	31	30	30	30	-	30	30	30	-	30				
88	WITG9024	26	12	31	30	50	50	-	50	50	50	-	50				
89	WITG9025	26	12	31	30	50	-	-	50	-	50	-	-				
BANK 1991		Irrigation date (das)															
		0	3	20	41	52	61	65	70	79	89	93	95	103	107	111	119	121
		Irrigation amount (mm)															
90	WITB9111	45	25	25	25	30	-	30	-	30	-	30	-	-	30	-	-	30
91	WITB9112	45	25	25	25	50	-	43	-	43	-	43	-	-	43	-	-	43
92	WITB9113	45	25	25	25	-	43	-	-	43	-	-	43	-	-	43	-	-
93	WITB9114	45	25	25	25	30	30	-	30	30	30	-	30	30	-	30	30	-
94	WITB9115	45	25	25	25	50	43	-	43	43	43	-	43	43	-	43	43	-
ART 1991		Irrigation date (das)															
		0	5	21	42	52	62	72	77	82	92	102	107	112	122			
		Irrigation amount (mm)															
95	WITA9111	50	30	30	30	-	50	-	50	-	50	-	50	-	-			
96	WITA9112	50	30	30	30	-	50	-	50	-	50	-	50	-	50			
97	WITA9113	50	30	30	30	-	50	-	-	50	-	50	-	-	50			
98	WITA9114	50	30	30	30	-	50	-	-	50	-	50	-	-	-			
99	WITA9115	50	30	30	30	50	50	50	-	50	50	50	-	50	-			
100	WITA9116	50	30	30	30	50	50	50	-	50	50	50	-	50	50			
ART 1992		Irrigation date (das)															
		0	6	19	39	51	61	71	74	81	91	101	105	112	122	132		
		Irrigation amount (mm)															
101	WITA9211	61	61	50	50	50	50	50	-	50	50	50	-	50	50	50		
102	WITA9212	61	61	50	50	50	50	50	-	50	50	50	-	50	50	-		
103	WITA9213	61	61	50	50	50	50	50	-	50	50	50	-	50	-	-		
104	WITA9214	61	61	50	50	-	50	-	-	50	-	50	-	-	50	-		
105	WITA9215	61	61	50	50	-	50	-	-	50	-	50	-	-	-	-		
106	WITA9216	61	61	50	50	-	50	-	-	50	-	-	-	-	-	-		
107	WITA9217	61	61	50	50	-	50	-	50	-	50	-	50	-	50	-		
108	WITA9218	61	61	50	50	-	50	-	50	-	50	-	50	-	-	-		
109	WITA9219	61	61	50	50	-	50	-	50	-	50	-	-	-	-	-		

One apparatus was assigned to each replicate and was positioned on a plot during treatment application. When not in use the apparatus were stationed outside the experimental area. In 1989, the water application amount was controlled by the duration of time required to apply the specified irrigation amount. In 1990, water flow meters were connected to each apparatus to enable more precise application of water.

The cv. Sengwa was used throughout the experiments in 1989 and 1990. For the trials conducted in 1991 and 1992, the cv. W170/84 was used. A seeding rate of 100 kg ha^{-1} was used throughout. Seed was sown by a small plot drill in 200 mm rows.

The gross plot size was 30 rows (6.0 m) x 7.5 m long (45 m^2). The outer six rows and the end 1.75 m of each row were considered as border rows and no measurements were taken from this part of the plot. Zadoks growth stages (GS 31, 39, 61, 75 and 87) were assessed in the central portion of the plot. Stem counts were carried out regularly in a permanent 2.0-m length of row near the centre of the plot. In all the trials at ART, but not at other sites, rows 7, 8, 9, 22, 23 and 24 were used for sampling plants for plant part dry matter determination. At harvest maturity, yield components were determined from a count of ears in a central 0.4 m^2 area, and the number and dry mass of kernels recorded from 30 selected ears. The yield calculated from yield components (YCYIELD) was computed as the product of the kernel number m^{-2} and the kernel dry mass. The central 10 row (2.0 m) x 4.0 m portion of the gross plot was reaped and threshed by hand and weighed to give a measure of field grain yield (FYIELD). The grain water content was determined with a Burrows Digital Moisture Meter on a sample of grain from each plot and yields were adjusted to 12.5 % water content.

Plant part dry matter was determined by harvesting all plants in a randomly-selected 1-m length of row (0.2 m^2) in each replicate at growth stages 39, 61, 75 and 87. The plant samples were processed as described in section 2.3.1. Similarly, kernel dry mass samples were harvested from randomly-selected 1-m lengths of row at approximately 10-d intervals starting 10 d after growth stage 61. These samples were harvested and processed as described in section 2.3.1.

An aluminium neutron probe access tube was placed in the

centre of each plot to a depth of 1.6 m prior to sowing. At frequent intervals the volumetric soil water content was mesured with a neutron probe (CPN Model 503DR Hydroprobe) at 0.25 m depth increments to 1.25 m. The neutron probe was calibrated with data collected from ART, RARS, GLEN and another experimental site at Concession (the regression comprised 252 data pairs; r = 0.913; calibration range of 0.093 to 0.410 $m^3 m^{-3}$). The water content of the top 0.125 m soil layer was determined gravimetrically and converted to a volumetric water content by multiplying by the field determined bulk density (Appendix 1).

2.3.3.2 Wheat irrigation dry down experiments

A set of experiments was conducted to determine the effect of severe water deficit stress on wheat water use and yield. These were referred to as dry down experiments because the wheat was irrigated adequately up to a particular growth stage but thereafter no further irrigation was applied, so the wheat dried the soil to a low water content. These experiments were conducted at ART 1989 and 1990, GLEN 1989 and 1990, and BANK 1991. The treatments varied from site to site (Table 2.6) and the allocation of the treatments to calibration or validation data sets is given in Table 2.7.

At ART 1989, there were six treatments, each applied to a large, unreplicated uniform soil area (0.16 ha). Four neutron probe access tubes were placed after sowing in the central area of each of the treatments. Irrigation was applied with overhead sprinkler irrigation, and the amount of irrigation applied measured with four rain guages located within the field. Field yield, adjusted to 12.5 % kernel water content (FYIELD) was assessed from four, 5 m x 5 m randomly selected harvested areas. Yield components were determined as described in section 2.3.3.1.

At the other sites, each treatment was applied to four small plots measuring 6 m x 7.5 m. These plots were adjacent to one another, and because treatments were not being compared *per se*, but rather the effect of water regime on each individual treatment was being evaluated, no randomization was considered

necessary. These treatments received their emergence and 21 d irrigations from overhead sprinklers, but all other irrigations were applied with the plot irrigation apparatus described in Section 2.3.3.1. Neutron probe access tubes were placed in the centre of each plot after sowing, and soil water content measurements were taken at frequent intervals using the probe and method described in Section 2.3.3.1. At harvest maturity, a central net plot of 2 m x 4 m was harvested, threshed, weighed and the kernel water content measured for field yield (FYIELD) estimation. Stem counts, growth stages and yield components were determined as in Section 2.3.3.1. The yield component yield was calculated as described in section 2.3.3.1.

Table 2.6: List of the wheat irrigation dry down trials, their data set number, treatment code and associated irrigation dates and amounts.

Data set	Trial code	Treatment							
ART 1989		Irrigation date (das)							
		0	3	19	41	55	69	81	93
		Irrigation amount (mm)							
110	WDDA8921	30	15	-	-	-	-	-	-
111	WDDA8922	30	15	22	-	-	-	-	-
112	WDDA8923	30	15	22	32	-	-	-	-
113	WDDA8924	30	15	22	36	47	48	-	-
114	WDDA8925	30	15	22	31	45	55	37	28
GLEN 1989		Irrigation date (das)							
		0	5	21	39	51	64		
		Irrigation amount (mm)							
115	WDDG8921	50	25	30	-	-	-		
116	WDDG8922	50	25	30	30	50	50		
ART 1990		Irrigation date (das)							
		0	5	21	42	57	69		
		Irrigation amount (mm)							
117	WDDA9021	36	38	24	-	-	-		
118	WDDA9022	36	38	24	30	50	50		
GLEN 1990		Irrigation date (das)							
		0	5	22	41	56	66		
		Irrigation amount (mm)							
119	WDDG9021	26	12	31	-	-	-		
120	WDDG9022	26	12	31	30	50	50		
BANK 1991		Irrigation date (das)							
		0	3	20	41	52	61	70	
		Irrigation amount (mm)							
121	WDDB9111	45	25	25	25	-	-	-	
122	WDDB9112	45	25	25	25	50	45	45	

Table 2.7: Calibration and validation data set allocation in the irrigation timing and dry down trials.

Site	Year	Data set numbers	Calibration	Validation
Wheat Irrigation Timing trials				
ART	1989	70 to 74	+	
GLEN	1989	75 to 79		+
ART	1990	80 to 84		+
GLEN	1990	85 to 89	+	
BANK	1991	90 to 94		+
ART	1991	95 to 100		+
ART	1992	101 to 109	+	
Wheat Irrigation Dry Down Trials				
ART	1989	110 to 114	+	
GLEN	1989	115 to 116	+	
ART	1990	117 to 118		+
GLEN	1990	119 to 120		+
BANK	1991	121 to 122		+

2.4 CERES-Wheat formatted experiment data files

Data files, conforming in content to the IBSNAT (1986) format, were created for each experimental series (i.e., sowing date x cv., sowing date x seeding rate and irrigation trials). Because of the large number of data sets, the file names were modified slightly to enable easy identification of site, year and treatment. This section summarises the data files for each experimental series. The data files are available in ASCII format in the appropriately named (see below) subdirectories on the accompanying diskette.

2.4.1 Wheat sowing date x cultivar trials

The suite of 11 sowing date x cv. experiments for each cv. is summarised in the file *WHEXPPDm.DIR*, where *m* is the cv. number (1 = W170/84; 2 = Sengwa; 3 = Rusape; 4 = Angwa). In order to use one of these files with CERES-Wheat (WHV21.exe), the chosen experiment-cv. file name must be changed to *WHEXP.DIR*.

Within the *WHEXPPDm.DIR* file is a list of each input file related to each sowing date experiment, relevant to cv. *m*. Some

of these files are redundant, viz., FILE 4, FILE 7, FILE A and FILE B. These are named *JUNK0000.WH4(7,A or B)* and are common to all *WHEXPSDm.DIR* files. The important files are FILE 5, FILE 6 and FILE 8, and these are named for each data set-cv. treatment as follows:

WPD$YYnm.WHx,

where *$* represents the site code, which is the first letter of the site mnemonic, except SAVE, which has the code M for Mid-Save. The year of the experiment is defined by a two-digit code, *YY*. The sowing date within each experiment is defined by *n* (0 = all sowings, or 1 = 1st, 2 = 2nd, etc. sowing), while *m* is the cv. (note, *m* = 0 indicates file refers to all cvs.), and *x* is the FILE no. In some cases, *m* = 0 to indicate that the file applies to all cultivars (e.g., this is used with files 5 and 6). All these files are located in the subdirectory *WPDXCV* on the accompanying diskette.

Although FILES 5 and 6 are given, they were not used in the calibration and verification of CERES-Wheat under well watered conditions. Thus, the irrigation switch (IIRR) in FILE 8 was set to 4, indicating that there was no water stress and the water balance was not used. This is justified because the sowing date experiments were well irrigated (Appendix 1). The plant density of each sowing date-cv. combination was obtained from plant counts 14 das, and are the mean of the number of replicates in each experiment. The row spacing was set at 0.3 m, and the seeding depth at 20 mm in each FILE 8.

2.4.2 Sowing date x seeding rate experiments

The file *WHEXPSR.DIR* was created to contain the list of input files for all the sowing date x seeding rate experiments. In order for CERES-Wheat to run, this file must be renamed to *WHEXP.DIR*. Files 4, 7, A and B were named *JUNK0000.WHx* and are common to all experiments as described in Section 2.4.1. To identify each experiment, the file names for file nos. 5, 6 and 8 were coded *WSR$YYnp.WHx*, where *$* represents the site, coded as described in Section 2.4.1, *YY* is the year of experiment, *n* is the sowing date (0 = all sowings, or 1 = 1st, 2 = 2nd, 3 = 3rd sowing), and *p* is the seeding rate (0 = inclusive of all

seeding rates, or 1 = 30 kg ha^{-1}; 2 = 75 kg ha^{-1}; 3 = 120 kg ha^{-1}; and 4 = 165 kg ha^{-1}) and *x* represents the file number. All these files are located in subdirectory *WPDXSR* on the accompanying diskette.

As described in Section 2.4.1, files 5 and 6 are provided, but were not used. The plant densities associated with each treatment in each FILE 8 were obtained from the average plant counts at 14 das (Table 2.4). The row spacing was set at 0.3 m, and the seeding depth at 20 mm in each FILE 8.

2.4.3 Irrigation experiments

Files 5, 6 and 8 were created for each Irrigation Timing experiment listed in Table 2.5. The file names have the following syntax:

WIT$YYmi.WHx,

where *$* represents the site code (as above), *YY* is the year of the experiment, *m* is the cultivar (1 = W170/84, 2 = Sengwa), *i* = the treatment number (if *i* = 0, then file refers to all treatments in the experiment), and *x* is the file no. In each file 5, the initial soil water conditions for each layer were obtained from gravimetric and neutron probe measurements taken prior to sowing. The **.WH6* files were based on the dates and amounts of irrigation given in Table 2.5. Plant density data required for the **.WH8* files were obtained from average plant counts 14 das. Seeding depth was set at 25 mm and row width 0.2 m for all treatments. The file *WHEXPWIT.DIR* contains the list of files oppropriate to each experiment. For CERES-Wheat, this must be renamed *WHEXP.DIR*. All these files are located in subdirectory *IRRIG* on the accompanying diskette.

The files for the Irrigation Dry Down experiments were created similarly to those for the Irrigation Timing experiments. File names have the following syntax:

WDD$YYmi.WHx.

For the **.WH5* files, initial soil water contents were estimated from the adjacent Irrigation Timing trials, because no pre-sowing mesurements of soil water were taken owing to the neutron probe access tubes only being installed after sowing. Irrigation dates and amounts were obtained from Table 2.6, and

plant densities were obtained from average plant counts 14 das. The file *WHEXPWDD.DIR* contains the list of files appropriate to each experiment. For CERES-Wheat, this file must be renamed *WHEXP.DIR*. All these files are located in the subdirectory *IRRIG* on the accompanying diskette.

2.4.4 Soil profile properties

The file *SPROFILE.WH2* contains a list of all the soil profiles used in the irrigation trials. The inputs SALB, U, and SWCON were estimated from the soil surface colour, texture and estimated permeability, respectively (Table 2.8). The drained upper limits, lower limits and saturated soil water contents for each soil were estimated by studying the *in situ* changes in soil water content through the season. Drained upper limits were estimated from soil water measurements two to three days after early season irrigations, while lower limits were estimated from soil water measurements at the end of the season. The Irrigation Dry Down experiments were mostly used for determining the lower limits. Although laboratory measured soil water retention data were obtained for some of the soils (Appendix 1), these were only helpful in estimating the saturated soil water contents, as there was little agreement between field observed upper and lower limits and soil water retention at -0.10 and -1.5 MPa, respectively. This concurs with the observations of Ritchie (1981b).

Table 2.8: Estimated SALB, U, SWCON and the total drained upper limit (TDUL), total lower limit (TLL) and total plant extractable soil water (TESW) for each 1.375 m soil profile used in the irrigation experiments.

Site	Year	SALB	U	SWCON	TDUL	TLL	TESW
			cm		$m^3\ m^{-3}$		
ART	1989	0.13	5	0.50	0.378	0.262	0.116
ART	1990	0.13	5	0.50	0.417	0.295	0.122
ART	1991	0.13	5	0.50	0.359	0.244	0.115
ART	1992	0.13	5	0.50	0.352	0.199	0.153
BANK	1992	0.20	3	0.65	0.209	0.110	0.099
GLEN	1989	0.14	4	0.55	0.252	0.129	0.123
GLEN	1990	0.14	4	0.55	0.257	0.156	0.101

3 VALIDATION OF CERES-WHEAT VERSION 2.10

One of the important requirements to be met before a crop simulation model can be employed for decision making is, *inter alia*, to verify that the model is technically correct for the given task (Rasmussen, 1991). Models are, however, by their very nature simplifications of the real world, and therefore the "technical correctness" of a model is hard to define or affirm. The process of evaluating the suitability of a model for a given task has been termed validation and may be defined as the "comparisons of predictions of a verified model with experimental observations other than those used to build and calibrate the model, and the identification and correction of errors in the model until it is suitable for its intended purpose" (Whisler *et al.*, 1986). This definition clearly states the need for independent data sets on which to validate models, a view held by all rigorous modellers. It also encompasses the evolutionary nature of modelling and the need or opportunity for continual improvement of model content and performance. This chapter deals with the validation of CERES-Wheat version 2.10 (WHV21) on independent data sets of well-watered (Table 2.3) and deficit irrigated (Table 2.7) wheat and thereby points to areas of required improvement for application in Zimbabwe.

3.1 Evaluation of model performance

For evaluating model performance against observed data, the procedures described by Willmott (1982) were followed. From a set of n pairs of observed (O) and predicted (P) data, the following indices were computed:

Mean absolute error (MAE):

$$MAE = n^{-1} \sum_{i=1}^{n} |P_i - O_i| \qquad 3.1$$

Index of agreement (IoA):

$$IoA = 1 - \left[\sum_{i=1}^{n} (P_i - O_i)^2 \Big/ \sum_{i=1}^{n} (|P'_i| + |O'_i|)^2 \right], \quad 0 \le IoA \le 1, \qquad 3.2$$

where

$$P'_i = P_i - \overline{O}, \quad 3.3$$

and

$$O'_i = O_i - \overline{O}. \quad 3.4$$

Mean square error (MSE):

$$MSE = MSEs + MSEu, \quad 3.5$$

where MSEs = systematic mean square error and MSEu = unsystematic mean square error, and are defined as:

$$MSEs = n^{-1} \sum_{i=1}^{n} (\hat{P}_i - O_i)^2, \quad 3.6$$

$$MSEu = n^{-1} \sum_{i=1}^{n} (P_i - \hat{P}_i)^2, \quad 3.7$$

and

$$\hat{P}_i = a + bO_i, \quad 3.8$$

where a is the intercept and b the slope of the least-squares regression of P_i on O_i. The correlation coefficient, r, was computed from the least-squares regression of P_i on O_i.

3.2 Validation of CERES-Wheat version 2.10 under well-watered conditions

3.2.1 Determination of genetic coefficients

The WHV21 model requires seven genetic coefficients (Table 1.4). Although guidelines exist for choosing these (Godwin *et al.*, 1989), iteration is required to refine them for a particular data set. The calibration data set (Table 2.3) was thus used to iteratively select genetic coefficients for the four cultivars used in this study, *viz.*, W170/84, Sengwa,

Rusape and Angwa. These were applied to the independent data set (Table 2.3) for validation of model performance. Because the model source code was not altered during this exercise, some iteration was also performed with the independent data set, so as to achieve the best possible correlation between predicted and observed data for the selected phenotypic and yield component variables.

The process of iteration involved, firstly, the refinement of phasic development and secondly, the refinement of yield components, with the objective of equating the average observed and predicted variables. The vernalization and photoperiod coefficients (P1V and P1D, respectively) were set to zero, because, firstly, the cultivars used were considered spring types and therefore required little or no vernalization, and secondly, although the cultivars may be sensitive to photoperiod, the change in photoperiod over the typical sowing dates and wheat growing areas in Zimbabwe are minimal (see Figure 1.6). Summerfield *et al.* (1991) stated that in photoperiod sensitive genotypes maintained in a given constant photoperiod, the rate of progress towards flowering is a linear function of temperature. Thus, the duration of pre-anthesis phasic development was adjusted only with PHINT.

The duration of grain-filling was adjusted with coefficient P5. The WHV21 model allows P5 to vary between zero and nine, but all cultivars in this study required P5 greater than nine. The input routines in subroutine IPVAR (Table 1.2) were therefore modified to allow input of P5 > nine. The chosen genetic coefficients are given (Table 3.1).

Godwin *et al.* (1989) reported P5 values of thirty cultivars in the range 2.0 to 6.0. The large P5 coefficients for the cultivars in this study suggests either a longer grain-filling period or a difference in measurement procedures for wheat in Zimbabwe than for those cultivars in the USA. The average period from anthesis to physiological maturity of the four cultivars in this study was ca. 50 d (from Table 3.1). Mashiringwani and Schweppenhauser (1992) noted relatively long grain-fill durations (40 to 54 d) for wheat cultivars in Zimbabwe, as did van Keulen and de Milliano (1984) for spring wheat in Zambia. The similarities of these reports with the

observations of this study suggest that the actual grain-fill duration rather than measurement errors are the reason for the high P5 coefficients. McMaster, Wilhelm and Morgan (1992), working with winter wheat in Britain, reported grain-fill durations of about 15 d shorter than the mean in this study.

The duration of grain-filling is temperature dependent (Sofield, *et al.*, 1977), which may account for the differences in the time durations quoted above, but the model should account for this. Genetic variability for the duration of grain filling has been reported (Bruckner and Frohberg, 1987). Mashiringwani and Schweppenhauser (1992) noted that genotypes with specific adaptation to cool environments had a low grain filling rate but a long duration of grain filling. The apparent longer grain-filling period of wheat in Zimbabwe may therefore be due to genetic differences, particularly since the majority of wheat breeding occurs on the cool highveld.

For the yield component data, the first genetic coefficient set was G1, the potential number of kernels per plant, which gives the number of grains m^{-2} (GPSM) when multiplied by PLANTS. From the first approximation of GPSM with an estimated coefficient, $G1_{est}$, G1 was calculated from the average observed and predicted GPSM data, $GPSM_o$ and $GPSM_p$, respectively, as follows:

$$G1 = G1_{est} \times GPSM_o / GPSM_p . \qquad 3.8$$

The G3 coefficient, which determines tiller production and ear density (TPSM), was the next coefficient set. Once a reasonable agreement between observed and predicted TPSM was obtained, G2 was adjusted to improve the prediction of kernel mass (PGRNWT).

Table 3.1: Genetic coefficients used in the validation of CERES-Wheat v. 2.10 under well-watered conditions.

	Cultivar			
Coefficient	W170/84	Sengwa	Rusape	Angwa
PHINT (°C d)	136	112	120	105
P1V	0.0	0.0	0.0	0.0
P1D	0.0	0.0	0.0	0.0
P5	16.6	19.0	16.2	15.8
G1	4.6	5.2	4.8	4.8
G2	2.1	0.8	2.2	2.0
G3	4.2	2.9	3.5	2.7

3.2.2 Phasic development

The statistical results of the performance of WHV21 are given (Table 3.2), while the raw data are appended (Appendix 2). The average predicted time from sowing to growth stages TS, 39, 61 and 87 were in close agreement for each cultivar, with the mean absolute error (*MAE*) mostly within 10% of the observed average and the index of agreement (*IoA*) was greater than 0.7 for all cultivars and growth stages, except TS and 87 in Angwa. However, in all but one (TS in W170/84) case, the systematic mean square error (*MSEs*) comprised a large proportion of the total mean square error (*MSE*), indicating that the model produced biased estimates of phasic develoment. This was also evidenced by slopes (*b*) less than one and positive y-intercepts (*a*). This is illustrated for cultivar W170/84 (Figure 3.1).

These results therefore showed that WHV21 was overestimating phase duration in the warmer environments where actual phasic development was fast and underestimating phase duration in the cooler environments where actual phasic development was slow. Whether this anomaly was due wholly to setting the P1D

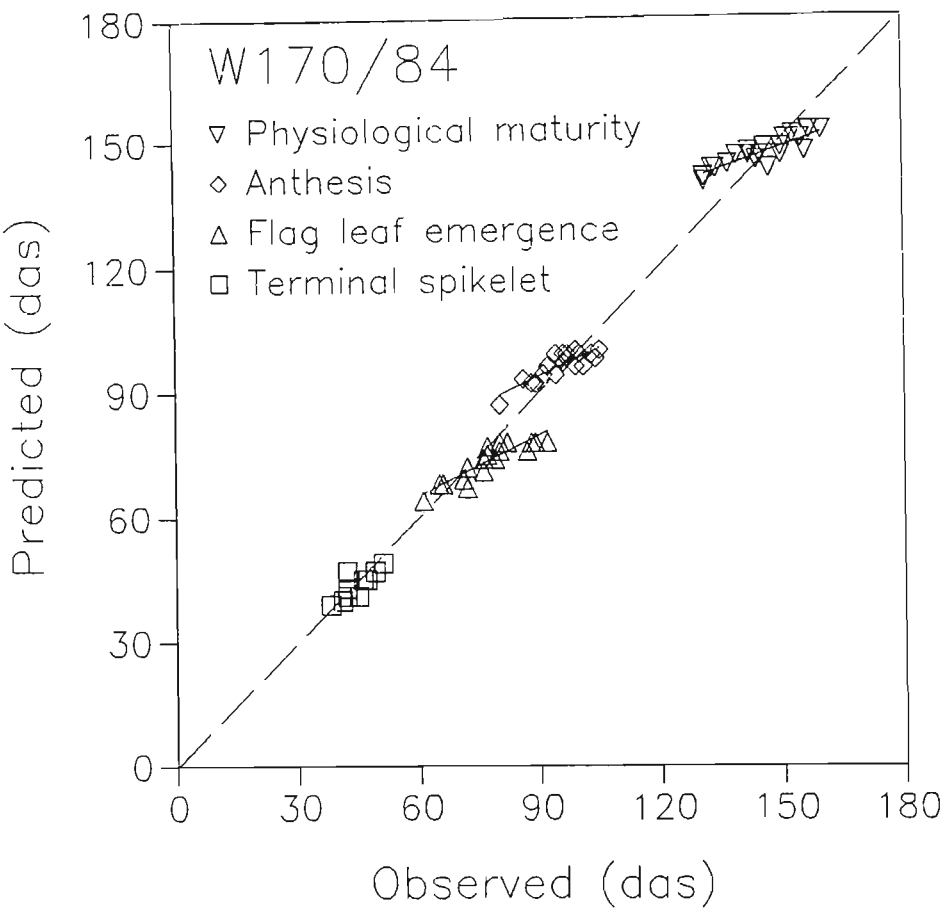

Figure 3.1: Predicted *versus* observed days after sowing (das) to four growth stages in cultivar W170/84 simulated by the original CERES-Wheat version 2.10 model on the well-watered validation data sets.

coefficient to zero and assuming photoperiod insensitivity for all cultivars is doubtful. Photoperiod changes over the range of sowing dates and sites were minimal in comparison to temperature differentials. To illustrate: firstly, the photoperiod change at ART from a 26 April sowing to a 6 June sowing is only 27 min and a cultivar would have to be extremely sensitive for development to be markedly hastened purely due to the photoperiod changes. The modelled change in relative development rates between the two sowings given above for a sensitive cultivar (P1D = 3) is 0.04, while that of an insensitive cultivar (P1D = 1) is 0.01. Secondly, the difference in photoperiod between the warmest site (DOMA) and the coolest site (ART) for a given sowing date was minimal (e.g., for a 26 April sowing, the photoperiod difference between ART and DOMA is only 1.2 min), whereas the relative

Table 3.2: The performance of CERES-Wheat version 2.10 in predicting phasic development of four cultivars under well watered conditions.

	Growth stage			
Parameter	TS	39	61	87
W170/84				
$\bar{O}$	44	78	96	145
$\bar{P}$	44	74	96	146
MAE	2.0	4.6	3.5	5.3
IoA	0.88	0.78	0.83	0.74
MSEs	1.91	30.81	13.39	34.56
MSEu	3.89	4.34	2.91	2.59
MSE	5.80	35.15	16.30	37.15
b	0.672	0.487	0.447	0.341
a	13.9	36.1	53.6	96.9
r	0.791	0.881	0.864	0.880
n	10	20	20	20
Sengwa				
$\bar{O}$	33	63	83	139
$\bar{P}$	37	61	82	138
MAE	3.1	3.6	3.6	5.1
IoA	0.74	0.87	0.86	0.74
MSEs	12.75	14.36	15.95	28.36
MSEu	2.65	2.94	3.76	3.74
MSE	15.40	17.30	19.71	32.10
b	0.611	0.553	0.516	0.341
a	16.2	26.3	38.7	90.5
r	0.837	0.919	0.894	0.814
n	10	20	20	20
Rusape				
$\bar{O}$	36	67	88	138
$\bar{P}$	39	66	87	139
MAE	3.9	4.4	4.5	5.8
IoA	0.74	0.84	0.82	0.72
MSEs	17.70	22.41	25.23	36.46
MSEu	2.20	2.24	1.92	3.19
MSE	19.90	24.65	27.15	39.65
b	0.500	0.472	0.430	0.319
a	21.2	33.7	48.9	94.6
r	0.869	0.933	0.933	0.846
n	10	20	20	20
Angwa				
$\bar{O}$	31	61	79	133
$\bar{P}$	35	57	76	132
MAE	4.0	4.5	5.0	7.1
IoA	0.68	0.80	0.81	0.67
MSEs	19.10	27.35	31.77	55.48
MSEu	2.90	2.15	2.63	3.02
MSE	22.00	29.50	34.40	58.50
b	0.522	0.527	0.480	0.280
a	18.5	24.8	37.92	94.3
r	0.810	0.935	0.931	0.852
n	10	10	10	10

temperature differences are greater (e.g., for the 40 d period beginning 26 April, DOMA accumulated 714°C d, whereas ART accumulated 624°C d). Finally, this observed bias was not consistent from phase to phase but was exaggerated with each successive phase (i.e., *MSEs* increased relative to *MSE* and *b* decreased with each successive phase). Therefore, the bias was not only due to an error in estimating TS, but indicates that the thermal time durations of all the growth stages were at fault, and needed improvement.

3.2.3 Ear density, yield components and yield

Scatter plots of the predicted and observed yield components and yield data are given (Figure 3.2). The statistical results of the performance of WHV21 in predicting ear density and yield components are given (Table 3.3), while the raw data are appended (Appendix 2). The WHV21 model was generally poor in predicting final TPSM and GPSM, as indicated by low and, in some cases, negative *r* and high *MSE*. This may have been partly due to the narrow range of observed data. There was good agreement between predicted and observed PGRNWT, as shown by high *IoA* and *r* (> 0.7) and low *MSE*. For PGRNWT in Sengwa, Rusape and Angwa, *MSEs* was a low percentage of *MSE* (less than 50 %), whereas in W170/84, the *MSEs* was a much larger percentage of *MSE* (70 %).

Yield, calculated from the product of GPSM and PGRNWT (YCYIELD), was poorly predicted (low *IoA* and *r*), although, on average, there was reasonable accuracy, with the *MAE* within 15 % of $\bar{O}$. However, when the predicted YCYIELD was adjusted to 12.5 % grain water content to give an estimate of predicted field yield (FYIELD) and then compared with actual field-measured yield, the correlation between predicted and observed data was even poorer and *MAE* a greater percentage of observed FYIELD. These poor correlations between predicted and observed yield are mostly accounted for by the inadequate prediction of GPSM and errors in measured GPSM, although variation in predicted PGRNWT and errors in measured kernel mass no doubt also played a role, albeit a lesser one. On the whole, the variability of the measured yield, GPSM and PGRNWT was low

(coefficients of variation < 19 %, data not shown), and though not discounting this variabilty, it was concluded that improvements in the functions used to predict GSPM and PGRNWT were warranted. Field-measured yield was consistently lower than yield calculated from measured yield components. This is a feature of most studies and therefore needs to be incorporated into the model estimates of field yield.

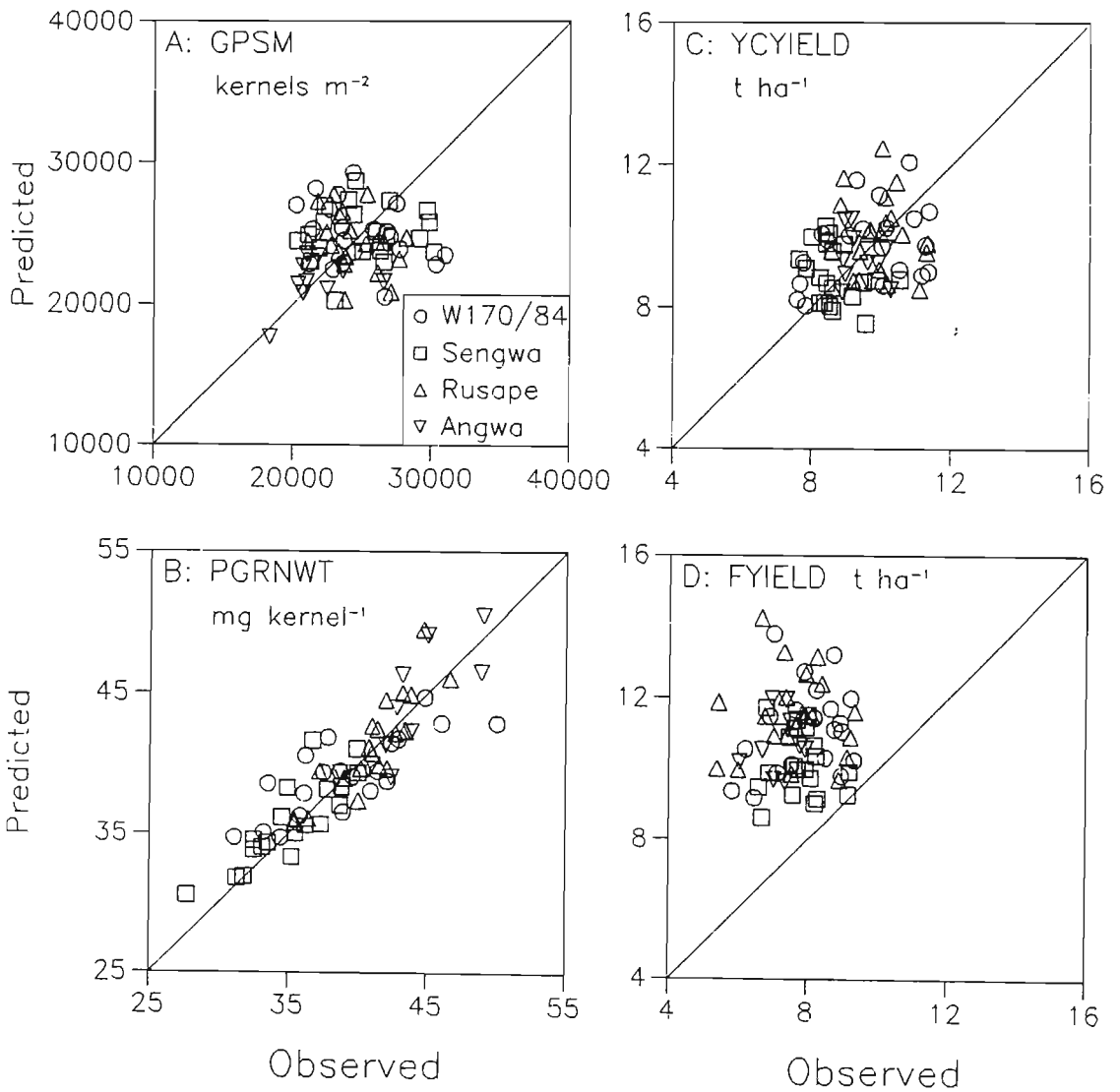

Figure 3.2: Predicted *versus* observed kernel number (GPSM), kernel dry mass (PGRNWT), yield component calculated yield (YCYIELD) and field-measured yield (FYIELD) of four wheat cultivars simulated by the original CERES-Wheat version 2.10 model on the well-watered validation data sets.

Table 3.3: The performance of CERES-Wheat v. 2.10 in predicting ear density (TPSM) and yield components (kernel wt., PGRNWT; kernel number, GPSM; field yield, FYIELD, corrected to 12.5 % kernel water content; and yield computed from yield components, YCYIELD) of four cultivars under well-watered conditions.

	TPSM Ears m^{-2}	PGRNWT mg $kernel^{-1}$	GPSM kernels m^{-2}	FYIELD t ha^{-1}	YCYIELD t ha^{-1}
W170/84					
$\bar{O}$	384	39.2	24768	7.97	9.66
$\bar{P}$	414	39.2	24925	11.17	9.77
MAE	48	2.38	3342	3.201	1.177
IoA	0.56	0.83	0.21	0.38	0.63
MSEs	2168	5.91	13205516	10.772	0.846
MSEu	1084	2.94	4131034	1.378	0.980
MSE	3252	8.85	17336551	12.150	1.826
b	0.244	0.475	-0.246	0.303	0.299
a	321	20.6	31017	8.76	6.89
r	0.328	0.788	-0.333	0.259	0.366
n	20	20	20	20	20
Sengwa					
$\bar{O}$	450	35.0	25070	7.81	8.71
$\bar{P}$	478	35.7	24986	10.18	8.91
MAE	47	1.41	3046	2.371	1.023
IoA	0.56	0.91	0.41	0.34	0.21
MSEs	1303	0.84	7879069	6.207	0.884
MSEu	1782	2.52	3479123	0.774	0.545
MSE	3085	3.36	11358192	6.981	1.429
b	0.418	0.809	0.072	-0.104	-0.327
a	290	7.4	23180	10.99	11.75
r	0.362	0.846	0.116	-0.082	-0.293
n	20	20	20	20	20
Rusape					
$\bar{O}$	407	40.9	24431	7.60	9.96
$\bar{P}$	437	41.2	24401	11.48	10.05
MAE	44	1.32	2758	3.882	1.093
IoA	0.42	0.92	0.16	0.30	0.29
MSEs	1686	0.15	6734122	16.391	0.777
MSEu	1328	2.88	3557825	1.448	1.095
MSE	3014	3.03	10291947	17.840	1.872
b	0.014	1.049	-0.332	-0.015	-0.158
a	431	-1.7	32500	11.59	11.62
r	0.011	0.876	-0.324	-0.014	-0.114
n	20	20	20	20	20
Angwa					
$\bar{O}$	439	43.7	21652	7.20	9.41
$\bar{P}$	446	43.9	21572	10.77	9.42
MAE	39	1.95	1598	3.576	0.779
IoA	0.68	0.89	0.59	0.27	0.30
MSEs	230	0.04	2201151	12.936	0.451
MSEu	1749	5.09	2088074	0.592	0.441
MSE	1979	5.13	4289225	13.528	0.892
b	0.641	1.022	0.293	0.262	-0.323
a	164	-0.78	15224	8.89	12.46
r	0.509	0.813	0.391	0.174	-0.239
n	10	10	10	10	10

3.2.4 Tillering

The ability of the wheat plant to tiller provides it with a degree of plasticity, whereby it may compensate for low plant densities or respond to favourable or unfavourable environmental conditions. Consequently, any wheat simulation model should adequately predict tiller development and senescence. The simulation outputs from the validation data sets showed that WHV21 was inadequate in its representation of tillering (two typical examples are given in Figure 3.3). Observations showed that tillering began about 15 d earlier than predicted and stem numbers (TILN) reached much greater peaks in the field than on the computer. This is an acknowledged weakness in WHV21 (Ritchie and Otter, 1984) and may be the major reason why poor correlations were obtained between predicted and observed ear densities.

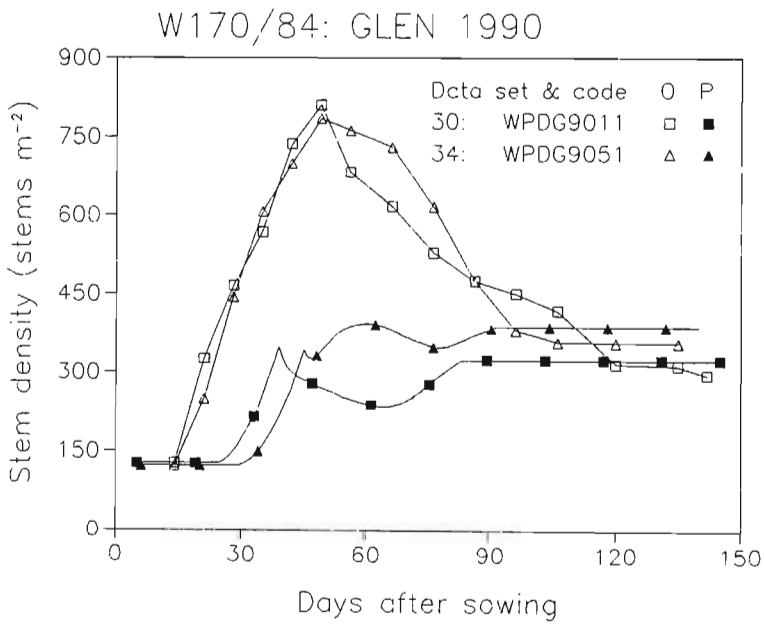

Figure 3.3: Observed (O, open symbols) and predicted (P, solid symbols) seasonal tillering profiles of cultivar W170/84 sown on two dates at GLEN in 1990 (data set and code defined in Table 2.3).

3.2.5 Leaf area index and dry matter accumulation

Dry matter determination and leaf area measurements were not made on any of the validation data sets listed in Table 2.3. This decision was taken so as to preserve those data sets, which had such measurements, for calibration and modification of WHV21. However, in 1986 a growth analysis study on wheat cultivars Sengwa and Rusape was undertaken at ART by the author. This study has not been published; the data are used here for validation of dry matter accumulation and leaf area index predictions of WHV21.

3.2.5.1 Growth analysis trial methods

The cultivars Sengwa and Rusape were sown in two adjacent 0.07 ha blocks on 25 May, 1986, at ART. Standard intensive wheat management practices were applied to the crops, and a total of approximately 530 mm water was applied with overhead sprinkler irrigation on a minimum eight day return interval. Thus, the wheat was well watered and grew under good conditions. The emerged plant densities were 231 and 180 plants m^{-2}, and the average yields, estimated from six-6 m^2 plots, were 7.05 and 7.12 t ha^{-1}, for Sengwa and Rusape, respectively.

Starting 23 das, and continuing through to physiological maturity, three random 0.2 m^2 plant samples were taken at weekly to two weekly intervals in each cultivar for leaf area and above-ground plant dry matter determination.

The leaf blade area of the three samples was determined as follows: In the early growth stages, when the number of leaves was small, the sum of the product of the length and breadth (ΣLB) and the leaf area (LA) of all the leaves were measured on one of the three samples. Leaf area was estimated by counting the number of dots, each representing 12.5 mm^2, on a clear plastic sheet overlayed on each leaf, which fell within the leaf margin. The leaf area of the other two samples was estimated from the sum of the product of the length and breadth of all the leaves in each sample multiplied by the ratio of LA/ΣLB estimated from the first samlpe. As the number of leaves increased with later growth stages, the number of leaves used

in the first sample to estimate ΣLB and LA was reduced to 30. The LA/ΣLB ratio determined from these 30 leaves was used on the total ΣLB on all three samples to estimate leaf area index (LAI).

The above-ground dry matter was determined as follows: The plants in each sample were separated into leaves, sheaths, stems, ears and grain sub-samples. When the size of samples was small, as in early growth stages, the entire set of sub-samples was dried in a forced-air oven at approximately 80°C for 24 hours and weighed to within 0.1 g. As the size of leaf and stem sub-samples increased, each sub-sample was divided into two sub-sub-samples in the ratio of approximately 1:3, and the fresh mass determined for each. The smaller sub-sub-sample was dried and the dry mass of the entire sub-sample estimated from the ratio of dry mass to fresh mass of the sub-sub-sample. This process was necessary because of oven space and time limitations. The sub-sample fresh mass of leaves and stems during full-canopy cover were mostly greater than 100 g. The total above-ground dry matter (BIOMAS) was calculated as the sum to the component sub-samples at each harvest.

The CERES-Wheat files appropriate to this section were named *WGAA8600.WHx*, and are given in subdirectory *WPDXCV* on the accompanying diskette. The experimental directory file (file *WHEXP.DIR*) is named *WHEXPGA.DIR*. The weather file *ARTF0112.W86* contains air temperature and rainfall records from ART but the solar radiation data were taken from Kutsaga weather records. The simulation output files were named *WGAA860m.Wx*.

3.2.5.2 Growth analysis trial simulation results

The WHV21 model predictions of the seasonal LAI profiles of Sengwa and Rusape were reasonably good in comparison to the measured data (Figure 3.4), especially in the period up to GS 39. However, after GS 39, WHV21, tended to under-predict LAI, particularly in Rusape. The measured data also indicated that maximum LAI was maintained for a longer period after GS39 than what the model predicted. Observations showed that it was only after anthesis and the beginning of grain-filling (GS 71) that rapid leaf senescence took place.

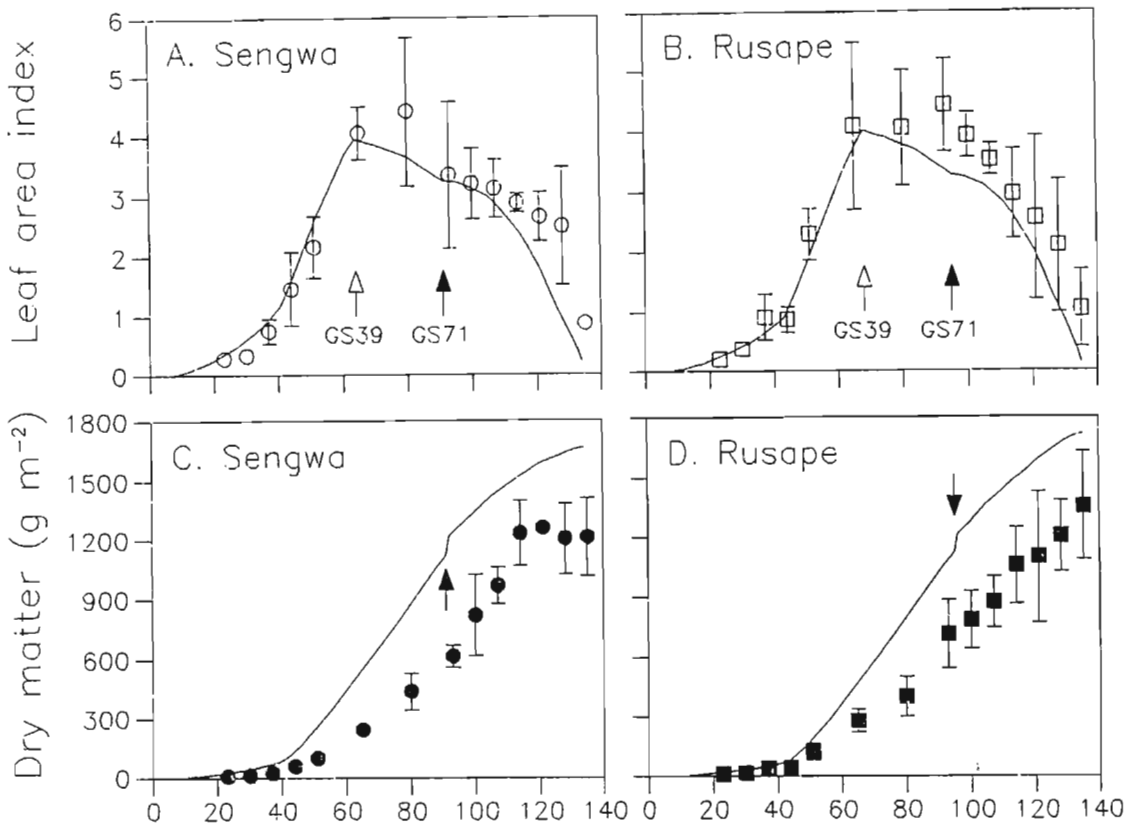

Figure 3.4: Observed (symbols ± SE) and predicted (solid line) leaf area indices and above-ground dry matter of two wheat cultivars grown at ART in 1986.

Above-ground total dry matter (BIOMAS) accumulation was grossly over-estimated by WHV21 in both Sengwa and Rusape. This may have been due to a number of components in the model, such as the over-estimation of the conversion ratio of intercepted PAR to PCARB (eqn. 1), the use of a too high extinction coefficient for PAR interception (0.85 in eqn. 1), and/or the use of incorrect partioning coefficients (Table 1.6). At the start of grain-filling (phase 5), BIOMAS showed a significant and probably atypical increase, due to the sudden appearance of grain dry mass (GRNWT).

3.3 Validation of CERES-Wheat version 2.10 under deficit-irrigated conditions

3.3.1 Methods

After validating the WHV21 model on the well-watered data set (Section 3.2), the model was applied to the irrigation trial validation data sets (Table 2.7) using the same genetic coefficients (Table 3.1) as those used for the well-watered data sets. The soil profile properties and root weighting factors for each experiment (given in file *SPROFILE.WH2*) were modified iteratively, so as to obtain close agreement between the output soil water balance and the measured soil water contents over the growth period. Model performance was evaluated using the procedures outlined in Section 3.1.

3.3.2 Soil water balance

In general, the predicted seasonal soil water balance compared well with observed measurements (Appendix 2). However, for some data sets (e.g., 73, 83 and 84), this was not so. This was attributed primarily to errors made in estimating the quantities of water applied and soil profile properties rather than errors in the model *per se* because, usually, the problem data sets were subsets of an experiment in which the majority of treatments showed close agreement between simulated and measured soil water contents. It was therefore concluded that the soil water balance subroutine (WATBAL) required less attention than the PHENOL and GROSUB subroutines.

3.3.3 Phasic development

The statistical results of the performance of WHV21 in predicting phasic development of wheat under deficit irrigation are given (Table 3.4), supported by scatter plots of the predicted and observed data (Figure 3.5). The raw data are appended (Appendix 2). The WHV21 model grossly over-predicted the timing of growth stages under deficit irrigation. Furthermore, there was a deterioration of precision compared to predictions made under well-watered conditions (cf. Table 3.2).

Table 3.4: The performance of CERES-Wheat v. 2.10 in predicting phasic development of wheat under deficit-irrigated conditions.

	Growth stage		
Parameter	39	61	87
$\bar{O}$	63	82	125
$\bar{P}$	68	89	140
MAE	6	7	15
IoA	0.852	0.814	0.424
MSEs	40.1	53.9	264.9
MSEu	5.3	7.4	9.0
MSE	45.4	61.3	273.9
b	0.559	0.656	0.429
a	32	35	87
r	0.932	0.921	0.802
n	27	27	27

Under deficit irrigation, observations showed that wheat phasic development was hastened with reduced irrigation frequency. The WHV21 model was unable to accommodate this effect, and thus for any irrigation treatment at a site, whether severely stressed or mildly stressed, the predicted time from sowing to each growth stage was identical. This highlighted an important shortcoming of the model.

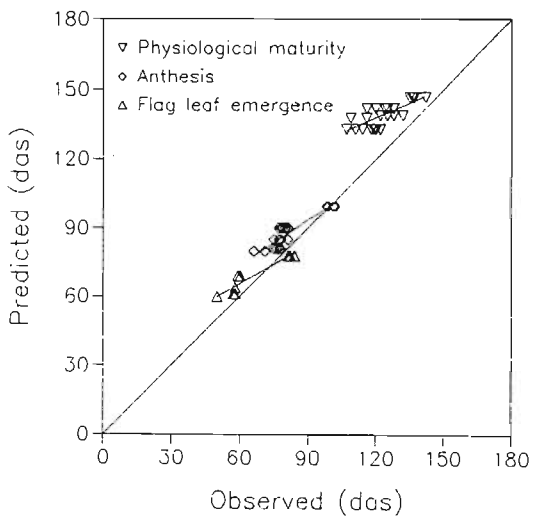

Figure 3.5: Predicted *versus* observed days after sowing (das) to three growth stages of wheat simulated by the original CERES-Wheat version 2.10 model on the deficit-irrigated validation data sets.

3.3.4 Tillering, ear density, yield components and yield

The seasonal pattern of tillering was poorly predicted as in the well-watered planting date trials (data not shown). Consequently, ear density at harvest (TPSM) was not precisely predicted (Table 3.5), as indicated by the high *MAE*. The *MSEs* also comprised a large proportion of the *MSE* (83 %).

Kernel mass was under predicted (Table 3.5 and Figure 3.6) and its *IoA* was low compared to that obtained under well-watered conditions. On the other hand, kernel numbers were predicted reasonably well compared to predictions under well-watered conditions. The modelled yield (YCYIELD), calculated as the product of these two components, exhibited close agreement with observed data (*IoA* > 0.83, *b* close to 1.0 and *r* > 0.86) but the *MAE* was large (> 1.6 t ha^{-1}), and *MSEs* comprised the larger proportion of the total *MSE*. Field yield was over-predicted.

Table 3.5: The performance of CERES-Wheat version 2.10 in predicting ear density (TPSM) and yield components (kernel mass, PGRNWT; kernel number, GPSM; field yield, FYIELD, corrected to 12.5 % kernel water content; and yield computed from yield components, YCYIELD) of wheat under deficit-irrigated conditions.

	TPSM Ears m^{-2}	PGRNWT mg kernel^{-1}	GPSM kernels m^{-2}	FYIELD t ha^{-1}	YCYIELD t ha^{-1}
$\bar{O}$	386	34.1	21975	5.51	7.36
$\bar{P}$	434	27.3	20682	6.73	5.89
MAE	85	8.14	4220	1.677	1.690
IoA	0.71	0.45	0.85	0.84	0.84
MSEs	7987	55.2	5155538	2.012	2.184
MSEu	1614	34.8	24197995	2.148	1.683
MSE	9601	89.9	29353533	4.160	3.868
b	0.371	0.235	0.750	1.374	1.071
a	291	19.3	4155	-0.84	-2.00
r	0.744	0.157	0.746	0.874	0.871
n	27	27	27	27	27

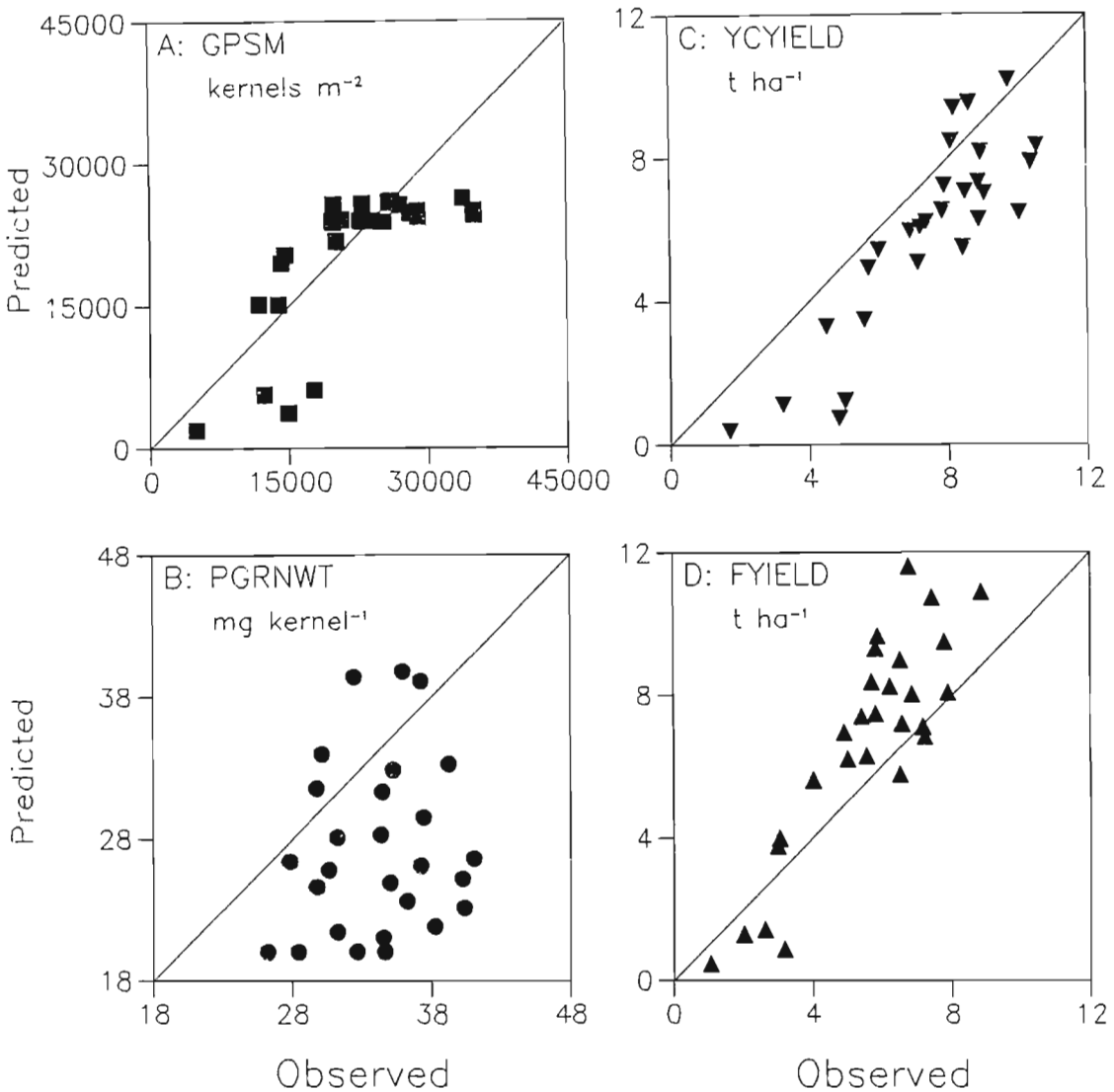

Figure 3.6: Predicted *versus* observed kernel number (GPSM), kernel dry mass (PGRNWT), yield component calculated yield (YCYIELD) and field-measured yield (FYIELD) of wheat simulated by the original CERES-Wheat version 2.10 model on the deficit-irrigated validation data sets.

3.4 Conclusion

Under well-watered conditions, WHV21 gave reasonable but biased predictions of crop phasic development, leaf area develoment and kernel mass. Under deficit irrigated conditions, phasic development and kernel mass were poorly predicted but kernel numbers were predicted fairly well. The greatest shortcomings of WHV21 appeared to be in the estimation of dry matter accumulation and tillering, the inconsistent prediction of yield components and the inability of the model to cater for the hastening of phasic development under water deficit stress. Consequently, the model required improvements of the following:

- duration of growth phases, with an ability to hasten phasic development under water deficit stress;
- growth routines, particularly dry matter accumulation and leaf area production and senescence;
- tiller development and senescence;
- the relationship between GPP and STMWT, with a facility to account for frost reductions to kernel numbers;
- kernel growth initiation and the rate of kernel growth;
- the ratio of field determined yield to yield calculated from yield components.

4 MODIFICATION OF CERES-WHEAT VERSION 2.10

Although WHV21 was shown to be reasonably accurate in predicting wheat phasic development, growth and yield (Chapter 3), the predictions appeared to be biased in some cases and imprecise in others. Consequently, it was concluded that WHV21 was in need of improvement. This chapter describes modifications made to WHV21, based on observations made in both the well-watered and deficit-irrigated calibration data sets (Tables 2.3 and 2.7), and compares the modified version (WHV22) with WHV21 on the validation data sets.

4.1 Phasic development

The WHV21 model divides plant phasic development into 8 stages (Table 1.5; Ritchie, 1991). Stages 8 (initiation of germination), 9 (germination to seedling emergence) and 6 (kernel ripening) are not considered here. Of these, stage 9 is perhaps the most important in terms of crop growth and development, but little difference was found between the observed and predicted times from sowing to emergence in the validation data sets (data not shown). Furthermore, unpublished data of the author indicated that the seeding depth function used by WHV21 to compute the thermal time requirement for emergence (given in Table 1.5) was adequate.

Of the other growth phases, terminal spikelet (TS), flag leaf emergence (GS39), anthesis (GS61) and physiological maturity (GS87) are the most definitive and easily recognisable. The end of phase 3 (defined as the end of pre-anthesis ear growth) and the start of phase 5 (defined as the start of linear grain filling) are the most difficult to identify in the field. Consequently, it was decided to concentrate on calibrating the definitive stages of emergence (EM) to TS, TS to GS39, GS39 to GS61 and GS61 to GS87. The end of pre-anthesis ear growth remains in the modified version, but as a component of the GS39 to GS61 phase. Similarly, the start of phase 5 has been included as a component of the GS61 to GS87 phase.

The rate of development (defined as the reciprocal of duration, t, d^{-1}) of a growth phase increases linearly with an increase in average air temperature (T, °C) above a base or threshold air temperature (T_b, °C), at which duration is infinite, to an optimum air temperature (T_o, °C), at which rate is fastest and duration shortest (Squire, 1990). The relation between $1/t$ and mean T, $\bar{T}$, between T_b and T_o can be determined by a linear regression of the form:

$$1/t = a + b\bar{T}. \qquad 4.1$$

The apparent T_b equals the x-intercept ($-a/b$) and the thermal time duration (TTD, °C d) of the growth phase is equal to $1/b$ (Summerfield *et al.*, 1991). This process of calculating TTD is appropriate for predicting plant development only if several conditions are met (Ritchie and NeSmith, 1991):

1. the temperature response of the development rate is linear over the range of temperatures experienced;
2. the air temperature does not decrease below T_b for a significant part of many days during the growing season;
3. air temperature does not exceed an upper threshold temperature for a significant part of the day; and
4. the growing region of the plant has the same mean temperature as $\bar{T}$.

Conditions 1, 2 and 3 were readily met in this study. Condition 4 was considered to be a problem only during stage 1, when the growing point (crown) of wheat is close to or below the soil surface. In this case the soil surface or crown temperature would be a better measure of T than screened air temperature (Ritchie and NeSmith, 1991). However, with the lack of instrumentation and readily available soil temperature data, this problem was ignored and the assumption was made that the crown temperature was in direct proportion to the measured screened air temperature.

A further problem is the definition of daily average air temperature. The average air temperature calculated from the mean of the maximum and minimum air temperatures recorded once per day may differ from the actual mean daily temperature and thereby introduce bias into accummulated air temperatures (Ritchie and NeSmith, 1991). Ritchie and NeSmith argued,

however, that such biases were likely to be small and insignificant. From a linear regression[1] of the mean of the daily maximum and minimum air temperatures on the mean daily air temperature calculated from the mean of the mean hourly air temperatures measured at ART Farm during the period October 1989 to September 1991 (see Section 2.2.1), it was found that the bias was in the order of 0.5 °C ($y = 0.46 + 1.00x$, $r^2 = 0.965$, data not given). Since this bias was small and consistent ($b = 1.00$) across the range of mean air temperatures recorded, it was ignored. Thus, in this study, the mean daily air temperature was calculated from the mean of the daily maximum and minimum screened air temperatures.

4.1.1 Phase 1: Emergence to terminal spikelet

It was assumed that the dominant factor governing the rate of development from EM to TS was air temperature (see Section 3.1 and 3.2 for discussion on this assumption). Since the proposed use of this modified version of CERES-Wheat is for spring wheat cultivars in Zimbabwe, it was decided to remove the vernalisation and COLD routines from WHV21. The photoperiod functions remain, but in a modified way (details given below).

Linear regressions of the rate of development from EM to TS on the mean air temperature for the same period were computed for each cultivar (W170/84, Sengwa, Rusape and Angwa). For all cultivars the regressions were significant[2] (Table 4.1). The y-intercepts of W170/84, Sengwa and Rusape were not significantly different from one another, but all were significantly different from Angwa. The regression slope of W170/84 was significantly different from that of Angwa, but the regression slopes of Sengwa and Rusape were not different from either W170/84 and Angwa. The x-intercepts of all cultivars differed significantly.

These results imply that *TTD* and T_b for phase 1 are cultivar

---

[1] All linear regressions were computed using PlotIT version 2.0, 1993, Scientific Programming Enterprises, Haslett, MI, USA.

[2] Throughout this thesis, statistical significance of results was computed at P = 0.05.

specific. WHV21 assumes that T_b is constant (0 °C) but *TTD* varies with genotype. Other wheat models also follow this rationale for phase 1 or pre-anthesis development. For example, Maas and Arkin (1980) and O'Leary *et al.* (1985) define T_b as 4 °C, while van Keulen and Seligman (1987) and Singels (1990) define T_b as 0 °C. For simplicity, this approach was maintained in the modified version, WHVZIM22. The mean T_b (x-intercept) calculated for the four cultivars in Table 4.1 was 4.4 °C but in view of the models of Maas and Arkin (1980) and O'Leary *et al.* (1985), T_b was set at 4 °C.

Using T_b equal to 4 °C, linear regressions were computed for the calibration data sets using the following relationship

$$1/t = b(\bar{T} - T_b) \qquad 4.2$$

The slopes of each cultivar were significantly different (Table 4.2). The *TTD* for each cultivar was calculated as the reciprocal of the slope, and results showed that TTD varied significantly from 291 °C d in Angwa to 446 °C d in W170/84.

The genetic coefficient P1 is defined for WHVZIM22 as the *TTD* of phase 1 growth with a T_b (TBASE) of 4 °C. For model input, P1 replaces P1V in *GENETICS.WH9*, and is scaled from 0 to 6 such that

$$TTD = 200 + 50 \times P1, \qquad 4.3$$

where *TTD* is the thermal time sum for EM to TS, °C d. The P1 values for W170/84, Sengwa, Rusape and Angwa were set as 4.9, 2.4, 3.0 and 1.8, respectively.

To allow for photoperiod sensitivity among genotypes, the approach taken was based on the observations of Summerfield *et al.* (1991). They stated that the rate of progress towards flowering (in this case TS) was a linear function of air temperature and photoperiod and that, in most cases, these two factors do not interact. Photoperiods in Zimbabwe are in the range of 11.55 to 14.25 h at the Southern-most border. The average photoperiod during the phase 1 growth in this study at ART was 11.89 h (range 11.79 to 12.19 h) and similar at other sites. It was assumed that, with this average and narrow range of photoperiods used for calibration, the dominant factor

Table 4.1: Statistical parameters of the linear regressions of the rate of development from emergence to terminal spikelet (d^{-1}) on the mean air temperature of four wheat cultivars using the well-watered calibration data set.

	Cultivar			
Parameter	W170/84	Sengwa	Rusape	Angwa
n	29	29	29	29
y-intercept (d^{-1})	-0.0060	-0.0118	-0.0121	-0.0301
SE y-intercept (d^{-1})	0.00272	0.00630	0.00630	0.00728
y-intercept 95 % confidence interval	(-0.0115, -0.0004)	(-0.0247 0.0011)	(-0.0265, 0.0022)	(-0.0450, -0.0151)
slope (d^{-1} $°C^{-1}$)	0.00205	0.00309	0.00290	0.00446
SE slope (d^{-1} $°C^{-1}$)	0.000175	0.000399	0.000450	0.000460
slope 95 % confidence interval	(0.00169, 0.00241)	(0.00227, 0.00391)	(0.00198, 0.00382)	(0.00352, 0.00540)
x-intercept (°C)	2.9	3.8	4.2	6.7
SE x-intercept[3]	0.003	0.006	0.007	0.007
x-intercept 95 % confidence interval	(2.89, 2.91)	(3.81, 3.83)	(4.16, 4.19)	(6.69, 6.71)
r	0.914	0.830	0.779	0.882
TTD (inverse of slope (°C d)	488	323	345	224
TTD 95 % confidence interval[4]	(402, 573)	(237, 409)	(235, 454)	(177, 271)

[3] $$SE_{x\text{-}intercept} = \sqrt{(SE_{slope})^2 + (SE_{y\text{-}intercept})^2}$$

[4] $$SE_{TTD} = SE_{slope} / slope^2$$

Table 4.2: Statistical parameters of the linear regressions of the rate of development from emergence to terminal spikelet (d^{-1}) on the average air temperature minus the base temperature (4 °C), i.e. $1/d = b\ (T - T_b)$, of four wheat cultivars using the calibration data set.

	Cultivar			
Parameter	W170/84	Sengwa	Rusape	Angwa
n	29	29	29	29
slope (d^{-1} °C^{-1})	0.00224	0.00313	0.00285	0.00344
SE slope (d^{-1} °C^{-1})	0.000018	0.000046	0.000055	0.000059
slope 95 % confidence interval	(0.00220, 0.00228)	(0.00304, 0.00323)	(0.00274, 0.00297)	(0.00332, 0.00356)
r	0.999	0.997	0.995	0.996
TTD (inverse of slope) (°C d)	446	319	351	291
TTD 95 % confidence interval	(454, 438)	(321, 317)	(509, 336)	(302, 280)

controlling development was air temperature. Furthermore, it was assumed that, regardless of photoperiodic sensitivity, all cultivars would require a cultivar-specific TTS (°C d) to complete phase 1 growth at an average photoperiod of 11.89 h. With longer or shorter photoperiods, the rate of development of sensitive cultivars would be a linear function of photoperiod. In other words, a photoperiod of 11.89 h was considered optimum and the following functions were used to compute the relative development rate (DF) and daily thermal time (DTT, °C) as a function of the photoperiod sensitivity coefficient, P1D:

$$DF = 1 - (11.89 - HRLT) \times 25 \times P1D, \quad 11.55 \leq HRLT \leq 14.25 \qquad 4.4$$

and, in terms of Fortran assignment code

$$DTT = DTT \times DF \qquad 4.5$$

where *HRLT* is the photoperiod (h) and P1D in Eqn. 4.4 is equal to the scaled P1D coefficient divided by 500. The scaled P1D coefficient may vary from 0 to 3.

The concept used in Eqn. 4.4 has little, or no, physiological basis, in that photoperiodic influences on plants act in other ways than by increasing or decreasing thermal accumulation. This comment also applies to the photoperiod

function used in WHV21. Nevertheless, Eqn. 4.4 provides an empirical means of adjusting development rate for photoperiod sensitivity and it is included simply because photoperiod sensitivity is common in wheat genotypes and it was considered necessary to include such a function in the event that the model was to be used, for example, for evaluating summer wheat production in Zimbabwe when photoperiods are longer than in winter. It is stressed, though, that the relationship is untested, would need verification, and is basically unused in this excercise, since P1D is set to zero for all cultivars.

4.1.2 Leaf emergence

Leaf emergence (i.e., leaf collar emergence) is not simulated in WHV21. It was decided to include leaf emergence in WHVZIM22 because of the reasons given in Section 2.5.2.

Using data from ART 1990, GLEN 1989 and SHAM 1990, emerged leaf number was plotted as a function of thermal time (T_b = 4 °C) after emergence (Figure 4.1). It was evident that the rate of leaf emergence prior to TS was greater than after TS. Discontinuity of rates of wheat leaf appearance and emergence have been reported in the literature and have been attributed to the change in phase from vegetative to reproductive growth (Baker *et al.*, 1986; Cao and Moss, 1991). The calibration data set also showed that, in most cases, the variation in total leaf number was mainly due to differences in leaf number prior to TS. Most data sets produced three leaves after TS, but total leaf numbers ranged from eight to 11. Thus, two sets of linear regressions were performed for each cultivar: one for leaves up to TS, and the other for the last three leaves. The statistical results are given (Table 4.3).

For all four cultivars the pre- and post-TS regressions were significant ($r > 0.86$, $n > 25$), but within either the pre- or post-TS leaves, the similarity of slopes and intercepts of the four cultivars indicated that the regressions were not significantly different. Consequently, the cultivar data were pooled and from the linear regressions on these pooled data (Table 4.3) the thermal time for leaf emergence (PHINTLE, °C d leaf^{-1}, T_b = 4 °C) in the pre- and post-TS phases were calculated

as the inverse of the respective slopes. This yielded the following:

Leaf number 1: PHINTLE = 28.5 °C d leaf^{-1}

Leaf 2 to TS: PHINTLE = 62.7 °C d leaf^{-1}

Last three leaves: PHINTLE = 92.4 °C d leaf^{-1}

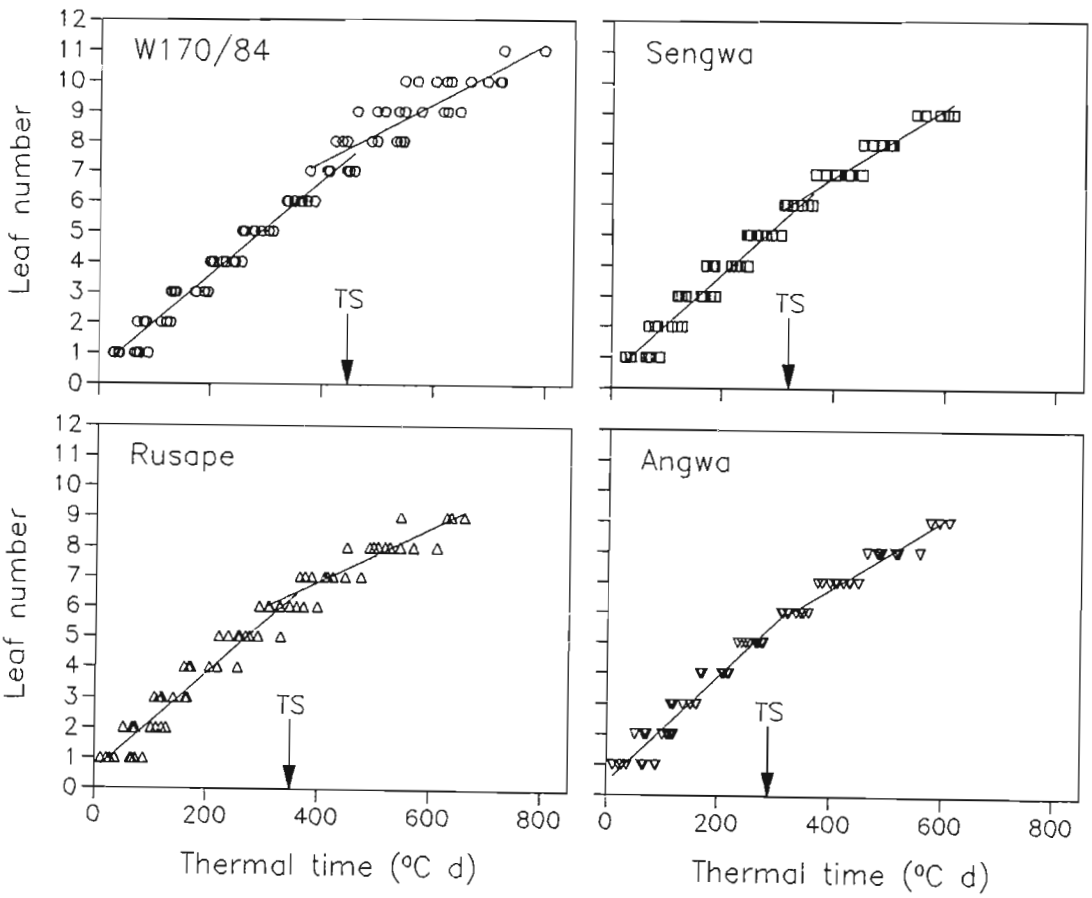

Figure 4.1: The relationship between leaf emergence and thermal time accumulation (T_b = 4 °C) of four wheat cultivars.

Table 4.3: Statistical parameters of the linear regressions of leaf number on thermal time (T_b = 4 °C) from emergence for leaves prior to and post TS for four cultivars in data sets from ART 1990, GLEN 1989 and SHAM 1990.

	Cultivar				
Parameter	W170/84	Sengwa	Rusape	Angwa	Pooled
Leaves prior to TS					
n	60	50	50	47	207
y-intercept (leaf no.)	0.5	0.4	0.6	0.4	0.55
SE y-int. (leaf no.)	0.11	0.12	0.14	0.12	0.06
y-intercept 95 %	(0.26,	(0.19,	(0.32,	(0.18,	(0.42,
cofidence interval	0.71)	0.67)	0.88)	0.67)	0.68)
slope (leaves °C^{-1} d^{-1})	0.016	0.017	0.016	0.017	0.016
SE slope (leaves °C^{-1} d^{-1})	0.0005	0.0006	0.0007	0.0007	0.0003
slope 95 %	(0.015,	(0.015,	(0.015,	(0.016,	(0.015,
confidence interval	0.016)	0.018)	0.018)	0.019)	0.017)
r	0.976	0.969	0.956	0.966	0.966
Leaves post TS					
n	34	26	27	29	116
y-intercept (leaf no.)	3.4	2.3	3.3	2.3	2.6
SE y-int. (leaf no.)	0.55	0.31	0.38	0.26	0.21
y-intercept 95 %	(2.28,	(1.70,	(2.51,	(1.76,	(2.18,
confidence interval	4.53)	2.98)	4.07)	2.83)	3.00)
slope (leaves °C^{-1} d^{-1})	0.010	0.011	0.009	0.011	0.011
SE slope (leaves °C^{-1} d^{-1})	0.0010	0.0007	0.0008	0.0006	0.0004
slope 95 %	(0.008,	(0.010,	(0.007,	(0.010,	(0.010,
confidence interval	0.012)	0.013)	0.010)	0.012)	0.012)
r	0.869	0.961	0.914	0.967	0.925

4.1.3 Phase 2: Terminal spikelet to end of leaf growth

In the WHV21 model, phase 2 takes three phyllochrons (i.e., P2, °C d, equals PHINT x 3). The data presented above (Section 4.1.2) agrees with this, in that the flag leaf was usually the third leaf to emerge after TS. In order to confirm that the *TTD* of phase 2 was not cultivar specific, the field estimated *TTD* of TS to GS39 was calculated for each cultivar over the calibration data sets (in the field, GS39 was estimated independently of the leaf number counts, and was estimated as the time when the majority of the population of plants was at GS39). Cultivars were not significantly different for the *TTD*

Table 4.4: The thermal time duration (T_b = 4 °C) from terminal spikelet to flag leaf emergence of four wheat cultivars, averaged over the calibration data sets (n = 29, excluding sets 50 to 54, where TS was not determined).

	Cultivar				
	W170/84	Sengwa	Rusape	Angwa	Mean
Mean	286	288	302	301	294
SE	32.5	28.5	37.2	33.7	33.5
95 % confidence limits	(220, 353)	(229, 346)	(226, 378)	(231, 370)	

of phase 2 (Table 4.4). Thus, the cultivar mean of 294 °C d was used in WHVZIM22 for the duration of phase 2 growth. This is similar to that computed from PHINTLE x 3 (277 °C d).

First node (GS31) appearance is a useful indicator for N fertilizer management, but the prediction of GS31 is not catered for in WHV21. On average across the calibration data sets, GS31 occurred four to 11 days after TS, depending on cultivar (Table 4.5). With the use of T_b equal to 4 °C, the thermal time from TS to GS31 for the four cultivars ranged from 47 to 114 °C d, but the data were variable, and cultivars not significantly different. Consequently, the thermal time from TS to GS31 (TT31) was set at the cultivar average of 82 °C d.

Table 4.5: The average time and thermal time duration (T_b = 4 °C) of the terminal spikelet (TS) to first node (GS31) phase.

	Cultivar				
Parameter	W170/84	Sengwa	Rusape	Angwa	Mean
	Time (d)				
Average	4	11	7	8	8
SE	3.2	2.7	3.0	2.7	3.6
	Thermal time (°C d)				
Average	47	114	83	86	82
SE	34.8	28.1	35.6	39.1	41.8

4.1.4 Phase 3: End of leaf growth to anthesis

In the WHV21 model, phase 3 ends with the end of pre-anthesis ear growth and is assumed to equal two phyllochrons, even though no new leaves are produced during this growth phase. In WHVZIM22, this stage was extended to the start of anthesis. The *TTD* (T_b = 4 °C) of GS39 to GS61 was calculated for all calibration data sets appropriate to each cultivar and it was found that, on average, cultivars did not differ significantly (Table 4.6). The mean *TTD* for GS39 to GS61 was 217 °C d, which is greater than PHINTLE x 2. Therefore, P3, the *TTD* for phase 3, was set at 217 °C d.

It was considered necessary to maintain the WHV21 growth stage "end of pre-anthesis ear growth" because it is used in GROSUB. In WHV21, anthesis occurs 80 °C d (T_b = 0 °C d) into phase 4. This is equivalent to 64 °C d (T_b = 4 °C d) when the mean daily air temperature is 20 °C (which is approximately the mean annual daily air temperature in Zimbabwe (Department of Meteorological Services, 1981). Thus, in WHVZIM22, the end of pre-anthesis ear growth was initially set at 64 °C d before anthesis, or 153 °C d into phase 3, with a T_b of 4 °C.

Table 4.6: The thermal time duration (T_b = 4 °C) from flag leaf emergence to anthesis of four wheat cultivars, averaged over the calibration data sets. (Cultivar Angwa was not included in sets 50 to 54.)

	Cultivar				
	W170/84	Sengwa	Rusape	Angwa	Mean
n	34	34	34	29	131
Mean	217	219	211	202	217
SE	25.6	19.5	34.1	27.3	30.8
95 % confidence limits	269)	(165, 259)	(179, 281)	(141, 258)	(146,

4.1.5 Phase 4 and 5: Anthesis to physiological maturity

The WHV21 model sets the duration of phase 4 (the period from the end of pre-anthesis ear growth to the beginning of grain filling) as 200 °C d (T_b = 0°C). Anthesis occurs 80 °C d into phase 4, so the beginning of grain filling occurs 120 °C d after anthesis. The phase 5 growth period is a linear function of a genetic coefficient P5 (Table 1.5). In the WHVZIM22 model, the period from anthesis (GS61) to physiological maturity (GS87) is considered as one complete growth phase. The start of grain filling in relation to anthesis is dealt with in Section 4.2.5, where the process of kernel filling is discussed.

Linear regressions of the rate of development from GS61 to GS87 on the mean air temperature during this period were computed for each cultivar using the calibration data set (Figure 4.2). The statistical inferences from the results (Table 4.7) indicated that the x- and y-intercepts and the slopes of the four cultivars were not significantly different. Singels (1991) made the assumption that similarity of slope and y-intercept of such cultivar regressions implied that apparent base temperatures were the same for the cultivars studied. Hence, on averaging the x-intercept values, the apparent base temperature was computed as 3.0 °C. Reported base temperatures in wheat models for the anthesis to maturity period range from 0 °C (van Keulen and Seligman, 1987), 1 °C (Ritchie, 1991), 5 °C (Maas and Arkin, 1980) to 8 °C (O'Leary, Connor and White, 1985; Singels, 1991). It was decided to use a T_b of 3 °C for the period GS61 to GS87.

Although the slopes of the cultivar regressions of the rate of post-anthesis development on mean air temperature were not significantly different at P = 0.05 (Table 4.7), at P = 0.10, the slopes of Sengwa and Rusape were significantly different, although neither was significantly different from W170/84 or Angwa (statistics not shown). This was considered sufficient justification to assume that the duration of the post-anthesis phase is genetotype specific, in line with the assumption of WHV21. Consequently, linear regressions (using Eqn 4.2) were computed for each cultivar for the GS61 to GS87 phase. The statistical results (Table 4.8) indicated that the slope of the

regression for Sengwa was significantly less than that of the other cultivars, while the slope of the regression for Angwa was greater than that of W170/84, but not that of Rusape.

The reciprocal of the slope yields the *TTD* of the post-anthesis period or the thermal time to maturity (*TTM*, °C d) (Table 4.8). The range of *TTM* was 735 to 826 °C d. To convert this from a scaled P5 genetic coefficient, the following relationship was used

$$TTM = 400 + 100 \times P5, \qquad 4.6$$

where P5 may vary from zero to six. Based on this, the P5 genetic coefficients for the four cultivars were set at 3.7, 4.3, 3.6 and 3.4 for W170/84, Sengwa, Rusape and Angwa, respectively.

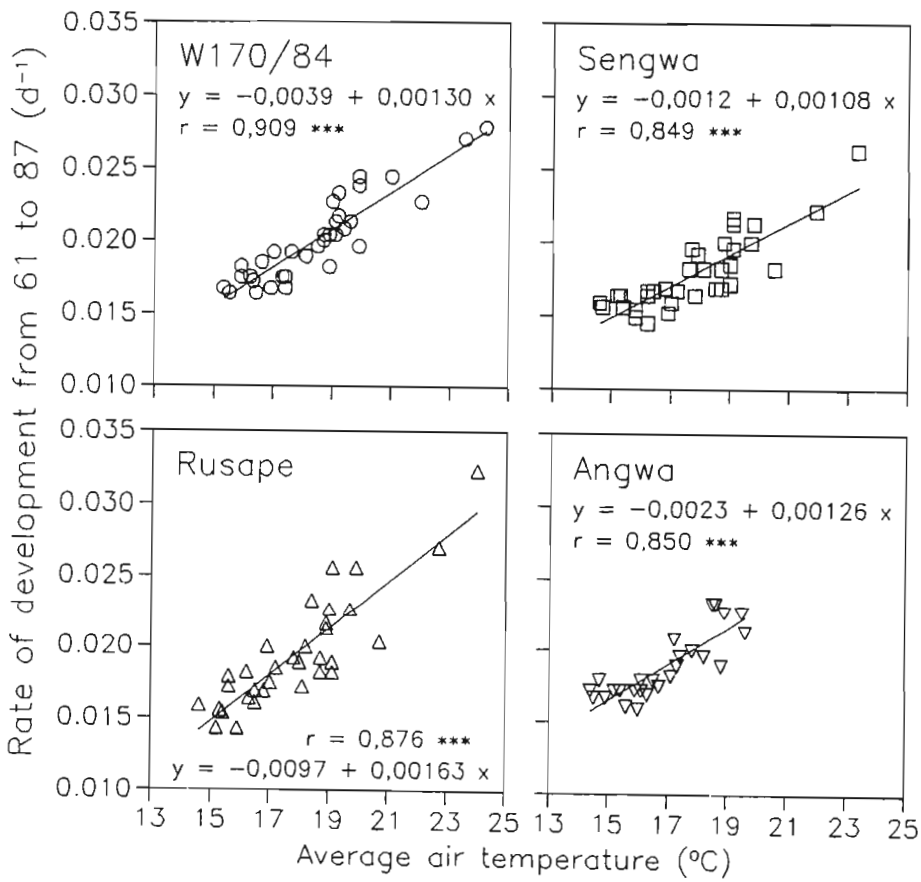

Figure 4.2: The rate of development from anthesis (61) to physiological maturity (87) of four wheat cultivars as a function of average air temperature during the phase.

Table 4.7: Statistical parameters of the linear regressions of the rate of development from anthesis to physiological maturity (d^{-1}) on the average air temperature of four wheat cultivars using the calibration data set (note, Angwa was not included in data sets 50 to 54).

Parameter	Cultivar W170/84	Sengwa	Rusape	Angwa
n	34	34	34	29
y-intercept (d^{-1})	-0.0039	-0.0012	-0.0097	-0.0023
SE y-intercept (d^{-1})	0.00195	0.00212	0.00286	0.00255
y-intercept 95 % confidence interval	(-0.0078, 0.0001)	(-0.0056, 0.0031)	(-0.0155, -0.0039)	(-0.0076, 0.0029)
slope (d^{-1} $°C^{-1}$)	0.00130	0.00108	0.00163	0.00126
SE slope (d^{-1} $°C^{-1}$)	0.000105	0.000118	0.000158	0.000150
slope 95 % confidence interval	(0.0011, 0.0015)	(0.0008, 0.0013)	(0.0013, 0.0020)	(0.0010, 0.0016)
x-intercept (°C)	3.0	1.2	5.9	1.8
SE x-intercept	0.002	0.002	0.003	0.003
x-intercept 95 % confidence interval	(2.966, 2.974)	(1.146, 1.154)	(5.927, 5.933)	(1.835, 1.845)
r	0.909	0.849	0.876	0.850

Table 4.8: Statistical parameters of the linear regressions of the rate of development from anthesis to physiological maturity (d^{-1}) on the average air temperature minus the base temperature (4 °C), i.e., using Eqn. 4.3, of four wheat cultivars using the calibration data set (note, Angwa was not included in sets 50 to 54). The thermal time from antheis to maturity (*TTM*) is also given.

Parameter	Cultivar W170/84	Sengwa	Rusape	Angwa
n	34	34	34	29
slope (d^{-1} $°C^{-1}$)	0.00130	0.00121	0.00132	0.00136
SE slope (d^{-1} $°C^{-1}$)	0.000014	0.000016	0.000023	0.000016
slope 95 % confidence interval	(0.00127, 0.00133)	(0.00118, 0.00124)	(0.00127, 0.00136)	(0.00133, 0.00140)
r	0.998	0.997	0.995	0.998
TTM (reciprocal of slope) (°C d)	770	826	757	735

4.1.6 Water deficit stress effect on phasic development

The WHV21 model was unable to account for the observed hastening of plant development under conditions of water deficit stress (see Section 3.3.2). Plant temperature has been shown to increase under conditions of water deficit stress (Ehrler *et al.*, 1978; Jackson, 1982). The slowing or inhibition of plant evaporation through lower water fluxes and/or stomatal closure under water deficit conditions decreases evaporative cooling and results in higher leaf temperatures (Eastin and Sullivan, 1984). This may act to hasten plant development in the same way as do increased ambient air temperatures. Consequently, DTT was made to increase under conditions of water deficit by the following Fortran assignment statement:

$$DTT = DTT \times (1.5 - 0.5 \times SWDF2) \qquad 4.7$$

where SWDF2 is the soil water deficit factor used to reduce leaf and stem extension growth and tillering. The form of Eqn 4.7 was chosen through iteration.

4.1.7 Validation of phenolgy modifications

The modifications given above were incorporated into the Fortran source code supplied with the WHV21 model and compiled using the Microsoft® FORTRAN Optimizing Compiler version 4.01. The phenological genetic coefficients applied to each cultivar are given (Table 4.9). Coefficient P1 for Rusape was increased from 3.0 to 3.1, as this improved the prediction of TS. The coefficients for the other cultivars were unchanged from those formulated and given above. The modified CERES-Wheat version (WV22) was applied to both the well-watered and deficit-irrigated validation data sets (Tables 2.3 and 2.7) and model performance evaluated according to the procedures given in Section 3.1.

The statistical results of the performance of WHVZIM22 in predicting phasic development under well-watered and deficit-irrigated conditions are given (Tables 4.10 and 4.11, respectively) and the raw data are appended (Appendix 4). From a comparison of the statistical parameters in Table 4.9 with

Table 4.9: Phenological genetic coefficients used in the validation of CERES-Wheat version 2.2 under well-watered conditions.

	Cultivar			
Coefficient	W170/84	Sengwa	Rusape	Angwa
PHINT (°C d)	136	112	120	105
P1	4.9	2.4	3.1	1.8
P1D	0.0	0.0	0.0	0.0
P5	3.7	4.3	3.6	3.4

those in Table 3.2, it is clear that in each cultivar under well-watered conditions, the modifications improved the predictions of wheat phasic development. In each case, WHVZIM22 decreased the *MAE* and increased the *IoA* relative to WHV21.

Under deficit-irrigated conditions, WHVZIM22 also improved predictions of wheat phasic development compared to WHV21 (Table 4.11). This was particularly so for GS87, where the *MAE* decreased from 15 with WHV21 to six with WHVZIM22. This was accompanied by a corresponding increase in the *IoA* from 0.424 with WHV21 to 0.866 with WHVZIM22.

These improvements in the prediction of GS39, GS61 and GS87 for both the combined well-watered and deficit-irrigated validation data sets are graphically presented (Figure 4.3) and the statistics of comparison are given (Table 4.12). As in either the well-watered of deficit-irrigated comparisons, the combined data showed marked improvements of WHVZIM22 over WHV21 in the prediction of wheat phasic development.

However, the revised model remains somewhat biased ($b < 1.0$) in predicting phasic development, especially under well watered conditions (Table 4.10) and this may warrant further improvement in the future. Nevertheless, on the combined data sets, the *MAE* of growth stage prediction with WHVZIM22 was less than or equal to five days (Table 4.12), which according to Maas and Arkin (1980b) approximates the magnitude of observational error in growth stage determination.

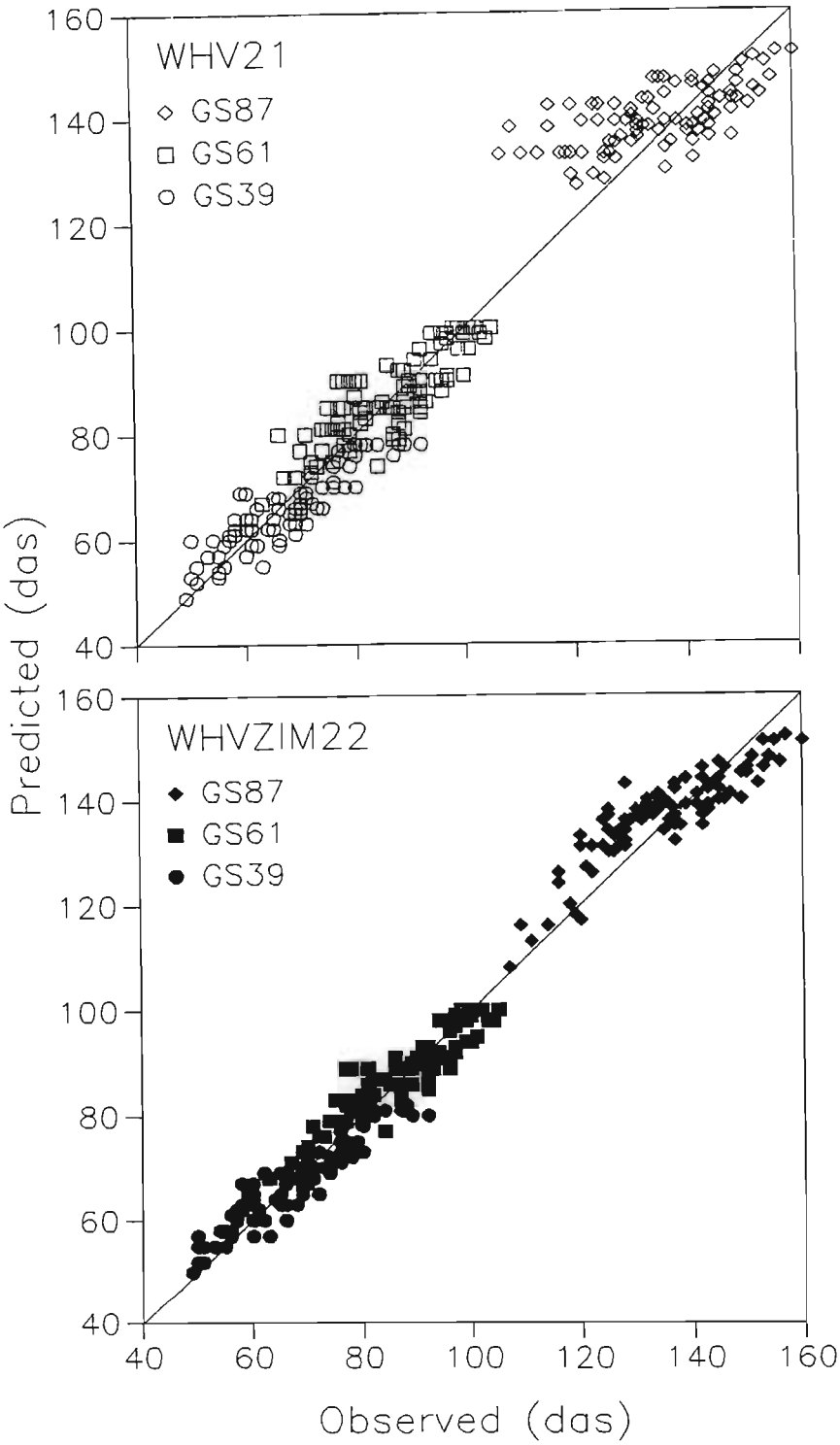

Figure 4.3: Comparison of the original (WHV21) and revised (WHVZIM22) CERES-Wheat models in the prediction of flag leaf emergence (GS39), anthesis (GS61) and physiological maturity (GS87). The straight line is the 1:1 line and not the regression line of least squares.

Table 4.10: The performance of revised CERES-Wheat model (WHVZIM22) in predicting phasic development of four cultivars under well watered conditions.

	Growth stage				
Parameter	TS	31	39	61	87
W170/84					
$\bar{O}$	44	46	78	96	145
$\bar{P}$	45	53	75	95	145
MAE	1.8	7.2	3.5	2.8	4.5
IoA	0.89	0.49	0.88	0.90	0.84
MSEs	0.70	52.73	14.01	7.42	22.26
MSEu	6.90	21.07	7.49	4.68	3.94
MSE	7.60	73.80	21.50	12.10	26.20
b	0.935	0.640	0.640	0.597	0.461
a	3.7	23.7	25.5	37.9	77.9
r	0.804	0.344	0.881	0.874	0.897
n	10	20	20	20	20
Sengwa					
$\bar{O}$	33	43	63	83	139
$\bar{P}$	34	43	63	84	141
MAE	1.9	3.1	2.4	3.3	4.2
IoA	0.91	0.84	0.94	0.91	0.83
MSEs	1.52	3.31	4.61	8.60	20.50
MSEu	3.48	9.44	4.39	5.70	3.90
MSE	5.00	12.75	9.00	14.30	24.40
b	0.701	0.659	0.702	0.619	0.467
a	10.1	14.0	18.8	32.5	75.7
r	0.837	0.723	0.924	0.888	0.883
n	10	20	20	20	20
Rusape					
$\bar{O}$	36	43	67	88	138
$\bar{P}$	37	46	67	87	139
MAE	2.4	4.3	3.1	3.5	5.0
IoA	0.91	0.78	0.93	0.91	0.82
MSEs	3.79	12.05	7.70	13.07	26.50
MSEu	3.61	12.80	5.55	3.18	3.45
MSE	7.40	24.85	13.25	16.25	29.95
b	0.660	0.613	0.671	0.591	0.420
a	12.9	19.5	21.7	35.0	80.6
r	0.875	0.684	0.920	0.941	0.895
n	10	20	20	20	20
Angwa					
$\bar{O}$	31	37	61	79	133
$\bar{P}$	31	38	59	80	134
MAE	2.1	2.4	2.5	3.5	6.5
IoA	0.87	0.87	0.94	0.93	0.76
MSEs	3.74	3.28	7.42	10.54	43.61
MSEu	3.56	3.72	3.08	4.36	3.09
MSE	7.30	7.00	10.50	14.90	46.70
b	0.572	1.059	0.711	0.624	0.350
a	13.1	-0.4	15.8	29.9	87.0
r	0.807	0.871	0.948	0.933	0.896
n	10	10	10	10	10

Table 4.11: The performance of the revised CERES-Wheat model (WHVZIM22) in predicting phasic development of wheat under deficit-irrigated conditions.

	Growth stage			
Parameter	31	39	61	87
$\bar{O}$	48	63	82	125
$\bar{P}$	49	69	87	130
MAE	3	6	6	6
IoA	0.939	0.870	0.871	0.866
MSEs	3.3	40.2	34.9	34.6
MSEu	7.8	5.1	9.6	19.1
MSE	11.0	45.3	44.4	53.7
b	1.172	0.671	0.742	0.905
a	-7	26	27	18
r	0.931	0.953	0.920	0.889
n	27	27	27	27

Table 4.12: Statistical camparison of the performance of the original CERES-Wheat model (WHV21) with the modified version (WHVZIM22) in predicting phasic development of wheat under combined well-watered and deficit-irrigated conditions.

	Growth stage			
Parameter	31	39	61	87
WHV21				
$\bar{O}$	NS[1]	67	86	135
$\bar{P}$	NS	66	87	140
MAE	NS	5	5	8
IoA	NS	0.894	0.889	0.643
MSEs	NS	18.6	13.5	85.0
MSEu	NS	13.0	20.1	19.7
MSE	NS	31.6	33.6	104.7
b	NS	0.593	0.645	0.301
a	NS	26	32	99
r	NS	0.864	0.822	0.622
n	NS	97	97	97
WHVZIM22				
$\bar{O}$	45	67	86	135
$\bar{P}$	47	67	87	137
MAE	4	4	4	5
IoA	0.894	0.938	0.929	0.909
MSEs	3.8	9.9	10.8	20.7
MSEu	17.0	10.3	10.8	15.1
MSE	20.9	20.2	21.6	35.8
b	0.968	0.702	0.690	0.643
a	3	20	28	50
r	0.840	0.916	0.903	0.889
n	97	97	97	97

[1] NS indicates that growth stage 31 is not simulated by WHV21

4.2 Modifications to the growth subroutine

The WHV21 model showed a number of limitations in predicting dry matter accumulation, tillering and yield (Chapter 3). These were considered serious enough to justify extensive review and modification of the GROSUB source code. In addition, the changing of the phasic development routines impacted on GROSUB, thereby necessitating a review thereof. This Section describes the changes made to GROSUB and shows how these changes improved the model performance. Wherever possible, changes were based on observations made in the calibration data sets or on published literature. However, a number of modifications involved calibrating coefficients iteratively using the calibration data sets or simply by rationalizing existing functions.

4.2.1 Dry matter accumulation

Dry matter accumulation (CARBO) in CERES-Wheat is based on the conversion of intercepted photosynthetically active radiation (IPAR) into potential biomass production (PCARB) (Eqn. 1.1). PCARB is moderated by a temperature function (PRFT) and a soil water deficit function (SWDF1). Each of these were modified.

4.2.1.1 PAR Interception

In WHV21, IPAR is calculated as an exponential function of green leaf area index (LAI):

$$IPAR = 1 - EXP(-k.LAI), \qquad 4.8$$

where k is the extinction coefficient (Kasanga and Monsi, 1954). In order to verify and modify this function, two experiments were conducted to obtain paired measurements of IPAR and LAI. These were the sowing date x seeding rate experiment at ART in 1989 (Section 2.3.2) and an unpublished cultivar x seeding rate experiment conducted by the author at ART in 1990. This latter experiment consisted of cultivars W170/84 and Sengwa sown at three seeding rates (6, 12 and 18 g m^{-2}) in a factorial experimental design replicated three times in randomized complete blocks. The plot size was 20 rows

at 0.2 m by 7.5 m, with a 0.5 m path between plots. Seed was sown by a small plot drill on 18 May, 1990 and resulting plant stands ranged from 94 to 363 plants m^{-2}. The trial was irrigated with a total of approximately 450 mm water and standard intensive management practices were applied to promote optimum growth.

At intervals through the season in both trials paired measurements of PAR interception and LAI were made. PAR interception was determined from the ratio of below- and above-canopy records of the difference in millivolt output from clear glass and infra-red filtered 380 mm long tube Delta-T (United Kingdom) solarimeters. The above-canopy measurements were taken at approximately 1.2 m above ground level, with the tubes horizontal and in the same orientation as the below-canopy measurements. For the below-canopy measurements, the pair of tube solarimeters were positioned level on the ground spanning a single row of wheat in the central portion of each plot. The records were taken between 12.00 and 14.00 local standard time on cloudless days. Although this procedure was similar to that used by Puckeridge and Donald (1967), it is recognised that interception is least at solar noon and may underestimate the daily integrated PAR interception (Hammer and Vanderlip, 1989). Unfortunately, lack of appropriate equipment precluded the use of integrated PAR measurements or the corroboration of the relationship between integrated PAR interception and instantaneous midday intercepted PAR, such as provided by Charles-Edwards and Lawn (1984).

The LAI was determined from randomly selected 0.18 m^2 (in the 1989 experiment) or 0.20 m^2 (in the 1990 experiment) whole plant samples. The samples were collected on the day of the PAR interception measurements, and the upper leaf blade area determined with an electro-optical system similar to that described by Clarke and McCaig (1985).

The relationship between IPAR and LAI for this data set is presented (Figure 4.4). The extinction coefficient, k, established from the least-squares nonlinear regression of IPAR on LAI was 0.31. The WHV21 model sets k = 0.85, while Singels (1990) used k = 0.45. As a first attempt, Eqn. 4.8 was modified by setting k = 0.31, but this resulted in insufficient dry

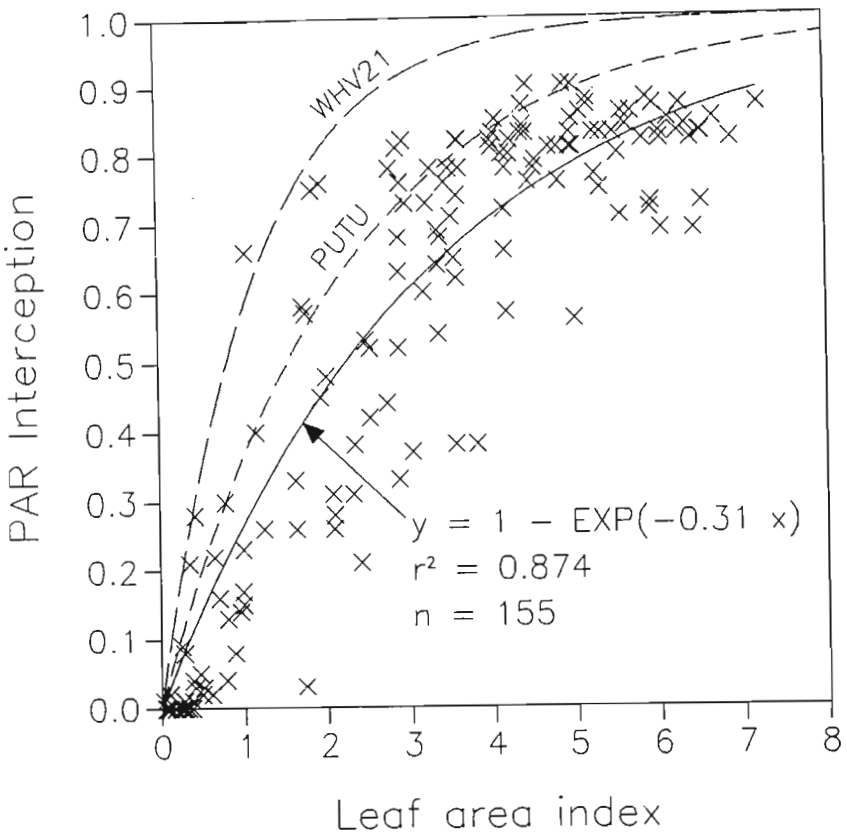

Figure 4.4: The relationship between PAR interception and leaf area index of wheat.

matter accumulation. Therefore, k was set equal to 0.45, as per Singels (1990).

On examination of the seasonal progression of PAR interception, it was noted that after ear emergence, IPAR remained high, even when LAI decreased due to leaf senescence. The wheat ear intercepts PAR and may contribute significantly to yield (Simpson, 1968). No relationship between IPAR and TPSM could be found in the literature. Therefore, as a first approximation, the following function was used to relate IPAR to ear density (TPSM) (Figure 4.5):

$$IPAR = 1 - EXP(-0.004 \times TPSM), \qquad 4.9$$

A small extinction coefficient was employed since ears tend to be of cylindrical form and maintain an erect architecture until maturity.

Since ears are only fully emerged from the canopy at about the time of anthesis, the following Fortran routine was included in WHVZIM22 to maintain IPAR at a maximum from

anthesis through to maturity:

```
IPAR1=(1-EXP(-0.45*LAI))
IPAR2=(1-EXP(-0.004*TPSM))
IF (ISTAGE.LE.3) THEN
    IPAR=IPAR1
ELSE
    IPAR=AMAX1(IPAR1,IPAR2)
ENDIF
```

In a well tillered crop (TPSM ≈ 400 tillers m^{-2}), IPAR will remain above 0.80 if the LAI declines below 3.6.

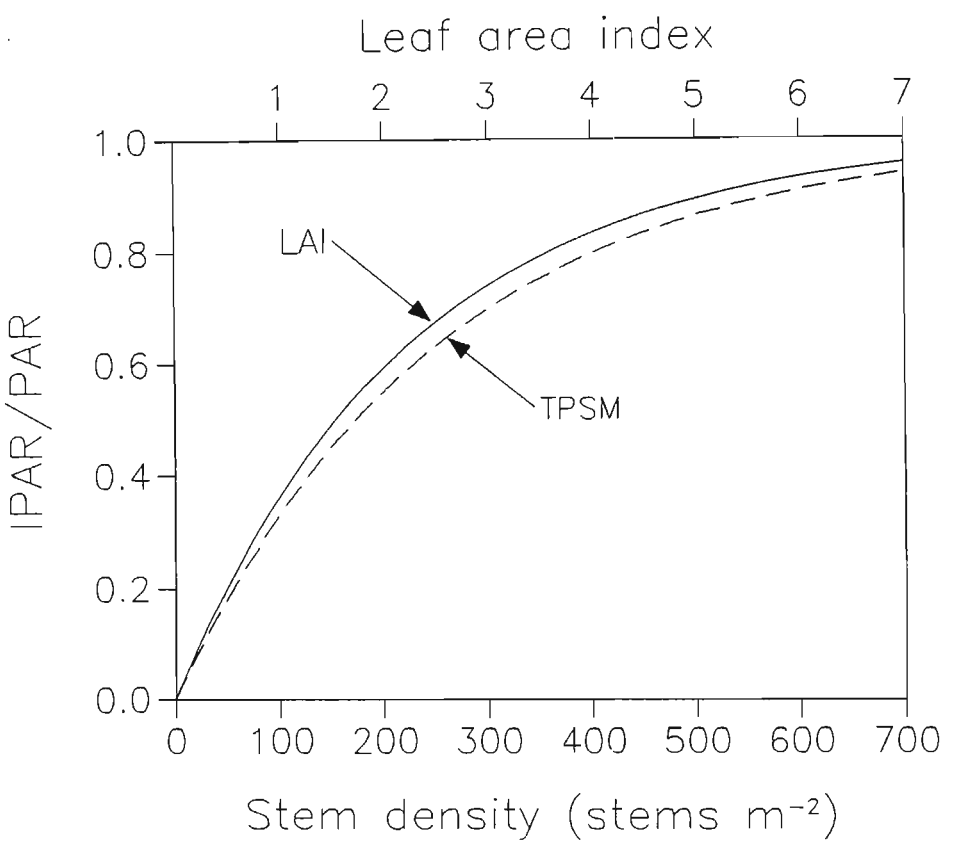

Figure 4.5: The interception of PAR as a function of leaf area index (LAI) and the number of tiller per square metre (TPSM) in the modified model, WHVZIM22.

4.2.1.2 Potential and actual dry matter production

Despite reducing the extinction coefficient, k, in Eqn. 1.1, from 0.85 to 0.45, dry matter production during the pre-anthesis growth stages remained greater than that measured in the calibration data sets. Therefore, the exponent of PAR in Eqn. 1.1 was reduced from 0.6 to 0.5, and the equation re-arranged:

$$PCARB = \frac{7.5 \times (IPAR \times PAR)^{0.5}}{PLANTS} \qquad 4.10$$

This improved the biomass predictions on the cooler sites, but when applied to a warm site such as SAVE (data sets 50 to 54, Table 2.3), yields were very much lower than observed. This was ascribed to incorrect air temperature functions: DT (daytime air temperature) and PRFT.

With the use of the hourly air temperature data set collected at ART (Section 2.2.1), the function used to determine DT was re-evaluated. It was found that DT calculated from

$$DT = 0.75 \times TEMPMX + 0.25 \times TEMPMN \qquad 4.11$$

over-predicted the mean daytime temperature computed from the mean of the mean hourly temperatures from the sixth to the seventeenth hour. By iteration, the following function was incorporated in WHVZIM22:

$$DT = 0.70 \times TEMPMX + 0.30 \times TEMPMN. \qquad 4.12$$

This improvement in predicting DT is shown (Figure 4.6).

The photosynthetic reduction factor for temperature (PRFT) in WHV21 is a parabolic function with an optimum of 18 °C and a range of 20 °C on either side of the optimum. This function was considered inadequate, in that PCARB is reduced below optimum whenever DT is not equal to 18 °C, whereas van Keulen and Seligman (1987), citing Wardlaw (1974), state that optimum photosynthetic performance of wheat occurs over a wide temperature range under field conditions. Furthermore, in light of the poor performance of WHV21 under warm conditions (data sets 50 to 54), it was considered necessary to maintain CARBO

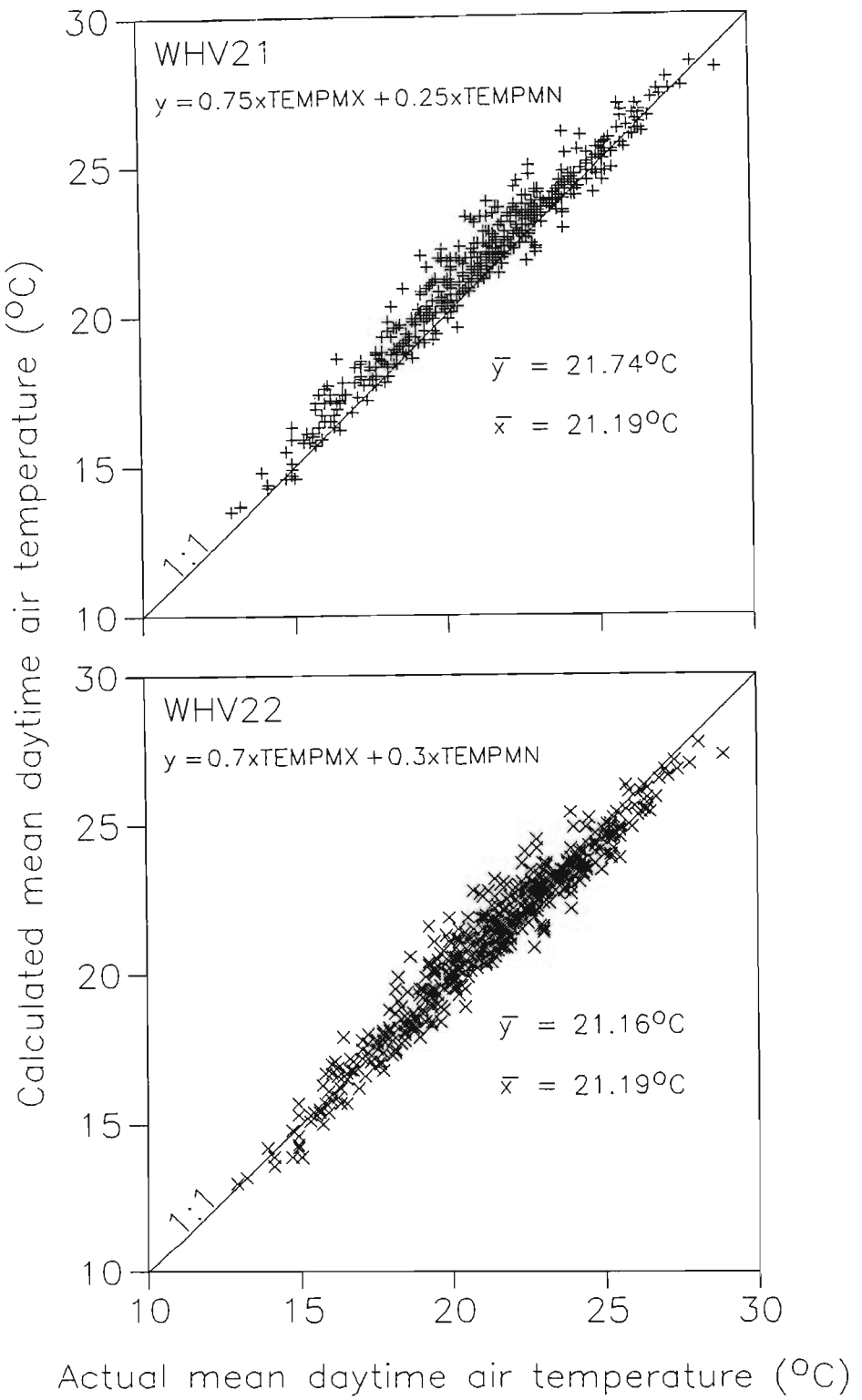

Figure 4.6: Comparison of the calculated mean daytime air temperature with the actual mean daytime air temperature of WHV21 and WHVZIM22 on a data set collected at ART.

at an optimum level over as wide a temperature range as possible. Consequently, the photosynthetic temperature function of van Keulen and Seligman (1987) was used in place of that given in WHV21. This function is illustrated and compared with the PRFT function of WHV21 in Figure 4.7.

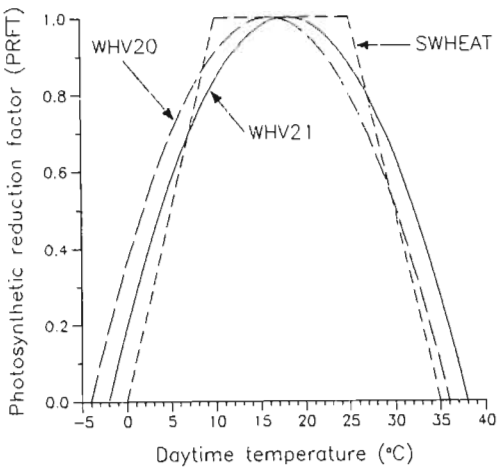

Figure 4.7: The photosynthetic reduction factor for temperature (PRFT) of an old version of CERES-Wheat (WHV20), a recent version (WHV21) and of SWHEAT (van Keulen and Seligman, 1987).

Potential dry matter production is also moderated by a soil water deficit factor (SWDF1), which in WHV21 is a linear function of the ratio of actual root water uptake to potential plant evaporation (TRWU/EP1). Although photosynthesis has been shown by Johnson, Frey and Moss (1974) to be linearly related to plant evaporation, their experiment was conducted in confined soil volumes where the plants may not have had the opportunity to adjust to stress imposition. Shimshi, Mayoral and Atsmon (1982), noted that the decrease in CO_2 fixation with decreasing Ψ_{leaf} was more gradual than the corresponding decrease in leaf permeability. They concluded that this may indicate that stomatal closure was not the major factor controlling CO_2 fixation, whereas stomatal closure is closely related to a decrease in transpiration. However, in a review on water stress and plant growth, Turner and Burch (1983) stated that decreases in the rate of photosynthesis as a result of water deficits generally arise from stomatal closure. They also concluded that, in general, stomatal resistance remains low as Ψ_{leaf} decreases until a threshold potential is reached below which

stomatal resistance increases markedly, although this threshold potential varies with species, leaf position within the canopy, leaf age, growth conditions and rate of stress imposition.

The SWDF1 function is a direct expression of canopy conductance in that it relates root water uptake to potential EP. Indirectly, the SWDF1 factor is an expression of Ψ_{leaf}, in that the balance between TRWU and plant evaporation dictates Ψ_{leaf} responses. Therefore, it may be concluded that reductions in PCARB due to water deficit are not a linear function of TRWU/EP1, but rather a curvilinear function, where reductions to PCARB become progressively greater as the magnitude of the stress increases. SWDF1 was thus changed:

$$SWDF1 = 1-(1-TRWU/EP1)^{1.5} \qquad 4.13$$

This is illustrated together with the original WHV21 function (Figure 4.8). It should be noted that the function approaches linearity when TRWU/EP1 decreases below about 0.6.

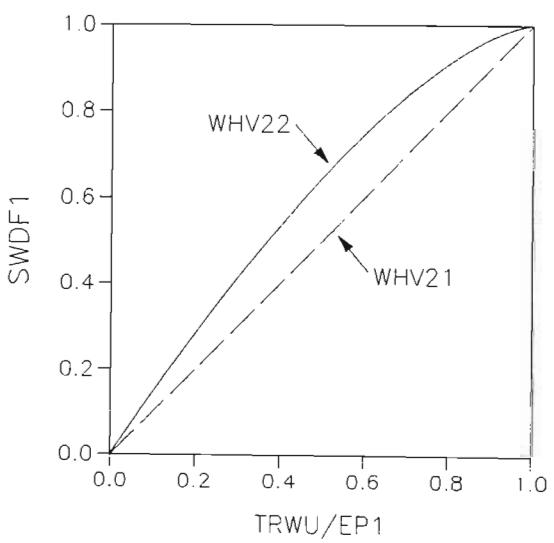

Figure 4.8: The soil water deficit factor number one (SWDF1) of WHV21 and WHVZIM22 as related to the actual root water uptake to potential eveporation ratio (TRWU/EP1).

In growth phase five, WHV21 has a function to simulate the influence of leaf aging and assimilate demand on the rate of photosynthesis:

$$CARBO = CARBO \times \left[1-\left(1.2-0.8\times\frac{SWMIN}{STMWT}\right)\times\frac{SUMDTT+100}{P5+100}\right], \qquad 4.14$$

where SWMIN is the stem weight (STMWT, g plant^{-1}) at the end of pre-anthesis ear growth. It was apparent from the validation of WHV21 under deficit-irrigated conditions that kernel mass was underpredicted (Section 3.3.3). This was partly attributed to this leaf aging/assimilate demand function (Eqn. 4.14). After numerous attempts to improve this function without success, it was discarded in favour of a simpler leaf aging function:

$$CARBO = CARBO \times [1 - 10000\,(SUMDTT - 0.9 \times P5)^4 / P5^4] \qquad 4.15$$

which is only called when SUMDTT is greater than 0.9 x P5.

4.2.1.3 Assimilate partitioning

The WHV21 model partitions assimilate between roots and shoots in discrete proportions as a function of growth phase (Table 1.6). These were changed with the objective of making PTF a continuous function of crop age.

Throughout growth phase one, WHV21 sets the minimum daily root growth as 0.35 x CARBO. The balance of CARBO is partitioned to leaf growth. In WHVZIM22, at plant emergence the PTF is set at 0.5, but is increased with crop age to 0.7 at the end of ISTAGE 1 (Table 4.13). This modification was based on the data presented by van Keulen and Seligman (1983). The minimum daily root growth was set as (1 - PTF) x CARBO, with the balance of CARBO partitioned to leaf growth, as in WHV21. For each of the other growth phases, PTF was made a function of SWDF1 and crop age. In ISTAGE 5, PTF was set at 1.00 and the function in WHV21 relating PTF to the ratio of SWMIN:STMWT was removed.

Table 4.13: The proportion of CARBO partitioned to shoot growth (PTF) as a function of SWDF1 and crop age in WHVZIM22.

ISTAGE	PTF
1	≤ 0.50 + 0.20 x TDU/P1
2	0.60 + 0.10 x SWDF1 + 0.15 x SUMDTT/P2
3	0.80 + 0.05 x SWDF1 + 0.05 x SUMDTT/P3
4	0.85 + 0.05 X SWDF1 + 0.10 x SUMDTT/P4
5	1.00

During ISTAGE 2, stem growth begins. In WHV21, the proportion of shoot CARBO assigned to stem growth (GROSTM) is a linear function of crop age:

$$GROSTM = (0.15 + 0.12 \times SUMDTT / PHINT) \times CARBO \times PTF \qquad 4.16$$

Thus, at the start of ISTAGE 2, GROSTM consumes 0.15 of CARBO x PTF, and at the end of ISTAGE 2, GROSTM consumes 0.51 of CARBO x PTF. This function (Eqn 4.14) was changed to an exponential equation (4.15) for three reasons. Firstly, it was observed in the field that stem growth was initially slow. Secondly, at the start of phase two, leaf growth is still a major component of plant growth. Thirdly, at the end of phase two, stem growth is probably a greater proportion of CARBO x PTF than 0.51, as used by WHV21, since leaf growth is drawing to an end with the emergence of the flag leaves.

$$GROSTM = (0.05 \times EXP(2.65 \times SUMDTT / P2)) \times CARBO \times PTF \qquad 4.17$$

Thus, in WHVZIM22, at the start of phase two, GROSTM consumes 0.05 of CARBO x PTF, but at the end of phase two, GROSTM consumes 0.71 of CARBO x PTF.

During stem growth, WHV21 allows a proportion of STMWT to be consumed for respiratory loss. This loss is a constant proportion of DTT. Since the T_b of the DTT calculation was changed in WHVZIM22, the STMWT respiratory loss constant was changed from 0.000267 to 0.000375 g plant^{-1} °C^{-1} d^{-1}.

4.2.2 Leaf area accumulation and senescence

As indicated in Section 3.2.5.2, WHV21 tended to under-predict LAI. Therefore, it was considered necessary to modify the functions in WHV21 to improve LAI predictions.

In WHV21, leaf area production during phase one is calculated from the product of the rate of leaf appearance and the rate of expansion of growing leaves. In WHVZIM22, the leaf emergence rate (TI, based on PHINTLE) was used in place of the leaf appearance rate. Thus,

$$TI = DTT / PHINTLE, \qquad 4.18$$

where PHINTLE is growth stage dependent (Section 4.1.2).

In order to evaluate the relationship between plant leaf area growth on the main stem (PLAGMS) and leaf emergence, data were collected in the wheat irrigation dry down experiment at GLEN in 1989 (data set 116). At plant emergence, three plants were selected in each of the four plots. At the emergence of each main stem leaf on these plants, the length and breadth of the leaf was measured, and the leaf area (cm^2) calculated as the length (mm) x breadth (mm) x 0.00867. This coefficient was derived from the wheat growth analysis trial (Section 3.2.5.1). The cumulative main stem leaf area was plotted against leaf number and an exponential curve was fitted by eye to the data (Figure 4.9). This was differentiated for use in WHVZIM22:

$$\frac{dPLAGMS}{dCUMPH} = 2.7 \times EXP(0.3 \times CUMPH) \qquad 4.19$$

The daily PLAGMS is calculated from the product of *dPLAGMS/dCUMPH* and the daily phyllochron interval (TI).

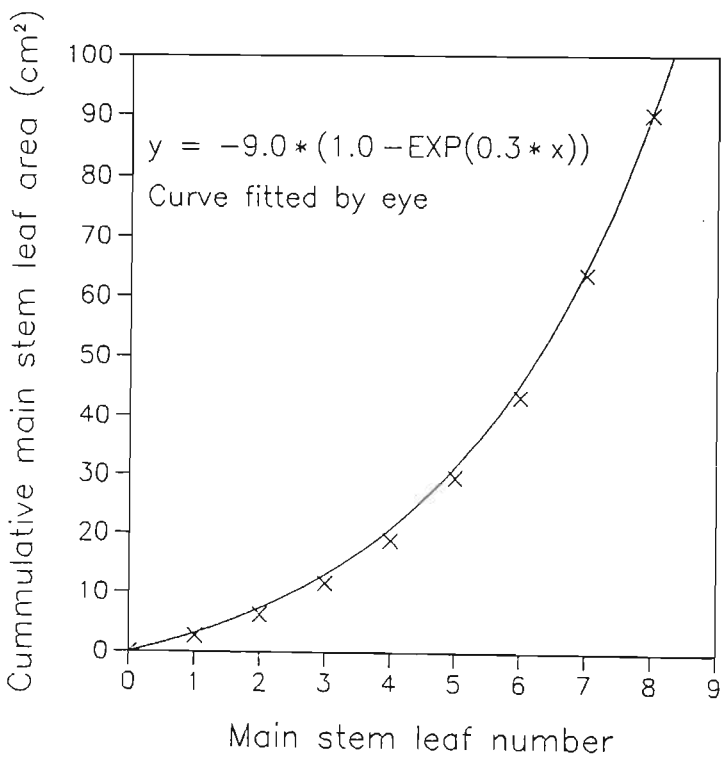

Figure 4.9: The cumulative main stem leaf area as a function of the emerged leaf number of wheat.

In WHV21, daily PLAGMS is moderated by a temperature factor (EGFT) and SWDF2. It was found that under severe stress (e.g., data set 110), SWDF2 was indequate in reducing PLAGMS. Therefore, another water deficit factor (W1) was introduced. This reduces PLAGMS when the soil water content in the top soil layer declines below 0.2 of the extractable soil water in that layer:

$$W1 = (SW(1) - LL(1)) / (DUL(1) - LL(1)) \quad 4.20$$

$$IF\ W1 < 0.2,\ W1 = W1 \times 5 \quad 4.21$$

$$IF\ W1 \geq 0.2,\ W1 = 1.0 \quad 4.22$$

The daily total plant leaf area growth (PLAG) in WHV21 is calculated from:

$$PLAG = PLAGMS \times (0.3 + 0.7 \times TILN) \quad 4.23$$

However, this relationship had to be changed because of modifications made to the tillering routines (see Section 4.3):

$$PLAG = PLAGMS \times (0.4 + 0.6 \times TILN) \quad 4.24$$

Leaf growth is calculated from

$$GROLF = PLAG / AWR, \quad 4.25$$

where AWR is the upper leaf blade area to leaf blade plus sheath dry mass ratio ($cm^2\ g^{-1}$). In WHV21 during phase one growth, the AWR is dependent on plant age:

$$AWR = 150 - 0.075 \times TDU, \quad 4.26$$

where TDU is the cumulative thermal development units in phase one. During phase two, WHV21 uses an AWR of 115 $cm^2\ g^{-1}$.

In a study of wheat in wide ranging tropical environments, Midmore, Cartwright and Fischer (1984) noted that the specific leaf area at 35 das varied substantially (a range of 192 to 480 $cm^2\ g^{-1}$). However, it was not clear whether their reported specific leaf areas included leaf sheath dry mass or not. On the other hand, van Keulen and Seligman (1983) stated that the specific leaf area of wheat generally varies between narrow bounds around 200 $cm^2\ g^{-1}$ (excluding leaf sheath dry mass).

In order to clarify this, leaf area and leaf dry mass data collected from the wheat sowing date x cultivar experiments at ART in 1988 and 1989 were examined. Data appropriate to growth phase one (GS22 from ART 1988) gave a mean AWR of 208 $cm^2\ g^{-1}$ ($\pm 17.8\ cm^2\ g^{-1}$, n = 20). For growth phase two, a linear regression of the leaf blade area on the leaf blade plus sheath dry mass was computed using all data for GS22, GS31 and GS39 (except WPDA8811 GS31, WPDA8815 GS39 and WPDA8921 GS31, which appeared erroneous). This regression (Figure 4.10) gave a mean AWR of 125 $cm^2\ g^{-1}$ ($\pm 3.1\ cm^2\ g^{-1}$, n = 97). Based on these results, Eqn 4.26, was modified for inclusion in WHVZIM22:

$$AWR = 200 - 75 \times TDU / P1 \qquad 4.27$$

Thus, during phase one, AWR declines from 200 to 125 $cm^2\ g^{-1}$. In growth phase two, the AWR was set at 125 $cm^2\ g^{-1}$ in WHVZIM22.

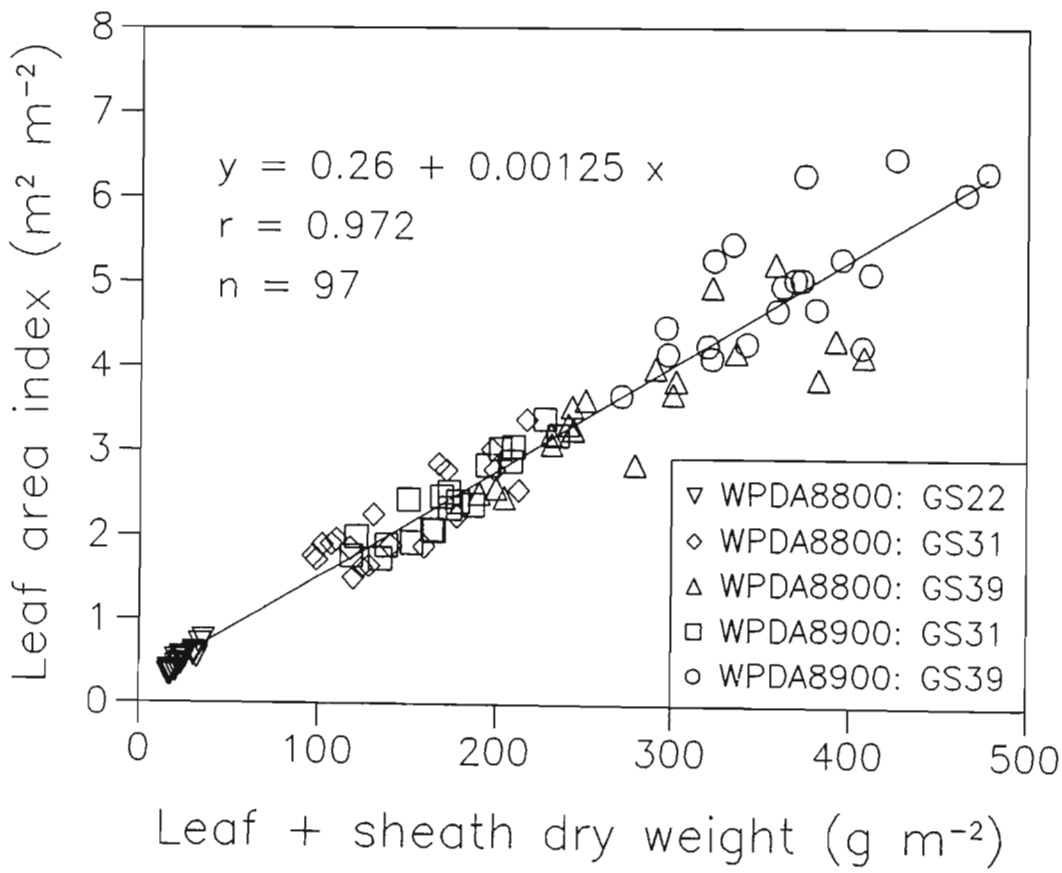

Figure 4.10: The relationship between leaf area index and the leaf plus sheath dry mass.

During growth phase two, the WHV21 model acts to reduce leaf area *via* reducing CARBO and PTF by coefficient SWDF1. This was considered to be inadequate because leaf expansion is known to be one of the physiological processes most sensitive to water stress (Hsiao, 1973). Boyer (1970) noted that upon the imposition of water stress, the rate of leaf enlargement of soyabean, sunflower and maize was affected earlier than the rate of photosynthesis. He proposed that this may lead to an accumulation of photosynthate either in the leaf or other portions of the plant. This suggests that the AWR may decline under conditions of mild stress, when leaf enlargement is restricted but not photosynthesis. Therefore, the AWR was moderated by SWDF2, so as to reduce plant leaf area accumulation under conditions of stress which do not necessarily reduce CARBO or PTF:

$$PLA = PLA + GROLF \times 125 \times SWDF2, \qquad 4.28$$

where PLA is the total cumulative plant leaf area ($cm^2 \cdot plant^{-1}$), GROLF is the proportion of CARBO partitioned to leaf growth ($g\ plant^{-1}$) and 125 is the AWR ($cm^2\ g^{-1}$).

Leaf area decline between GS39 and GS71 appeared to be too rapid in WHV21 (see Section 3.2.5.2). Consequently, in growth phase three, the function used to calculate the plant leaf area loss rate (PLALR) in WHV21 was changed from

$$PLALR = 0.0003 \times DTT \times GPLA \qquad 4.29$$

to

$$PLALR = 0.0002 \times DTT \times GPLA, \qquad 4.30$$

where GPLA is the green plant leaf area ($cm^2\ plant^{-1}$).

Finally, it was noted that at physiological maturity leaf weight (LFWT, $g\ plant^{-1}$) comprised a large proportion (ca. 15 %) of BIOMAS with WHV21, whereas observations in data sets 10 to 14 showed that LFWT usually comprised a smaller proportion (ca. 9 %) of BIOMAS at physiological maturity. Consequently, the leaf weight loss routine of WHV21 was modified from

$$LFWT = LFWT + GROLF - LFWT \times 0.000267 \times DTT \times (1 - SENLA/PLA) \qquad 4.31$$

to

$$LFWT = LFWT + GROLF - LFWT \times 0.005 \times DTT \times SENLA^2 / PLA^2, \qquad 4.32$$

where SENLA is the cumulative senescent leaf area (cm^2 $plant^{-2}$).

4.2.3 Tillering

The ability of WHV21 to predict the tillering patterns of the data sets in this study was weak (Section 3.2.4 and 3.3.3). Therefore, the tillering routines of WHV21 underwent extensive revision. These revisions were based on the fact that the primary determinants of tillering are air temperature, solar irradiance, plant density and plant water status. Nutrition, especially N nutrition, is important for tillering but is not considered here for the reasons given in the Introduction.

Field observations of the tillering of wheat in all the data sets exhibited the same basic pattern: tillering began when the plant had two to four main stem leaves; tiller numbers then increased rapidly and reached a peak at about the time of TS or GS31; thereafter they declined in number through to the early grain-fill period. In nearly every data set, except those severely water-stressed, stem numbers were greater at TS than at plant emergence and maturity, while ear counts at harvest were greater than plant counts at emergence. Based on these general observations, tillering was made to begin earlier in growth phase one, the rate of tillering in growth phase one was made a function of plant density, air temperature and solar irradiance, and the modified tiller dry matter accumulation routines were extended into growth phase four.

From the sowing date x seeding rate experiments (Table 2.4), the reciprocal of the tiller production rate per unit solar irradiance (tillers $plant^{-1}$ $(MJ\ m^{-2})^{-1}$) and per daily thermal time (tillers $plant^{-1}$ $(°C\ d)^{-1}$) between 14 das and peak tiller number for each treatment were plotted against plant density (Figure 4.11). These plots indicated that as plant density increased, the production of each tiller required the accumulation of a greater amount of thermal time and solar irradiance.

The interaction of air temperature and solar irradiance on tillering has been demonstrated by Friend (1965). His data

indicated that over a wide range of air temperatures (10 to 30 °C), the tiller production rate increased with increasing light intensity[5], but at a decreasing rate depending on temperature (Figure 4.12). Tillering was greatest over all light intensities and at an air temperature of 20 °C. At high light intensities (> 1000 ft-candles) tillering appeared to be limited by cool air temperatures (< 20 °C), whereas at high air temperatures (> 25 °C), tillering was reduced over the full range of light intensities.

In order to simulate these interacting effects (Figures 4.11 and 4.12), the following Fortran statements were included in growth phase one of WHVZIM22 to replace the WHV21 tiller production routine:

```
600     IF (CUMPH.LT.2.5) GOTO 700
        TC1=DTT/(0.52*PLANTS)
        TC2=SOLRAD/(0.79*PLANTS)
        TRF=1
        IF(DTT.GT.20)THEN
           TRF=1-(DTT-20)/12
           IF(TRF.LT.0)TRF=0.
        ENDIF
        TILN=TILN+TRF*AMIN1(W1,SWDF2)*AMIN1(TC1,TC2)
700     IF(TILN.LT.1)TILN=1
```

where CUMPH = the cumulative phyllochrons (emerged leaves) after emergence,

TC1 = tiller no. increment per daily thermal time as a function of plant density,

TC2 = tiller no. increment per unit daily irradiance as a function of plant density, and

TRF = tillering reduction factor for air temperatures greater than 24 °C.

The W1 soil water deficit factor (Eqn 4.20) was included in this routine because it was noted in data set 110, which received no irrigation after plant emergence, that tillering was markedly reduced once the surface soil had dried despite the total profile water content being relatively high. Nodal

---

5 currently an inappropriate measure in the plant sciences

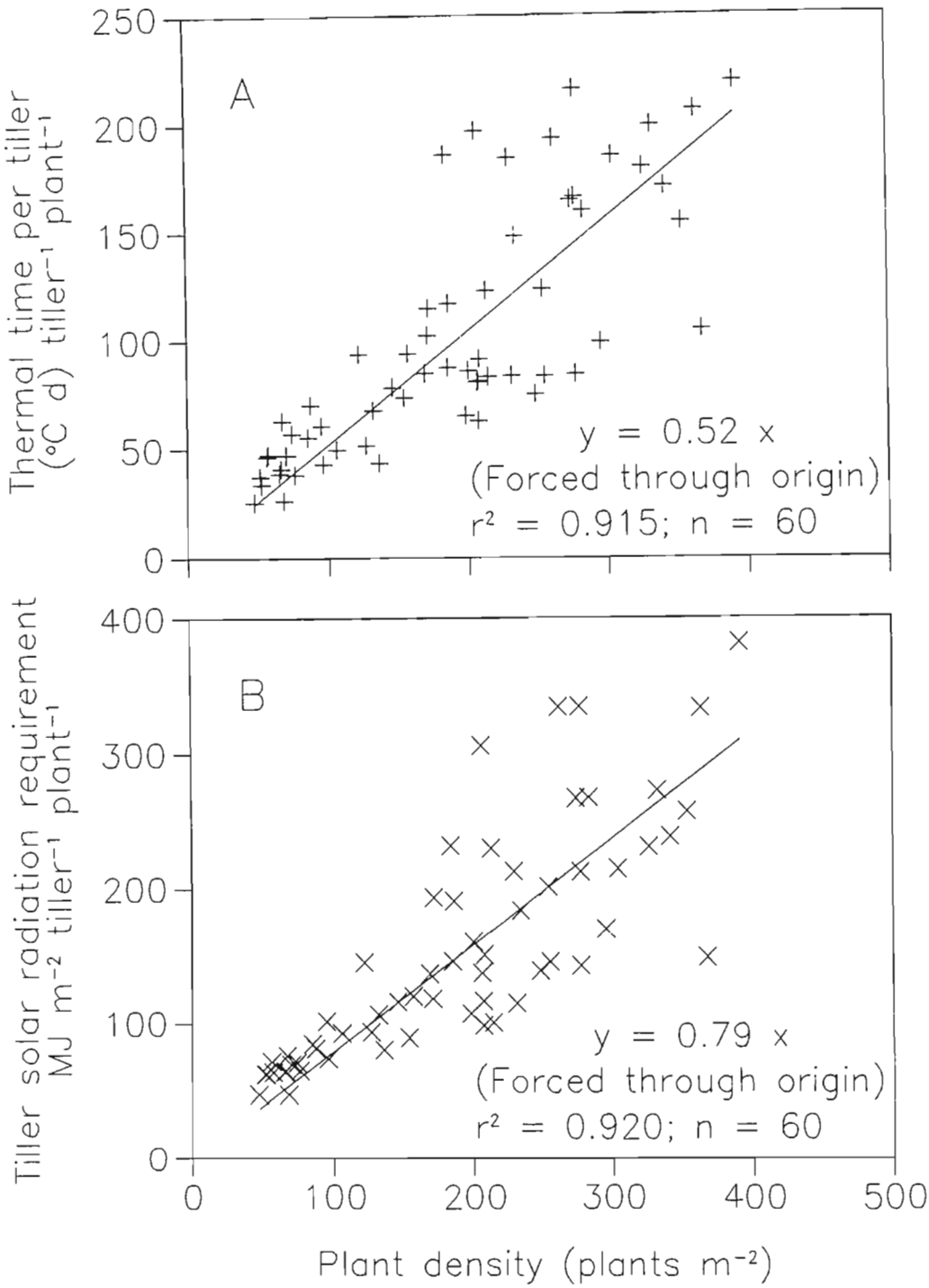

Figure 4.11: The A. thermal time (T_b = 4 °C) and B. solar irradiance requirement for tiller production as a function of plant density.

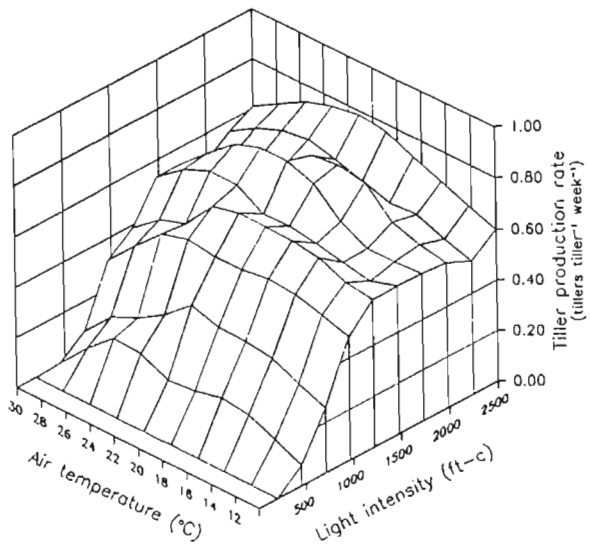

Figure 4.12: The interaction of light intensity and air temperature effects on the tiller production rate of wheat (data from Friend, 1966).

root growth is inhibited by dry surface soil (Musick and Porter, 1990) and roots arising and supporting developing tillers tend to be shallower than seminal and mainstem nodal roots (Rickman, Klepper and Belford, 1985). Therefore, it may be expected that dry surface soil would reduce tillering of wheat, especially in early growth phases.

The simulated interaction of mean daily air temperature and daily solar irradiance (MJ m^{-2}) on the tiller production rate of wheat at a plant density of 150 m^{-2} is illustrated (Figure 4.13). It shows that at mean daily air temperatures of 20 to 24 °C, the tiller production rate increases linearly with irradiance. At higher mean daily air temperatures, tiller production rate declines over all levels of irradiance and is zero at a mean daily air temperature of 36 °C. At mean daily air temperatures less than 20 °C, the tiller production rate increases with irradiance up to a point whereafter temperature limits tillering regardless of the level of irradiance.

In the WHV21 model, tiller production and senescence during growth phases two and three is dependent on the balance between the assimilate available (i.e., the actual daily stem growth, STMWT) and the number of tillers that this assimilate can support for growth, based on the potential growth of a single tiller under optimum conditions. As given in Section 4.2.1, the function to predict STMWT in growth phase two was changed (Eqn

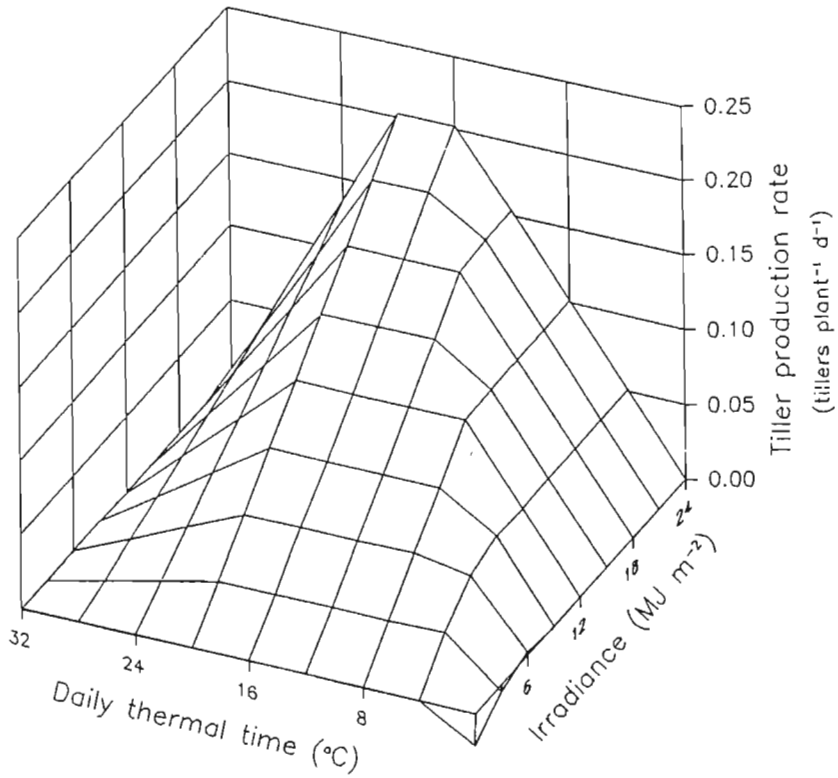

Figure 4.13: Illustration of the tiller production rate function used in WHVZIM22.

4.17). Thus, the equations to predict optimum tiller growth also had to be changed. Tillering was also extended into growth phase four. These changes were made through iteratively assessing and improving modifications on the sowing date x seeding rate calibration data set.

In growth phase two, the function to predict the optimum mass of a single tiller (TILSW, g tiller^{-1}) was changed to an exponential function, in line with the exponential function used to predict STMWT:

$$TILSW = TILSW + G3 \times 0.0004 \times EXP\left[(1.425 - 0.0008 \times (PLANTS - 90)) \times \frac{SUMDTT}{PHINTLE}\right] \quad 4.33$$

The effect of plant competition was included in Eqn 4.33, so as to decrease the potential gain in TILSW under high plant densities.

During phases three, TILSW was simulated by:

$$TILSW = TILSW + G3 \times DTT \times 0.0035, \quad 4.34$$

while TILSW was simulated by

$$TILSW = TILSW + G3 \times DTT \times 0.003, \qquad 4.35$$

during growth phase four.

Once the optimum tiller stem mass (TILSW) has been calculated, the model adjusts tiller numbers with a function that uses the ratio (RTSW) of the actual stem mass (STMWT) to the potential tiller mass (TILSW x TILN). If STMWT is less than the potential tiller mass (i.e., RTSW < 1) then tiller numbers are decreased. Observations showed that tiller numbers also decrease under conditions of soil water deficits. Thus, the RTSW function used to adjust tiller numbers was moderated by soil water deficit factors. In growth phase two,

$$RTSW = \frac{STMWT + GROSTM}{TILSW \times TILN} \times AMIN1(W1, SWDF2), \qquad 4.36$$

while in growth phases three and four,

$$RTSW = \frac{STMWT + GROSTM}{TILSW \times TILN} \times SWDF1. \qquad 4.37$$

This ensured that under water deficits, tiller senescence was increased.

During growth phase one, tillering was assumed not to be under genetic control, as in WHV21. During growth phases two, three and four, the genetic coefficient used to control TILSW, G3, was retained, but because the equations used to predict TILSW were changed, the equation used to convert the scaled G3 coefficient to the actual G3 coefficient (in subroutine *ECHO*) also had to be changed:

$$G3_{actual} = 0.35 \times G3_{scaled}, \quad 0 < G3_{scaled} \leq 6. \qquad 4.38$$

The new scaled and actual G3 coefficients for the four cultivars used in this study (Table 4.14) were set by iteration on the well-watered calibration and validation data sets.

Table 4.14: The scaled and actual G3 genetic coefficients ($G3_{scaled}$ and $G3_{actual}$, respectively) for the four wheat cultivars used in the WHVZIM22 model.

Cultivar	$G3_{scaled}$	$G3_{actual}$
	g tiller^{-1} d^{-1}	
W170/84	4.0	1.40
Sengwa	3.4	1.12
Rusape	3.9	1.37
Angwa	3.3	1.16

4.2.4 Kernel numbers and the effect of frost

The WHV21 model calculates the number of kernels per plant (GPP) from the product of STMWT at the end of growth phase four (i.e., GS71) and a genetic coefficient (G1). In order to verify this, the STMWT at GS71 and GPP data collected from the sowing date x cultivar trials at ART 1988, 1989 and 1990 and from RARS in 1988, and from the sowing date x seeding rate trial conducted at ART in 1990 were analysed. It was found, however, that because of the difficulty of visually determining GS71 in the field, the STMWT data at GS71 was variable. Consequently, the STMWT data at GS61 was utilized. For each cultivar, regressions, of the form $y = bx$, of GPP on STMWT at GS61 were computed (Table 4.15).

Each regression was highly significant. The slope for cultivar W170/84 was significantly less than that for Sengwa but neither was different from Rusape or Angwa. W170/84 is a tall-strawed, leafy cultivar, and therefore the lower G1 coefficient for this cultivar compared to that of Sengwa was not surprising. This supports the concept of a genetic coefficient for kernel number determination.

Thus, the basic function to compute GPP from the product of STMWT and G1 was retained, but the function was moved from the end of growth phase four to the time of anthesis. This would facilitate future verification of this relationship.

Table 4.15: Statistical parameters for the linear regressions of the number of kernels per plant on the stem plus ear dry mass (STMWT) at anthesis of four wheat cultivars using calibration data sets 1 to 14, 25 to 24 and 61 to 63.

	Cultivar			
Parameter	W170/84	Sengwa	Rusape	Angwa
n	17	28	17	17
slope (kernels g^{-1})	49.1	58.6	55.4	54.6
SE slope (kernels g^{-1})	1.98	1.34	2.82	3.43
slope 95 % confidence interval	(44.9, 53.5)	(55.8 61.3)	(49.5 61.4)	(47.3 61.9)
r	0.987	0.993	0.980	0.970

From Table 4.15, the actual G1 genetic coefficient averaged 54.4 kernels (g STMWT)$^{-1}$ at anthesis. For input purposes in file *GENETICS.WH9*, the G1 coefficient was scaled from zero to six and converted to the actual G1 coefficient in subroutine *ECHO* by

$$G1_{actual} = 20 + 10 \times G1_{scaled}, \quad 0 < G1_{scaled} \leq 6. \qquad 4.39$$

The new scaled G1 genetic coefficients used in WHVZIM22 for the four cultivars are given (Table 4.16). These were established by iteration on the sowing date x cultivar calibration and validation data sets.

Table 4.16: The scaled, actual and measured G1 genetic coefficients for the four wheat cultivars used in the WHVZIM22 model.

Cultivar	Scaled	Actual	Measured
	kernels g^{-1}		
W170/84	3.2	52	49
Sengwa	3.4	54	59
Rusape	3.3	53	55
Angwa	2.9	49	55

Frost is a sporadic but potentially disastrous problem in wheat production in Zimbabwe (Alvord, 1971; Mashiringwani, 1990b). This is because wheat is grown during winter and frost around the time of anthesis may cause floral sterility and reductions in kernel numbers. Although factors such as the rate of temperature decline, plant cold hardening, the presence or absence of ice nucleators (including certain bacteria) and the plant part and growth stage affect the extent of cold temperature injury to wheat (Gusta and Chen, 1987), it is generally recognised that the reproductive structures may be injured by air temperatures below -1.8 °C between the time of ear emergence and early grainfill (Livingstone and Swinbank, 1950; Single and Marcellos, 1974; Single, 1985).

Although Mashiringwani (1990b) reported that cultivars may show differential response to frost during reproductive growth, his results were not conclusive and there are no "frost resistant" cultivars available to Zimbabwean farmers. Therefore, the recommended strategy to avoid frost damage is to time plantings so that anthesis occurs when the probability of frosts is low (Alvord, 1971; MacRobert, 1990). The problem with this, though, is that it may cause the grainfill period to occur during the warm to hot weather of spring and thereby reduce potential kernel mass, and early rain may interfere with harvest and reduce kernel quality. In view of this constraint to wheat production in Zimbabwe, it was considered necessary to incorporate a function in CERES-Wheat that would account for frost or low temperature damage to kernel numbers.

Frost in Zimbabwe is mostly of the radiation type (Law, 1979), requiring clear skies, calm winds and a dry atmosphere for its occurrence. Two types of radiation frost are recognised (Savage, 1980): 1. Black frost, which occurs when vegetation is frozen without the formation of ice crystals on the vegetation surface. The meteorological condition associated with black frost is when the air and vegetal temperatures are less than 0 °C but above the dewpoint temperature. 2. Hoar frost or white frost is the deposition of interlocking ice crystals, formed by sublimation, on exposed objects. The temperature condition required for hoar frost is for the air and object temperatures to be both less than 0 °C and less than or equal to the dewpoint

air temperature. Hoar frosts are generally less damaging than black frosts, because with black frosts it is the cell sap that freezes, causing a disruption of cell activity often resulting in cell death. With hoar frost, during the formation of surface ice, energy is released by the latent heat of fusion, which is absorbed by the vegetal surface. The ice formed in a hoar frost may also act as an insulator against further vegetal temperature decrease.

The problem of simulating cold temperature damage to kernel numbers lie firstly in predicting the exposed minimum air temperature from the screened minimum air temperature, and secondly in establishing a relationship between the exposed minimum air temperature and the extent of injury. These two factors are considered independently.

Law (1968) presented a simple means of forecasting frost at night from the previous-day's wet- and dry-bulb temperatures. However, the minimum weather data set used by WHV21 does not include the wet-bulb temperature and so this method was unsuitable in this instance. Law (1979), however, presented another simple model for prediciting the probability of frost occurrence over Zimbabwe. This model was based on four general observations: 1. due to the latitude effect alone, frost may be expected more in the south of Zimbabwe than the north; 2. the average winter season dewpoint temperatures are lower in the south-western parts of Zimbabwe than the north-eastern parts; 3. frost is more likely at high than low altitude; and 4. there is a tendency for frost to occur more frequently in valleys and lower slopes than on upper slopes and mountains. Law rationalized these four factors into three correction indices, which when summed for a particular location gives an estimate of the number of occasions per year when the air temperature at ground level is expected to decrease below 0 °C. The lower the total correction factor, the greater the frequency of ground air temperatures less than 0 °C. These correction factors were: 1. a combined latitude and dewpoint correction factor (Figure 4.14); 2. an altitude correction factor, which ranged from 9 at low altitude to -6 at a high altitude; and 3. an exposure factor (Figure 4.15).

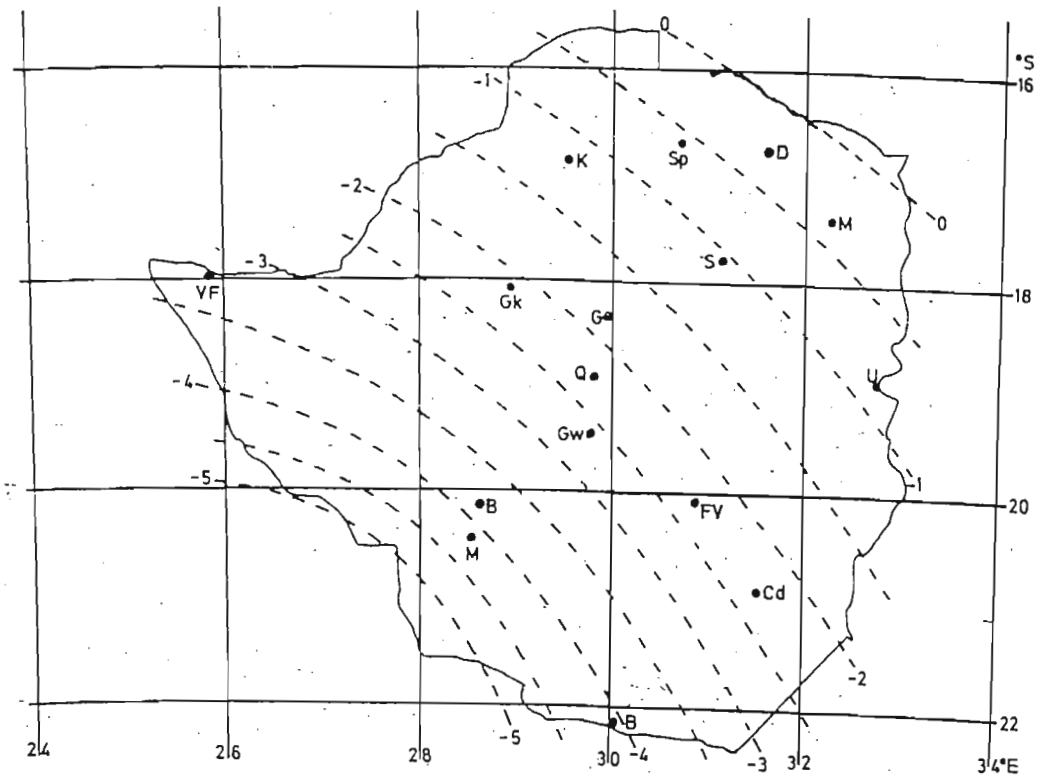

Figure 4.14: Map of Zimbabwe showing the isolines of the combined latitude and dewpoint correction factor (from Law, 1979). The greater the correction factor, the less likelihood of frost occurrence.

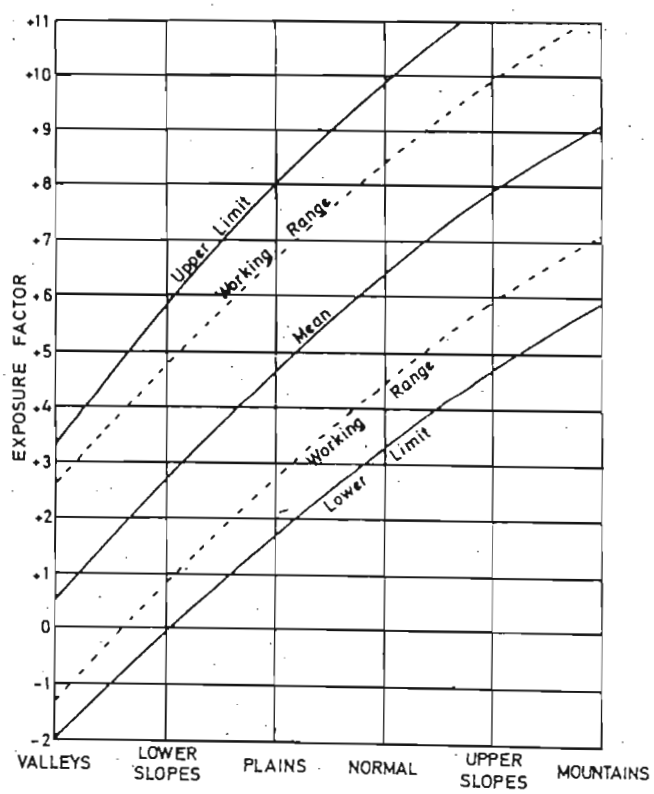

Figure 4.15: The exposure factor for frost incidence (from Law, 1979). The greater the factor, the less the likelihood of frost occurrence.

This scheme of Law (1979) was used as a basis to predict the exposed minimum air temperature from the screened minimum air temperature (TEMPMN, °C). The map given by Law (1979) to estimate the combined latitude and dewpoint correction factor (LATFACT; Figure 4.14) was converted to a mathematical function by multiple nonlinear regression analysis:

$$LATFACT = 8.7 - 0.0518 \times LAT^2 - 0.00564 \times XLONG^2 + 0.0000395 \times (LAT \times XLONG)^2. \quad 4.40$$

The altitude correction factor (ALTFACT) was converted to a mathematical function by linear regression analysis:

$$ALTFACT = 12.06 - 0.00987 \times ALT, \quad 4.41$$

where ALT is the altitude, m above mean sea level, of the site and is read into WHVZIM22 from the weather file (*FILE 1*) by subroutine *IPWTH*. The exposure factor (EXPFACT) is estimated for a location from Figure 4.15 and input into WHVZIM22 by subroutine *IPWTH* from the weather file (*FILE 1*). In subroutine *IPWTH*, the total correction factor (TF) is calulated as

$$TF = LATFACT + ALTFACT + EXPFACT. \quad 4.42$$

It was assumed that the minimum air temperature around a wheat ear (i.e., the exposed minimum air temperature) would be the same as the ground minimum air temperature (GROUNDT, °C), as recorded at a weather station. Using minimum ground and screened air temperature data collected at ART during the period October 1989 to September 1991 (see Section 2.2.1) and extracted from the Department of Meteorological Services records for Henderson Research Station for the period May to September, 1990 and 1991, linear regressions of GROUNDT on TEMPMN were computed (Figure 4.16). The slopes of the two regressions were significantly different and intersected at TEMPMN equal to 12 °C, with the slope for ART greater than that of Henderson. It was postulated that the difference in slope was due to differences in the total correction factor (TF) between the two sites (Table 4.17). In other words, the greater the total correction factor (i.e., the lower the probability of frost occurrence), the lower the slope of the GROUNDT *versus*

Table 4.17: The altitude (ALT, m), the altitude correction factor (ALTFACT), the combined latitude and dewpoint correction factor (LATFACT), the estimated exposure factor (EXPFACT) and the total correction factor (TF) for ART and Henderson Research Station (HEND).

Site	ALT	ALTFACT	LATFACT	EXPFACT	TF
ART	1500	-2.75	-1.04	3.5	-0.29
HEND	1292	-0.69	-1.01	3.5	1.80

TEMPMN curve. Thus, it was assumed that at a site that was highly susceptible to radiation frost (e.g., a site on the lower slopes of a high altitude area), one would expect a sharp gradient between TEMPMN and GROUNDT, especially under calm conditions with a temperature inversion. On the other hand, at a site that was not prone to frost, there would be a decreased gradient between the minimum temperature recorded in a screen and that recorded on the ground.

In order to establish the linear relationship between GROUNDT and TEMPMN for a site, it was assumed firstly, that any regression would pass through TEMPMN equal to 12 °C, and GROUNDT equal to 8.65 °C, secondly, that the slope of the regression was linearly related to Law's total correction factor (TF), and thirdly, that the GROUNDT would always be at least 3.35 °C less than TEMPMN. Based on the data from ART and Henderson (Figure 4.16 and Table 4.17), the y-intercept (aa) of the GROUNDT *versus* TEMPMN curve was calculated as

$$aa = -7.08 + 2.08 \times TF, \quad aa \leq -3.35 \qquad 4.43$$

while the slope (bb) was calculated as

$$bb = (8.65 - aa)/12. \qquad 4.44$$

Equations 4.43 and 4.44 were inserted in subroutine *IPWTH*. From them, the GROUNDT is estimated from the TEMPMN in subroutine *GROSUB* of WHVZIM22.

The second problem of predicting low temperature damage to wheat kernel numbers was establishing a causal relationship between GROUNDT and GPP. Two year's of field experiments were conducted at ART in 1989 and 1990 in an attempt to establish

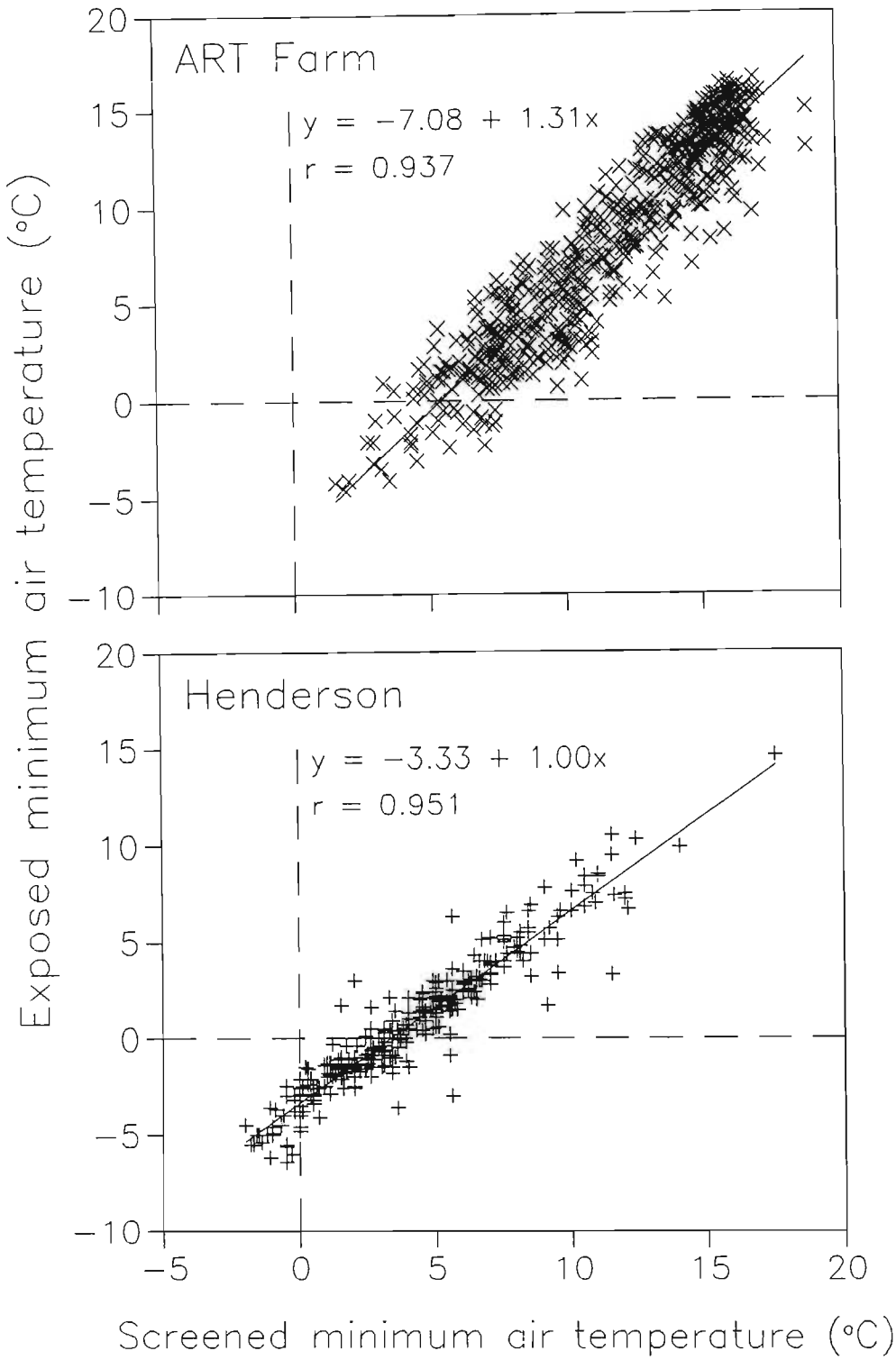

Figure 4.16: The relationship between the ground minimum air temperature and the screened minimum air temperature at ART and Henderson Research Station.

such a relationship, but these were a failure because of difficulties in matching anthesis with periods of low air temperatures and in assessing kernel number losses. These experiments were therefore abandoned in favour of a simple empirical approach.

Singels (1990) used a linear relationship to reduce the potential grain growth rate when the minimum air temperature declined below -1.5 °C. However, in a review of frost injury to wheat, Single (1985) indicated that the greatest effect of low temperature damage during reproductive growth was on kernel numbers and not kernel growth rate. Recognising that the period of greatest sensitivity is from ear emergence to early grainfill, a multiplicative low temperature factor was introduced into WHVZIM22 during growth phases three and four. This factor (FROST) is an exponenetial function of GROUNDT:

$$FROST = 1 - EXP[-0.65 \times (GROUNDT + 10)], \quad 0 \leq FROST \leq 1. \qquad 4.45$$

At the end of growth phase three,

$$GPP = STMWT \times G1 \times \prod_{i=1}^{n} FROST_i \qquad 4.46$$

where n is the number of days during the period between the end of ear growth and anthesis when GROUNDT < 0 °C. During growth phase four,

$$GPP = GPP \times FROST. \qquad 4.47$$

These functions were not verified with actual data, due to lack of data, but when they were included in WHVZIM22, they contributed to improved predictions of GPSM (see Section 4.2.8.2). Furthermore, although they are by no means perfect, they do provide a means by which to assess the risks associated with early planted wheat which may be exposed to low temperatures during reproductive growth.

4.2.5 Kernel growth

Kernel growth in WHV21 begins at the start of growth phase five, with the initial kernel mass equal to 3.5 mg kernel^{-1}. This, when multiplied by GPP and PLANTS causes a sudden and probably atypical increase in BIOMAS (see Section 3.2.5.2). It was therefore considered necessary to begin kernel growth in a gradual fashion during growth phase four. However, the end of growth phase four was not defined in the modification of the PHENOL subroutine (Section 4.1.5) and so it is dealt with here, together with the accumulation of kernel mass.

Kernel dry mass data were collected from the sowing date x cultivar trials at ART 1989 and 1990, GLEN 1989 and SHAM 1990, as described in Section 2.3.1. In order to establish the start of the linear grainfilling period, regression analyses of kernel mass on thermal time (T_b = 3 °C) after anthesis were computed for each cultivar-data set. All regressions were highly significant (data not shown), and although many of the x-intercepts computed from the regressions within a cultivar were significantly different from one another, there was no distinct trend or obvious reason for this variation. Consequently, the data for each cultivar were pooled and new regressions computed (Table 4.18). These regressions showed that the x-intercepts of W170/84, Sengwa and Angwa were not significantly different, but all were different from Rusape. Since there is no provision in WHV21 for the duration of phase four to be genotype specific, this convention was maintained in WHVZIM22. The data for the four cultivars were thus pooled and the resultant regression statistics (Table 4.18) indicated that the mean duration of the lag phase was 136 °C d (T_b = 3 °C).

Table 4.18: Statistical parameters of the pooled linear regressions of kernel mass on thermal time (T_b = 3 °C) after GS61 for four cultivars in data sets from ART 1989 and 1990, GLEN 1989 and SHAM 1990.

	Cultivar				
Parameter	W170/84	Sengwa	Rusape	Angwa	Pooled
n	66	76	74	70	286
x-intercept (°C d)	142	141	123	142	136
SE x-int. (°C d)	0.7	0.7	0.9	1.1	0.5
x-intercept 95 % confidence interval	(141., 143.)	(140., 142.)	(121., 125.)	(140., 144.)	(135., 137.)
slope (mg kernel^{-1} °C^{-1} d^{-1})	0.060	0.052	0.060	0.066	0.059
SE slope (mg kernel^{-1} °C^{-1} d^{-1})	0.0014	0.0013	0.0018	0.0021	0.0010
slope 95 % confidence interval	(0.057, 0.063)	(0.049, 0.055)	(0.057, 0.064)	(0.062, 0.070)	(0.057, 0.061)
r	0.983	0.979	0.969	0.968	0.960

It was assumed that kernel growth begins one quarter of the way through growth phase four, with the growth rate, G2R (mg kernel^{-1} d^{-1}) increasing linearly from zero to G2 with crop age:

$$G2R = G2 \times (1-(1-SUMDTT/P4)/0.75) \qquad 4.48$$

and

$$GROGRN = RGFILL \times GPP \times G2R \times 0.001, \qquad 4.49$$

where GROGRN is the potential daily growth rate of kernels per plant (g plant^{-1} d^{-1}), RGFILL is the relative kernel filling rate defined as a function of the maximum and minimum air temperatures (Ritchie and Otter, 1984) and 0.001 is a conversion factor from g to mg.

Kernel growth rates of wheat range between 1.0 and 2.5 mg kernel^{-1} d^{-1} (Sofield *et al.*, 1977). In this study, the kernel growth rates determined from regressions of kernel dry mass on days after GS61 for the four cultivars in the sowing date x cultivar experiments were similar, but somewhat lower (range 0.7 to 1.4 mg kernel^{-1} d^{-1}, data not shown). Although there was a trend for the mean kernel growth rates to be cultivar specific (the mean kernel growth rates of W170/84, Sengwa, Rusape and Angwa were 1.03, 0.86, 1.07 and 1.13 mg kernel^{-1} d^{-1}, respectively), the data were variable and the means not

significantly different. Nevertheless, the provision for genetic control of potential kernel growth rate was maintained in WHVZIM22, but the scaling factor was changed:

$$G2_{actual} = 0.4 \times G2_{scaled}, \quad 0 < G2_{scaled} \leq 6. \qquad 4.50$$

The G2 genetic coefficients were established iteratively for each cultivar on the well-watered calibration and validation data sets (Table 4.19). The actual G2's for the four cultivars corresponded reasonably well with the measured mean kernel growth rates given above.

Table 4.19: The scaled and actual potential kernel growth rates ($G2_{scaled}$ and $G2_{actual}$, respectively) of the four wheat cultivars used in WHVZIM22.

Cultivar	$G2_{scaled}$	$G2_{actual}$
	mg kernel^{-1} d^{-1}	
W170/84	3.10	1.24
Sengwa	2.42	0.97
Rusape	3.06	1.22
Angwa	3.16	1.26

During sensitivity analyses of some of these modifications, it was noted that under environmental conditions that favoured a long duration of phase five growth, kernel mass often exceeded 50 mg in some cultivars. Maximum observed kernel masses in the calibration data sets rarely exceeded 50 mg (Appendix 4). Cultivars also exhibited different mean and maximum kernel masses. Maas and Arkin (1980) set a maximum allowable kernel mass of 50 mg in their model. In order to include an upper limit to kernel mass in WHVZIM22, it was assumed that maximum kernel mass (MAXGWT, mg kerenel^{-1}) was a function of genotype, kernel growth rate and grain-fill duration:

$$MAXGWT = (P5 - 136) \times G2/16, \quad 40 \leq MAXGWT \leq 50, \qquad 4.51$$

where *(P5 - 136)* is the duration of the linear kernel growth phase (phase five, °C d), G2 is the optimum kernel growth rate (mg kernel^{-1} d^{-1}), and *16* is the optimum air temperature (°C) for kernel growth and phase five duration. During growth phase five, if (GRNWT+GROGRN)/GPP exceeds MAXGWT, then GROGRN is set to zero, and all of CARBO x PTF from then on is assimilated into the stem.

The adequate prediction of kernel mass under conditions of deficit irrigation proved difficult (Section 3.3.3). Mogensen and Talukder (1987) reported increased kernel growth rates under water stress, while Sofield *et al.* (1977) noted an increase in the kernel growth rate with an increase in air temperature. Despite these reports, however, the kernel growth rate data collected in the wheat irrigation trials at ART in 1989 and 1992 did not provide much corroborative support (Table 4.20). Nevertheless, at ART 1989, the lowest and nearly significantly different kernel growth rate was obtained on the well watered treatment (data set 73). Furthermore, at ART 1992, the kernel growth rates were the same whether the wheat was irrigated through to physiological maturity on a 10 d, 15 d or 20 d cycle, although in each of these irrigation regimes, the early termination of irrigation tended to reduce kernel growth rates slightly.

These results from ART (Table 4.20) do not explicitly show whether short term water deficit stress increased or decreased kernel growth rates, since the calculated kernel growth rate was averaged over the whole duration of kernel filling. However, in view of the report by Mogensen and Talukder (1987), the relative kernel growth rate factor (RGFILL) was made to increase under conditions of water deficit stress during growth phase five:

$$RGFILL = RGFILL \times (2 - SWDF1), \quad 0.5 \leq SWDF1 < 1.0 \qquad 4.52$$

$$RGFILL = RGFILL \times (1 + SWDF1), \quad 0.0 \leq SWDF1 < 0.5 \qquad 4.53$$

The contribution of stem-stored non-structural carbohydrate is recognised in WHV21 as a source of assimilate for kernel growth. This may be particularly important when water deficits

develop during reproductive growth (Gallagher, Biscoe and Hunter, 1976; Mogensen and Talukder, 1987; Pheloung and Siddique, 1991). The WHV21 model accumulates this reserve pool of assimilate during growth phase four if the STMWT during this period exceeds the STMWT at the end of growth phase three (i.e., the end of pre-anthesis ear growth). The definition of the end of growth phase three was changed in WHVZIM22 from the end of pre-anthesis ear growth to anthesis (see Section 4.1.4). Consequently, the end of pre-anthesis ear growth was set at 153 °C d (T_b = 4 °C) after the start of growth phase 3. However, due to problems in adequately predicting kernel mass under deficit irrigated conditions, the timing of the end of pre-anthesis ear growth was reduced to 100 °C d (T_b = 4 °C) to enable the contribution of more stem-stored reserves to kernel growth.

Table 4.20: The statistical parameters pertaining to the slope of the regressions of kernel dry mass on time after GS61 of treatments in the wheat irrigation trials at ART in 1989 and 1992.

Data set	b	SE	Confidence limits Lower	Upper	r
	mg kernel^{-1} d^{-1}				
ART 1989					
70	1.04	0.061	0.87	1.21	0.993
71	0.93	0.073	0.72	1.13	0.988
72	0.94	0.049	0.80	1.08	0.994
73	0.79	0.035	0.69	0.89	0.996
74	0.96	0.054	0.81	1.11	0.994
ART 1992					
101	1.32	0.037	1.23	1.42	0.998
102	1.35	0.061	1.19	1.50	0.995
103	1.26	0.036	1.17	1.35	0.998
104	1.31	0.120	1.01	1.62	0.980
105	1.19	0.069	1.01	1.37	0.992
106	1.20	0.045	1.09	1.32	0.996
107	1.36	0.030	1.28	1.43	0.999
108	1.18	0.104	0.92	1.45	0.981
109	1.22	0.081	1.01	1.42	0.989

4.2.6 Root depth

In a comparison of the root depth (RTDEP, cm) increments of the WHV21 and WHVZIM22 models in the irrigation trial calibration data sets, it was noted that the rate of root extension of WHVZIM22 was slower than that of WHV21 in growth phase zero but exceeded that of WHV21 in later growth phases (data not shown). Consequently, the RTDEP functions were modified. In growth phase nine,

$$RTDEP = RTDEP + 0.11 \times DTT, \qquad 4.54$$

and in the other growth phases,

$$RTDEP = RTDEP + 0.20 \times DTT \times AMIN1((SWDF1 \times 2), SWDF), \qquad 4.55$$

where AMIN1 is the Fortran statement for select the minimum value of an array and SWDF is a soil water deficit factor for the soil level where the root front is growing.

4.2.7 Field yield

The WHV21 model predicts the dry mass grain yield of wheat from the yield components kernel number (GPSM, kernels m^{-2}) and kernel dry mass (SKERWT, mg $kernel^{-1}$). This has been termed the yield component yield (YCYIELD). The farmer, on the other hand, is familiar with a field yield (FYIELD) at a standard kernel water content of 12.5 %. If YCYIELD is converted to a field yield at 12.5 % kernel water content, then FYIELD is greater than YCYIELD. This approach was used in evaluating the yield predictions of WHV21 in chapter 3, but it was noted that the simulated FYIELD grossly over-estimated observed FYIELD. In these experiments, both YCYIELD (from a small sample) and FYIELD (from a large, threshed sample) were measured, and from the calibration data sets it was found that, on average, FYIELD at 12.5 % kernel water content was less than oven-dry YCYIELD. This is not unexpected, in that spatial variability, sampling errors and grain losses are usually greater from large threshed samples than small selected samples. By iteration on the validation data set, the factor to convert simulated YCYIELD to FYIELD in WHVZIM22 was set at 0.85.

4.2.8 Validation of the modifications made to the growth subroutines

The genetic coefficients used in the validation exercise were those given in Tables 4.9, 4.14, 4.16 and 4.19. The file *GENETICS.WH9* was renamed *GENETICS.V22* for WHVZIM22, in order to easily distinguish between the two versions. All other input files were identical, except the weather files (*FILE 1*), which, in the first line, contain the additional information of site altitude (ALT, m) and the exposure factor (EXPFACT, no units). Both WHV21 and WHVZIM22 can use these modified weather files.

4.2.8.1 Leaf area index and dry matter accumulation

The growth analysis trial, described in Section 3.2.5.1, was used to compare the above-ground total dry matter (BIOMAS) accumulation and leaf area index (LAI) simulations of WHV21 and WHVZIM22. The WHVZIM22 model simulated higher LAI values over the whole growth period of cultivars Sengwa and Rusape compared to WHV21 (Figure 4.17). This was considered an improvement, especially from GS39 onwards, in that the WHV21 model tended to under-predict LAI in Sengwa after GS71 and in Rusape around the time of GS71.

The simulation of BIOMAS accumulation by WHVZIM22 was slightly greater than that of WHV21 in the early growth stages (i.e., prior to TS) (Figure 4.17). However, after TS, WHVZIM22 accumulated less BIOMAS than WHV21, and predictions were closer to measured data, especially during grain-filling. Furthermore, the uncharacteristic sudden increase in BIOMAS at the start of growth phase five observed with the use of WHV21 was eliminated with WHVZIM22. Thus, in terms of LAI and BIOMAS simulation, WHVZIM22 showed some marked improvements over the WHV21 model on this particular data set.

4.2.8.2 Ear density, yield components and yield

The statistical results of the performance of WHVZIM22 in predicting ear density and yield components for wheat grown under well-watered conditions (Table 4.21) and under deficit-

irrigated conditions (Table 4.22) are given, while the raw data are appended (Appendix 5). These two tables may be compared to Tables 3.3 and 3.5, respectively. The statistical comparison of WHV21 and WHVZIM22 on the complete set of well-watered and deficit-irrigated validation data sets is also given (Table 4.23).

On the well-watered data set, WHVZIM22 did not improve the prediction of TPSM at maturity compared to WHV21, since in each cultivar the *IoA* was less with WHVZIM22 than WHV21. Nevertheless, neither model was particularly good in predicting TPSM at maturity under well-watered conditions, and WHVZIM22 produced lower *MAE*'s in Sengwa, Rusape and Angwa.

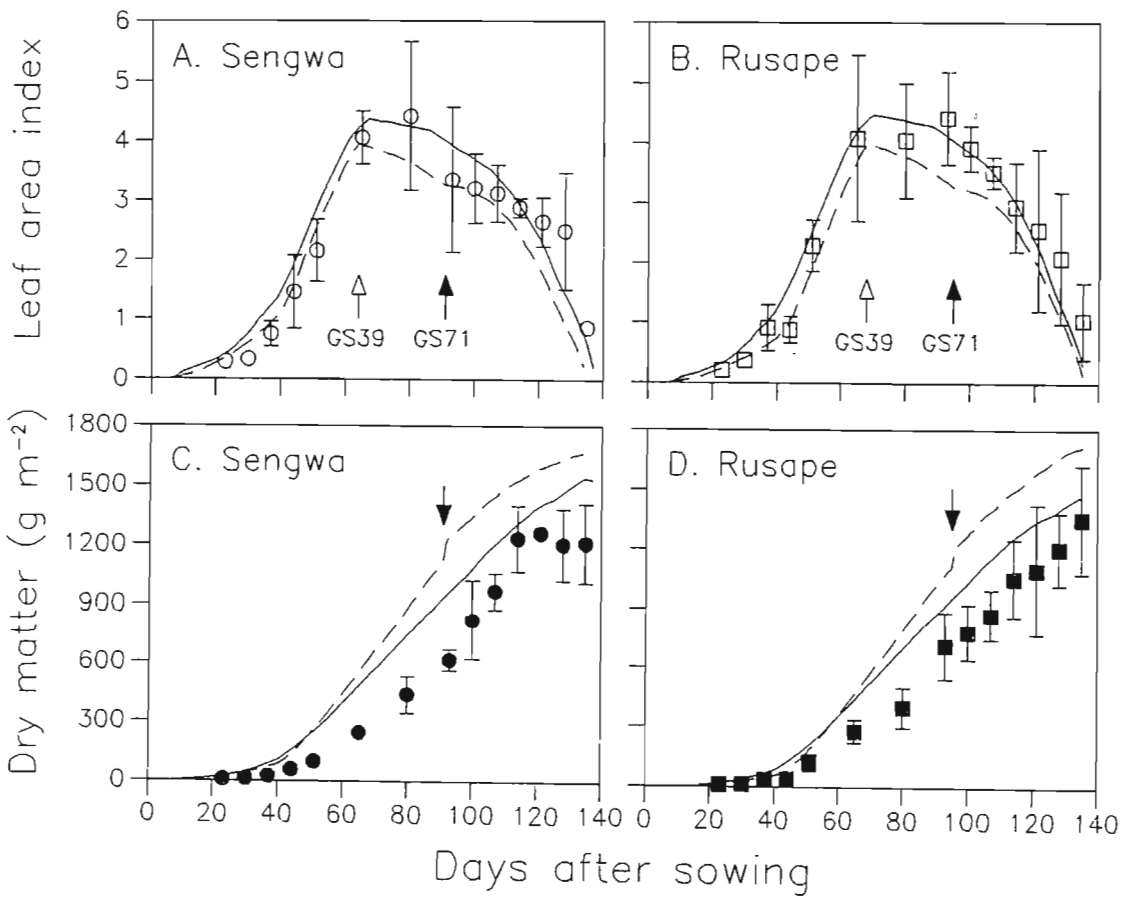

Figure 4.17: Simulated (dashed line, WHV21 and solid line, WHVZIM22) and observed leaf area index and total above-ground dry matter of two cultivars of wheat grown at ART 1986.

On the other hand, TPSM at maturity was predicted more accurately by WHVZIM22 under deficit irrigation (Table 4.22) and in the complete set (Table 4.23) than by WHV21. This was indicated by higher *IoA*, *b* and *r* and lower *MAE* in these data sets with the use of WHVZIM22 than with WHV21.

Kernel mass predictions by WHVZIM22 under well-watered conditions were improved in cultivars W170/84, Sengwa and Rusape, but not in Angwa (comparing Tables 4.21 and 3.3). Under deficit irrigation, WHVZIM22 performed better than WHV21 in predicting kernel mass (comparing Tables 4.22 and 3.5) but under conditions of severe water stress (e.g., data sets 117 to 122) WHVZIM22 predictions of kernel mass remained well below measured kernel mass. When evaluated over all validation data sets, the *IoA* and *r* of kernel mass prediction by WHVZIM22 were slightly greater than those of WHV21, whereas the *MAE* and *b* of WHVZIM22 were slightly worse than those of WHV21. Kernel number predictions were improved by WHVZIM22 compared to predictions by WHV21 in the well-watered, deficit-irrigated and complete data sets.

The prediction of field yield (FYIELD) was improved by the use of WHVZIM22 compared to predictions by WHV21 in both the well- and deficit-irrigated data sets (comparing Tables 3.3 with 4.21, and 3.5 with 4.22). However, the FYIELD predictions of WHV21 given in chapter 3 were grossly over-estimated because of the adjustment of YCYIELD for kernel water content. Thus, in order to sensibly compare the FYIELD predictions of WHVZIM22 with those of WHV21, the YCYIELDs computed by WHV21 were converted to FYIELDs by a factor of 0.85 (see section 4.2.7 for an explanation). Using the combined data sets, WHVZIM22 improved the prediction of FYIELD compared to WHV21 (Table 4.23 and Figure 4.18). Prediction of the yield component-yield (YCYIELD) was improved by WHVZIM22 when evaluated over all data sets (Table 4.23), but in the individual well-watered and deficit-irrigated data sets, WHVZIM22 did not always show an improvement (Tables 4.21 and 4.22).

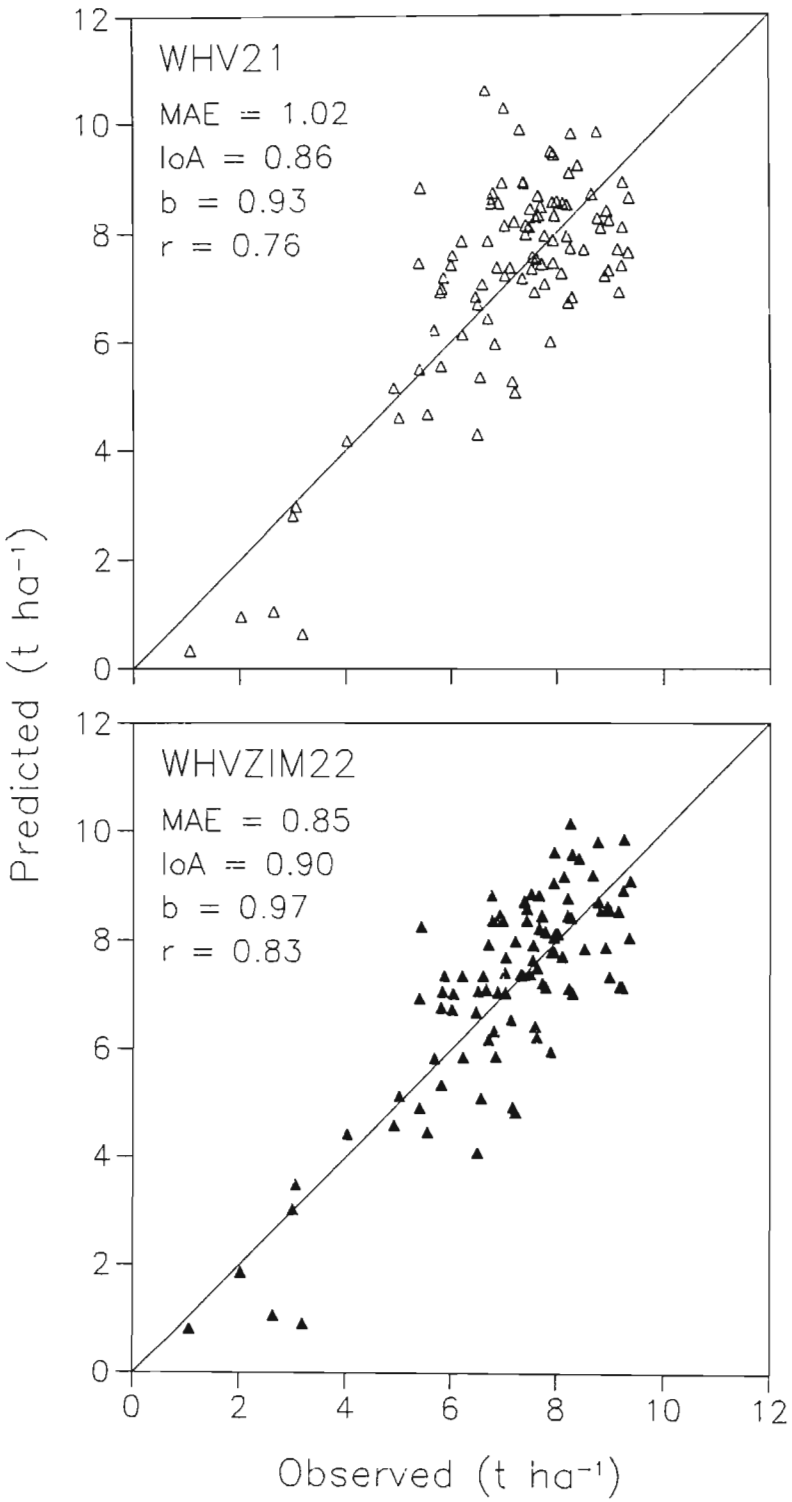

Figure 4.18: Comparison of the predictions by WHV21 and WHVZIM22 with the observed field yield of wheat in all the validation data sets.

Table 4.21: The performance of WHVZIM22 in predicting ear density (TPSM) and yield components (kernel mass, PGRNWT; kernel number, GPSM; field yield, FYIELD; and yield computed from yield components, YCYIELD) of wheat under well-irrigated conditions.

	TPSM Ears m^{-2}	PGRNWT mg $kernel^{-1}$	GPSM kernels m^{-2}	FYIELD t ha^{-1}	YCYIELD t ha^{-1}
W170/84					
$\bar{O}$	384	39.2	24768	7.97	9.66
$\bar{P}$	414	40.0	24281	8.24	9.70
MAE	52	2.45	2640	0.791	1.076
IoA	0.43	0.85	0.43	0.76	0.72
MSEs	2978	3.6	7487453	0.260	0.527
MSEu	869	6.5	4737113	0.637	1.067
MSE	3847	10.1	12224566	0.897	1.594
b	0.031	0.631	0.076	0.587	0.443
a	402	15.3	22401	3.56	5.42
r	0.049	0.754	0.101	0.608	0.487
n	20	20	20	20	20
Sengwa					
$\bar{O}$	450	35.0	25070	7.81	8.71
$\bar{P}$	465	35.5	24704	7.41	8.72
MAE	44	1.47	2883	0.648	1.007
IoA	0.46	0.92	0.54	0.58	0.22
MSEs	1498	0.2	5616527	0.345	0.921
MSEu	1255	3.3	5156649	0.422	0.608
MSE	2754	3.5	10773177	0.767	1.529
b	0.088	0.976	0.226	0.378	-0.385
a	425	1.3	19048	4.46	12.07
r	0.097	0.858	0.288	0.373	-0.324
n	20	20	20	20	20
Rusape					
$\bar{O}$	407	40.9	24431	7.60	9.96
$\bar{P}$	413	40.4	24390	8.35	9.82
MAE	36	1.38	2274	0.970	0.980
IoA	0.25	0.94	0.50	0.68	0.51
MSEs	1265	1.0	2365769	0.899	0.310
MSEu	717	2.1	4156187	0.450	0.988
MSE	1982	3.1	6521956	1.349	1.298
b	-0.245	1.296	0.211	0.481	0.289
a	513	-12.6	19234	4.69	6.94
r	0.249	0.935	0.198	0.631	0.215
n	20	20	20	20	20
Angwa					
$\bar{O}$	439	42.9	21652	7.20	9.41
$\bar{P}$	452	42.4	22156	7.95	9.35
MAE	32	2.11	1456	0.754	0.831
IoA	0.66	0.88	0.76	0.58	0.25
MSEs	662	1.6	1137761	0.607	0.482
MSEu	895	3.7	2541408	0.263	0.476
MSE	1557	5.2	3679169	0.870	0.958
b	0.414	1.024	0.551	0.625	-0.365
a	270	-2.3	10218	3.46	12.78
r	0.472	0.855	0.587	0.535	-0.259
n	10	10	10	10	10

Table 4.22: The performance of WHVZIM22 in predicting ear density (TPSM) and yield components (kernel mass, PGRNWT; kernel number, GPSM; field yield, FYIELD; and yield computed from yield components, YCYIELD) of wheat under deficit-irrigated conditions.

	TPSM Ears m^{-2}	PGRNWT mg $kernel^{-1}$	GPSM kernels m^{-2}	FYIELD t ha^{-1}	YCYIELD t ha^{-1}
$\bar{O}$	386	34.1	21975	5.51	7.36
$\bar{P}$	360	28	21176	5.06	5.95
MAE	53	8.06	3617	0.976	1.729
IoA	0.88	0.53	0.89	0.90	0.83
MSEs	2627	46.2	3546766	0.202	1.950
MSEu	2460	34.6	17933239	1.328	1.990
MSE	5086	80.9	21480006	1.530	3.940
b	0.638	0.603	0.768	0.949	0.982
a	113	6.9	4305	-0.16	-1.26
r	0.840	0.379	0.800	0.845	0.831
n	27	27	27	27	27

Table 4.23: The performance of WHV21 and WHVZIM22 in predicting ear density (TPSM) and yield components (kernel mass, PGRNWT; kernel number, GPSM; field yield, FYIELD; and yield computed from yield components, YCYIELD) of wheat with all data sets in the well-watered and deficit-irrigated validation experiments.

	TPSM Ears m^{-2}	PGRNWT mg $kernel^{-1}$	GPSM kernels m^{-2}	FYIELD t ha^{-1}	YCYIELD t ha^{-1}
WHV21					
$\bar{O}$	409	37.7	23662	7.10	8.86
$\bar{P}$	441	36.1	23291	7.25	8.53
MAE	57	3.52	3225	1.024	1.230
IoA	0.69	0.80	0.78	0.86	0.85
MSEs	3106.4	2.7	3358371	0.04	0.12
MSEu	1698.3	26.0	13292881	1.63	2.11
MSE	4804.7	28.7	16651252	1.67	2.23
b	0.404	1.034	0.616	0.927	1.065
a	276	-2.9	8709	0.68	-0.91
r	0.599	0.712	0.620	0.764	0.782
n	97	97	97	97	97
WHVZIM22					
$\bar{O}$	409	37.7	23662	7.10	8.86
$\bar{P}$	409	35.8	23324	7.17	8.43
MAE	46	3.58	2761	0.852	1.200
IoA	0.82	0.81	0.83	0.90	0.85
MSEs	863.7	3.9	2572694	0.008	0.185
MSEu	2460.7	23.1	10134269	1.149	1.963
MSE	3324.4	27.0	12706962	1.158	2.149
b	0.616	1.128	0.665	0.966	1.025
a	158	-6.7	7594	0.31	-0.65
r	0.688	0.761	0.699	0.827	0.781
n	97	97	97	97	97

4.2.8.3 Tillering

The modifications made to the tillering routines of WHV21 improved the prediction of the seasonal progression of tiller production and senescence of wheat, although these were by no means perfect. Examples of this general improvement are given for a well-watered site (*WPDG9000*; Figures 4.19 and 4.20) and a deficit-irrigated site (*WDDA9020*; Figure 4.21). The general shape of the seasonal tillering profiles predicted by WHVZIM22 followed the course of observed stem densities better than that of WHV21, especially during growth phase one. Furthermore, as discussed in Section 4.2.8.2, above, final TPSM predictions by WHVZIM22 were improved on average over all the data sets.

4.2.8.4 Soil water balance

The modifications made to WHV21 made little impact on the seasonal soil water balance predictions, which, on the whole, were good (data presented in Appendix 2; see Section 3.3.2). However, in some instances, the soil water contents predicted by WHVZIM22 were slightly less than those predicted by WHV21, especially after TS. This may have been due to the higher LAI values predicted by WHVZIM22 causing greater EP compared to WHV21, but the differences in soil water contents were small and considered insignificant to warrant further modifications.

4.2.8.5 Root depth

Soil pits were dug on four occasions in treatment 114 of the wheat irrigation dry down trial at ART 1989 in order to observe the depth of root penetration. The modifications made to the root depth increment functions (Eqn 54 and 55) slowed the rate of root depth growth but the simulated progress of root penetration was similar to that observed in the field (Figure 4.22).

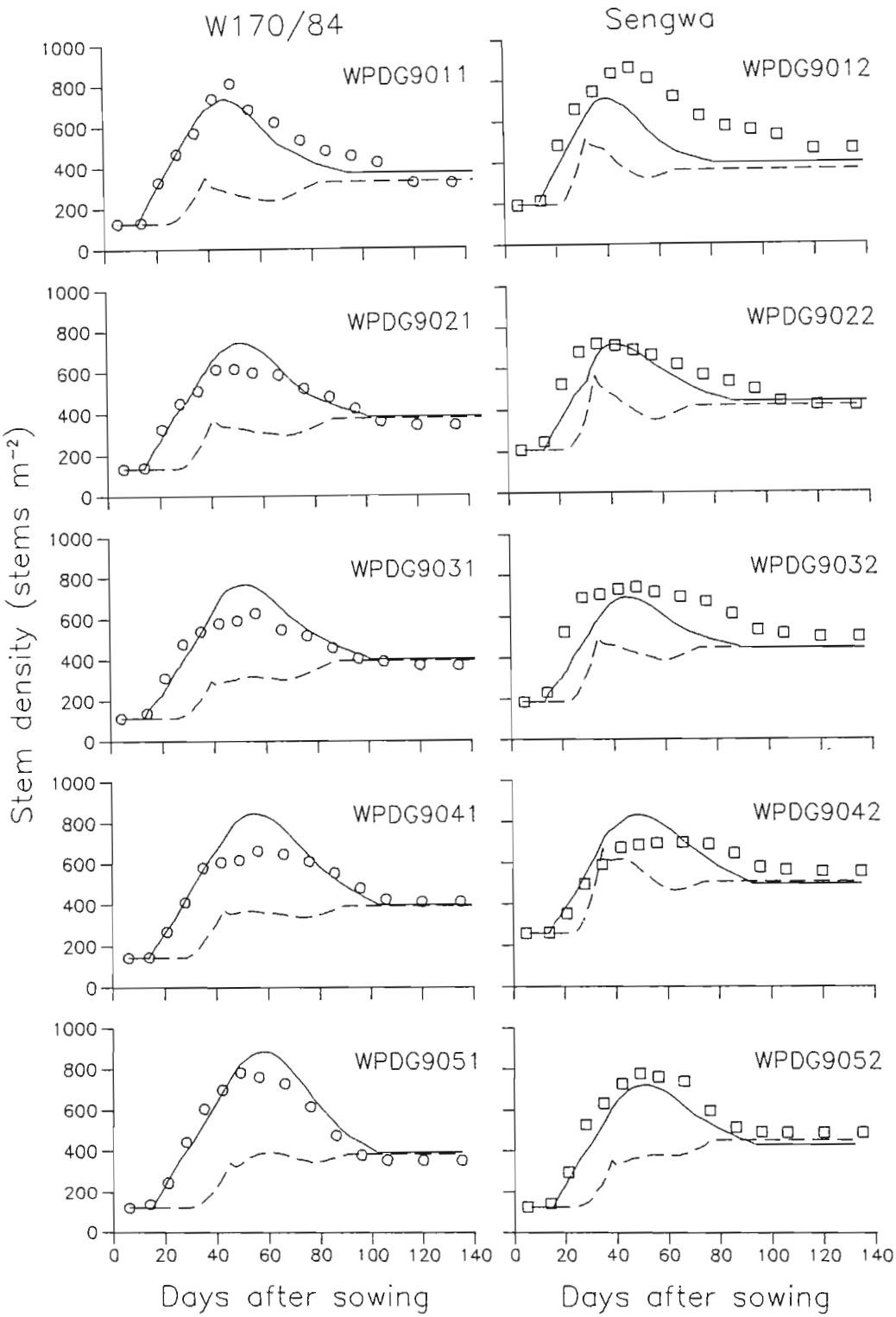

Figure 4.19: The predicted (dashed lines, WHV21 and solid lines, WHVZIM22) and observed tillering patterns of wheat cultivars W170/84 and Sengwa in the GLEN 1990 validation set.

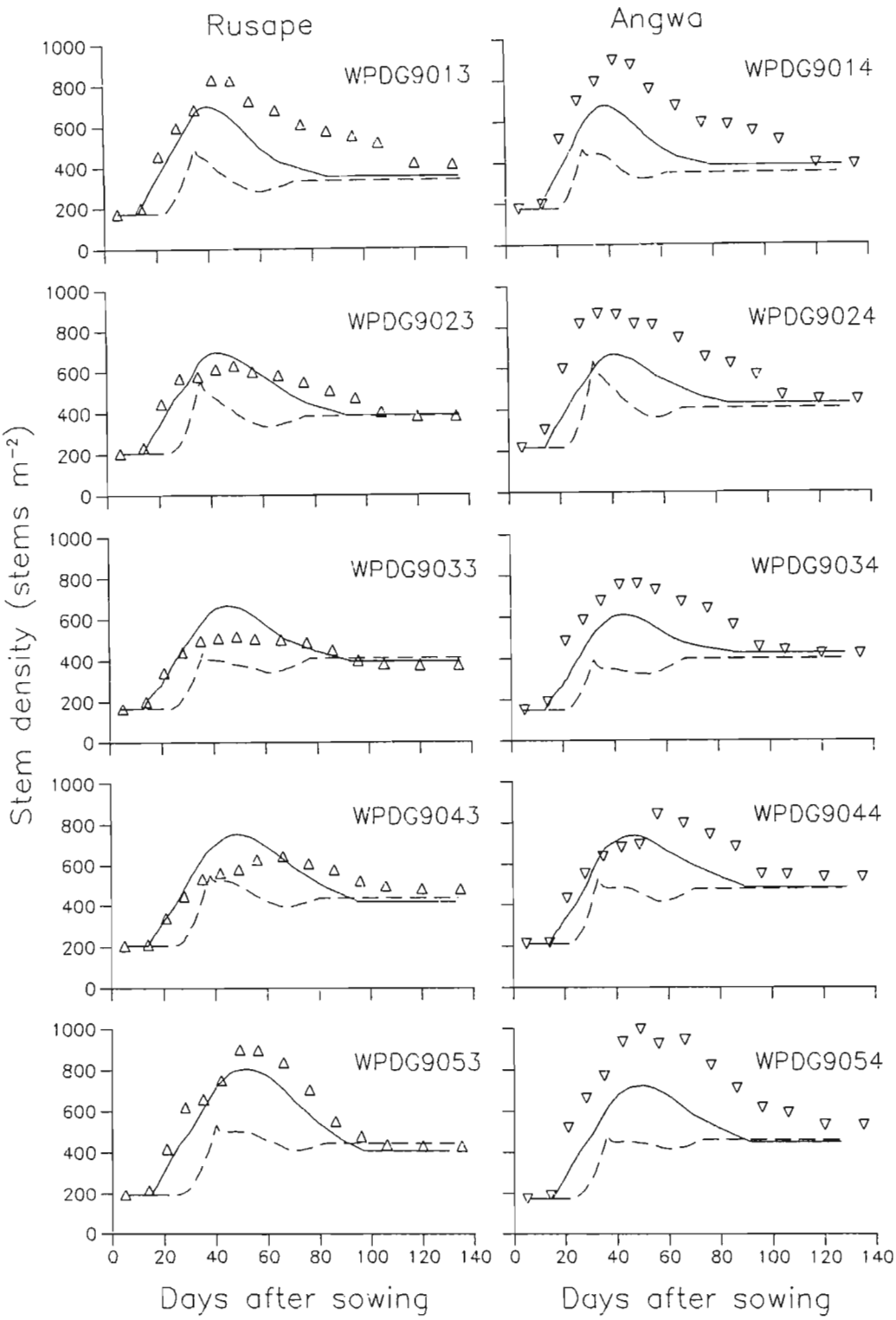

Figure 4.20: The predicted (dashed lines, WHV21 and solid lines, WHVZIM22) and observed tillering patterns of wheat cultivars Rusape and Angwa in the GLEN 1990 validation set.

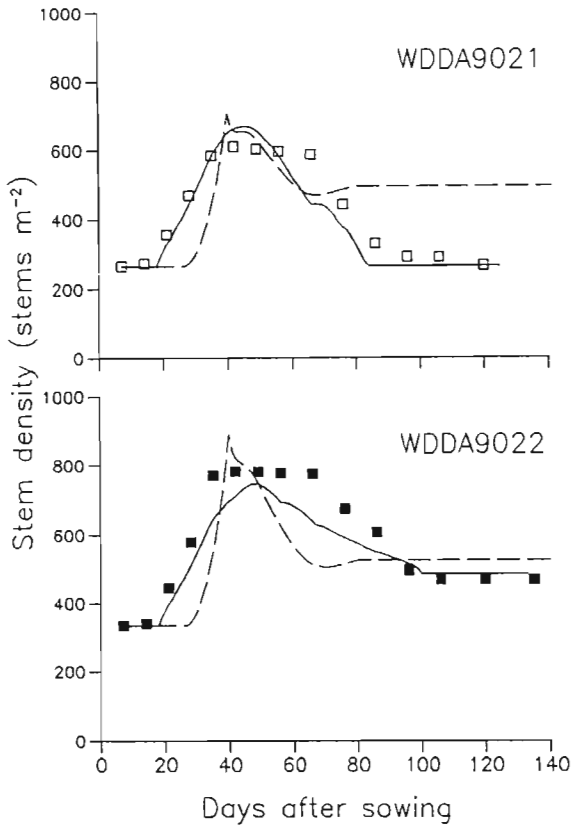

Figure 4.21: The predicted (dashed lines, WHV21 and solid lines, WHVZIM22) and observed tillering patterns of wheat grown under deficit-irrigated conditions at ART 1990.

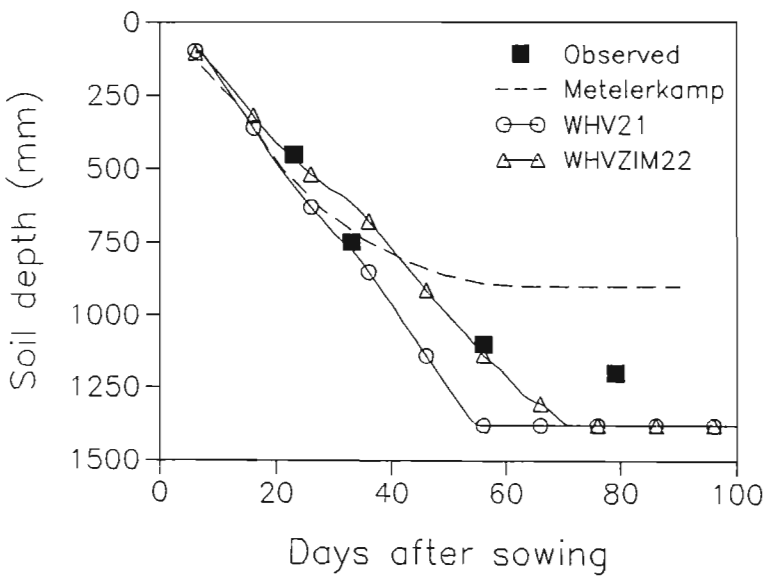

Figure 4.22: The simulated (WHV21, WHVZIM22 and Metelerkamp, 1980) root depth growth of wheat and four observed depths of root penetration at ART 1989.

4.3 Conclusion

The modifications made to the CERES-Wheat version 2.10 model contributed to a better all-round performance of the model when evaluated on the validation data sets. In particular, the simulation of the timing of phasic development, the prediction of tiller production and senescence and the estimation of field yield were improved, especially under deficit-irrigated conditions. This, therefore, provides reasonable justification to apply the model to evaluate wheat irrigation strategies in Zimbabwe. The inclusion of a procedure to account for low temperature damage to kernel numbers around the time of anthesis also gives the model greater flexibility for application in Zimbabwe. Nevertheless, any application of the revised model to production problems must recognize that the model is not a perfect predictor of yield and that it does not account for nutrient dynamics or pest stresses.

5 APPLICATION OF THE MODIFIED CERES-WHEAT MODEL TO EVALUATE WHEAT PRODUCTION STRATEGIES

Crop simulation models provide a rapid and relatively inexpensive means of evaluating production strategies (Singels and de Jager, 1991). However, their use must be cautioned by the assumptions and limitations of the model (Hanks and Ritchie, 1991). The CERES-Wheat model has been used in a number of diverse applications (e.g., Bacsi, Thornton and Dent, 1991; Booysen, 1987; McGregor and Thornton, 1990; Rodrigues, *et al.*, 1990; Savdie *et al.*, 1991). Similarly, the CERES-Maize model (Jones and Kiniry, 1986), which has a number of routines resembling those of CERES-Wheat, has been used to evaluate crop production options (e.g., Alocilja and Ritchie, 1989; Liu, Botner and Sakamoto, 1989; Thornton and MacRobert, 1993).

The CERES-Wheat version 2.10 model (Godwin, Ritchie, Singh and Hunt, 1989) was modified extensively for application in Zimbabwe (Chapter 4). This modified version (WHVZIM22) was shown to give improved predictions of phenology and yield over the original version in a wide range of environments. This chapter describes the application of WHVZIM22 to the evaluation of wheat sowing date and irrigation options in Zimbabwe.

The WHVZIM22 model does not account for plant nutrient synthesis or the influence of diseases, insects or weeds. The model therefore assumes that plant nutrients are non-limiting and apart from genetic, soil, water and weather limitations, all other production variables are assumed to be optimal. This assumption is reasonably plausible in Zimbabwe because, firstly, most farmers apply sufficient fertilizers to wheat (Whingwiri, Mataruka and Ntungakwa, 1984), secondly, the standard of wheat management is generally high and, thirdly, pest and disease problems are usually minimal.

5.1 The simulation of optimum sowing dates of wheat

The choice of sowing date is one of the first options faced by farmers growing wheat. Many factors influence this decision, such as the availability of water for irrigation, the perceived

risk of frost occurring at the time of anthesis, the previous crop harvest date, the proposed sowing date of the following crop and the area of wheat to be grown. The general recommendation is for wheat to be planted as early in May as possible but, in frost prone areas, this must be late enough to avoid potential frost damage at anthesis (MacRobert, 1990). Also, since some cultivars differ in their duration of vegetative growth, those that flower later may be planted earlier. This section evaluates the use of WHVZIM22 in predicting optimal sowing dates of two wheat cultivars in Zimbabwe.

5.1.1 Methods

Zimbabwe is divided into three broad regions based on altitude. These are the highveld (altitude > 1400 m), the middleveld (900 to 1400 m) and the lowveld (altitude < 900 m). Apart from edaphic characteristics, the major environmental difference is in air temperature, with the highveld generally cooler then the lowveld. Wheat is grown in all three regions. Consequently, three sets of weather files were created to allow for the simulation of wheat yield in these three regions. These weather files were derived from the Department of Meteorological Services, Government of Zimbabwe, weather records for the period 1981 to 1990. For the highveld, middleveld and lowveld, the records from the Kutsaga Research Station (KUTS), Banket Research Station (BANK) and Buffalo Range (BUFF) weather stations, respectively, were chosen to be representative of each region (summary statistics given in Table 5.1). The weather files are given on the accompanying diskette, and are named *KUTS0112.WYY*, *BANK0112.WYY* and *BUFF0112.WYY*, where *YY* is the last two digits of the year.

Fifteen sowing date treatments were established. The first sowing date was on day 78 (19 March) and the others were spaced at seven day intervals through to day 176 (25 June). This spanned the normal planting date range of wheat in Zimbabwe. For each treatment the simulation was run without the soil water balance in order to determine the potential yield in the absence of water deficit stress. The plant density was set at

Table 5.1: Site location, and the mean daily total radiant density, mean daily maximum and minimum air temperatures and the mean annual rainfall of the three weather stations for the 10 yr period 1981 to 1990.

Parameter	KUTS Highveld	BANK Middleveld	BUFF Lowveld
Latitude (° south)	17.92	17.32	21.02
Longitude (° east)	31.13	30.40	31.58
Altitude (m)	1480	1244	430
Total daily radiant density (MJ m^{-2})	20.2	20.6	21.1
Maximum air temperature (°C)	25.2	27.1	30.6
Minimum air temperature (°C)	11.5	13.9	16.4
Annual rainfall (mm)	718	806	494

200 plants m^{-2} and the seeding depth was 20 mm. The simulation was carried out on cultivars W170/84 and Sengwa, using the genetic coefficients given in Chapter 4, for each of the 10 yr of weather records for the three stations. The mean and standard error of the yields were computed for each station.

5.1.2 Results and discussion

The simulated yield response of wheat to sowing date for the three altitude regions is given (Figure 5.1). For any sowing date at a site, the yield of W170/84 was greater than that of Sengwa. This is similar to that observed in the field, where, on average over 78 variety trials, W170/84 produced a 0.59 t ha^{-1} yield advantage over Sengwa (J.R. Tattersfield, 1993, personal communication).

In either Sengwa or W170/84, the mean yields for each sowing date were greatest on the highveld and least on the lowveld, with the differences being as much as 4 t ha^{-1}. This trend is similar to field observations but the simulated difference appears greater than observed differences. Mashiringwani (1993) reported mean yields of four cultivars evaluated in small plot variety trials of 7.39 t ha^{-1} on the highveld and 5.64 t ha^{-1} on the lowveld. Differences in yield between the highveld and lowveld of Zimbabwe have been attributed to the higher temperatures of the lowveld hastening development and thereby

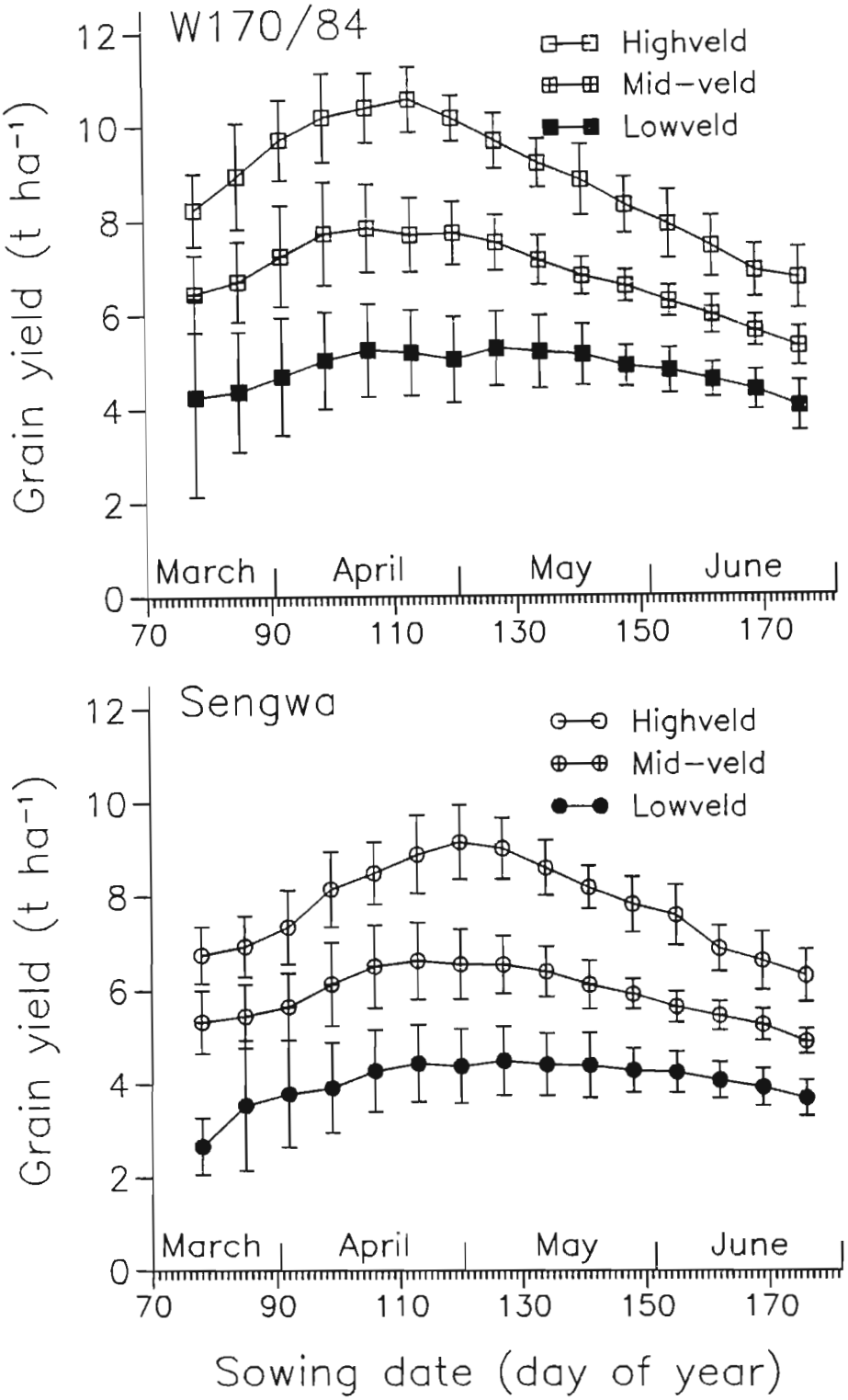

Figure 5.1: The simulated mean yield of wheat cultivars W170/84 and Sengwa in response to sowing date at three locations representative of the highveld (Kutsaga), middleveld (Banket) and lowveld (Buffalo Range).

reducing both sink size and source duration (Cackett and Wall, 1971). The simulated mean yield of W170/84 of over 10 t ha^{-1} on a 23 April sowing is not unrealistic. A farmer in Zimbabwe achieved field-scale yield of over 10 t ha^{-1} with cultivar W170/84 in 1993 (Grant, 1993).

The effect of sowing date on the yield of both W170/84 and Sengwa was most distinct on the highveld. With W170/84, highest yields were obtained with a 23 April sowing, whilst with Sengwa, highest yields were obtained with a 30 April sowing. With sowings on either side of this optimum, yields were less. Similar results were obtained on the middleveld and the lowveld, but the decrease in yield with earlier or later plantings was not as great as on the highveld. In each region, the SE of yield tended to be greater with the earlier sowings than the later sowings, particularly in W170/84.

This distinct optimum sowing date on the highveld and the difference in optimum sowing date between W170/84 and Sengwa is not unlike field observations and is in line with current recommendations. In both W170/84 or Sengwa the optimum sowing date resulted in anthesis occurring during the period end of July and early August. This coincides with a decrease in the probability of frost occurrence (Law, 1989) and yet is early enough to enable grain-filling to proceed prior to the high air temperatures normally experienced in late September and October. This observation that optimum yields are obtained when the anthesis date occurs immediately prior to the period of rapid temperature increase was also proposed by Fischer (1985).

In conclusion, this simulation exercise showed that the WHVZIM22 model predicted wheat yields in response to planting date in a logical and expected fashion. However, yield prediction under lowveld conditions appeared to be lower than observations and the model may require further development for such environments. On the middleveld and highveld, simulated yields indicated that sowings in late April and early May would, on average, give the highest yields under optimum conditions.

5.2 Simulated response of wheat to irrigation

Wheat production in Zimbabwe is currently dependent on irrigation. Consequently, the efficient use of irrigation water is essential. In recent years, farmers have been advised to reduce their irrigation application per unit area and use the water thus saved to grow a larger area (MacRobert, 1992). This method of irrigation has been termed deficit irrigation (James, 1988), but the *modus operandi* of deficit irrigation is not well defined, although some principles have been proposed for use in Zimbabwe (MacRobert, 1992). These principles were mainly derived from small-plot experimental results (Agricultural Research Trust, 1987 to 1992), corroborated by observations made by the author on the field scale application of deficit irrigation. However, the general applicability of deficit irrigation to wheat in Zimbabwe is not fully understood because of the limited number of environments in which the field experiments that have been conducted.

MacRobert and Savage (1991) used a slightly modified version of CERES-Wheat to evaluate a wide range of possible irrigation regimes applied on three soil types. Their results indicated that deficit irrigation was most appropriate on deep, high water holding capacity soils, and that optimal irrigation strategies were characterized by a gradual depletion of soil water from establishment through to maturity. This section describes the use of the WHVZIM22 model in evaluating deficit irrigation strategies over three soil types and two multi-year environments.

5.2.1 Methods

Fifteen irrigation treatments were created (Table 5.2) for simulation on three soil types at two locations. The choice of the irrigation treatments was based on personal experience with the criteria that they were both potentially suitable for deficit irrigation and feasible within a farmer's constraints. An irrigation efficiency of 85 % was used.

The fifteen treatments were applied on three soil types: ART 1990, GLEN 1990 and BANK 1991 (Table 5.3), which, for

Table 5.2: Irrigation treatments applied to each of the three soil types at the highveld and middleveld locations (Note: Treatments 1 to 9 were all irrigated at 0, 5, 20 and 40 das with 50, 25, 25 and 50 mm, respectively, and treatments 10 to 15 were all irrigated at 0, 5, 20 and 35 das with 35, 35 25 and 35 mm, respectively. Thereafter, the irrigation treatments were imposed, and the number of cycles given in the table refers to the number of cycles after the four establishment irrigations described above.)

	Highveld				Middleveld			
Treatment Number	Total water	No. of cycles	Irrig. cycle^{-1}	Irrig. interval	Total water	No. of cycles	Irrig. cycle^{-1}	Irrig. interval
	mm		mm	d	mm		mm	d
1	650	10	50	11	550	8	50	11
2	600	9	50	12	500	7	50	12
3	550	8	50	13	450	6	50	13
4	500	7	50	14	450	6	50	14
5	450	6	50	15	400	5	50	15
6	450	6	50	16	400	5	50	16
7	400	5	50	17	350	4	50	17
8	400	5	50	18	350	4	50	18
9	350	4	50	19	300	3	50	19
10	550	12	35	9	480	10	35	9
11	515	11	35	10	445	9	35	10
12	480	10	35	11	410	8	35	11
13	445	9	35	12	375	7	35	12
14	410	8	35	13	340	6	35	13
15	375	7	35	14	340	6	35	14

simplicity, were also coded Clay, Loam and Sand, respectively (the textural analyses of these soils are given in Appendix 1, Table A1.5). These soils differed in their available water contents (Clay = 0.124 m^3 m^{-3}, Loam = 0.101 m^3 m^{-3} and Sand = 0.081 m^3 m^{-3}).

The two locations were Kutsaga Research Station (representing the highveld) and Banket Research Station (representing the middleveld). The treatments differed slightly at the two locations. Less irrigation was applied on the middleveld because the wheat had a shorter growth duration due to warmer air temperatures at that location compared to the highveld (see Table 5.1). For all treatments, the sowing date was set as 10 May, the plant density was 200 plants m^{-2} and the seeding depth was 20 mm.

The WHVZIM22 model was used to simulate the yield of wheat for all combinations of irrigation treatment and soil type using ten years (1981 to 1990) of weather data from the two locations. The simulation results were analyzed both from a yield and economic point of view. For the economic evaluation,

the gross margin per unit area (GM, ZW$[1] ha^{-1}) was calculated as follows:

$$GM = Y \times Y_p - IRR \times IRR_c - NIRR \times NIRR_c - Y \times HARV_c - CONST_c, \quad 5.1$$

where Y = grain yield, t ha^{-1}

Y_p = price of wheat grain, ZW$1450 t^{-1}

IRR = applied irrigation, mm

IRR_c = cost of irrigation water, ZW$8 mm^{-1} (only energy costs and repairs and maintenance)

NIRR = number of irrigation applications

$NIRR_c$ = cost of applying one irrigation cycle, ZW$12 $cycle^{-1}$

$HARV_c$ = cost of harvesting and transporting grain, ZW$30 t^{-1}

$CONST_c$ = constant production costs, independent of irrigation application (e.g., seed, fertilizer and tractor operating costs), ZW$2000 ha^{-1} for the highveld and ZW$16000 ha^{-1} for the middleveld (lower for the middleveld because of the lower yield potential).

The grain price was the ruling price for wheat for the 1993 harvest year, while the costings were obtained from the Agricultural Research Trust (I. Gaylard, 1993, personal communication). The total GM was calculated as that which could be earned if the water used in treatment one was applied to each other treatment.

5.2.2 Results and discussion

The yield of wheat increased with increasing application of water on both the highveld and middleveld and on all soil types (Figures 5.2 and 5.3). However, the response was a typical curvilinear production function, with yields reaching a maximum with the application of 468 mm net (550 mm gross, treatment 3) on the highveld and 383 mm net (450 mm gross, treatment 10) on the middleveld. The maximum yield simulated on the highveld was similar to that reported by MacRobert and Mutemeri (1988). They

[1] Note, at the time of writing, ZW$5.60 ≈ US$1.00

Table 5.3: Soil profile characteristics (lower limit, LL, drained upper limit, DUL, and saturated, SAT, soil water contents, and the root weighting factor, W) of the three soils used in the simulations.

Depth	LL	DUL	SAT	SW	W
m			$m^3\ m^{-3}$		
ART 1990 (Clay)					
0.13	0.210	0.360	0.390	0.300	1.000
0.25	0.270	0.407	0.417	0.370	0.700
0.25	0.340	0.454	0.460	0.435	0.400
0.25	0.300	0.422	0.430	0.400	0.200
0.50	0.300	0.415	0.430	0.400	0.100
GLEN 1990 (Loam)					
0.13	0.130	0.235	0.260	0.170	1.000
0.25	0.135	0.240	0.265	0.210	0.800
0.25	0.165	0.265	0.292	0.245	0.600
0.25	0.165	0.265	0.306	0.255	0.300
0.50	0.165	0.265	0.304	0.260	0.100
BANK 1991 (Sand)					
0.13	0.065	0.145	0.165	0.050	1.000
0.25	0.070	0.150	0.170	0.100	0.300
0.25	0.120	0.195	0.210	0.150	0.100
0.25	0.140	0.220	0.235	0.220	0.075
0.50	0.155	0.240	0.255	0.220	0.010

obtained a two-year mean maximum yield with the application of 570 mm gross.

At both locations, yields were lower, over the full range of irrigation application, on the sand than on the clay. This was attributed to the lower water holding capacity of the sand compared to the loam and clay. The simulated yields on the middleveld were consistently lower than those on the highveld. For a similar given amount of applied water, there was little yield difference between treatments irrigated with 35 mm per application (i.e., greater frequency of irrigation) compared to those irrigated with 50 mm per application. From a farmers' perspective, less frequent irrigations with large amounts are easier to manage.

The maximum GM was obtained on the highveld with the application of 468 mm net (550 mm gross, treatment 10) on all soil types (this was coincident with the maximum yield irrigation application). Conversely, on the middleveld, the amount of irrigation required to achieve the maximum GM

differed with soil type, with the sand requiring more water (treatment 10) than the clay (treatment 12).

If the principle of deficit irrigation was applied to these data, increased financial returns were obtained on the clay soil at both locations, but on the sand and loam soils these benefits were less apparent or non-existent at either location. Nevertheless, it is apparent that even on the sand and loam soil types, the application of more than about 450 mm net irrigation on the highveld and more than about 350 mm on the middleveld leads to reduced financial performance. However, the data does suggest that deficit irrigation is best suited to deep soils with high water holding capacities, and corroborates the recommendations of MacRobert (1992).

The intraseasonal irrigation regimes that produced maximum total gross margins were not consistent across locations, soil ypes or years. However, the treatments that showed the greatest frequency of maximum total gross margin were treatments five and ten (Figure 5.4). These two treatments were different in the total amount of water applied and in the frequency of irrigation application (Table 5.2). Treatment five applied less water at a lower frequency than treatment ten. Consequently, a greater potential area of wheat could be grown with the use of treatment five compared to treatment ten (Table 5.4). However, this did not always result in a greater mean total gross margin. Conversely, on average, the use of less water, applied at a lower frequency, resulted in greater total costs in each situation and these were not always off-set by increased returns. This would be a detraction to the use of deficit irrigation. Nevertheless, on the middleveld, deficit irrigation (treatment five) produced greater returns per dollar invested (i.e., the ratio of total income to total costs) than treatment ten, indicating that the greater costs were more than off-set by the greater returns.

The risk associated with reduced irrigation application (as implied by the standard error of the total GM) increased with a decrease in the amount of water applied (Figure 5.5). This was particularly the case on the highveld, where the yield response to irrigation was greater than on the middleveld. Soil type at a location did not appear to influence the level of

income variance as much as did the amount of irrigation. Increased risk is a feature of deficit irrigation (Martin, van Brocklin and Wilmes, 1989) and may be a reason why farmers tend apply more water than necessary (Stegman, 1983).

In conclusion, this simulation exercise indicated that, in general, less water was required on the middleveld than on the highveld to achieve maximum total gross margins. This was mainly to due to differences in the duration of growth at the two locations resulting in fewer irrigations being applied. Deficit irrigation was shown to be appropriate on soils with a high water holding capacity and could be applied on such soils in either the high- or middleveld. Soils with low water holding capacities in either environment were best irrigated with amounts of water that would achieve the maximum GM per unit area. Variability of mean total gross margin increased with a decrease in water application, particularly on the highveld.

These results show that the financial outcome of irrigation application to wheat depends on many factors, including, *inter alia*, weather conditions, soil type, area of crop grown, irrigation frequency, total irrigation, and the production costs and grain price. The process of advising farmers on the irrigation programme to be applied to their wheat is, therefore, not simple, but calls for an integrated approach that considers all the above factors. The use of a crop simulation model is a convenient and rapid means by which irrigation options can be evaluated in terms of yield, financial returns and practicality.

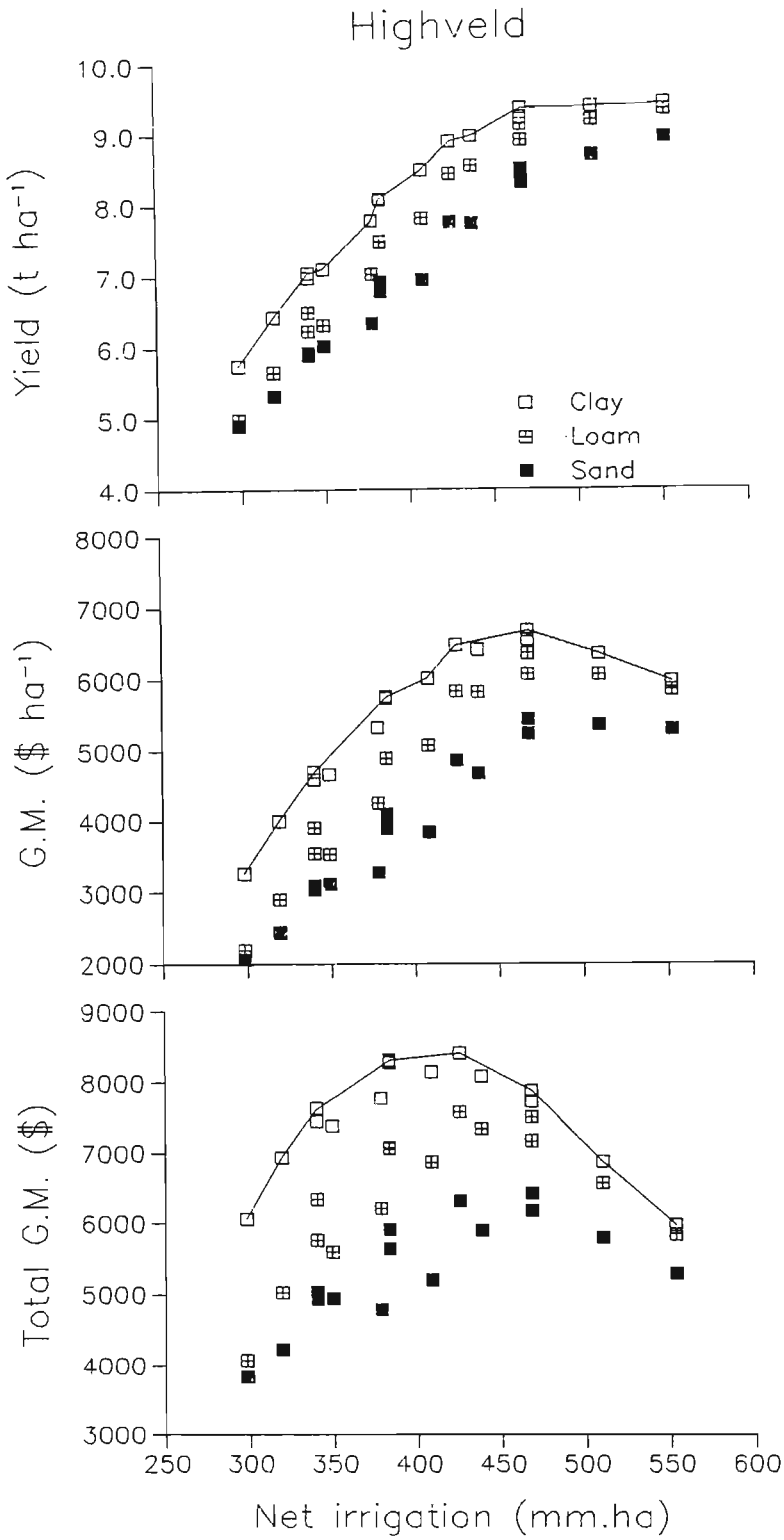

Figure 5.2: The simulated mean yield, gross margin (G.M.) and total G.M. of wheat in response to irrigation amount on three soil types at Kutsaga (representing the highveld).

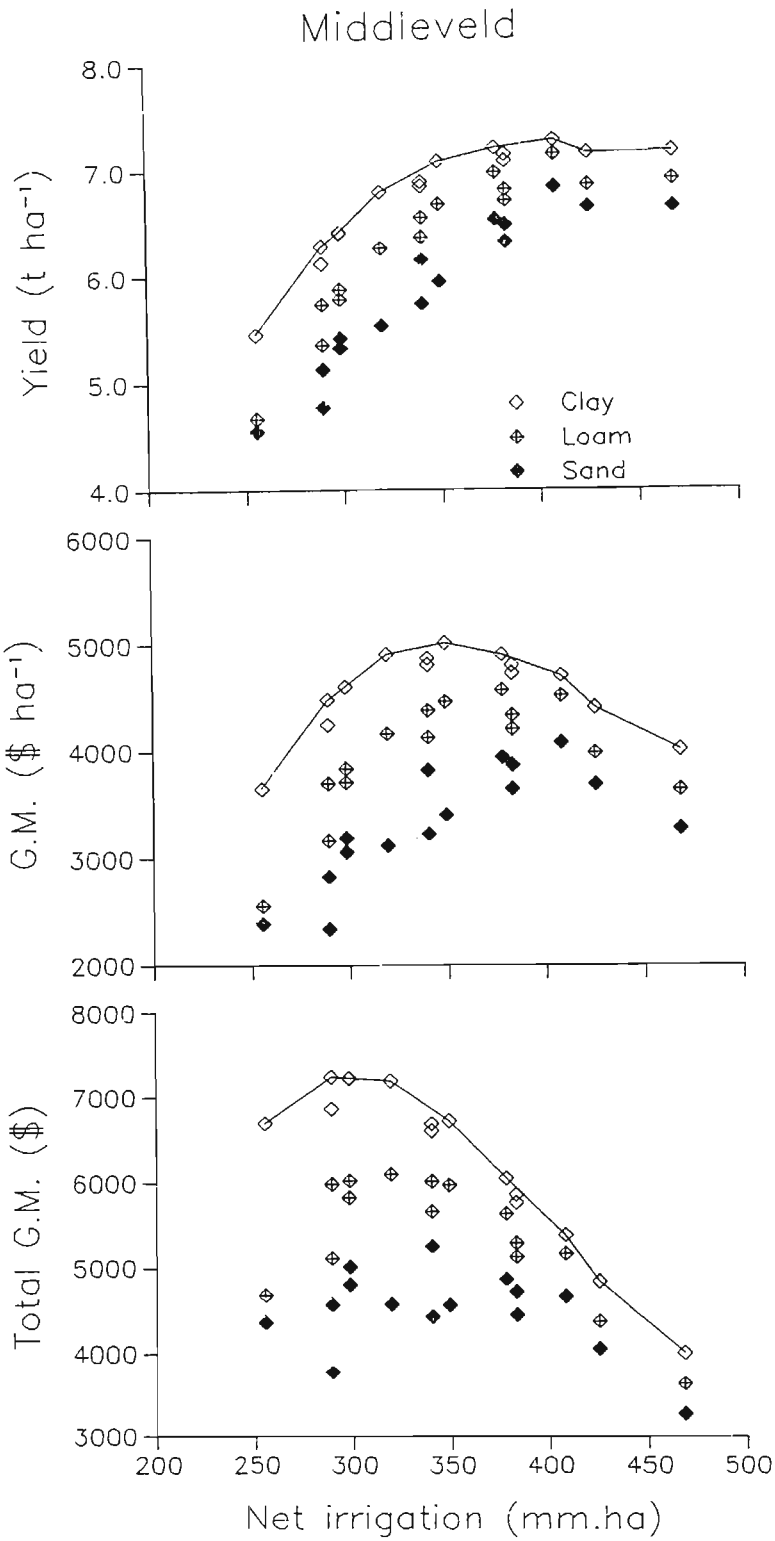

Figure 5.3: The simulated mean yield, gross margin (G.M.) and total G.M. of wheat in response to irrigation amount on three soil types at Banket (representing the middleveld).

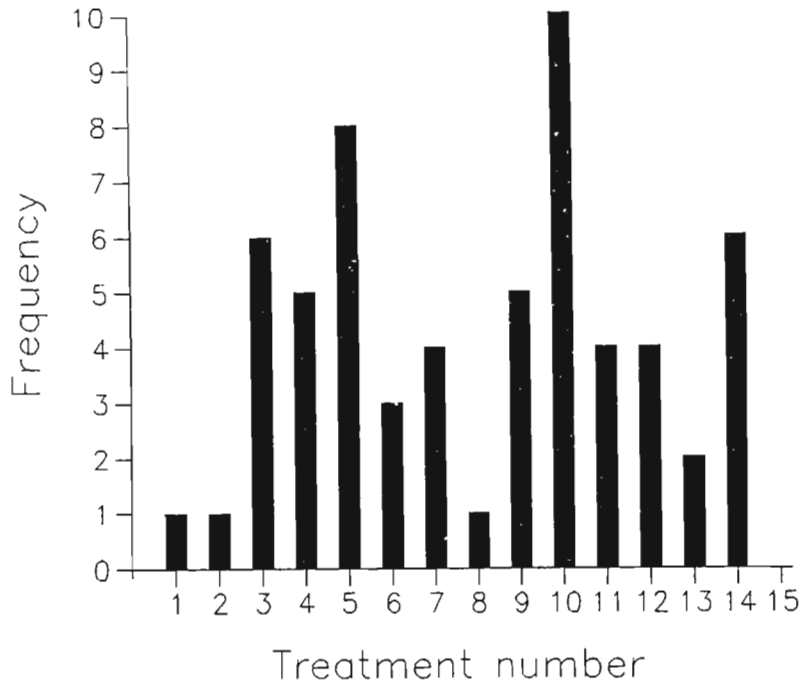

Figure 5.4: The frequency of individual year outcomes with which a treatment achieved the ten-year mean maximum total gross margin across all locations and soil types.

Table 5.4: The relative area (ha), and the simulated ten-year mean total cost (ZW$), total gross margin (ZW$) and return per dollar invested of treatments five and ten applied on two sites and three soil types.

Soil	Relative area 5	10	Total Cost 5	10	Total gross margin 5	10	Return per dollar 5	10
Highveld								
Clay	1.44	1.18	8612	8122	8311	7877	1.965	1.970
Loam	1.44	1.18	8628	8144	7074	7503	1.820	1.921
Sand	1.44	1.18	8562	8091	5907	6419	1.690	1.793
Middleveld								
Clay	1.63	1.35	7582	7134	6687	5387	1.882	1.755
Loam	1.63	1.35	7568	7129	6015	5167	1.795	1.725
Sand	1.63	1.35	7552	7118	5252	4664	1.695	1.655

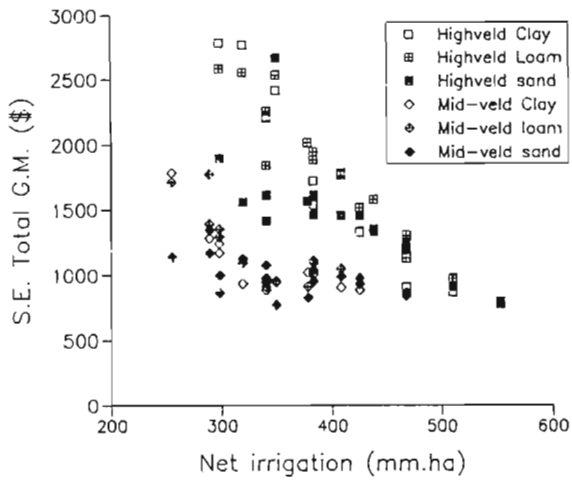

Figure 5.5: The simulated relationship between the standard error of the mean total gross margin (G.M.) and the net amount of water applied to wheat grown on three soil types on the highveld (Kutsaga) and the middleveld (Banket).

6 WHEAT IRRIGATION OPTIMIZATION PROGRAMME

Deficit irrigation is a viable management option in certain situations in Zimbabwe (Chapter 5). Despite this knowledge, though, there is no systematic method of advising a farmer on whether or not to undertake deficit irrigation of his wheat crop. Furthermore, even if a farmer decides to apply deficit irrigation to his crop, he is faced with many pre-season interacting choices, which may impact on profitability. These include, *inter alia*, how much water to apply, what area to grow, what frequency of irrigation is required and what will be the costs and returns? In view of these questions, an interactive computer irrigation optimization programme was developed to assist farmers decide on an irrigation strategy that would maximize the total gross margin of their wheat.

6.1 Programme description

The wheat irrigation optimization programme (WIRROPT6) was written in QuickBASIC 4.00 (Microsoft Corporation, Redmond, WA) and is useable on IBM AT-compatible computers operating under MS-DOS 3.1 or higher (Microsoft Corporation, Redmond, WA). WIRROPT6 uses the CERES-Wheat crop simulation model (Ritchie and Otter, 1984), as modified herein (WHVZIM22, Chapter 4), and incorporates economic and irrigation constraints to predict optimal irrigation policies for particular soil, cultivar and weather conditions. The programme aims to answer the following pre-season questions in the context of maximizing financial returns:

1. with a given water and land resource, what area of wheat should be grown to maximize the total gross margin?
2. with a given irrigation equipment infrastructure, what is the minimum return interval of irrigation to be employed and when should intra-seasonal irrigations be applied?
3. for a given optimal area of wheat, what will be the expected costs of production and returns?

The WIRROPT6 programme is modular based, with a main module supporting 20 subroutines (Table 6.1). The main module contains a menu, by which the user interacts with six input menus, which

Table 6.1: List of subroutines and their principle functions in WIRROPT6.

Subroutine	Description of function
CALDAT	Converts day of year to calendar date (*ex* WHVZIM22).
CONSTRAINTS	Enables input of user specified irrigation constraints: available land and water resources, minimum and maximum return intervals and irrigation application amount and efficiency.
CULTURE	Enables entry of user specified cultural practices: cultivar, sowing date, plant density and seeding depth.
CUMULATE	Accumulates stress indices (*ex* WHVZIM22).
DOTS	Prints dots on screen to indicate that the programme is working.
ECON	Enables entry of crop production cost information and grain price.
GROSUB	WHVZIM22 growth subroutine.
ID	Enables identification of run.
IRROPT	Procedure for selecting the treatments giving the maximum gross margins per unit area and per unit applied water.
MONTHCALC	Determines the alpha month from a numeric month.
OPENWTHFILE	Opens the selected weather file.
PHASEI	Initializes phenological variables (*ex* WHVZIM22).
PHENOL	Determines phenological stage (*ex* WHVZIM22).
PROGRI	Initializes all WHVZIM22 state variables.
READWTHFILE	Reads one day's weather records.
SIMULATION	Iteratively runs the WHVZIM22 subroutines.
SOIL	Enables input of the soil profile characteristics.
SOILRI	Initializes soil information (*ex* WHVZIM22).
WATBAL	Water balance subroutine (*ex* WHVZIM22).
WEATHER	Enables selection of appropriate weather file.

specify the identity, irrigation constraints, economic criteria and the soil, weather and cultural conditions appropriate to the farm in question. Once these parameters (described below) have been chosen, the main module iteratively calls the WHVZIM22 subroutines PROGRI, SOILRI, PHASEI, PHENOL, GROSUB and WATBAL to simulate irrigation application dates, phenology and yield. The output irrigation amounts and yield are converted into financial indices to determine the best irrigation regimes for the farm in question. These are listed for evaluation. Additionally, the programme provides the simulated dates of important growth stages, including the harvest date. The period

from physiological maturity to harvest was simulated using the algorithm developed by Chen and McClendon (1984). Although their model was used on soyabeans, Parsch *et al.* (1991) found it adequate for the prediction of grain drydown of wheat.

The ASCII source code of the WIRROPT6 programme is supplied on the accompanying diskette (file name *WIRROPT6.bas* in subdirectory *WIRROPT*). A list of programme variables is given (Appendix 6). The programme may be run from within either the QuickBASIC 4.00 or MS-DOS QBasic 1.1 (Microsoft Corporation, Redmond, WA) environments by loading the file *WIRROPT6.bas* and selecting the "Start" command from the "Run" menu.

6.1.1 Input routines

6.1.1.1 Farm and run identification (subroutine *ID*)

Each optimization exercise is preceeded by an opportunity to identify the run, by specifying the farm name, a four-character code for the farm, a two-digit field identification number and a two-digit year code.

6.1.1.2 Irrigation constraints (subroutine *CONSTRAINTS*)

Most irrigation farms in Zimbabwe have relatively more arable land than irrigable land, as dictated by the irrigation water resources. The majority of irrigation schemes are hand moved, overhead sprinkler systems. Such schemes are flexible in that they can be extended relatively easily to cover a larger area than the original design. However, there is usually a maximum area to which the scheme may be expanded, as determined by underground or portable main lines and/or pump capacity. Once the field is laid out, the irrigation scheme becomes fairly rigid in terms of the frequency with which irrigation can be applied. Farmers generally lay out their irrigation network to cater for a minimum return interval, which is decided upon pre-season by taking into account factors such as the soil water holding capacity, crop water demand and potential evaporation.

The amount of irrigation that may be applied in one setting is dependent on the nozzle discharge, sprinkler spacing and set

duration. Most irrigation schemes have sprinkler spacings of 12 m x 18 m or 18 m x 18 m, and nozzle discharges of around 1 $m^3 h^{-1}$. Water application rates therefore range between 4 and 7 mm h^{-1}. The set duration is usually between six and 12 hours, with shorter durations applied on the sandier, lower water holding capacity soils. Twelve hour set durations are generally favoured, though, because they enable two moves per day during daylight hours. More frequent irrigation pipe changes require night moves, which can be difficult. Thus, on a 12 h set time (usually taken as 11.5 h to account for the time taken in moving the pipes), gross irrigation application amounts range between 45 and 80 mm (a common standard is 55 mm on high water holding capacity soils). Irrigation application efficiencies vary greatly but a figure of 85 % is commonly used.

Water used in wheat production is derived from river flow, surface storage and underground reserves. Farmers relying on underground reserves have the least knowledge of the total quantity of water available, but they generally know the hourly pump capacity of a well. Farmers extracting water from dams and rivers usually have defined water rights, which specify the seasonal quantities of water that may be pumped. Thus, wherever a farmer obtains his water, he can estimate the total quantity of water available to him for a given season.

The irrigation constraints facing a farmer are therefore:

1. the amount of potentially irrigable land available (*POTAREA*, ha),
2. the total seasonal amount of water available (*WATRES*, ML),
3. the minimum return interval (*MinInterval*, d),
4. the maximum return interval (*MaxInterval*, d),
5. the normal, full set irrigation application amount (*IrrApp*, mm), and
6. the irrigation efficiency (*EffIrr*, %).

The subroutine *CONSTRAINTS* enables the user to input these data for a particular situation.

6.1.1.3 Economic criteria (subroutine *ECON*)

The major wheat production cost variables are irrigation and fertilizer. In this exercise, irrigation costs were considered

the dominant variable costs. Consequently, the programme requires the following production costs:

1. The cost of irrigation water (*IrrCost1*, ZW$ mm^{-1}). This represents the cost of delivering one mm of water to the field and may be comprised of energy costs, repairs and maintenance, depreciation on equipment and labour.
2. The cost of applying one cycle of irrigation (*IrrCost2*, ZW$ $cycle^{-1}$). Since this exercise considers both the total amount of irrigation applied and the frequency of irrigation, it was considered necessary to include a cost component related to irrigation frequency. Since irrigation schemes in Zimbabwe are mainly hand-moved sprinkler systems, this cost component is mostly composed of labour costs.
3. The harvest and transport cost (*HarvCost*, ZW$ t^{-1}). Irrigation application amount affects yield. Therefore, a harvest and transport cost needed to be included. This cost accounts for the harvesting operation and the transport of the grain to market.
4. The constant costs of production (*ConstCost*, ZW$ ha^{-1}). Certain costs of wheat production are essentially independent of irrigation amount. These include the costs of land preparation, seed and fertilizer. Although fertilizer application, especially N fertilizer, is linked to yield potential, it was considered unnecessary to specifically include it in the model, especially since the model assumes that nutrients are non-limiting. Furthermore, research has indicated that wheat responds similarly to nitrogen fertilizer application over a range of water application amounts (Agricultural Research Trust, 1988).

In order the calculate the gross margin per ha (*GMha*, ZW$ ha^{-1}) and other financial indices, the programme also prompts for the net price of wheat grain (*NetPrice*, ZW$ t^{-1}), which is the grain price less marketing costs.

6.1.1.4 Weather file selection (subroutine *WEATHER*)

Eight representative weather files are included with the programme (Table 6.2). These are listed in the file *WTH.DIR*, which together with the actual weather data files, conform to

Table 6.2: Characteristics of the representative weather files available for use with the WIRROPT6 programme.

						Mean annual		
Code	Name	LAT	XLONG	ALT	EXPFACT	SOLRAD	TEMPMX	TEMPMN
		°S	°E	m		MJ m^{-2}	°C	°C
BANK	Banket	17.32	30.40	1244	5.0	20.5	26.9	13.9
BUFF	Buffalo Range	21.02	31.58	430	5.0	21.2	30.3	16.4
DARW	Mount Darwin	16.47	31.35	966	5.0	21.9	28.1	14.4
HEND	Henderson	17.58	31.00	1292	3.5	20.3	26.8	9.8
KADO	Kadoma	18.32	29.88	1150	4.0	21.9	28.6	14.6
KARO	Karoi	16.83	29.62	1343	4.0	22.2	25.8	13.7
KUTS	Kutsaga	17.92	31.13	1480	4.5	20.2	24.9	11.5
MVUR	Mvurwi	17.03	30.51	1480	5.0	19.9	24.5	12.0

the IBSNAT file conventions (IBSNAT, 1986), except that the weather file extensions for these particular files are *.RND* and not *.WYY* as specified by IBSNAT (where *YY* is the last two digits of the year). These weather files were created from records obtained from the Department of Meteorological Services, Government of Zimbabwe. For each site, ten years (1981 to 1990) of minimum data set weather records were compiled. From these, one weather file was created for each site by randomly selecting, for each day of the year, one set of weather records for that day of year from one of the ten years of records. This was considered a convenient and adequate way of creating a representative weather file for each location for use in this simulation excercise. Weather conditions during the winter period (1 May to 30 September) of Zimbabwe do not vary greatly (Table 6.3) and creating a representative weather file by randomly selecting records was considered a better method than using averages, because averages tend to mask extremes. However, it is recognised that the taking of random samples destroys short term serial correlations that exist in weather data. The user may add weather files to the file *WTH.DIR*, as required.

6.1.1.5 Soil profile selection (subroutine *SOIL*)

A representative soil profile is selected from a screen displayed list. The programme utilizes the file *SPROFILE.WH2*, which has the same format as that required for WHVZIM22

Table 6.3: The ten year (1981 to 1990) mean (± SE) cumulative daily solar radiant density (MJ m^{-2}), mean (± SE) cumulative mean daily air temperature (°C) and the mean total rainfall for the period 1 May to 30 September at eight locations.

Location	Solar irradiance	Air temperature	Rainfall
BANK	2907 ± 56	2743 ± 88	16
BUFF	2715 ± 81	3096 ± 218	46
DARW	3131 ± 51	2750 ± 126	10
HEND	2836 ± 67	2278 ± 65	16
KADO	3069 ± 69	2861 ± 88	9
KARO	3294 ± 66	2646 ± 90	16
KUTS	2950 ± 75	2339 ± 74	18
MVUR	2872 ± 176	2372 ± 72	17

(conforming to IBSNAT, 1986). A summary of the soil profiles provided for use with WIRROPT6 is given (Table 6.4). Additional soil pedons may be added at the user's discretion.

The actual initial soil water content of each soil layer may be specified by the user, if known. Alternatively, the user may simply specify the percent depletion of the profile available water content. If this latter option is chosen, the programme adjusts the soil water content of each layer to give the initial soil water content required for the proper functioning of *WATBAL*. Soil water is preferentially depleted from surface layers in a cascading manner.

Table 6.4: Characteristics of the soil profiles available for use with WIRROPT6.

Location and soil description		SALB	U	SWCON	CN2	LL	DUL	SAT
			mm			$m^3\ m^{-3}$		
ART Farm 1988	Salisbury 5.E2	0.13	4	0.20	60	0.243	0.370	0.413
ART Farm 1989	Salisbury 5.E2	0.13	4	0.20	60	0.262	0.378	0.415
ART Farm 1990	Salisbury 5.E2	0.13	4	0.20	60	0.293	0.417	0.429
ART Farm 1991	Salisbury 5.E2	0.13	4	0.20	60	0.235	0.385	0.401
ART Farm 1992	Salisbury 5.E2	0.13	4	0.20	60	0.211	0.350	0.384
Glendale 1989	Wooler Farm	0.14	4	0.50	60	0.148	0.288	0.304
Glendale 1990	Wooler Farm	0.14	2	0.40	60	0.517	0.258	0.291
Rattray Arnold	Salisbury 5E.2	0.14	5	0.50	60	0.225	0.338	0.374
Concession	Zanadu Farm	0.20	3	0.60	60	0.191	0.320	0.348
Banket sand	Doonside Farm	0.18	1	0.25	60	0.122	0.203	0.220
Kutsaga sand	Harare 5G.2	0.20	2	0.70	60	0.035	0.128	0.175

6.1.1.6 Crop cultural practices (subroutine *CULTURE*)

The WIRROPT6 programme presents the user with a choice of cultivars derived from the file *GENETICS.V22*. This file has the same format and genetic coefficients as those required by WHVZIM22. Additional cultivars may be added to the list at the user's discretion. Following cultivar selection, the user is prompted to enter the sowing date, plant density (plants m^{-2}) and seeding depth (cm).

6.1.2 Irrigation optimization routines

The WIRROPT6 programme seeks to find the intraseasonal irrigation regime that maximizes the total gross margin within the constraints of land and water availability. The process for doing this is simple. Firstly, all irrigation regimes have the same establishment procedure. This procedure (accomplished in subroutine *WATBAL*) applies irrigation water on the day of sowing, five days after sowing (das) (if necessary) and at 21 das in quantities that ensure that the whole soil profile is at or near the upper limit of plant available water by 21 das. The only constraint is that the amount of irrigation applied with each irrigation must be equal to either a full or a half application of the normal full set irrigation (*IrrApp*) as specified in subroutine *CONSTRAINTS*. This procedure conforms to the establishment principles given by MacRobert (1992) and they are practical in terms of a farmer's capability.

Secondly, the programme loops once through WHVZIM22 to simulate the potential yield by irrigating whenever 30 % of the profile available soil water has been depleted. This irrigation triggering level of soil water depletion has been cited as one that will achieve maximum yields (James, 1988). No regard is taken of the *IrrApp* or *MinInterval* specified by the user, since the aim is to simulate the maximum yield.

From the maximum yield and the total irrigation amount applied, the *GMha*, ZW$ ha^{-1}, is calculated from:

$$GMha = YIELD \times NetPrice - IrrApp \times IrrCost1 - Nirr \times IrrCost2 - YIELD \times HarvCost - ConstCost, \quad 6.1$$

where *YIELD* is the predicted field yield, t ha^{-1}. The area of wheat that could be grown (*AREA*, ha) is calculated from *WATRES* divided by the total irrigation application (*TotIrr*, mm ha^{-1}), multiplied by 100 to convert mm ha^{-1} to ML ha^{-1}. The gross margin per unit of applied water (*GMmm*, ZW$ mm^{-1}) is calculated by dividing *GMha* by *IrrApp*. The total costs (*TOTCOST*, ZW$) and the total gross margin (*TotGM*, ZW$) are computed from the product of the *AREA* and the sum of the costs per ha and from the product of *AREA* and *GMha*, respectively. These indices provide the starting point from where the programme begins to seek the irrigation regime that will maximize total gross margin.

The programme continues to loop through the WHVZIM22 crop simulation model, incrementing the minimum irrigation return interval by one day with each loop, starting with *MinInterval* and ending with *MaxInterval*. Irrigation after establishment (i.e., after 21 das) is applied only if the number of days from the last irrigation is greater than or equal to the current irrigation interval and if the profile soil water content has been depleted by, at least, the amount *IrrApp x EffIrr*. On the completion of each loop, the *GMha*, *GMmm*, *TotGM* and *TOTCOST* are calculated and displayed. The programme selects the irrigation regime(s) that produce the maximum *GMha* and the maximum *TotGM* and displays the irrigation schedule and plant characteristics of each for evaluation by the user.

6.2 Irrigation optimization example

As an example of the use of WIRROPT6, the programme was run on two soil types differing in water holding capacity, *viz.*, a low water holding capacity soil (Kutsaga: mean profile available water content of 0.093 m^3 m^{-3}) and on a high water holding capacity soil (ART 1991: mean profile available water content of 0.150 m^3 m^{-3}) (Table 6.4). The same weather file and cultural conditions were applied to both soils (Table 6.5). The irrigation application amounts and the minimum and maximum return intervals differed according to soil type. A high water application rate (55 mm per set) and longer return intervals were applied on the ART 1991 soil, whereas a low water application rate (40 mm per set) and shorter return intervals

were applied on the Kutsaga soil. These application rates are common on such soil types in Zimbabwe. The constant costs of production were set lower on the Kutsaga soil than the ART soil in anticipation of lower yields on the Kutsaga soil.

The WIRROPT6 programme was executed from within the QuickBASIC 4.00 environment on an IBM AT-compatible 80486 computer running at 25 MHz under MS-DOS 6. The optimization time for each soil type was ca. four to five minutes. The duration of the optimization process depends partly on the time taken for the user to interact with the input routines.

Table 6.5: Input specifications used in the irrigation optimization example on two soil types.

Parameter	ART 1991	Kutsaga
Identification		
Farm name	ART Farm	Kutsaga
Farm code	ARTF	KUTS
Field code	01	02
Year	93	93
Run code	ARTF9301	KUTS9302
Irrigation constraints		
Area of land available, ha	100	100
Quantity of water available, ML	400	400
Maximum return interval, d	17	15
Minimum return interval, d	10	8
Normal full set application, mm	55	40
Irrigation efficiency, %	85	85
Economic criteria		
Net price of wheat, ZW$ t^{-1}	1450	1450
Irrigation water cost, ZW$ mm^{-1}	8	8
Irrigation application cost, ZW$ $cycle^{-1}$	12	12
Harvesting and transport cost, ZW$ t^{-1}	30	30
Constant costs of production, ZW$ ha^{-1}	2000	1600
Weather file		
Number	1	1
Name	KUTS0112.RND	KUTS0112.RND
Soil profile characteristics		
Number	4	11
Name	ART 1991	Kutsaga
Available water depletion, %	30	40
Cultural conditions		
Cultivar	W170/84	W170/84
Sowing date	12 May	12 May
Plant density, plants m^{-2}	200	200
Seeding depth, cm	2	2

The first output screen (Table 6.6 for the ART soil and Table 6.9 for the Kutsaga soil) presents the phenological development, yield and yield components of the first optimization loop. This loop establishes the potential yield for the site, sowing date and cultivar. The simulated potential yields for the two soil types were equal. This is principally because irrigation is applied to ensure a non-limiting soil water balance. However, because the application rates for the two soils were different, the attainment of potential yield on the ART soil required a minimum return interval of seven days, whereas the minimum return interval for potential yields on the Kutsaga soil was five days (Tables 6.7 and 6.10, respectively). Nevertheless, the total water application and potential crop areas were similar for each soil type.

The simulated effects of lengthening the irrigation interval from the minimum to maximum intervals are given for the ART soil (Table 6.7) and for the Kutsaga soil (Table 6.10). The optimization procedure on the ART soil indicated that potential yields and maximum gross margins per unit area could be achieved with either a ten, 11 or 12 d minimum irrigation interval. The use of any of these cycle lengths would enable the production of 69 ha with the available water resources. However, with a lengthening of the irrigation interval beyond 12 d, less water per unit area was required, thereby enabling a greater area of production, and although the yield and gross margin per unit area declined, the gross margin per unit of water increased, as did the total gross margin. The maximum total gross margin was achieved with a minimum irrigation interval of 15 d.

This, therefore, presents two options on the ART soil. The hypothetical farmer may aim for maximum gross margin per unit area with a frequent irrigation schedule. Alternatively, he could reduce the water application per unit area by irrigating less frequently, and thereby grow a larger area and achieve greater total profits. To help distinguish between these two alternatives, the programme presents the total cost and total gross margin data, together with the irrigation schedule and crop development information (Table 6.8). The farmer's choice may depend on factors such as attitude to risk (bearing in mind

that the long term variability of yield and total gross margin tends to increase with a decrease in water application (Figure 5.5)), the relationship between total costs and returns and the practicality of the proposed irrigation schedule. For example, if the farmer grew 86 ha with a 15 d minimum irrigation interval, his costs would by $34626 greater than if he grew 69 ha on a 10 d interval, but his total gross margin would be increased by $58796, which more than off-sets the increased cost. However, if the increased cost incurred added finance charges, there may not be any advantage in the 15 d interval over the 10 d interval.

On the Kutsaga soil, both the maximum gross margin per unit area and the maximum total gross margin were achieved with a minimum return interval of eight days (Table 6.10). With a lower frequency of irrigation, a greater area of wheat could be grown, but total costs increased and the total gross margin decreased. Thus, for this particular case, the choice of irrigation management is simple, and the simulated irrigation schedule and crop development information is presented (Table 6.11) to assist the user in deciding the intraseasonal allocation of water.

6.3 Conclusion

The WIRROPT6 irrigation optimization programme is a relatively simple and "friendly" programme to work with, and provides a means by which a farmer or advisor can rapidly and conveniently evaluate irrigation management options on wheat. The user may loop through the programme *ad infinitum*, changing any of the input variables to assess new options and alternatives.

However, WIRROPT6 can only be viewed as a management aid within the context of the limitations of the modified CERES-Wheat model. Although this model has shown reasonable accuracy in the prediction of wheat yield under irrigated conditions in Zimbabwe, it is not a perfect predictor of yield, and suffers from the inadequacy of not simulating nutrient dynamics or pest problems. The WIRROPT6 programme also uses historical weather to predict a likely outcome from a particular set of irrigation, soil, cultivar and economic conditions for use in

a future situation. In cognisance of future uncertainty, the simulated output of WIRROPT6 must be used with caution. The best use of the programme would be to give guidelines on the area of wheat to grow and the minimum return interval that should be planned for. The actual intra-seasonal allocation of water should be carried out using real-time information of crop water use, as dictated by weather, soil, crop and management conditions.

Table 6.6: The first output screen generated by WIRROPT6 during the simulated optimization of irrigation of wheat on the ART soil. (Price is the net price of wheat grain, Irr is the irrigation water cost, App is the irrigation application cost, Harv is the harvesting cost and Const is the constant costs of production. DAP is the days after planting.)

```
                        Simulation has begun
                        ====================

Code: ARTF9301     Weather: KUTS0112.RND   Soil:  4 (16)  Cv: W170/84
Price=$1450/t  Irr=$8.00/mm.ha  App=$12.00/cycle  Harv=$30/t Const=$2000/ha

                  Event                          Date      DAP
                  -------------------------      ------    ---
                  Sowing date :                  12 May      0
                  Germination :                  13 May      1
                  Emergence   :                  18 May      6
                  Terminal spikelet :            30 Jun     49
                  First node :                    9 Jul     58
                  Flag leaf emergence :          30 Jul     79
                  Flowering started :            22 Aug    102
                  Begin grain-filling :           1 Sep    112
                  Physiological maturity :       12 Oct    153
                  Harvest maturity :             21 Oct    162

   Yield = 10.08 t/ha; Ear density = 451 per m^2; Kernel mass = 43.1 mg
   Kernels per plant = 138 ;          Kernels per square metre = 27520

                        Press <Enter> to continue
```

Table 6.7: The second output screen generated by WIRROPT6 during the simulated optimization of irrigation of wheat on the ART soil. The table shows the effect of incrementing the minimum irrigation interval (Irr Int) from *MinInterval* to *MaxInterval* on the total irrigation applied (Tot Irr), yield, gross margin per unit area (G M, $/ha), gross margin per unit of applied water (G M, $/mm), the area of wheat that could be grown within the constraints of land and water availability, the total cost (Tot cost) and the total gross margin (Tot GM).

```
                Searching for maximum total gross margin
                ========================================
Code: ARTF9301     Weather: KUTS0112.RND   Soil:  4 (16)  Cv: W170/84
Price=$1450/t  Irr=$8.00/mm.ha  App=$12.00/cycle  Harv=$30/t  Const=$2000/ha

Irr Int    Tot Irr     Yield      G M        G M       Area     Tot Cost      Tot GM
 days        mm         t/ha      $/ha       $/mm       ha         $            $
------     -------     -----      ----       ----      ----     --------     --------
   7         670       10.08      6788       10.1       60       467536       405384
  10         578       10.08      7562       13.1       69       488617       523790
  11         578       10.08      7562       13.1       69       488617       523790
  12         578       10.08      7562       13.1       69       488617       523790
  13         523        9.73      7511       14.4       77       504634       575002
  14         523        9.71      7491       14.3       77       504601       573465
  15         468        8.91      6809       14.6       86       523243       582586
  16         468        8.77      6603       14.1       86       522871       564997
  17         413        7.82      5714       13.9       97       546009       554076

Maximum gross margin per ha on a 10 d interval; GM/ha = $7562
Maximum gross margin per mm on a 15 d interval; GM/mm = $14.56
Maximum total gross margin on a 15 d interval; MaxTotGM = $ 582586

Optimization process took  3.8 minutes

Press <Enter> to continue
```

Table 6.8: The third (A) and fourth (B) output screens generated by WIRROPT6 during the simulated optimization of irrigation of wheat on the ART soil. The table shows the irrigation regime, crop growth characteristics and summary economic details of the irrigation regime that produced A. the maximum gross margin per unit area and B. the maximum gross margin per unit of applied water.

A. The irrigation regime and characteristics of the 'maximum GM/ha regime':

Code: ARTF9301 Weather: KUTS0112.RND Soil: 4 (16) Cv: W170/84
Price=$1450/t Irr=$8.00/mm.ha App=$12.00/cycle Harv=$30/t Const=$2000/ha

Irrigation application Date	DAP	mm	Interval days	AWD %
12 May	0	55	-	30
2 Jun	21	28	21	15
22 Jun	41	55	20	36
7 Jul	56	55	15	38
20 Jul	69	55	13	38
1 Aug	81	55	12	36
17 Aug	97	55	16	39
28 Aug	108	55	11	39
7 Sep	118	55	10	38
17 Sep	128	55	10	41
27 Sep	138	55	10	48
		578 mm gross		
		491 mm net		

Growth stage	Date	DAP
Leaf three	2 Jun	21
First node	9 Jul	58
Flag leaf	30 Jul	79
Anthesis	22 Aug	102
P. maturity	12 Oct	153
Harvest	21 Oct	162

Yield = 10.08 t/ha
Area = 69 ha

G M per ha = $7562/ha
G M per mm = $13.09/mm

Total G M = $ 523790
Total Cost = $ 488617

Press <Enter> to continue

B. The irrigation regime and characteristics of the 'maximum GM/mm regime':

Code: ARTF9301 Weather: KUTS0112.RND Soil: 4 (16) Cv: W170/84
Price=$1450/t Irr=$8.00/mm.ha App=$12.00/cycle Harv=$30/t Const=$2000/ha

Irrigation application Date	DAP	mm	Interval days	AWD %
12 May	0	55	-	30
2 Jun	21	28	21	15
22 Jun	41	55	20	36
7 Jul	56	55	15	38
22 Jul	71	55	15	45
6 Aug	86	55	15	52
21 Aug	101	55	15	52
5 Sep	116	55	15	68
20 Sep	131	55	15	89
		468 mm gross		
		397 mm net		

Growth stage	Date	DAP
Leaf three	2 Jun	21
First node	9 Jul	58
Flag leaf	30 Jul	79
Anthesis	22 Aug	102
P. maturity	8 Oct	149
Harvest	19 Oct	160

Yield = 8.91 t/ha
Area = 86 ha

G M per ha = $6809/ha
G M per mm = $14.56/mm

Total G M = $ 582586
Total Cost = $ 523243

Press <Enter> to continue

Table 6.9: The first output screen generated by WIRROPT6 during the simulated optimization of irrigation of wheat on the Kutsaga soil. (Price is the net price of wheat grain, Irr is the irrigation water cost, App is the irrigation application cost, Harv is the harvesting cost and Const is the constant costs of production. DAP is the days after planting.)

```
                        Simulation has begun
                        ====================

Code: KUTS9302     Weather: KUTS0112.RND   Soil: 11 (31)  Cv: W170/84
Price=$1450/t  Irr=$8.00/mm.ha  App=$12.00/cycle  Harv=$30/t  Const=$1600/ha

                  Event                          Date       DAP
                  -------------------------      ------     ---
                  Sowing date :                  12 May       0
                  Germination :                  13 May       1
                  Emergence   :                  18 May       6
                  Terminal spikelet :            30 Jun      49
                  First node :                    9 Jul      58
                  Flag leaf emergence :          30 Jul      79
                  Flowering started :            22 Aug     102
                  Begin grain-filling :           1 Sep     112
                  Physiological maturity :       12 Oct     153
                  Harvest maturity :             21 Oct     162

   Yield = 10.08 t/ha; Ear density = 451 per m^2; Kernel mass = 43.1 mg
   Kernels per plant = 138 ;          Kernels per square metre = 27520

                        Press <Enter> to continue
```

Table 6.10: The second output screen generated by WIRROPT6 during the simulated optimization of irrigation of wheat on the Kutsaga soil. The table shows the effect of incrementing the minimum irrigation interval (Irr Int) from *MinInterval* to *MaxInterval* on the total irrigation applied (Tot Irr), yield, gross margin per unit area (G M, $/ha), gross margin per unit of applied water (G M, $/mm), the area of wheat that could be grown within the constraints of land and water availability, the total cost (Tot cost) and the total gross margin (Tot GM).

```
                Searching for maximum total gross margin
                ========================================
Code: KUTS9302     Weather: KUTS0112.RND   Soil: 11 (31)  Cv: W170/84
Price=$1450/t  Irr=$8.00/mm.ha  App=$12.00/cycle  Harv=$30/t  Const=$1600/ha

Irr Int     Tot Irr    Yield     G M       G M      Area     Tot Cost     Tot GM
  days        mm       t/ha      $/ha      $/mm      ha         $           $
-------     -------    -----     -----     -----     ----     --------    --------
    5         666      10.08      7142      10.7       60       448582      428667
    8         600      10.09      7739      12.9       67       459651      515938
    9         560       9.45      7156      12.8       71       467389      511176
   10         520       8.89      6697      12.9       77       476517      515118
   11         480       8.16      5995      12.5       83       486740      499561
   12         440       7.26      5051      11.5       91       498357      459205
   13         400       6.54      4361      10.9      100       512832      436065
   14         400       6.16      3820       9.6      100       511691      382026
   15         360       5.48      3177       8.8      100 *     476430      317705

Maximum gross margin per ha on a  8 d interval; GM/ha = $7739
Maximum gross margin per mm on a  8 d interval; GM/mm = $12.90
Maximum total gross margin on a  8 d interval; MaxTotGM = $ 515938

Optimization process took  5.1 minutes

Press <Enter> to continue
```

Table 6.11: The third output screens generated by WIRROPT6 during the simulated optimization of irrigation of wheat on the Kutsaga soil. The table shows the irrigation regime, crop growth characteristics and summary economic details of the one irrigation regime that produced both the maximum gross margin per unit area and the maximum gross margin per unit of applied water.

The irrigation regime and characteristics of the 'maximum GM/ha regime':

Code: KUTS9302 Weather: KUTS0112.RND Soil: 11 (31) Cv: W170/84
Price=$1450/t Irr=$8.00/mm.ha App=$12.00/cycle Harv=$30/t Const=$1600/ha

Irrigation application Date	DAP	mm	Interval days	AWD %
12 May	0	40	-	40
16 May	4	20	4	11
2 Jun	21	20	17	19
16 Jun	35	40	14	38
28 Jun	47	40	12	41
9 Jul	58	40	11	42
18 Jul	67	40	9	40
26 Jul	75	40	8	39
5 Aug	85	40	10	41
17 Aug	97	40	12	41
25 Aug	105	40	8	41
2 Sep	113	40	8	45
10 Sep	121	40	8	43
18 Sep	129	40	8	57
26 Sep	137	40	8	67
4 Oct	145	40	8	79
		600 mm gross		
		510 mm net		

Growth stage	Date	DAP
Leaf three	2 Jun	21
First node	9 Jul	58
Flag leaf	30 Jul	79
Anthesis	22 Aug	102
P. maturity	12 Oct	153
Harvest	21 Oct	162

Yield = 10.09 t/ha
Area = 67 ha

G M per ha = $7739/ha
G M per mm = $12.90/mm

Total G M = $ 515938
Total Cost = $ 459651

Press <Enter> to continue

SUMMARY AND CONCLUSION

The CERES-Wheat version 2.10 model (Ritchie and Otter, 1984; WHV21) was found to be inaccurate and biased in predicting the phenological development of wheat in Zimbabwe, particularly under deficit irrigated conditions. The simulation of tillering by WHV21 was poor and the model tended to over-predict dry matter accumulation and under-predict leaf area indices. The yield component and grain yield predictions were generally imprecise. On the other hand, for most data sets, the simulated soil water contents were similar to the measured soil water contents. These inconsistencies prompted a revision of the phenological and growth subroutines of the model. These revisions were mostly based on experimental data collected from seven years of field research in Zimbabwe.

Modifications to the phenological subroutine (PHENOL) included removing the vernalization procedure, changing the thermal time requirements and base temperatures for growth phases one to five, adding the simulation of leaf emergence and the prediction of Zadoks growth stage 31, and adding a function to hasten phasic development under conditions of plant water deficit (Section 4.1). These modifications improved the predictive ability of the model (Section 4.1.7). On average over all the validation data sets, the revised model (WHVZIM22) had lower mean absolute errors and higher Index of Agreements for the prediction of Zadoks growth stages 39, 61 and 87 compared to WHV21 (Table 4.12).

Many changes were made to the growth subroutine (Section 4.2). Some were minor calibrations of empirical equations, whilst others were significant changes. The over-prediction of dry matter accumulation was rectified by reducing the extinction coefficient in the exponential PAR interception equation. Field data indicated that wheat ears played a significant role in PAR interception. Consequently, an exponential equation was added to allow for PAR interception by ears during growth phases three to five. The photosynthetic reduction factor for temperature (PRFT) was changed to the one given by van Keulen and Seligman (1987), whilst the daytime temperature equation was calibrated on a Zimbabwean data set.

The progression of assimilate partitioning to roots, leaves, stems and grains was made a continuous changing function of plant age, as apposed to the discontinuous functions given in WHV21. Minor adjustments were made to the leaf area production and senescence routines.

The tiller production routines were radically changed (Section 4.2.3). Field data indicated that the main factors affecting tiller production were air temperature, solar irradiance and plant density. A tiller production rate function, based on these three factors, was developed and inserted in growth phase one in place of the routine given in WHV21. Tillering was also made to begin when the third leaf was half emerged, which was earlier than that of WHV21. Tillering routines were extended into growth phase four, and the equations used to predict the potential dry matter accumulation of a tiller were modified to accommodate the changes made to other sections of the growth subroutine. These changes markedly improved the capacity of the model to predict the seasonal progression of tillering under both well-watered and deficit-irrigated conditions (Section 4.2.8.3).

Frost damage to wheat kernel numbers is a problem at times in Zimbabwe. A procedure was developed to predict kernel number loss due to low temperatures (Section 4.2.4). The method firstly determines the exposed minimum temperature from the screen minimum temperature, based on an frost susceptibility index given by Law (1979). Secondly, kernel numbers are reduced whenever the exposed minimum air temperature declines below 0°C.

Kernel growth was made to begin gradually during growth phase four (Section 4.2.5). In view of inadequate predictions of kernel mass under conditions of water deficits, kernel growth rate was made to increase under conditions of water stress. Additionally, the timing of the completion of pre-anthesis ear growth was retarded to enable the accumulation of more stem stored assimilate for later transfer to kernel growth. On average, these changes contributed to improved predictions of kernel mass (Section 4.2.8.2), but under conditions of severe water deficits, predicted kernel mass remained below observed data, indicating that this area of the model needs further review and improvement.

The prediction of field yield was improved, on average over all the validation data sets, by WHVZIM22 compared to WHV21. The mean absolute error of field yield prediction declined from 1.02 t ha^{-1} with WHV21 to 0.85 t ha^{-1} with WHVZIM22, while the Index of Agreement increased from 0.86 to 0.90 (Table 4.23). This was considered sufficient justification to apply the revised model to evaluate management strategies of wheat in Zimbabwe (Chapter 5).

The revised model was first used to evaluate the optimum sowing date of wheat at three locations in Zimbabwe. The model was run on ten-years of weather data for sites representing the high-, middle- and lowvelds. The WHVZIM22 model predicted yields in response to sowing date in a logical and expected fashion, with maximum yields occurring with late April to early May sowings. This sowing date effect was most significant on the highveld. Simulated yields for any sowing date were greater on the highveld than on the middle- and lowvelds, while the cultivar W170/84 consistently produced greater mean yields than Sengwa.

Secondly, the revised model was used to evaluate the economics of a range of irrigation strategies on the middle- and highvelds. These results indicated that, in general, less water was required to achieve maximum gross margins on the middleveld than on the highveld. Furthermore, it was evident that deficit irrigation was appropriate only on the soil with a high water holding capacity, and that as the amount of water applied to wheat was reduced, the long-term variability of returns increased.

As in the simulation of the wheat sowing date response, the simulation of wheat under deficit irrigation produced logical results. Thus, the model was considered suitable for use as a management tool. A wheat irrigation optimization programme was thus developed using the QuickBASIC 4.00 programming language (Chapter 6). This programme, named WIRROPT6, uses the modified WHVZIM22 model and incorporates economic and irrigation constraints to predict optimal irrigation policies for particular soil, cultivar and weather conditions. The programme is relatively simple in content and use, and provides a means by which a farmer or advisor can rapidly and conveniently

evaluate irrigation management options on wheat. However, the optimization solutions are only as good as the model and the supplied input data, so they must be interpreted cautiously.

The example presented with the irrigation optimization programme (Section 6.2) showed, in a small way, how crop simulation models could become extremely useful crop management tools. The major limitation of this particular programme is that it does not include the simulation of nutrient dynamics or pest and disease problems. Neither is it linked to other crop models, which would enable multi-season optimization of management objectives, and be of significant use in determining the optimum allocation of limited resources, such as water. These options therefore present future opportunities for crop simulation models.

REFERENCES

Acevedo, E., T.C. Hsiao and D.W. Henderson. 1971. Immediate and subsequent growth responses of maize leaves to changes in water status. Plant Physiol. 48:631-636.

Agricultural Research Trust. 1987. ART Winter Report. Supplement to The Farmer including Tobacco News, 24 March, 1988.

Agricultural Research Trust. 1988. ART Winter Report. Supplement to The Farmer including Tobacco News, 23 March, 1989.

Agricultural Research Trust. 1989. ART Winter Report. Supplement to The Farmer including Tobacco News, 29 March, 1990.

Agricultural Research Trust. 1990. ART Winter Report. Supplement to The Farmer, 7 March, 1989.

Agricultural Research Trust. 1991. ART Winter Report. Supplement to The Farmer, 12 March, 1992.

Agricultural Research Trust. 1992. ART Winter Report. Supplement to The Farmer, 18 March, 1993.

Alocilja, E.C. and J.T. Ritchie. 1989. Simulation-dual criteria optimization in agricultural production. ASAE Paper no. 89-7025.

Alocilja, E.C. and J.T. Ritchie. 1990. The application of SIMOPT2:RICE to evaluate profit and yield-risk in upland rice production. Agric. Sys. 33:315-326.

Alvord, E.D. 1971. Sowing date of wheat on sandveld soils in the highveld in relation to frost incidence at flowering. Rhod. Agric. J. 68:15-18.

Anonymous. 1974. An inexpensive thermometer shelter. Climate Information Sheet no. 63. Department of Meteorological Services, Government of Zimbabwe.

Bacsi, Z., P.K. Thornton and J.B. Dent. 1991. Impacts of future climate change on Hungarian crop production: An application of crop growth simulation models. Agric. Sys. 37:435-450.

Baker, J.T., P.J. Pinter, R.J. Reginato and E.T. Kanemasu. 1986. Effects of temperature on leaf appearance in spring and winter wheat cultivars. Agron. J. 78:605-613.

Barlow, E.W.R., R. Munns, N.S. Scott and A.H. Reisner. 1977. Water potential, growth and polyribosome content of the stressed wheat apex. J. Exp. Bot. 28:909-916.

Begg, J.E. and N.C. Turner. 1976. Crop water deficits. Adv. Agron. 28:161-217.

Belford, R.K., B. Klepper and R.W. Rickman. 1987. Studies of intact shoot-root systems of field grown winter wheat. 2. Root and shoot development patterns as related to nitrogen fertilizer. Agron. J. 79:310-319.

Bidinger, F., R.B. Musgrave and R.A. Fischer. 1977. Contribution of stored pre-anthesis assimilate to grain yield in wheat and barley. Nature 270:431-433.

Blum, A., J. Mayer, and G. Gozland. 1983. Association between plant production and some physiological components of drought resistance in wheat. Plant Cell Environ. 6:219-225.

Blum, A., S. Ramaiah, E.T. Kanemasu and G.M. Paulsen. 1990. Wheat recovery from drought stress at the tillering stage of development. Field Crops Res. 24:67-85.

Booysen, J. 1987. The development of a crop specific drought index for winter wheat. Unpublished Ph.D. thesis. The University of Nebraska, Lincoln. (Diss.Abs.1988.49 950B).

Boyer, J.S. 1970. Leaf enlargement and metabolic rates in corn, soybean, and sunflower at various leaf water potentials. Plant Physiol. 46:233-235.

Boyer, J.S. and H.G. McPherson. 1974. Physiology of water deficits in cereal crops. Adv. Agron. 27:1-23.

Bras, R.L. and J.R. Cordova. 1981. Intraseasonal water allocation in deficit irrigation. Water Resources Res. 17:866-874.

Bruckner, P.L. and R.C. Frohberg. 1987. Rate and duration of grain fill in spring wheat. Crop Sci. 27:451-455.

Cackett, K.E. 1968. Irrigation of wheat. Unpublished paper presented at the Irrigation Symposium, Salisbury, June, 1969.

Cackett, K.E. 1970. Irrigation of wheat: a detailed explanation on scheduling. Modern Farming, 1970, pp. 29-41.

Cackett, K.E. 1972. Introduction. In: Cackett, K.E. (ed.) Lowveld Irrigated Wheat. Rhod. Agric. J. Tech. Bull. No. 14.

Cackett, K.E. and P.C. Wall. 1971. The effect of altitude and season length on the growth and yield of wheat (*Triticum aestivum* L.) in Rhodesia. Rhod. J. Agric. Res. 9:107-120.

Cao, W. and D.N. Moss. 1991. Phyllochron change in winter wheat with planting date and environmental changes. Agron. J. 83:396-401.

Carter, D.L. 1987. Water relations and irrigation. In: E.G. Heyne (ed.) Wheat and wheat improvement. Agron. Monogr. no. 13 (2nd Ed.), ASA, Madison.

Charles-Edwards, D.A. and R.J. Lawn. 1984. Light interception by grain legume row crops. Plant, Cell Environ. 7:247-251.

Chaturvedi, G.S., P.K. Aggarwal, A.H. Singh, M.G. Joshi and S.K. Sinha. 1981. Effect of irrigation on tillering of wheat, triticale and barley in a water-limited environment. Irrig. Sci. 2:225-235.

Chen, L.H. and R.W. McClendon. 1984. Selection of planting schedule for soybeans via simulation. Trans. ASAE 27:29-32.

Clarke, J.M. and T.N. McCaig. 1985. A versatile, inexpensive microcomputer-based leaf area measurement system. Agron. J. 77:966-968.

Cooper, J.L. 1980. The effect of nitrogen fertilizer and irrigaiton frequency on a semi-dwarf wheat in south-east Australia. 1. Growth and yield. Aust. J. Exp. Agric. Anim. Husb. 20:359-364.

Cutford, H.W., C.A. Campbell, Y.W. Jame, J.M. Clarke and R.M. DePauw. 1988. Growth characteristics, yield components and rate of grain development of two high-yielding wheats, HY320 and DT367, compared to two standard cultivars, Neepawa and Wakooma. Can. J. Plant Sci. 68:915-928.

Davidson, D.J. and P.M. Chevalier. 1990. Preanthesis tiller mortality in spring wheat. Crop Sci. 30:832-836.

de Jager, J.M., W.H. van Zyl, B.E. Kelbe, and A. Singels. 1987. Research on a weather service for scheduling the irrigation of winter wheat in the Free State region. Water Research Commission Report no. 117/1/87. Water Research Commission, Pretoria, RSA.

Department of Meteorological Services. 1981. Climate Handbook of Zimbabwe. Government of Zimbabwe.

Eastin, J.D. and C.Y. Sullivan. 1984. Environmental stress influences on plant persistence, physiology and production. In: M.B. Tesar (ed.) Physiological basis of crop growth and development. ASA, CSSA, and SSSA, Madison, WI, USA.

Edwards, I.B. 1971. Cultivation. In: Irrigated winter wheat in Rhodesia. Rhod. Agric. J. Tech. Bull. no. 12, pp 1-6.

Edwards, I.B. 1974. The wheat situation in Rhodesia. In: Proc. of a Wheat Symposium, Pretoria, 9 October, 1974. Tech. Comm. no. 162, Department of Agricultural Technical Services, Pretoria, RSA.

Ehrler, W., S.B. Idso, R.D. Jackson and R.J. Reginato. 1978. Wheat canopy temperature: Relation to plant water potential. Agron. J. 70:251-256.

English, M.J. 1981. The uncertainty of crop models in irrigation optimization. Trans. ASAE 24:917-921,928.

English, M.J. 1990. Deficit irrigation. 1. Analytical framework. J. Irrig. Drain. Div. Am. Soc. Civ. Eng. 116:399-412.

English, M.J., L. James and C.-F. Chen. 1990. Deficit irrigation. 2. Observations in Columbia Basin. J. Irrig. Drain. Div. Am. Soc. Civ. Eng. 116:413-426.

English, M.J. and G.S. Nuss. 1982. Designing for deficit irrigation. J.Irrig.Drain.Div.Am.Soc.Civ.Eng. 108:91-106.

English, M.J. and G.T. Orlob. 1978. Decision theory applications and irrigation optimization. Contribution no. 174. California Water Resources Center, University of California, Davis, CA, USA.

Epperson, J.E., J.E. Hook and Y.R. Mustafa. 1992. Stochastic dominance analysis for more profitable and less risky irrigation of corn. J. Prod. Agric. 5:243-247.

Epperson, J.E., J.E. Hook and Y.R. Mustafa. 1993. Dynamic programming for improving irrigation scheduling strategies of maize. Agric. Sys. 42:85-101.

Evans, L.T., I.F. Wardlaw and R.A. Fischer. 1975. Wheat. In: L.T. Evans (ed.) Crop physiology - some case histories. Cambridge Univ. Press, Cambridge.

Faci, J.M. and E. Fereres. 1980. Response of grain sorghum to variable water supply under two irrigation frequencies. Irrig. Sci. 3:149-159.

Fischbach, P.E. and B.R. Somerholder. 1974. Irrigation design requirements for corn. Trans. ASAE 17:162-165,171.

Fischer, R.A. 1985. Physiological limitations to producing wheat in semitropical and tropical environments and possible selection criteria. In: Wheats for more tropical environments. CIMMYT, Mexico.

Fischer, R.A. and R.M. Hagan. 1965. Plant water relations, irrigation management and crop yield. Expl. Agric. 1:161-177.

Fischer, R.A. and G.D. Kohn. 1966. The relationship of grain yield to vegetative growth and post-flowering leaf area in the wheat crop under conditions of limited moisture. Aust. J. Agric. Res. 17:281-295.

Fischer, R.A., J.H. Lindt and A. Glave. 1977. Irrigation of dwarf wheats in the Yaqui Valley of Mexico. Expl. Agric. 13:353-367.

Fonken, D.W., J.C. Steele and P.E. Fischbach. 1974. Sprinkler irrigation design criteria for sugar beets. Trans. ASAE 17:889-891.

Frank, A.B., J.F. Power, and W.O. Willis. 1973. Effect of temperature and plant water stress on photosynthesis, diffusion resistance and leaf water potential in spring wheat. Agron. J. 65:777-780.

French, V. and T. Hodges. 1984. Comparison of crop phenology models. Agron. J. 77:170-171.

Friend, D.J.C. 1965. Tillering and leaf production in wheat as affected by temperature and light intensity. Can. J. Bot. 43:1063-1076.

Gajri, P.R. and S.S. Prihar. 1983. Effect of small irrigation amounts on the yield of wheat. Agric. Water Manag. 6:31-41.

Gajri, P.R., S.S. Prihar, H.S. Cheema and A. Kapoor. 1991. Irrigation and tillage effects on root development, water use and yield of wheat on coarse textured soils. Irrig. Sci. 12:161-168.

Gallagher, J.N. 1979. Field studies of cereal leaf growth. 1. Initiation and expansion in relation to temperature and ontogeny. J. Exp. Bot. 30:625-636.

Gallagher, J.N., P.V. Biscoe and B. Hunter. 1976. Effects of drought on grain growth. Nature 264:541-542.

Garvin, R. 1976. Some aspects of winter wheat production in the Salisbury Group. In: R.A. Winkfield (ed.) In Communique, No. 8. Government Printer, Government of Rhodesia.

Godwin, D.C., J.T. Ritchie, U. Singh, and L.A. Hunt. 1989. A user's guide to CERES-Wheat v.2.10. International Fertilizer Development Center, Muscle Shoals, Alabama, USA.

Grant, P.M. 1993. Winter Serials. Ten tonne wheat achieved. The Farmer, 18 November, 1993, p. 7.

Gregory, P.J., M. McGowan and P.V. Biscoe. Water relations in winter wheat. 2. Soil water relations. J. agric. Sci., Camb. 91:103-116.

Gusta, L.V. and T.H.H. Chen. 1987. The physiology of water and temperature stress. In: E.G. Heyne (ed.) Wheat and wheat improvement. Agron. Monogr. no. 13 (2nd Ed.), ASA, Madison.

Hanks, R.J. 1974. Model for predicting plant yield as influenced by water use. Agron. J. 66:660-665.

Hanks, R.J. and V.P. Rasmussen. 1982. Predicting crop production as related to plant water stress. Adv. Agron. 35:193-215.

Hanks, R.J. and J.T. Ritchie. 1991. Introduction. In: J. Hanks and J.T. Ritchie (eds.) Modeling plant and soil systems. Agron. Mongr. 31. ASA, CSSA, SSSA, Madison, WI, USA.

Hunsaker, D.J. and D.A. Bucks. 1987. Wheat yield variability in level basins. Trans. ASAE 30:1099-1104.

Heermann, D.F., D.L. Martin, R.D. Jackson, and E.C. Stegman. 1990. Irrigation scheduling controls and techniques. In: B.A. Stewart and D.R. Nielsen (eds.) Irrigation of agricultural crops. Agron. Monogr. 30. ASA, CSSA, and SSSA, Madison, WI, USA.

Hexem, R.W. and E.O. Heady. 1978. Water production functions for irrigated agriculture. Iowa State Univ. Press, Ames, Iowa.

Hood, C.P., R.W. McClendon and J.E. Hook. 1987. Computer analysis of soybean irrigation management strategies. Trans. ASAE 30:417-423.

Howell, T.A. and E.A. Hiler. 1975. Optimization of water use efficiency under high frequency irrigation. 1. Evapotranspiration and yield relationship. Trans. ASAE 18:873-878.

Howell, T.A., E.A. Hiler and D.L. Reddell. 1975. Optimization of water use efficiency under high frequency irrigation. 2. System simulation and dynamic programming. Trans. ASAE 18:879-887.

Hsiao, T.C. 1973. Plant responses to water stress. Ann. Rev. Plant Physiol. 24:519-570.

Hsiao, T.C. 1990. Measurement of plant water status. In: B.A. Stewart and D.R. Nielsen (eds.) Irrigation of agricultural crops. Agron. Monogr. 30. ASA, CSSA and SSSA, Madison, WI.

Hurd, E.A. 1974. Phenotype and drought tolerance in wheat. Agric. Meteor. 14:39-55.

Husain, I. and D. Aspinall. 1970. Water stress and apical morphogenesis in barley. Ann. Bot. 34:393-407.

IBSNAT. 1986. Decision Support System for Agrotechnology Transfer (DSSAT). Technical Report 5. International Benchmark Sites Network for Agrotechnology Transfer, University of Hawaii.

IBSNAT. 1989. Proc. International Benchmark Sites Network for Agrotechnology Transfer Symp. Part 1. Dept. Agronomy and Soil Sciences, University of Hawaii.

Jackson, R.D. 1982. Canopy temerature and crop water stress. Adv. Irrig. 1:43-85.

James, L.G. 1988. Principles of farm irrigation system design. John Wiley and Sons, New York.

Johnson, R.C., D.W. Mornhinweg, D.M. Ferris and J.J. Heitholy. 1987. Leaf photosynthesis and conductance of selected *Triticum* species at different water potentials. Plant Physiol. 83:1014-1017.

Johnson, R.R., N.M. Frey and D.N. Moss. 1974. Effect of water stress on photosynthesis and transpiration of flag leaves and spikes of barley and wheat. Crop Sci. 14:728-731.

Johnson, R.R. and D.N. Moss. 1976. Effect of water stress on $^{14}CO_2$ fixation and translocation in wheat during grain filling. Crop Sci. 16:697-701.

Jones, C.A. and J.R. Kiniry. 1986. CERES-Maize. A simulation model of maize growth and development. Texas A & M University Press, College Station, USA.

Jones, H.G. 1977. Aspects of the water relations of spring wheat (*Triticum aestivum* L.) in response to induced drought. J. Agric. Sci., Camb. 88:267-282.

Kasanga, H. and M. Monsi. 1954. On the light transmission of leaves, and its meaning for the production of dry matter in plant communities. Japan J. Bot. 14:304-324.

Keim, D.L. and W.E. Kronstad. 1981. Drought response of winter wheat cultivars grown under field stress conditions. Crop Sci. 21:11-15.

Kirkham, M.B. and E.T. Kanemasu. 1983. Wheat. In: I.D. Teare and M.M. Peet (eds.) Crop water relations. John Wiley and Sons, New York.

Klepper, B., R.K. Belford and R.W. Rickman. 1984. Root and shoot development in winter wheat. Crop Sci. 76:117-122.

Klepper, B., R.W. Rickman and C.M. Peterson. 1982. Quantitative characterization of vegetative development in small cereal grains. Agron. J. 74:789-792.

Kobata, T., J.A. Palta and N.C. Turner. 1992. Rate of development of postanthesis water deficits and grain filling of spring wheat. Crop Sci. 32:1238-1242.

Krenzer, E.G., T.L. Nipp and R.W. McNew. 1991. Winter wheat mainstem leaf appearance and tiller formation vs. moisture treatment. Agron. J. 83:663-667.

Large, E.C. 1954. Growth stages in cereals: Illustration of the Feeks scale. Plant Path. 3:128-129.

Law, A.B. 1968. The use of wet- and dry-bulb thermometers to forecast frost at night in Rhodesia and frost protection in Rhodesia. Notes on Agricultural Meteorology no. 16. Department of Meteorological Services, Government of Rhodesia (now Zimbabwe).

Law, A.B. 1979. The prediction of the occurrence of frost over Zimbabwe Rhodesia. Notes on Agricultural Meteorology no. 15. Department of Meteorological Services, Government of Zimbabwe.

Lersten, N.R. 1987. Morphology and anatomy of the wheat plant. In: E.G. Heyne (ed.) Wheat and wheat improvement. Agron. Monogr. no. 13 (2nd Ed.), ASA, Madison.

Liu, W.T.H., D.M. Botner and C.M. Sakamoto. 1989. Application of CERES-Maize model to yield prediction of a Brazilian maize hybrid. Agric. Forest Meteor. 45:299-312.

Livingstone, J.E. and J.C. Swinbank. 1950. Some factors influencing the injury to winter wheat heads by low temperatures. Agron. J. 42:153-157.

Longmire, J., P. Ngobese, and S. Tembo. 1987. Wheat policy options in Zimbabwe and SADCC countries: Preliminary findings. In: M. Rukuni and C. Eicher (eds.) Proceedings of a Conference on Food Security Research in Southern Africa, Harare, Zimbabwe, 9-13 November, 1986. University of Zimbabwe, Harare, Zimbabwe.

Lupton, F.G.H. and M.J. Pinthus. 1969. Carbohydrate translocation from small tillers to spike producing shoots in wheat. Nature (Lond.) 221:129-144.

Maas, S.J. and G.F. Arkin. 1980a. TAMW: a wheat growth and development simulation model. Program and model documentation no. 80-3. Temple-Blackland Research Center, Temple, TX, USA.

Maas, S.J. and G.F. Arkin. 1980b. Initial validation of a winter wheat simulation model. Tech. Paper no. 80-4010, 1980 Summer Meeting, Am. Soc. of Agric. Eng.

Machado, S. 1992. The effect of different moisture regimes on the yield of seven spring wheat varieties in Zimbabwe. In: D.G. Tanner and W. Mwanyi (eds.) Seventh regional wheat workshop for eastern, central and southern Africa, CIMMYT, Mexico.

MacRobert, J.F. 1990. Wheat planting date considerations. The Farmer, 3 May, 1990.

MacRobert, J.F. 1992. Irrigation management for efficient use of water. 2. Deficit irrigation of wheat. The Farmer, 23 April, 1992.

MacRobert, J.F. 1993. Irrigation. In: P.D. Wells (ed.) Wheat Handbook. Zimbabwe Cereal Producers' Association, Harare.

MacRobert, J.F. and L.T. Mutemeri. 1988. The effect of the amount of irrigation on wheat. In: Agricultural Research Trust 1987 Winter Report. Supplement to The Farmer including Tobacco News, 24 March, 1988.

MacRobert, J.F. and M.J. Savage. 1991. The use of a crop simulation model to evaluate optimal irrigation strategies of wheat in Zimbabwe. Paper presented at the Southern African Irrigation Symposium, Elangeni Hotel, Durban, 4 to 6 June, 1991.

MacRobert, J.F., P.D. Wells and M.J. Savage. 1991. A survey of farm wheat root profiles. The Zimb. Sci. News 25:83-86.

Martin, D.L. 1984. Using crop yield models in optimal irrigation scheduling. Unpublished Ph.D. diss. Colorado State Univ., Fort Collins, CO, USA.

Martin, D.L., J.R. Gilley and R.J. Supalla. 1989. Evaluation of irrigation planning decisions. J. Irrig. Drain. Div. Am. Soc. Civ. Eng. 115:58-77.

Martin, D.L. and D.F. Heermann. 1984. Scheduling to maximize profit from deficit irrigation. ASAE Paper no. 84-2607.

Martin, D.L., D.F. Heermann, J.R. Gilley and J.W. Labadie. 1983. Optimal seasonal center pivot management. ASAE Paper no. 83-2004.

Martin, D.L., J. van Brocklin and G. Wilmes. 1989. Operating rules for deficit irrigation management. Trans. ASAE 32:1207-1215.

Mashiringwani, N.A. 1990a. Trends in production and consumption of wheat and the role of variety improvement in Zimbabwe. Zim. Agric. J. (In press).

Mashiringwani, N.A. 1990b. Wheat frost tolerance experiments: preliminary results. The Farmer, 12/19 April, 1990.

Mashiringwani, N.A. 1993. Crop variety release notice: Deka wheat. The Farmer, 28 January, 1993.

Mashiringwani, N.A. and M.A. Schweppenhauser. 1992. Phenotypic characters associated with yield adaption of wheat to a range of temperature conditions. Field Crops Res. 29:69-77.

McGregor, M.J. and P.K. Thornton. 1990. Information systems for crop management: Prospects and problems. J. Agric. Econ. 41:172-183.

McGugan, P. 1972. Irrigation studies. In: Cackett, K.E. (ed.) Lowveld Irrigated Wheat. Rhod. Agric. J. Tech. Bull. No. 14.

McMaster, G.S., W.W. Wilhelm and J.A. Morgan. 1992. Simulating winter wheat shoot apex phenology. J. Agric. Sci. (Camb.) 119:1-12.

Metelerkamp, H.R.R. 1968. Irrigation scheduling by means of Class A pan evaporation. Rhod. Agric. J. Tech. Bull. No.12.

Meyer, W.S. and G.C. Green. 1980a. Water use by wheat and plant indicators of available soil water. Agron. J. 72:253-256.

Meyer, W.S. and G.C. Green. 1980b. Leaf growth, phenological development and yield of wheat grown under different irrigation treatments. Water S.A. 6:21-26.

Midmore, D.J., P.M. Cartwright and R.A. Fischer. 1984. Wheat in tropical environments. 2. Crop growth and grain yield. Field Crops Res. 8:207-227.

Miller, D.E. and A.N. Hang. 1982. Deficit, high frequency sprinkler irrigation of wheat. Soil Sci. Soc. Am. J. 46:386-389.

Minhas, B.S., K.S. Parikh, and T.N. Srinivasan. 1974. Toward the structure of a production function for wheat yields with dated inputs of irrigation water. Water Resour. Res. 10:383-393.

Mogensen, V.O., H.E. Jensen and M.A. Rab. 1985. Grain yield, yield components, drought sensitivity and water use efficiency of spring wheat subjected to water stress at various growth stages. Irrig. Sci. 6:131-140.

Mogensen, V.O. and M.S.V. Talukder. 1987. Grain yield of spring wheat in relation to water stress. 2. Growth rate of grains during drought. Cer. Res. Comm. 15:247-253.

Monteith, J.L. 1986. How do crops manipulate water supply and demand? Phil. Trans. R. Soc. Lond. A316:245-259.

Morgan, J.M. 1977. Changes in diffusive conductance and water potential of wheat plants before and after anthesis. Aust. J. Plant Physiol. 4:75-86.

Morris, M.L. 1988. Comparative advantage and policy incentives for wheat production in Zimbabwe. CIMMYT Economics Working Paper 88/02. Mexico, D.F.: CIMMYT.

Morris, M.L. 1989. Wheat policy options in sub-Saharan Africa: The case of Zimbabwe. Agric. Econ. 3:115-129.

Munns, R. and R. Weir. 1981. Contributions of sugars to osmotic adjustment in elongating and expanded zones of wheat leaves during moderate water deficits at two light levels. Aust. J. Plant Physiol. 8:93-105.

Musick, J.T. 1989. Discussion: Effects of deficit irrigation and irrigation frequency on wheat yields. J. Irrig. Drain. Div. Am. Soc. Civ. Eng. 115:806-807.

Musick, J.T. and D.A. Dusek. 1980. Irrigated corn yield response to water. Trans. ASAE 23:92-98.

Musick, J.T. and K.B. Porter. Wheat. In: B.A. Stewart and D.R. Nielsen (eds.) Irrigation of agricultural crops. Agron. Monogr. 30. ASA, CSSA, and SSSA, Madison, WI, USA.

Ngobese, P. 1987. The economics of large-scale wheat production in Zimbabwe. Unpublished Masters Thesis, Virginia Polytechnic Institute and State University, Blacksburg, VA.

Ngobese, P.T. 1988. The economics of expanding commercial wheat production in Zimbabwe. In: M. Rukuni and R.H. Bernsten (eds.) Southern Africa: food security policy options. Proceedings of the Third Annual Conference on Food Security Research in Southern Africa, 1-5 November, 1987. Department of Agricultural Economics and Extension, University of Zimbabwe, Harare, Zimbabwe.

O'Leary, G.J., D.J. Connor and D.H. White. 1985. A simulation model of the development, growth and yield of the wheat crop. Agric. Sys. 17:1-26.

Oosterhuis, D.M. 1977. Developmental morphology of the spike of a Rhodesian spring wheat recorded with a scanning electron microscope. Rhod. J. Agric. Res. 15:65-77.

Oosterhuis, D.M. and P.M. Cartwright. 1983. Spike differentiation and floret survival in semidwarf spring wheat as affected by water stress and photoperiod. Crop Sci. 23:711-717.

Otter, S. and J.T. Ritchie. 1985. Validation of the CERES-Wheat model in diverse environments. In: W. Day and R.K. Atkin (eds.) Wheat growth and modelling. Plenum Press, New York.

Pandey, S. 1990. Risk-efficient irrigation strategies for wheat. Agric. Econ. 4:59-71.

Parsch, L.D., M.J. Cochran, K.L. Trice and H.D. Scott. 1991. Biophysical simulation of wheat and soybean to assess the impact of timeliness on double-cropping economics. In: J. Hanks and J.T. Ritchie (eds.) Modeling plant and soil systems. Agron. Mongr. 31. ASA, CSSA, SSSA, Madison, WI, USA.

Pheloung, P.C. and K.H.M. Siddique. 1991. Contribution of stem dry matter to grain yield in wheat cultivars. Aust. J. Plant Physiol. 18:53-64.

Pilbrough, S. and J.F. MacRobert. 1988. How much water? The Farmer including Tobacco News, 31 March, 1988, Harare, Zimbabwe.

Pleban, S and I. Israeli. 1989. Improved approach to irrigation scheduling programs. J. Irrig. Drain. Div. Am. Soc. Civ. Eng. 115:577-587.

Portas, C.A.M. and H.M. Taylor. 1976. Growth and survival of young plant roots in dry soil. Soil Sci. 121:170-175.

Porter, J.R. 1984. A model of canopy development of winter wheat. J. Agric. Sci., Camb. 102:383-392

Porter, J.R., P.D. Jamieson and D.R. Wilson. 1993. Comparison of the wheat simulation models ARCWHEAT2, CERES-Wheat and SWHEAT for non-limiting conditions of crop growth. Field Crops Res. 33:131-157.

Power, J.F. and J. Alessi. 1978. Tiller development and yield of standard and semidwarf spring wheat varieties as affected by nitrogen fertilizer. J. agric. Sci., Camb. 90:97-108.

Proffitt, A.P.B., P.R. Berliner and D.M. Oosterhuis. 1984. A comparative study of root distribution and water extraction efficiency by wheat grown under high and low frequency irrigation. Crop Prod. 13:3.

Proffitt, A.P.B., P.R. Berliner and D.M. Oosterhuis. 1985. A comparative study of root distribution and water extraction efficiency by wheat grown under high- and low-frequency irrigation. Agron. J. 77:655-662.

Puckridge, D.W. and C.M. Donald. 1967. Competition among wheat plants sown at a wide range of densities. Aust. J. Agric. Res. 18:193-211.

Quarrie, S.A. and H.G. Jones. 1977. Effects of abscisic acid and water stress on development and morphology of wheat. J. Exp. Bot. 28:192-203.

Rao, N.H., P.B.S. Sarma and S. Chander. 1988. A simple dated water-production function for use in irrigated agriculture. Agric. Water Manag. 13:25-32.

Rasmussen, V.P. 1991. Promises and problems of extending models to the grass roots level. In: J. Hanks and J.T. Ritchie (eds.) Modeling plant and soil systems. Agron. Mongr. 31. ASA, CSSA, SSSA, Madison, WI, USA.

Rasmussen, V.P. and R.J. Hanks. 1978. Spring wheat yield model for limited moisture conditions. Agron. J. 70:940-944.

Rawlins, S.L. and P.A.C. Raats. 1975. Prospects for high-frequency irrigation. Science 4188:604-610.

Rawson, H.M and C.M. Donald. 1969. The absorption and distribution of nitrogen after floret initiation in wheat. Aust. J. Agric. Res. 20:799-808.

Rickman, R.W., B. Klepper and R.K. Belford. 1985. Developmental relationships among roots, leaves and tillers in winter wheat. In: W. Day and R.K. Atkin (eds.) Wheat growth and modelling. Plenum Press, New York.

Riddell, J.A., G.A. Gries and F.W. Stearns. 1958. Development of spring wheat. 1. The effect of photoperiod. Agron. J. 50:735-738.

Ritchie, J.T. 1972. Model for predicting evaporation from a row crop with incomplete cover. Water Resources Res. 8:1204-1213.

Ritchie, J.T. 1981a. Water dynamics in the soil-plant-atmosphere system. Plant and Soil 58:81-96.

Ritchie, J.T. 1981b. Soil water availability. Plant Soil 58:327-338.

Ritchie, J.T. 1991. Wheat phasic development. In: J. Hanks and J.T. Ritchie (eds.) Modeling plant and soil systems. Agron. Mongr. 31. ASA, CSSA, SSSA, Madison, WI, USA.

Ritchie, J.T. and D.S. NeSmith. 1991. Temperature and crop development. In: J. Hanks and J.T. Ritchie (eds.) Modeling plant and soil systems. Agron. Mongr. 31. ASA, CSSA, SSSA, Madison, WI, USA.

Ritchie, J.T. and S. Otter. 1984. CERES-Wheat: A user oriented wheat yield model. Preliminary documentation. United States Department of Agriculture, Agricultural Research Service, ARS 38:159-175. AgRISTARS Publication no. YM-U3-04442-JSC-18892.

Ritchie, J.T., H.A. Nix, R.A. Fischer, H.J. Speirtz, Meyer, J.N. Gallagher, P. Dyke, E.J.M. Kirby, S. Otter, D.C. Godwin, J.W. Jones, C. Humphries and others. 1988. CERES Wheat Model, Fortran Source Code Listing, International Benchmark Sites Network for Agrotechnology Transfer, University of Hawaii. (Note, not all the initials of authors are given or known.)

Rodrigues, A., J.N. Trapp, O.L. Walker, and D.J. Bernardo. 1990. A wheat grazing systems model for the US Southern Plains: Part 1. Model description and performance. Agric. Syst. 33:41-59.

Saini, H.S. and D. Aspinall. 1981. Effect of water deficit on sporogenesis in wheat (*Triticum aestivum* L.). Ann. Bot. 48:623-633.

Saini, H.S. and D. Aspinall. 1982. Sterility in wheat (*Triticum aestivum* L.) induced by water deficit or high temperature: Possible mediation by abscisic acid. Aust. J. Plant Physiol. 9:529-537.

Savage, M.J. 1980. Agrometeorology 210 Course Notes. Department of Soil Science and Agrometeorology, University of Natal, Pietermaritzburg, South Africa.

Savdie, I., R. Whitewood, R.L. Raddatz and D.B. Fowler. 1991. Potential for winter wheat production in western Canada: A CERES model winterkill risk assessment. Can. J. Plant Sci. 71:21-30.

Shimshi, D., M.L. Mayoral and D. Atsmon. 1982. Responses to water stress in wheat and related wild species. Crop Sci. 22:123-128.

Simmons, S.R. 1987. Growth, development and phenology. In: E.G. Heyne (ed.) Wheat and wheat improvement. Agron. Monogr. no. 13 (2nd Ed.), ASA, Madison.

Simpson, G.M. 1968. Association between grain yield per plant and photosynthetic area above the flag-leaf node in wheat. Can. J. Plant Soil 48:253-260.

Single, W.V. 1985. Frost injury and the physiology of the wheat plant. Farrer Memorial Oration, 1984. J. Aust. Inst. Agric. Sci. 51:128-134.

Single, W.V. and H. Marcellos. 1974. Studies on frost injury to wheat. 4. Freezing of ears after emergence from the leaf sheath. Aust. J. Agric. Res. 25:679.

Singels, A. 1990. A modeling approach to determine strategies for minimizing risk in wheat production in the Orange Free State. Unpublished Ph.D. thesis, University of the Orange Free State, Bloemfontein, R.S.A.

Singels, A. 1992. Evaluating wheat planting strategies using a growth model. Agric. Sys. 38:175-184.

Singels, A. and J.M. de Jager. 1991. Evaluating different wheat production strategies for the Orange Free State using stochastic dominance techniques and a crop growth model. S. Afr. J. Plant Soil 8:113-118.

Singh, S.D. 1981. Moisture-sensitive growth stages of dwarf wheat and optimal sequencing of evapotranspiration deficits. Agron. J. 73:387-391.

Singh, P., H. Wolkewitz and R. Kumar. 1987. Comparative performance of different crop production functions for wheat (*Triticum aestivum* L.). Irrig. Sci. 8:273-290.

Smith, B. and R. Gasela. 1991. Wheat Strategy Paper. Zimbabwe Cereal Producers' Association in conjunction with the Grain Marketing Board, Harare, Zimbabwe.

Sofield, I., L.T. Evans, M.G. Cook and I.F. Wardlaw. 1977. Factors influencing the rate and duration of grain filling in wheat. Aust. J. Plant Physiol. 4:785-797.

Squire, G.R. 1990. The physiology of tropical crop production. CAB International, Wallingford, UK.

Stark, J.C. and T.S. Longley. 1986. Changes in spring wheat tillering patterns in response to delayed irrigation. Agron. J. 78:892-896.

Stegman, E.C., 1982. Corn grain yield as influenced by timing of evapotranspiration deficits. Irrig. Sci. 3:75-87.

Stegman, E.C. 1983. Irrigation Scheduling: Applied timing criteria. Adv. Irrig. 2:1-30.

Stegman, E.C., R.J. Hanks, J.T. Musick and D.G. Watts. 1981. Irrigation water management - adequate or limited water. In: Irrigation: Challenges of the 80's. Proc. Second Nat. Irrig. Symp., University of Nebraska, October 20-23, 1980. ASAE Publication 6-81.

Stegman, E.C., J.T. Musick, and J.I. Stewart. 1983. Irrigation water management. In: M.E. Jensen (ed.) Design and operation of farm irrigation systems. A.S.A.E. Monogr. no. 3, St. Joseph, MI, USA.

Steiner, J.L., R.C.G. Smith, W.S. Meyer, and J.A. Adeney. 1985. Water use, foliage temperature, and yield of irrigated wheat in southeastern Australia. Aust. J. Agric. Res. 36:1-11.

Stern, W.R. and E.J.M. Kirby. 1979. Primordium initiation at the shoot apex in four contrasting varieties of spring wheat in response to sowing date. J. Agric. Sci. 93:203-215.

Stewart, J.I., R.E. Danielson, R.J. Hanks, E.B. Jackson, R.M. Hagan, W.O. Pruitt, W.T. Franklin and J.P. Riley. 1977. Optimizing crop production through control of water and salinity levels in the soil. Utah Water Res. Lab., Logan, Utah.

Summerfield, R.J., E.H. Roberts, R.H. Ellis and R.J. Lawn. 1991. Towards the reliable prediction of time to flowering in six annual crops. 1. The development of simple models for fluctuating field environments. Expl. Agric. 27:11-31.

Talukder, M.S.V., V.O. Mogensen and H.E. Jensen. 1987. Grain yield of spring wheat in relation to water stress. 1. Effect of early drought on development of late tillers. Cereal Res. Comm. 15:101-107.

Tembo,S. and A. Senzanje. 1988. Water-use efficiency on commercial wheat farms in Zimbabwe. In: M. Rukuni and R.H. Bernsten (eds.) Southern Africa: food security policy options. Proceedings of the Third Annual Conference on Food Security Research in Southern Africa, 1-5 November, 1987. Department of Agricultural Economics and Extension, University of Zimbabwe, Harare, Zimbabwe.

Thompson, J.G. and W.D. Purves. 1978. A guide to the soils of Zimbabwe. Rhod. Agric. J. Tech. Hbook. no. 3.

Thornton, P.K., J.A. Blair-Fish and S.M.D. Wilson. 1991. Crop simulation modelling using a transputer-based parallel computer. Agric. Sys. 35:321-337.

Thornton, P.K. and J.F. MacRobert. 1993. The value of information concerning near-optimal nitrogen fertilizer scheduling . Agric. Sys. (In press).

Tottman, D.R. and H. Broad. 1987. The decimal code for the growth stages of cereals, with illustrations. Ann. Appl. Biol. 110:441-454.

Townley-Smith, T.F. and E.A. Hurd. 1979. Testing and selecting for drought resistance in wheat. In: H. Mussell and R.C. Staples (eds.) Stress physiology in crop plants. John Wiley and Sons, New York.

Turner, N.C. 1986. Adaption to water deficits: A changing perspective. Aust. J. Plant Physiol. 13:175-190.

Turner, N.C. and G.J. Burch. 1983. The role of water in plants. In: I.D. Teare and M.M. Peet (eds.) Crop water relations. John Wiley and Sons, New York.

van Keulen, H. and W.A.J. de Milliano. 1984. Potential wheat yields in Zambia - a simulation approach. Agric. Sys. 14:171-192.

van Keulen, H. and N.G. Seligman. 1987. Simulation of water use, nitrogen nutrition and growth of a spring wheat crop. Pudoc, Wageningen.

Vaux, H.J. and W.O. Pruitt. 1983. Crop-water production functions. Adv. Agron. 2:61-32.

Wardlaw, I.F. 1971. The early stages of grain development in wheat: Response to water stress in a single variety. Aust. J. Biol. Sci. 24:1047-1055.

Weir, A.H., P.L. Bragg, J.R. Porter, J.H. Rayner. 1984. A winter wheat model without water or nutrient limitations. J. Agric. Sci., Camb. 102:371-382.

Whingwiri, E.E., D. Mataruka and C. Ntungakwa. 1984. A survey of commercial wheat production practices in the Mazowe/Bindura area. Zimbabwe Agric. J. 81:139-141.

Whisler, F.D., B. Acock, D.N. Baker, R.E. Fye, H.F. Hodges, J.R. Lambert, H.E. Lemmon, J.M. McKinion and V.R. Reddy. 1986. Crop simulation models in agronomic systems. Adv. Agron. 40:141-208.

Whitlow, R. Wetland use and abuse in Zimbabwe. Trans. Zimb. Sci. Assoc. 65:24-33.

Wiegand, C.L. and J.C. Cuellar. 1981. Duration of grain filling and kernel weight of wheat as affected by temperature. Crop Sci. 21:95-101.

Willmott, C.J. 1982. Some comments on the evaluation of model performance. Bull. Am. Meteorol. Soc. 63:1309-1313.

Wilson, G. 1974. Planned watering of winter wheat. Modern Farming, Autumn, 1974, Harare, Zimbabwe.

Wilson, J.H. 1969. The influence of water on yield components of wheat. Rhod. J. Agric. Res. 7:129-133.

Yaron, D. and E. Bresler. 1983. Economic analysis of on-farm irrigation using response functions of crops. Adv. Irrig. 2:223-255.

Yaron, D. and G. Strateener. 1973. Wheat response to soil moisture and the optimal irrigation policy under conditions of unstable rainfall. Water Resources Res. 9:1145-1154.

Zadoks, J.C., T.T. Chang and C.F. Konzak. 1974. A decimal code for the growth stages of cereals. Weed Res. 14:415-421.

APPENDIX 1: SUPPLIMENTARY INFORMATION TO CHAPTER 2: MATERIALS AND METHODS

TABLE OF CONTENTS

Table A1.1: Summary of cultural practices applied to the sowing date trials.

Site	Year	Previous crop	Residue management	Land preparation	Fertilizer applied N	P_2O_5	K_2O	S	Soil analysis results pH	P_2O_5	K	Ca	Mg
					kg ha^{-1}					ppm	cmol kg^{-1}		
ART	1988	Maize	Burnt	Ploughed	176	102	90	48	4.6	41	0.37	6.66	1.77
ART	1989	Maize	Burnt	Ploughed	186	81	41	38	5.4	24	0.84	8.36	2.22
ART	1990	Maize	Incorporated	Ploughed	188	84	42	39	5.4	41	0.69	8.90	2.10
ART	1991	Maize	Burnt	Ploughed	186	84	42	39	5.1	44	0.49	8.03	2.46
DOMA	1991	Soyas	Incorporated	Disced	186	84	42	39	5.9	23	0.22	5.32	4.86
GLEN	1989	Maize	Silage	Chiselled	186	81	41	38	5.7	20	0.28	4.67	1.12
GLEN	1990	Maize	Silage	Chiselled	188	84	42	39	5.7	46	0.45	3.40	1.16
RARS	1988	Soyas	Incorporated	Ploughed	176	102	90	48	5.8	35	0.52	4.47	1.29
RARS	1989	Soyas	Incorporated	Ploughed	186	81	41	38	5.4	18	0.52	3.97	0.90
SAVE	1991	Cotton	Incorporated	Disced	136	42	21	20	5.8	68	0.62	9.37	3.69
SHAM	1990	Maize	Incorporated	Disced	188	84	42	39	5.9	22	0.90	8.25	3.25

Table A1.2: The day of year (doy) and approximate amount of irrigation applied or rainfall received (in parenthesis) in the wheat sowing date x cultivar and sowing date x seeding rate trials at the various sites (*continued on page 193*).

ART 1988		ART 1989		ART 1990		ART 1991		DOMA 1991	
doy	mm	doy	mm	doy	mm	doy	mm	doy	mm
116	22	114	30	114	22	115	25	115	24
126	22	118	15	119	(17)	116	(4)	118	(12)
135	29	129	15	124	22	117	(4)	119	(3)
145	22	135	30	129	14	120	16	123	20
155	22	139	7	134	14	124	25	128	10
172	22	144	11	138	14	129	16	134	20
182	24	149	11	145	22	135	25	138	(12)
193	29	154	15	148	14	141	8	144	20
202	44	158	7	155	14	145	25	149	10
212	44	168	15	159	14	150	8	155	20
221	44	179	15	169	14	156	25	161	10
229	44	188	44	179	14	161	8	171	20
238	44	199	44	188	44	171	25	180	25
247	44	208	44	199	44	180	25	191	35
254	44	216	44	209	44	191	35	201	44
272	44	226	44	220	44	201	45	211	44
280	44	235	44	230	44	211	45	221	44
286	36	244	44	241	44	222	45	232	44
	---	253	44	251	44	232	45	240	44
	624	262	44	261	44	243	45	249	44
		271	44	273	44	254	45	259	44
		279	30	284	44	266	45	271	44
			---		---	277	45	278	44
			641		635	288	16		---
							---		637
							650		

Table A1.2: *continued from page 192*

GLEN 1989		GLEN 1990		RARS 1988		RARS 1989		SHAM 1990		SAVE 1991	
doy	mm	doy	mm	doy	mm	doy	mm	doy	mm	doy	mm
116	50	116	20	116	25	115	45	117	37	116	30
126	50	120	(40)	123	25	119	12	119	(16)	120	22
129	50	126	30	129	25	121	(12)	122	15	126	30
133	25	130	15	136	15	125	20	126	15	129	30
136	25	137	25	142	20	129	12	131	34	138	40
139	12	141	12	154	20	135	32	134	(4)	147	30
144	12	146	25	161	8	140	27	136	26	157	22
146	4	151	12	173	25	149	11	141	22	169	35
149	12	157	25	185	25	154	11	146	20	182	40
157	25	162	12	195	45	158	10	151	20	188	35
160	12	169	13	206	45	168	24	157	38	196	51
170	25	180	12	216	45	178	28	161	18	207	47
181	25	190	50	227	45	188	35	171	20	213	32
191	50	200	50	237	45	198	45	181	25	220	30
201	50	209	50	248	45	206	28	191	26	230	38
216	50	219	50	257	45	214	39	200	24	234	50
228	50	228	50	266	45	218	(4)	209	34	241	30
237	50	238	50	276	45	223	34	218	46	248	35
245	50	249	50	285	30	231	35	227	40	253	46
253	50	258	50	285	(38)	240	40	236	45		---
261	50	268	50		---	248	46	244	44		673
266	35	277	50		661	256	35	253	56		
283	50		---			263	(3)	263	26		
	---		741			264	28	271	30		
	812					271	49		---		
						277	(6)		681		
						279	37				
						277	6				
						279	37				

							708				

Table A1.3: Summary of cultural practices applied to the wheat irrigation trials.

Site	Year	Sowing date		Previous crop	Land management	Fertilizer applied N	P_2O_5	K_2O	S	Soil analysis pH	P_2O_5	K	Ca	Mg
		date	doy			kg ha^{-1}					ppm	cmol kg^{-1}		
ART	1989	17 May	137	Maize	Ploughed	178	70	35	33	5.3	58	0.77	8.24	3.12
ART	1990	22 May	142	Maize	Ploughed	178	70	35	33	5.1	28	0.25	9.60	2.80
ART	1991	20 May	140	Maize	Ploughed	178	70	35	33	5.4	21	0.20	7.71	2.80
ART	1992	18 May	138	Maize	Ploughed	178	70	35	33	5.1	44	0.49	8.03	2.46
BANK	1991	19 May	139	Ley	Disced	178	70	35	33	6.6	27	0.20	1.03	1.89
CON	1990	18 May	138	Tobacco	Ploughed	188	50	50	33	5.5	55	0.40	2.51	0.64
GLEN	1989	8 May	128	Maize	Chiselled	178	70	35	33	5.7	20	0.28	4.67	1.12
GLEN	1990	16 May	136	Maize	Chiselled	175	64	32	30	5.1	72	0.75	3.13	1.05

Table A1.4: Soil bulk densities (Bd) and standard errors (SE), both in g cm^{-3}, of representative profiles.

	Depth (mm)					
	75	250	500	750	1000	1250
ART 1988						
Bd	1.18	1.22	1.07	1.03	1.00	1.12
SE	0.084	0.019	0.113	0.063	0.061	0.032
ART 1989						
Bd	1.17	1.19	1.16	1.12	1.19	1.29
SE	0.061	0.081	0.021	0.036	0.067	0.023
ART 1990						
Bd	1.25	1.37	1.34	1.32	1.32	1.32
SE	0.085	0.056	0.073	0.099	0.048	0.049
RARS 1988						
Bd	1.28	1.31	1.21	1.20	1.17	1.23
SE	0.070	0.093	0.081	0.032	0.046	0.033
RARS 1989						
Bd	1.25	1.35	1.10	1.09	1.10	1.13
SE	0.036	0.033	0.036	0.035	0.025	0.003
GLEN 1989						
Bd	1.51	1.60	1.59	1.62	1.54	1.55
SE	0.139	0.032	0.018	0.035	0.003	0.033
GLEN 1990						
Bd	1.51	1.49	1.42	1.39	1.44	1.40
SE	0.099	0.071	0.092	0.084	0.056	0.046
BANK 1991						
Bd	1.73	1.78	1.68	1.76	1.78	1.85
SE	0.090	0.092	0.029	0.021	0.046	0.091

Table A1.5: Texture and total exchangeable bases (TEB) of the soils at each site.

Depth m	Clay %	Silt %	Sand %	TEB cmol kg^{-1}
ART 1989				
0 - 0.25	65	20	15	8.6
0.25 - 0.50	74	12	14	7.6
0.50 - 0.75	68	17	15	8.0
0.75 - 1.00	67	17	16	7.1
1.00 - 1.25	63	14	23	6.6
RARS 1989				
0 - 0.25	56	11	33	5.7
0.25 - 0.50	69	11	20	7.0
0.50 - 0.75	65	9	25	7.6
0.75 - 1.00	59	11	30	5.1
1.00 - 1.25	66	9	26	6.6
GLEN 1989				
0 - 0.25	27	10	63	5.5
0.25 - 0.50	36	7	57	5.3
0.50 - 0.75	33	7	60	4.1
0.75 - 1.00	33	7	59	4.4
1.00 - 1.25	33	7	59	5.3
GLEN 1990				
0 - 0.13	23	9	68	4.9
0.13 - 0.38	26	10	64	4.8
0.38 - 0.63	26	12	62	5.2
0.63 - 0.88	34	12	54	5.1
0.88 - 1.13	40	8	52	4.9
1.13 - 1.38	40	10	50	5.2
SHAM 1990				
0 - 0.13	29	33	38	13.3
0.13 - 0.38	42	25	33	11.6
0.38 - 0.63	52	23	25	11.1
0.63 - 0.88	49	23	28	11.2
0.88 - 1.13	48	23	29	11.0
1.13 - 1.38	51	23	26	11.0
BANK 1991				
0 - 0.13	12	6	82	3.1
0.13 - 0.38	10	8	82	3.5
0.38 - 0.63	10	8	82	3.7
0.63 - 0.88	19	8	73	3.9
0.88 - 1.13	14	11	75	2.9
1.13 - 1.38	16	10	74	2.8
SAVE 1991				
0 - 0.13	22	21	57	20.5
0.13 - 0.38	22	21	57	21.8
0.38 - 0.63	20	17	63	21.5
0.63 - 0.88	14	7	79	13.2
0.88 - 1.13	20	17	63	25.9
1.13 - 1.38	20	15	65	24.0

Table A1.6: Soil particle density (Bd_p), bulk density (Bd), porosity (P) and soil water retention characteristics at some of the sites.

				Matric potential (MPa)				
Depth	Bd_p	Bd	P	-0.05	-0.10	-0.33	-2.0	-15.0
m	Mg m^{-3}	Mg m^{-3}	%	Soil water content ± SE (m^3 m^{-3})				
ART 1988								
0 - 0.28	2.83	1.11±0.05	60.9±1.7	0.400±0.024	0.348±0.019	0.293±0.018	0.266±0.021	0.216±0.012
0.28 - 0.50	2.82	1.23±0.06	56.2±2.1	0.414±0.001	0.387±0.006	0.352±0.011	0.330±0.010	0.294±0.011
0.50 - 0.65	2.82	1.09±0.05	61.3±1.8	0.407±0.016	0.374±0.019	0.327±0.023	0.304±0.026	0.263±0.020
0.65 - 1.00	2.85	1.00±0.06	65.0±2.0	0.407±0.011	0.364±0.014	0.304±0.016	0.277±0.034	0.238±0.010
1.00 - 1.50	2.86	1.12±0.04	60.6±1.4	0.421±0.011	0.380±0.013	0.322±0.012	0.267±0.008	0.230±0.014
RARS 1988								
0 - 0.28	2.75	1.40±0.06	49.0±2.4	0.367±0.017	0.339±0.016	0.290±0.008	0.269±0.005	0.225±0.013
0.28 - 0.55	2.79	1.27±0.07	54.5±2.6	0.376±0.017	0.342±0.015	0.290±0.016	0.280±0.022	0.235±0.019
0.55 - 0.90	2.82	1.18±0.03	58.0±0.9	0.373±0.005	0.334±0.002	0.277±0.002	0.258±0.008	0.222±0.001
0.90 - 1.40	2.83	1.20±0.13	57.6±4.6	0.376±0.022	0.338±0.027	0.283±0.032	0.262±0.037	0.224±0.022
GLEN 1989								
0 - 0.10	2.66	1.52±0.06	42.9±2.1	0.281±0.008	0.241±0.009	0.183±0.016	0.153±0.009	0.108±0.011
0.10 - 0.34	2.66	1.33±0.31	50.1±9.9	0.230±0.035	0.203±0.030	0.163±0.021	0.135±0.027	0.105±0.019
0.34 - 0.72	2.69	1.38±0.40	48.7±3.4	0.264±0.020	0.236±0.020	0.188±0.019	0.162±0.017	0.134±0.016
0.72 - 1.03	2.71	1.36±0.45	49.8±2.4	0.272±0.019	0.245±0.019	0.205±0.015	0.173±0.016	0.142±0.009
1.03 - 1.52	2.71	1.48±0.48	45.3±2.8	0.280±0.023	0.251±0.023	0.206±0.023	0.172±0.019	0.141±0.011

APPENDIX 2: RAW DATA PERTAINING TO THE VALIDATION OF CERES-WHEAT VERSION 2.10 UNDER WELL-WATERED AND DEFICIT-IRRIGATED CONDITIONS

TABLE OF CONTENTS

Page

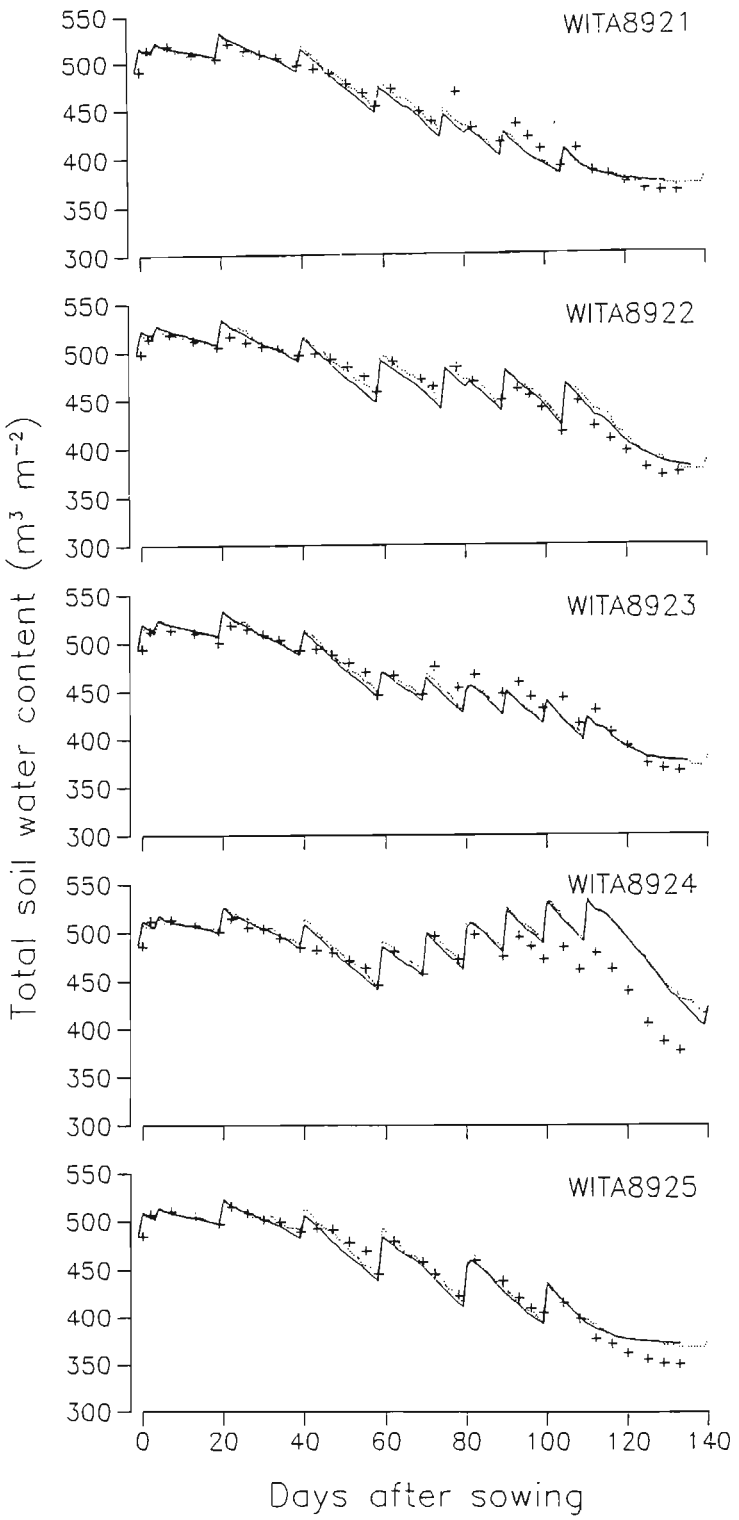

Figure A2.1: The predicted (dotted line: WHV21; solid line WHVZIM22) and observed (+) soil water contents for the wheat irrigation trial at ART 1989.

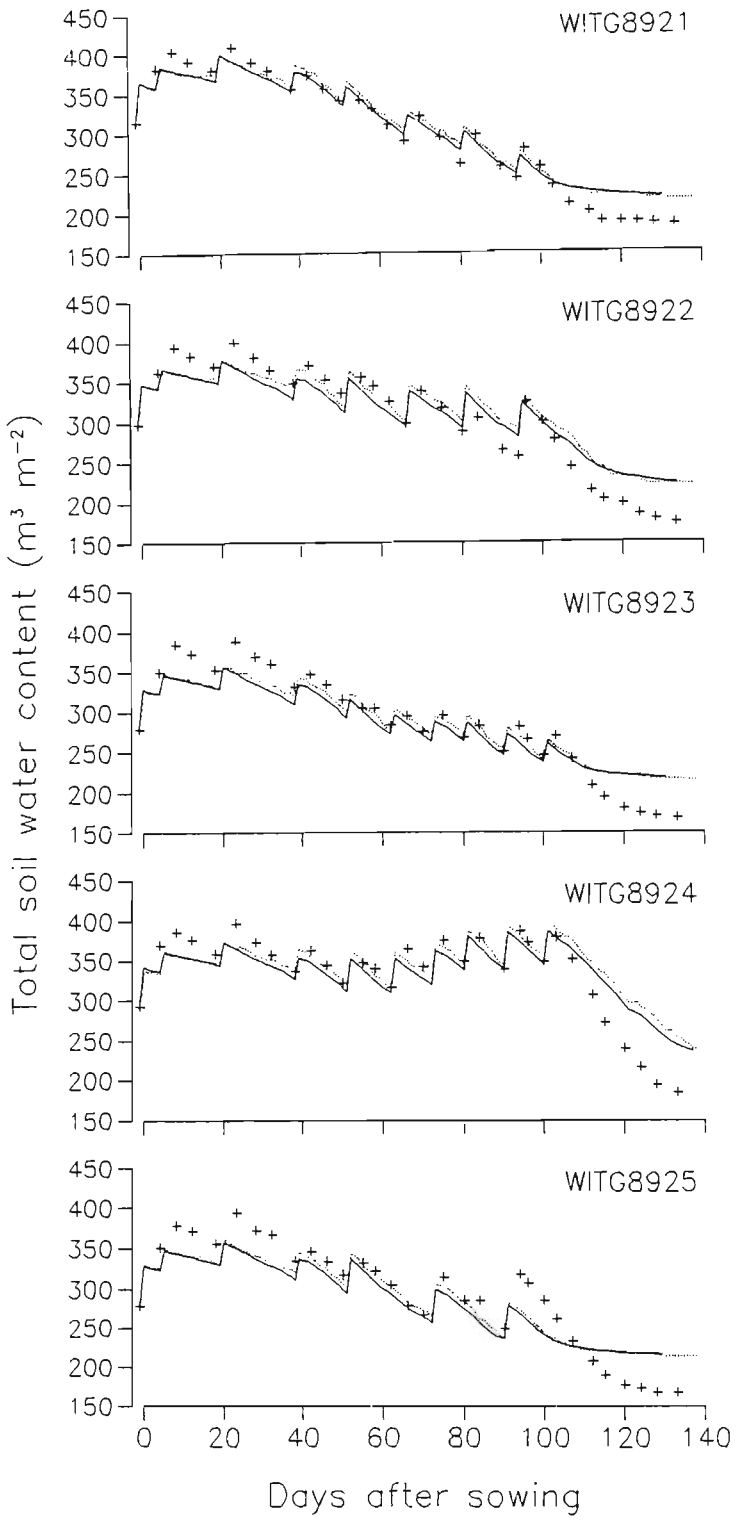

Figure A2.2: The predicted (dotted line: WHV21; solid line WHVZIM22) and observed (+) soil water contents for the wheat irrigation trial at GLEN 1989.

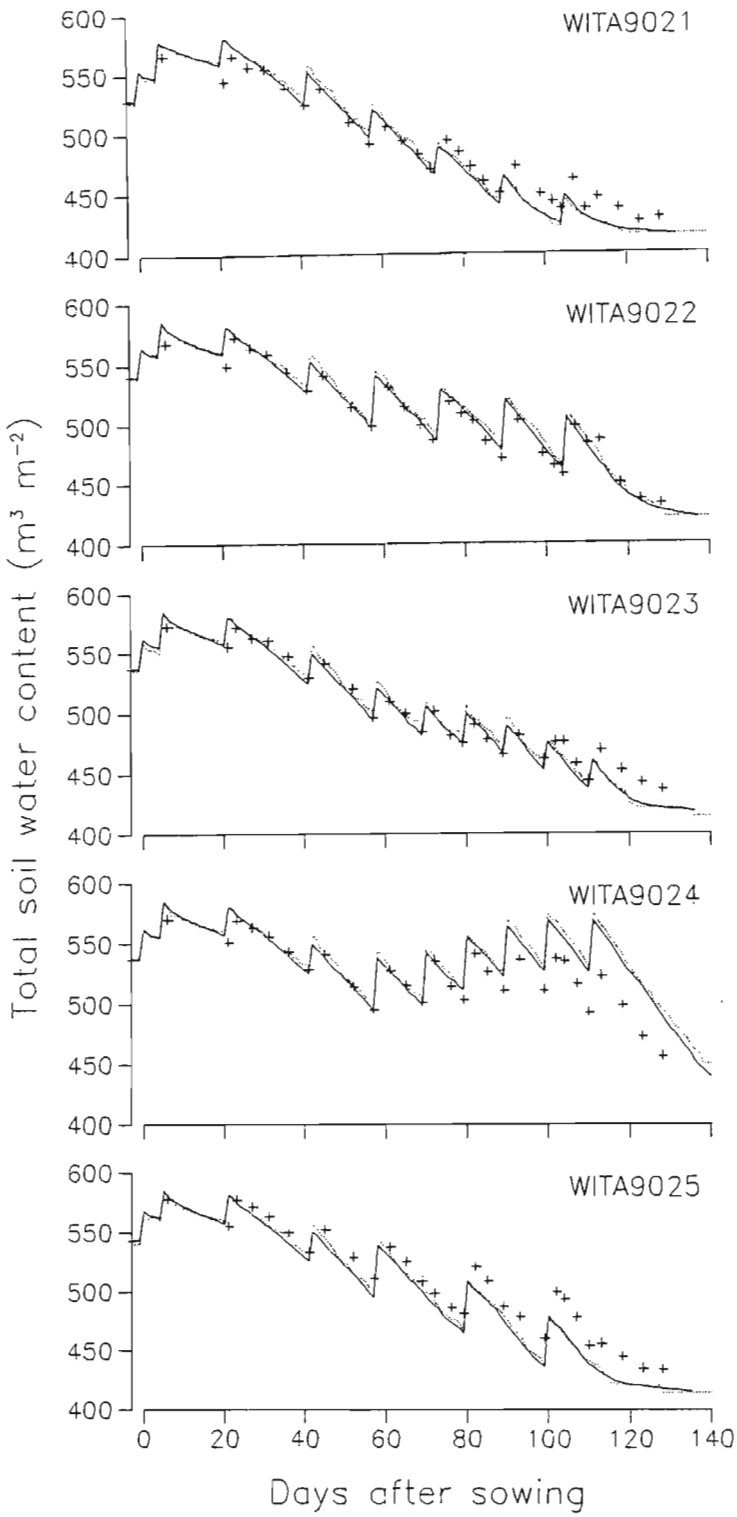

Figure A2.3: The predicted (dotted line: WHV21; solid line WHVZIM22) and observed (+) soil water contents for the wheat irrigation trial at ART 1990.

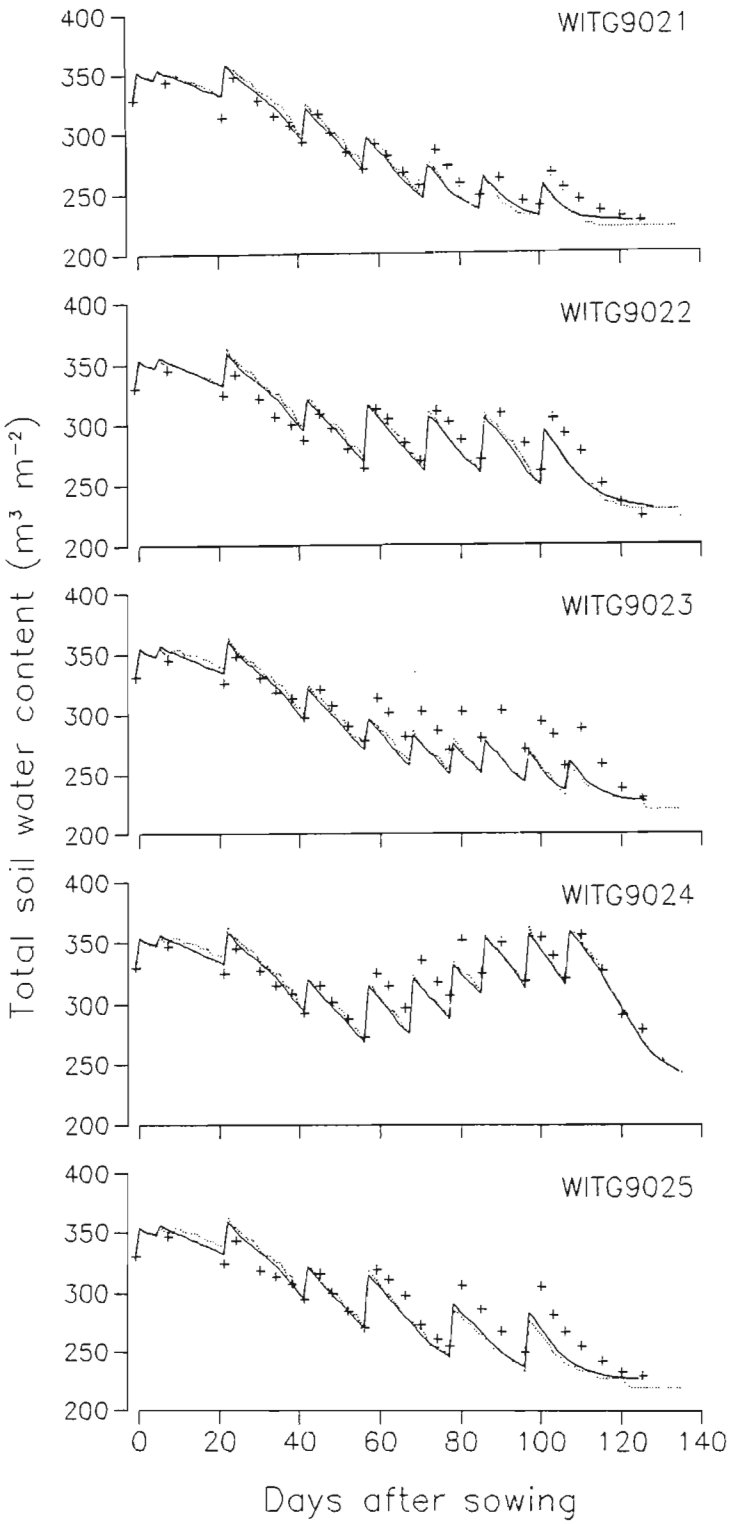

Figure A2.4: The predicted (dotted line: WHV21; solid line WHVZIM22) and observed (+) soil water contents for the wheat irrigation trial at GLEN 1990.

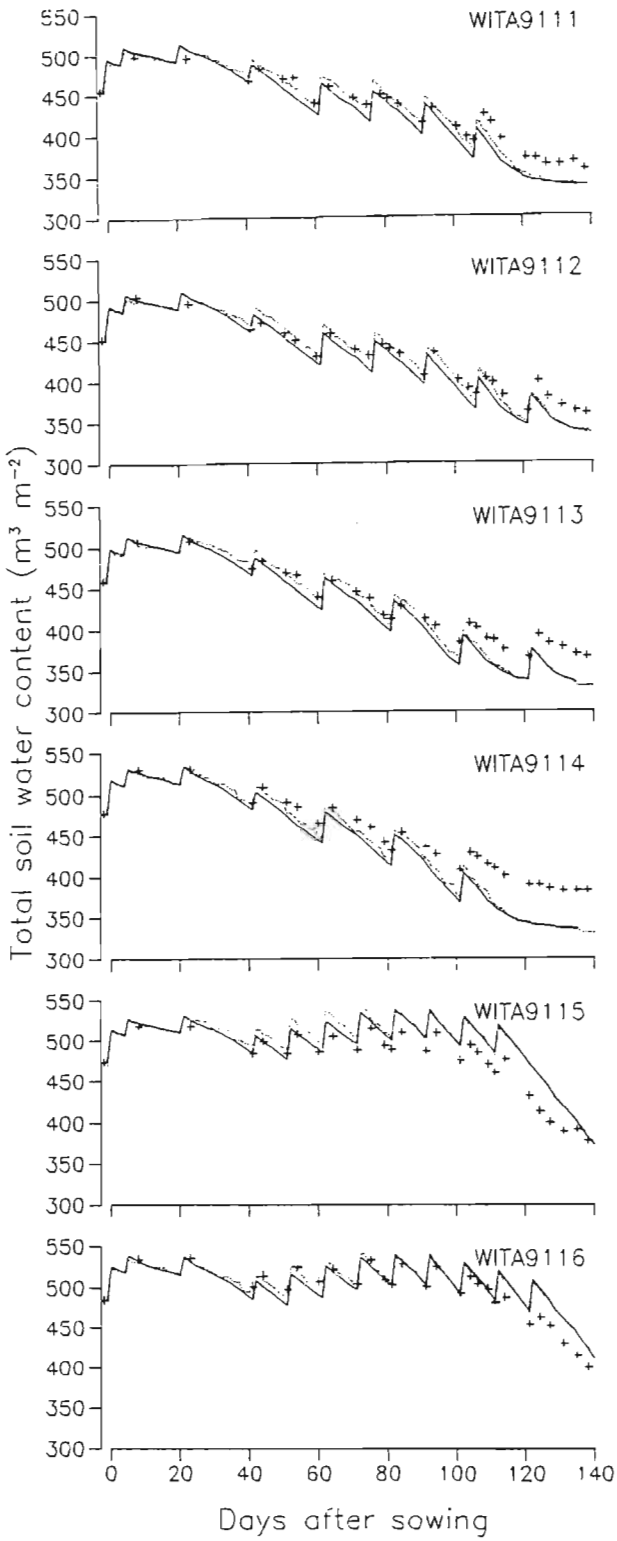

Figure A2.5: The predicted (dotted line: WHV21; solid line WHVZIM22) and observed (+) soil water contents for the wheat irrigation trial at ART 1991.

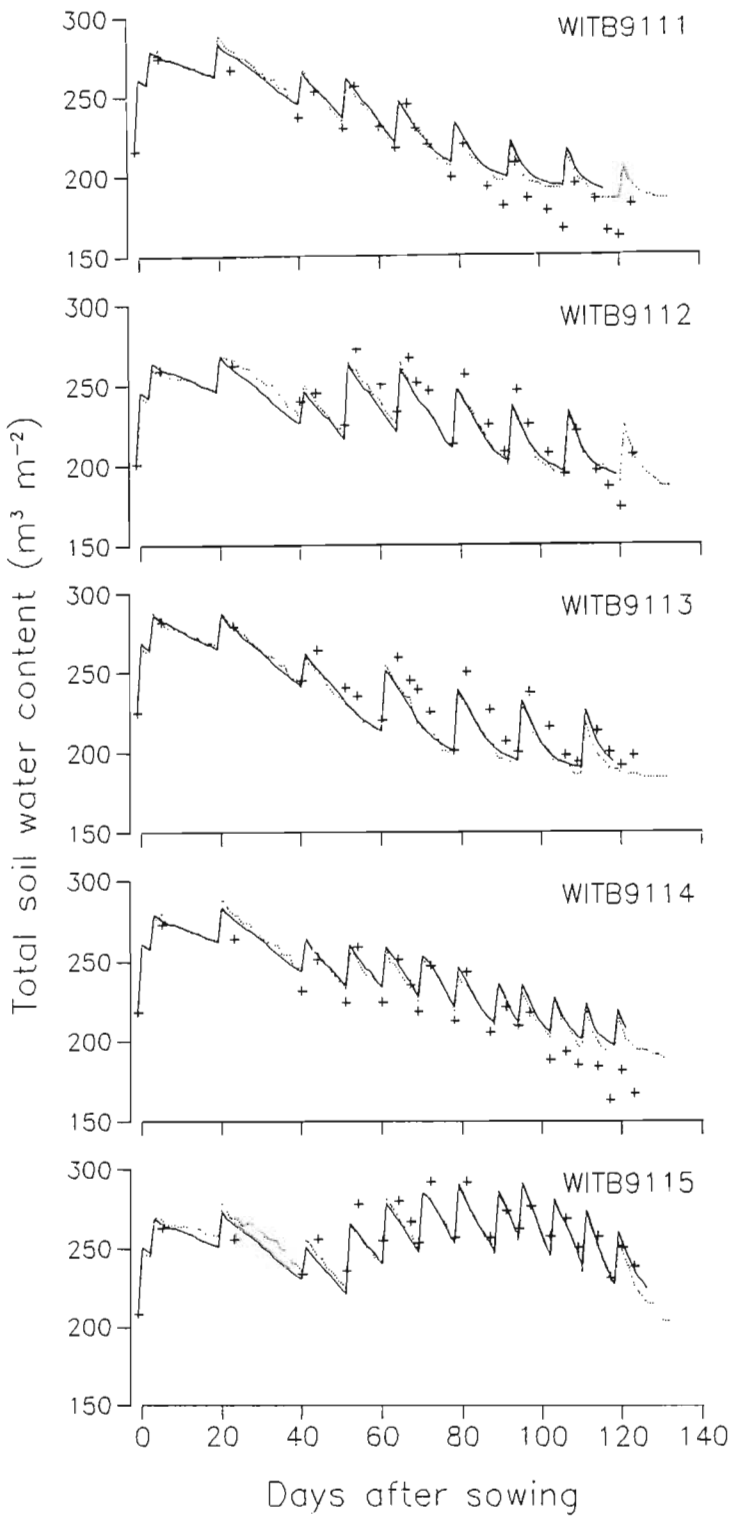

Figure A2.6: The predicted (dotted line: WHV21; solid line WHVZIM22) and observed (+) soil water contents for the wheat irrigation trial at BANK 1991.

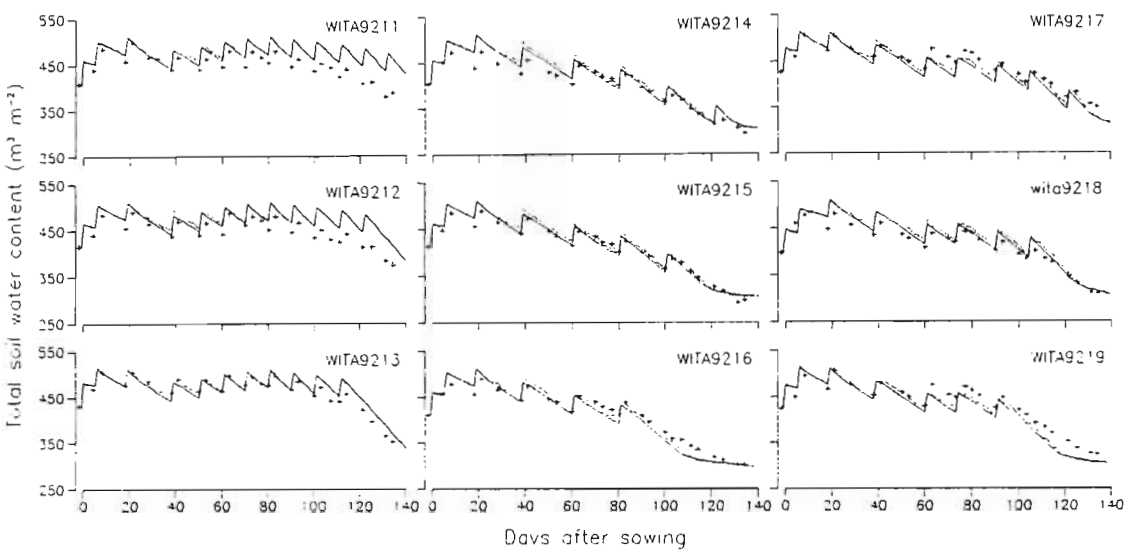

Figure A2.7: The predicted (dotted line: WHV21; solid line WHVZIM22) and observed (+) soil water contents for the wheat irrigation trial at ART 1992.

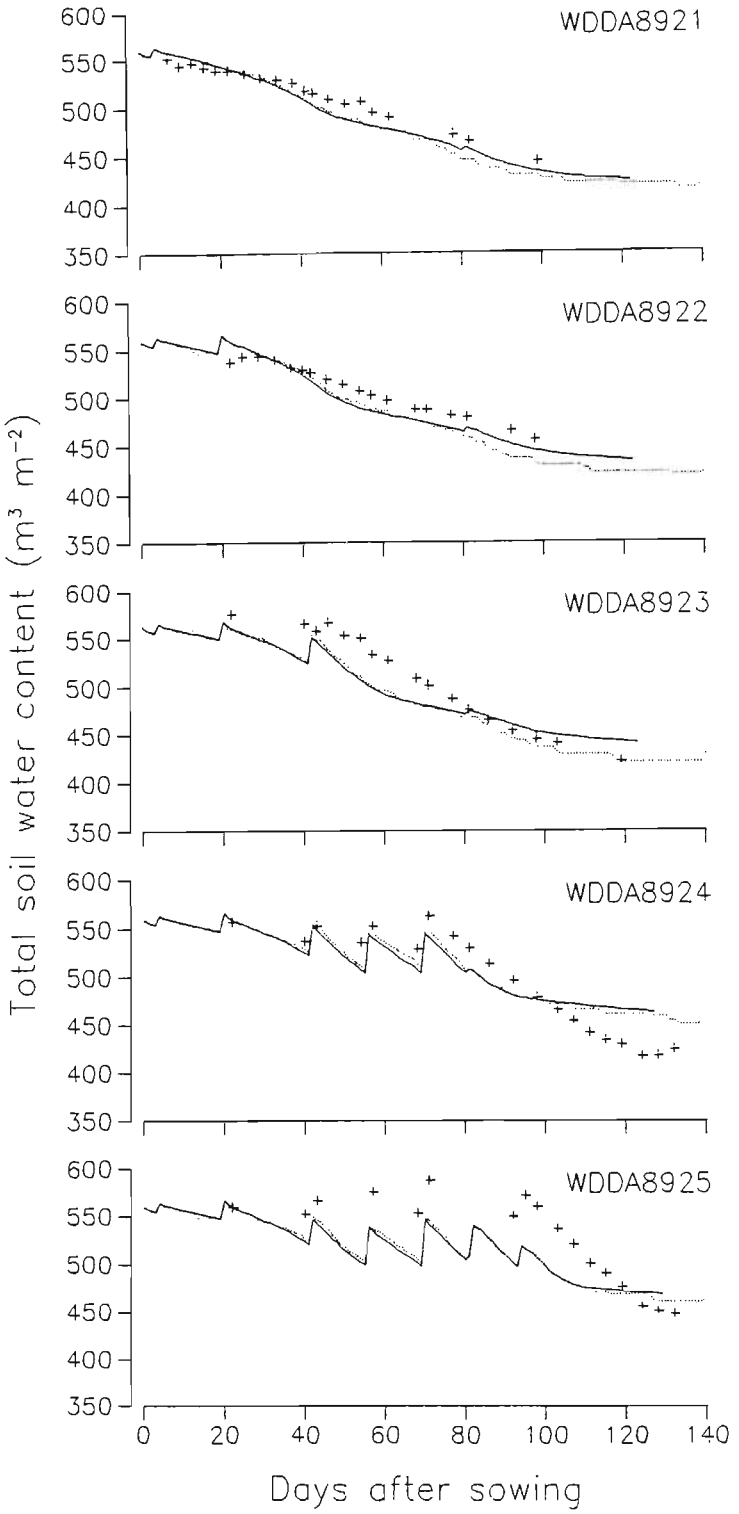

Figure A2.8: The predicted (dotted line: WHV21; solid line WHVZIM22) and observed (+) soil water contents for the wheat irrigation dry down trial at ART 1989.

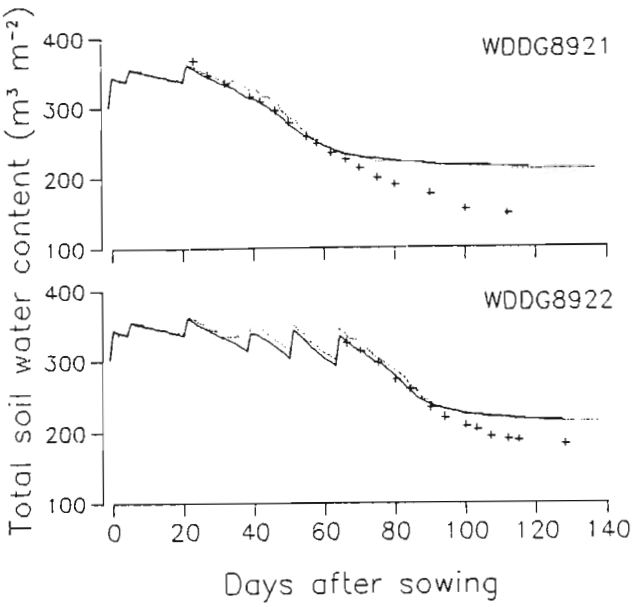

Figure A2.9: The predicted (dotted line: WHV21; solid line WHVZIM22) and observed (+) soil water contents for the wheat irrigation dry down trial at GLEN 1989.

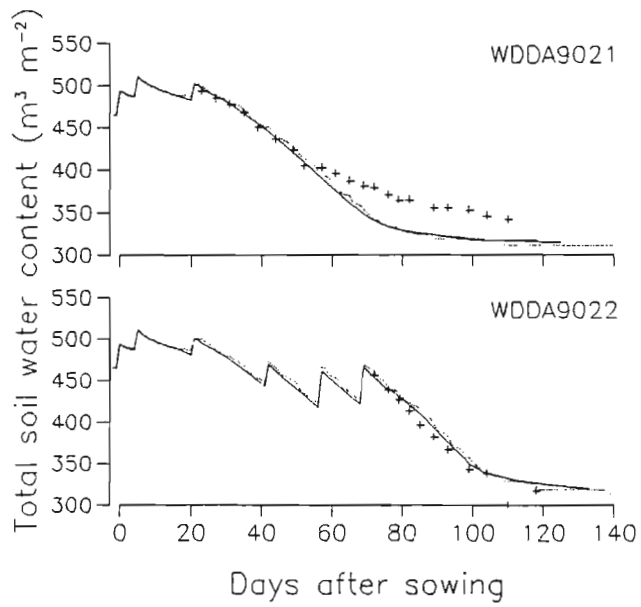

Figure A2.10: The predicted (dotted line: WHV21; solid line WHVZIM22) and observed (+) soil water contents for the wheat irrigation dry down trial at ART 1990.

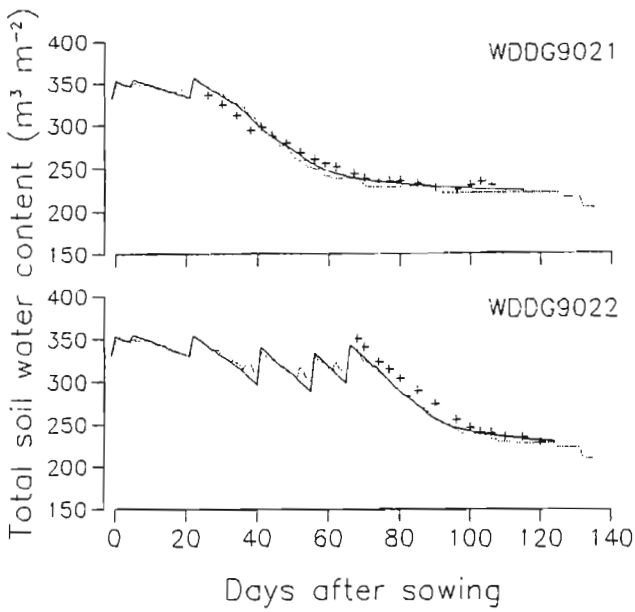

Figure A2.11: The predicted (dotted line: WHV21; solid line WHVZIM22) and observed (+) soil water contents for the wheat irrigation dry down trial at GLEN 1990.

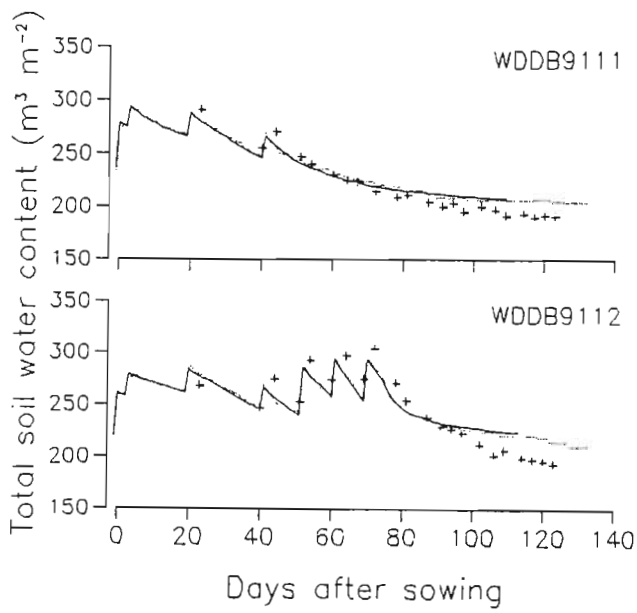

Figure A2.12: The predicted (dotted line: WHV21; solid line WHVZIM22) and observed (+) soil water contents for the wheat irrigation dry down trial at BANK 1991.

Table A2.1: Observed (O) and predicted (P) days from sowing to growth stages TS, 39, 61 and 87 of four cultivars under well-watered conditions (*continued on page 217*).

Data set	Trial code	TS		39		61		87	
		O	P	O	P	O	P	O	P
W170/84									
15	WPDR8911	45	41	76	71	99	96	157	152
16	WPDR8921	47	45	76	74	97	99	153	151
17	WPDR8931	42	47	77	77	99	100	151	150
18	WPDR8941	49	47	80	78	100	99	150	148
19	WPDR8951	51	49	82	78	97	98	144	145
30	WPDG9011	38	39	61	64	80	87	142	146
31	WPDG9021	42	41	66	68	88	92	142	147
32	WPDG9031	41	40	65	68	86	93	137	144
33	WPDG9041	42	43	72	72	91	94	133	143
34	WPDG9051	46	45	77	75	92	96	131	141
40	WPDA9111			79	74	103	99	160	152
41	WPDA9121			87	76	105	100	155	150
42	WPDA9131			92	78	105	100	156	147
43	WPDA9141			88	78	104	98	150	146
44	WPDA9151			89	78	101	96	147	143
45	WPDD9111			72	67	89	92	146	148
46	WPDD9121			71	69	94	94	145	146
47	WPDD9131			80	76	96	99	139	146
48	WPDD9141			82	78	94	99	134	143
49	WPDD9151			80	78	96	97	131	140
Sengwa									
15	WPDR8912	35	34	62	59	88	79	154	144
16	WPDR8922	35	37	65	62	88	84	150	143
17	WPDR8932	38	40	65	64	89	86	145	141
18	WPDR8942	36	40	68	65	89	85	145	138
19	WPDR8952	40	41	69	66	89	85	141	137
30	WPDG9012	26	32	51	52	67	72	132	138
31	WPDG9022	32	34	51	55	72	75	132	138
32	WPDG9032	30	34	55	57	74	77	132	136
33	WPDG9042	29	35	56	59	79	80	128	135
34	WPDG9052	32	38	60	62	81	82	126	133
40	WPDA9112			64	62	82	83	145	144
41	WPDA9122			69	63	92	85	149	141
42	WPDA9132			73	66	93	86	144	139
43	WPDA9142			74	66	92	86	145	136
44	WPDA9152			74	66	92	84	137	134
45	WPDD9112			55	54	73	74	137	139
46	WPDD9122			60	57	78	78	141	138
47	WPDD9132			58	62	81	84	136	137
48	WPDD9142			69	65	86	85	131	135
49	WPDD9152			70	66	84	85	128	132

Table A2.1: *continued from page 216*

Data set	Trial code	TS O	TS P	39 O	39 P	61 O	61 P	87 O	87 P
Rusape									
15	WPDR8913	37	37	68	63	92	85	153	145
16	WPDR8923	38	39	70	65	91	88	149	143
17	WPDR8933	39	42	71	68	92	90	145	142
18	WPDR8943	40	43	74	70	97	91	146	140
19	WPDR8953	47	44	76	71	95	90	142	138
30	WPDG9013	30	35	53	57	70	77	130	139
31	WPDG9023	30	36	54	60	75	81	133	138
32	WPDG9033	31	36	57	60	77	82	132	137
33	WPDG9043	32	38	60	64	82	85	127	135
34	WPDG9053	33	40	66	66	85	86	122	133
40	WPDA9113			69	65	89	89	149	144
41	WPDA9123			70	67	96	90	152	142
42	WPDA9133			78	70	100	91	143	140
43	WPDA9143			78	70	97	90	143	137
44	WPDA9153			80	70	96	88	138	135
45	WPDD9113			56	59	74	81	135	141
46	WPDD9123			61	62	87	85	139	139
47	WPDD9133			62	66	90	89	134	138
48	WPDD9143			70	69	90	90	129	136
49	WPDD9153			76	70	92	88	127	133
Angwa									
15	WPDR8914	33	32	63	55	84	74	149	136
16	WPDR8924	33	35	66	59	87	79	143	137
17	WPDR8934	34	38	66	60	87	80	142	135
18	WPDR8944	35	38	69	61	89	81	142	132
19	WPDR8954	39	39	71	63	88	82	137	130
30	WPDG9014	24	30	49	49	63	67	120	129
31	WPDG9024	25	33	50	53	69	72	126	132
32	WPDG9034	28	32	55	53	72	73	124	129
33	WPDG9044	28	33	56	55	76	75	126	128
34	WPDG9054	29	36	61	59	79	77	121	127

Table A2.2: Observed (O) and predicted (P) ear densities (TPSM) and yield components for four cultivars under well-watered conditions (*continued on page 219*).

Data Set	Trial code	TPSM O	TPSM P	Kernel wt. O	Kernel wt. P	Kernel no. O	Kernel no. P	Yield 12.5% O	Yield 12.5% P	Y.C. Yield O	Y.C. Yield P
		Ears m^{-2}		mg $kernel^{-1}$		kernel m^{-2}		t ha^{-1}			
W170/84											
15	WPDR8911	331	415	46.0	44.0	20203	26968	8.76	13.57	9.30	11.81
16	WPDR8921	454	438	41.4	40.2	27481	27071	8.25	12.45	11.37	10.89
17	WPDR8931	394	439	38.7	39.5	23510	25351	8.20	11.45	9.09	10.02
18	WPDR8941	465	431	36.1	39.0	30986	23468	7.55	10.45	11.17	9.15
19	WPDR8951	353	404	33.5	39.6	22876	22435	7.13	10.16	7.67	8.89
30	WPDG8911	296	324	44.8	45.4	21157	22820	7.66	11.85	9.48	10.37
31	WPDG9021	303	374	42.9	42.6	23673	24483	8.67	11.91	10.15	10.42
32	WPDG8931	381	395	42.1	39.7	26800	25090	8.78	11.39	11.28	9.97
33	WPDG9041	413	398	38.9	37.4	27033	24730	8.52	10.56	10.53	9.24
34	WPDG8951	359	387	33.2	36.1	23616	22905	6.47	9.45	7.84	8.27
40	WPDA9111	398	419	42.4	42.3	25790	25274	9.25	12.23	10.94	10.70
41	WPDA9121	360	400	39.6	39.7	21376	25280	8.95	11.48	8.47	10.04
42	WPDA9131	425	414	36.2	40.9	27729	23862	8.99	11.16	10.04	9.76
43	WPDA9141	457	404	37.5	40.3	30313	22809	9.35	10.51	11.35	9.19
44	WPDA9151	425	368	37.8	42.3	26633	20516	8.98	9.93	10.07	8.69
45	WPDD9111	332	441	50.0	43.7	21607	28163	7.02	14.06	10.80	12.30
46	WPDD9121	365	469	40.9	39.0	24331	29269	7.90	13.04	9.95	11.41
47	WPDD9131	378	463	35.8	36.6	23219	27682	6.92	11.59	8.31	10.15
48	WPDD9141	392	466	34.4	35.3	22598	26659	6.21	10.77	7.77	9.42
49	WPDD9151	397	433	31.1	35.6	24425	23667	5.83	9.62	7.60	8.42
Sengwa											
15	WPDR8912	433	447	36.7	41.7	21859	23936	7.72	11.40	8.01	9.97
16	WPDR8922	458	494	34.9	38.3	24387	26299	8.02	11.52	8.51	10.08
17	WPDR8932	415	491	34.5	36.2	22177	25792	8.20	10.68	7.65	9.34
18	WPDR8942	440	483	33.1	34.0	26019	25102	8.10	9.76	8.61	8.54
19	WPDR8952	453	492	32.5	33.8	26311	23767	8.29	9.17	8.54	8.03
30	WPDG9012	420	358	39.9	41.1	23026	20233	6.60	9.50	9.19	8.31
31	WPDG9022	392	419	38.8	38.4	21279	23011	7.63	10.11	8.25	8.84
32	WPDG9032	486	448	36.2	35.6	29130	24642	7.94	10.02	10.55	8.77
33	WPDG9042	537	509	33.1	34.0	29836	25755	7.73	10.00	9.87	8.75
34	WPDG9052	513	454	31.8	31.9	30154	23674	6.70	8.64	9.58	7.56
40	WPDA9112	415	465	40.0	39.4	21091	24870	7.97	11.19	8.43	9.79
41	WPDA9122	409	474	38.7	37.1	20325	24450	8.26	10.38	7.86	9.08
42	WPDA9132	456	450	35.5	35.0	26757	24824	9.22	9.94	9.51	8.70
43	WPDA9142	440	456	33.5	34.3	25029	23685	9.18	9.29	8.39	8.13
44	WPDA9152	486	480	32.5	34.5	26556	22942	8.22	9.04	8.62	7.91
45	WPDD9112	393	493	37.8	38.2	22282	26900	6.81	11.73	8.42	10.27
46	WPDD9122	424	492	37.3	35.7	24009	27318	7.62	11.15	8.96	9.76
47	WPDD9132	450	562	35.2	33.3	24504	28670	7.49	10.91	8.62	9.55
48	WPDD9142	496	543	31.3	31.8	26967	27257	6.89	9.91	8.45	8.67
49	WPDD9152	489	555	27.7	30.5	29700	26600	7.59	9.28	8.24	8.12

Table A2.2: *continued from page 218*

Data Set	Trial code	TPSM O	TPSM P	Kernel wt. O	Kernel wt. P	Kernel no. O	Kernel no. P	Yield 12.5% O	Yield 12.5% P	Y.C. Yield O	Y.C. Yield P
		Ears m^{-2}		mg $kernel^{-1}$		kernel m^{-2}		t ha^{-1}			
Rusape											
15	WPDR8913	412	437	46.6	46.0	22422	25025	8.28	13.17	10.44	11.52
16	WPDR8923	418	454	43.4	42.4	23347	26190	7.95	12.68	10.13	11.09
17	WPDR8933	433	449	41.5	39.9	24112	25158	8.13	11.49	10.00	10.05
18	WPDR8943	408	456	37.2	39.5	25273	24240	7.43	10.95	9.40	9.58
19	WPDR8953	417	454	39.0	39.0	26122	22161	7.54	9.87	10.19	8.64
30	WPDG9013	393	329	44.7	49.5	23731	20281	6.78	11.48	10.61	10.04
31	WPDG9023	385	383	43.2	45.0	23802	23346	7.39	12.02	10.29	10.51
32	WPDG9033	377	409	41.4	42.5	23256	23675	7.93	11.50	9.63	10.07
33	WPDG9043	471	437	40.2	39.7	28182	24667	7.67	11.20	11.32	9.80
34	WPDG9053	437	446	35.4	36.0	26544	24365	5.39	10.01	9.38	8.76
40	WPDA9113	392	423	42.0	44.5	21054	24383	8.41	12.41	8.84	10.86
41	WPDA9123	379	428	42.7	42.2	22715	24112	9.37	11.62	9.70	10.16
42	WPDA9133	438	411	40.8	41.2	27701	23172	9.24	10.91	11.30	9.54
43	WPDA9143	422	428	42.1	39.7	23675	22802	9.15	10.35	9.96	9.05
44	WPDA9153	423	413	41.0	40.8	27082	20824	8.91	9.70	11.11	8.49
45	WPDD9113	352	470	43.8	44.9	22913	27741	6.67	14.25	10.04	12.47
46	WPDD9123	355	466	41.0	42.7	21769	27226	7.32	13.29	8.93	11.63
47	WPDD9133	410	486	40.0	37.4	25343	27733	5.43	11.86	10.14	10.38
48	WPDD9143	401	493	36.4	36.1	23538	26505	7.03	10.95	8.57	9.58
49	WPDD9153	410	468	35.4	35.8	26047	24414	6.01	9.98	9.22	8.73
Angwa											
15	WPDR8914	417	432	45.0	49.1	20351	21365	6.98	11.98	9.15	10.49
16	WPDR8924	408	457	43.2	46.3	20738	22625	7.39	11.96	8.96	10.47
17	WPDR8934	444	492	43.8	42.3	21005	23494	7.51	11.35	9.21	9.93
18	WPDR8944	448	521	41.0	40.0	21776	23359	7.78	10.68	8.92	9.35
19	WPDR8954	421	465	42.4	39.1	20953	21542	7.36	9.64	8.89	8.43
30	WPDG9014	400	346	49.0	50.5	18332	17687	6.04	10.20	8.98	8.93
31	WPDG9024	416	405	48.9	46.5	20733	20757	7.21	11.04	10.14	9.66
32	WPDG9034	418	398	42.8	44.0	22472	21015	7.94	10.58	9.62	9.26
33	WPDG9044	498	477	42.0	41.4	23592	22313	6.71	10.56	9.91	9.24
34	WPDG9054	523	462	38.7	39.4	26569	21561	7.03	9.71	10.28	8.50

Table A2.3: Observed (O) and predicted (P) days from sowing to growth stages 39, 61 and 87 of wheat grown under deficit irrigation.

Data set	Trial code	39		61		87	
		O	P	O	P	O	P
75	WITG8921	57	61	77	81	122	139
76	WITG8922	58	61	76	81	128	139
77	WITG8923	57	61	77	81	128	139
78	WITG8924	58	61	78	81	132	139
79	WITG8925	58	61	75	81	125	139
80	WITA9021	58	64	78	85	120	142
81	WITA9022	58	64	78	85	125	142
82	WITA9023	58	64	77	85	125	142
83	WITA9024	58	64	78	85	128	142
84	WITA9025	58	64	78	85	124	142
90	WITB9111	60	69	79	90	114	133
91	WITB9112	59	69	78	90	119	133
92	WITB9113	60	69	77	90	120	133
93	WITB9114	60	69	81	90	118	133
94	WITB9115	60	69	80	90	122	133
95	WITA9111	82	78	99	100	136	147
96	WITA9112	82	78	98	100	137	147
97	WITA9113	81	78	99	100	137	147
98	WITA9114	82	78	98	100	135	147
99	WITA9115	84	78	102	100	142	147
100	WITA9116	84	78	101	100	142	147
117	WDDA9021	58	64	75	85	116	142
118	WDDA9022	58	64	81	85	125	142
119	WDDG9021	50	60	66	80	109	138
120	WDDG9022	50	60	71	80	116	138
121	WDDB9111	60	69	77	90	107	133
122	WDDB9112	60	69	80	90	111	133

Table A2.4: Observed (O) and predicted (P) ear densities (TPSM) and yield components of wheat grown under deficit irrigation.

Data Set	Trial code	TPSM		Kernel wt.		Kernel no.		Yield 12.5%		Y.C. Yield	
		O	P	O	P	O	P	O	P	O	P
		Ears m^{-2}		mg $kernel^{-1}$		kernel m^{-2}		t ha^{-1}			
75	WITG8921	512	442	27.8	26.4	28091	24735	5.81	7.46	7.82	6.53
76	WITG8922	583	452	29.7	31.5	34918	24941	6.51	8.98	10.36	7.86
77	WITG8923	480	453	31.2	28.1	28877	24959	6.84	8.02	9.02	7.01
78	WITG8924	589	432	30.1	33.9	34976	24509	7.79	9.50	10.53	8.31
79	WITG8925	508	442	30.6	25.8	28911	24352	6.56	7.18	8.85	6.28
80	WITA9021	369	505	36.2	23.6	19833	25675	4.91	6.92	7.18	6.06
81	WITA9022	387	489	35.2	32.8	22940	25740	5.86	9.65	8.07	8.44
82	WITA9023	444	505	34.4	31.3	25942	25993	5.80	9.30	8.92	8.14
83	WITA9024	509	503	37.2	39.1	26108	25966	6.76	11.60	9.71	10.15
84	WITA9025	450	497	34.3	28.3	25793	25868	5.68	8.37	8.85	7.32
90	WITB9111	208	356	38.2	20.4	11743	15558	3.00	3.63	4.48	3.17
91	WITB9112	268	374	40.2	25.1	14181	19861	4.02	5.70	5.70	4.99
92	WITB9113	233	359	40.3	23.0	13855	15077	3.06	3.96	5.58	3.47
93	WITB9114	262	369	41.0	26.6	14599	20932	5.01	6.36	5.99	5.57
94	WITB9115	349	376	39.2	33.6	20110	21792	6.22	8.37	7.88	7.32
95	WITA9111	357	432	35.0	24.9	19675	23907	7.22	6.80	6.89	5.95
96	WITA9112	388	433	37.4	29.5	22680	23935	7.88	8.07	8.47	7.06
97	WITA9113	341	435	37.2	26.1	19764	23771	7.17	7.09	7.35	6.20
98	WITA9114	375	441	34.5	21.0	20658	24061	6.50	5.77	7.12	5.05
99	WITA9115	442	427	32.4	39.4	25174	23822	7.43	10.73	8.15	9.39
100	WITA9116	409	432	35.9	39.8	23958	23915	8.83	10.88	8.59	9.52
117	WDDA9021	363	495	28.4	20.0	17682	6125	2.63	1.40	5.01	1.23
118	WDDA9022	566	526	29.7	24.4	33796	26273	5.40	7.33	10.02	6.41
119	WDDG9021	268	426	32.6	20.0	14871	3460	3.18	0.79	4.84	0.69
120	WDDG9022	443	505	31.2	21.3	26957	25592	5.55	6.23	8.40	5.45
121	WDDB9111	96	276	34.6	20.0	4940	1952	1.06	0.45	1.71	0.39
122	WDDB9112	236	342	26.2	20.0	12306	5639	2.02	1.29	3.22	1.13

APPENDIX 3: AVERAGE AIR TEMPERATURE AND DEVELOPMENT RATE DATA USED FOR THE CALIBRATION OF PHENOLOGICAL DEVELOPMENT IN WHVZIM22

TABLE OF CONTENTS

Table A3.1: Average air temperature (T, °C) and rate of development ($1/t$, d^{-1}) for specified growth stages of cultivar W170/84. Set refers to the data set numbers given in Table 2.3.

Set	GS10 - TS		GS10 - GS31		TS - GS39		GS39 - GS61		GS61 - GS87	
	T	$1/t$	T	$1/t$	T	$1/t$	T	$1/t$	T	$1/t$
1	16.4	0.0278	16.3	0.0233	14.7	0.0476	13.8	0.0435	15.5	0.0164
2	16.3	0.0278	15.8	0.0217	14.1	0.0435	14.2	0.0385	16.3	0.0172
3	15.7	0.0256	15.4	0.0213	14.0	0.0370	15.8	0.0476	16.6	0.0185
4	14.6	0.0227	14.4	0.0208	14.3	0.0435	14.1	0.0455	18.7	0.0204
5	14.1	0.0227	14.1	0.0213	13.9	0.0385	16.6	0.0556	19.1	0.0204
6	16.3	0.0286	16.3	0.0244	14.4	0.0370	14.4	0.0476	15.9	0.0182
7	15.5	0.0256	15.4	0.0238	14.0	0.0385	14.5	0.0476	17.0	0.0192
8	14.8	0.0233	14.8	0.0222	14.3	0.0400	14.3	0.0455	19.2	0.0217
9	14.1	0.0233	14.1	0.0217	14.3	0.0417	16.6	0.0500	19.2	0.0233
10	15.9	0.0256	15.6	0.0227	13.7	0.0385	13.2	0.0476	16.4	0.0164
11	14.7	0.0256	14.7	0.0217	14.8	0.0357	13.3	0.0500	17.3	0.0175
12	14.5	0.0238	14.6	0.0222	13.7	0.0345	14.7	0.0476	18.7	0.0200
13	14.2	0.0217	14.2	0.0196	13.7	0.0333	16.4	0.0588	18.9	0.0204
14	13.5	0.0208	13.7	0.0196	14.7	0.0370	18.3	0.0714	19.1	0.0213
20	16.7	0.0286	16.3	0.0244	14.4	0.0333	14.3	0.0526	16.2	0.0175
21	15.9	0.0286	15.4	0.0227	14.5	0.0313	14.1	0.0588	17.4	0.0175
22	15.1	0.0263	15.1	0.0233	14.3	0.0333	14.7	0.0556	18.5	0.0196
23	14.8	0.0250	14.7	0.0227	14.0	0.0323	15.7	0.0667	19.6	0.0213
24	14.4	0.0250	14.3	0.0238	14.6	0.0323	17.9	0.0714	19.9	0.0238
25	15.9	0.0270	15.8	0.0233	14.5	0.0370	14.7	0.0455	15.3	0.0167
26	14.9	0.0263	14.9	0.0213	14.8	0.0323	13.8	0.0526	15.9	0.0175
27	14.7	0.0244	14.6	0.0208	14.3	0.0357	13.6	0.0455	17.6	0.0192
28	14.7	0.0233	14.7	0.0204	13.9	0.0313	14.9	0.0476	19.0	0.0227
29	14.3	0.0204	14.4	0.0192	14.1	0.0345	16.2	0.0625	19.9	0.0244
35	18.7	0.0303	18.7	0.0256	17.5	0.0417	15.8	0.0455	16.9	0.0167
36	18.1	0.0313	18.0	0.0294	16.0	0.0417	16.0	0.0500	17.4	0.0167
37	17.4	0.0294	17.6	0.0323	15.5	0.0455	15.5	0.0455	18.1	0.0189
38	16.7	0.0278	16.8	0.0303	15.9	0.0370	15.6	0.0588	19.4	0.0208
39	16.2	0.0278	16.2	0.0286	15.3	0.0345	17.4	0.0556	21.0	0.0244
50	NR[§]	NR	19.7	0.0294	19.6	0.0169	19.2	0.0667	18.9	0.0182
51	NR	NR	18.7	0.0270	19.1	0.0169	17.6	0.0625	19.9	0.0196
51	NR	NR	18.7	0.0313	18.2	0.0154	20.2	0.0714	24.2	0.0278
52	NR	NR	18.7	0.0294	18.9	0.0172	17.5	0.0476	22.0	0.0227
53	NR	NR	18.7	0.0294	18.2	0.0159	17.6	0.0588	23.5	0.0270

[§]TS was not recorded at this site.

Table A3.2: Average air temperature (T, °C) and rate of development ($1/t$, d^{-1}) for specified growth stages of cultivar Sengwa. Set refers to the data set numbers given in Table 2.3.

Set	GS10 - TS		GS10 - GS31		TS - GS39		GS39 - GS61		GS61 - GS87	
	T	$1/t$	T	$1/t$	T	$1/t$	T	$1/t$	T	$1/t$
1	16.1	0.0385	16.5	0.0263	15.8	0.0417	14.3	0.0526	14.6	0.0159
2	16.6	0.0323	16.0	0.0244	14.0	0.0455	14.1	0.0526	15.8	0.0149
3	16.4	0.0370	15.5	0.0227	13.9	0.0357	14.4	0.0476	16.4	0.0167
4	14.9	0.0333	14.8	0.0238	14.1	0.0313	13.9	0.0556	17.9	0.0192
5	14.2	0.0303	14.1	0.0238	14.0	0.0333	14.2	0.0588	19.0	0.0185
6	16.1	0.0400	16.3	0.0278	15.8	0.0476	14.1	0.0435	15.2	0.0164
7	16.3	0.0370	15.5	0.0256	13.9	0.0417	14.3	0.0476	16.2	0.0164
8	15.3	0.0370	14.9	0.0263	14.1	0.0370	14.2	0.0455	17.6	0.0182
9	14.1	0.0313	14.0	0.0244	14.3	0.0417	14.3	0.0455	19.1	0.0213
10	16.0	0.0345	15.9	0.0250	13.7	0.0370	14.8	0.0476	15.4	0.0156
11	15.6	0.0333	14.7	0.0256	14.1	0.0357	13.3	0.0435	16.8	0.0169
12	14.1	0.0323	14.5	0.0233	14.5	0.0333	13.7	0.0435	18.1	0.0182
13	14.1	0.0313	14.2	0.0213	13.9	0.0294	14.7	0.0455	18.8	0.0200
14	13.9	0.0286	13.6	0.0204	13.8	0.0323	16.6	0.0556	19.1	0.0196
20	16.8	0.0385	16.5	0.0270	14.7	0.0357	14.9	0.0500	15.8	0.0154
21	16.3	0.0370	15.5	0.0256	14.5	0.0357	14.2	0.0500	17.0	0.0159
22	15.2	0.0357	15.1	0.0263	14.7	0.0370	14.3	0.0500	17.8	0.0164
23	14.6	0.0370	14.7	0.0278	14.4	0.0357	14.5	0.0500	18.7	0.0182
24	14.4	0.0370	14.5	0.0263	14.1	0.0323	15.8	0.0526	19.8	0.0213
25	16.5	0.0370	15.9	0.0278	14.4	0.0417	14.8	0.0435	14.7	0.0156
26	15.2	0.0357	15.0	0.0250	14.3	0.0357	14.9	0.0500	15.3	0.0164
27	14.7	0.0357	14.6	0.0256	14.8	0.0385	13.9	0.0417	16.2	0.0167
28	14.5	0.0333	14.7	0.0227	14.4	0.0313	13.6	0.0476	17.7	0.0196
29	14.6	0.0313	14.5	0.0227	13.9	0.0323	14.8	0.0455	19.1	0.0217
35	19.7	0.0455	18.7	0.0313	17.4	0.0417	15.9	0.0588	16.2	0.0145
36	18.1	0.0500	18.1	0.0370	17.9	0.0476	15.5	0.0455	16.9	0.0152
37	17.6	0.0476	17.5	0.0385	16.0	0.0417	16.1	0.0526	17.2	0.0167
38	17.9	0.0455	17.4	0.0370	15.5	0.0417	15.5	0.0455	18.5	0.0169
39	16.0	0.0417	16.1	0.0323	15.9	0.0385	15.6	0.0526	19.7	0.0200
50	NR	NR	20.3	0.0370	19.9	0.0222	19.0	0.0500	18.7	0.0169
51	NR	NR	19.0	0.0345	19.1	0.0204	19.2	0.0667	19.0	0.0172
52	NR	NR	18.4	0.0333	19.0	0.0208	17.4	0.0625	20.5	0.0182
53	NR	NR	18.6	0.0333	18.4	0.0196	17.7	0.0556	21.9	0.0222
54	NR	NR	19.0	0.0385	18.3	0.0192	17.6	0.0588	23.3	0.0263

Table A3.3: Average air temperature (T, °C) and rate of development ($1/t$, d^{-1}) for specified growth stages of cultivar Rusape. Set refers to the data set numbers given in Table 2.3.

Set	GS10 - TS		GS10 - GS31		TS - GS39		GS39 - GS61		GS61 - GS87	
	T	$1/t$	T	$1/t$	T	$1/t$	T	$1/t$	T	$1/t$
1	16.2	0.0370	16.5	0.0263	15.7	0.0435	14.3	0.0526	15.2	0.0143
2	16.5	0.0303	16.0	0.0244	14.2	0.0435	13.9	0.0625	15.9	0.0143
3	16.0	0.0294	15.5	0.0227	13.6	0.0455	14.6	0.0500	16.5	0.0161
4	14.8	0.0313	14.8	0.0238	14.2	0.0333	13.9	0.0556	18.1	0.0172
5	13.9	0.0250	14.1	0.0238	14.4	0.0435	14.2	0.0588	19.1	0.0182
6	16.3	0.0286	16.4	0.0250	14.6	0.0455	14.0	0.0500	15.6	0.0179
7	15.8	0.0303	15.4	0.0233	14.1	0.0370	14.2	0.0400	16.9	0.0200
8	15.0	0.0313	14.8	0.0233	14.1	0.0313	14.4	0.0435	18.4	0.0233
9	13.9	0.0263	14.1	0.0222	14.4	0.0357	16.5	0.0500	19.1	0.0256
10	12.9	0.0303	16.1	0.0270	17.7	0.0417	14.8	0.0500	15.4	0.0154
11	15.2	0.0294	14.7	0.0256	14.3	0.0370	13.3	0.0500	16.8	0.0169
12	14.2	0.0303	14.5	0.0233	14.0	0.0323	14.3	0.0500	18.0	0.0189
13	14.3	0.0286	14.3	0.0233	13.6	0.0294	15.1	0.0526	18.9	0.0213
14	13.9	0.0250	13.5	0.0227	14.1	0.0313	17.0	0.0833	18.9	0.0213
20	16.8	0.0357	16.5	0.0270	14.7	0.0333	14.6	0.0526	15.6	0.0172
21	16.1	0.0313	15.4	0.0238	14.5	0.0357	13.9	0.0526	17.0	0.0175
22	15.0	0.0333	15.1	0.0250	14.8	0.0313	14.1	0.0455	18.2	0.0200
23	14.7	0.0313	14.7	0.0263	14.3	0.0345	15.0	0.0500	18.9	0.0217
24	14.4	0.0286	14.4	0.0250	14.5	0.0333	16.7	0.0556	19.9	0.0256
25	16.5	0.0370	15.9	0.0278	14.4	0.0357	14.9	0.0526	14.6	0.0159
26	15.2	0.0357	15.0	0.0278	14.4	0.0333	14.8	0.0556	15.3	0.0156
27	14.7	0.0345	14.6	0.0270	14.8	0.0333	13.6	0.0526	16.3	0.0164
28	14.6	0.0323	14.7	0.0238	14.3	0.0294	13.5	0.0556	17.8	0.0192
29	14.6	0.0286	14.5	0.0227	13.7	0.0278	15.7	0.0714	19.0	0.0227
35	19.6	0.0417	18.7	0.0303	17.5	0.0435	15.7	0.0435	16.2	0.0182
36	17.9	0.0455	18.1	0.0370	17.8	0.0455	15.5	0.0455	16.5	0.0169
37	17.5	0.0417	17.4	0.0400	16.0	0.0400	16.6	0.0455	17.2	0.0185
38	17.7	0.0435	17.6	0.0400	15.7	0.0357	15.3	0.0435	18.7	0.0192
39	16.0	0.0400	16.1	0.0333	15.7	0.0323	16.2	0.0500	19.7	0.0227
50	NR	NR	20.3	0.0370	19.8	0.0208	18.9	0.0476	18.7	0.0182
51	NR	NR	19.0	0.0345	19.2	0.0196	18.7	0.0588	19.1	0.0189
52	NR	NR	18.4	0.0333	18.9	0.0185	17.7	0.0625	20.7	0.0204
53	NR	NR	18.6	0.0333	18.2	0.0175	18.1	0.0500	22.7	0.0270
54	NR	NR	18.9	0.0370	18.3	0.0179	18.7	0.0500	24.0	0.0323

Table A3.4: Average air temperature (T, °C) and rate of development ($1/t$, d^{-1}) for specified growth stages of cultivar Angwa. Set refers to the data set numbers given in Table 2.3.

Set	GS10 - TS		GS10 - GS31		TS - GS39		GS39 - GS61		GS61 - GS87	
	T	$1/t$	T	$1/t$	T	$1/t$	T	$1/t$	T	$1/t$
1	16.0	0.0435	16.3	0.0323	16.3	0.0435	13.9	0.0556	14.4	0.0172
2	16.6	0.0400	16.4	0.0294	14.7	0.0400	13.7	0.0526	15.6	0.0161
3	16.5	0.0385	15.8	0.0270	14.1	0.0370	13.9	0.0500	16.1	0.0172
4	15.1	0.0357	14.8	0.0256	14.0	0.0370	13.9	0.0435	17.4	0.0196
5	14.2	0.0313	13.8	0.0256	14.0	0.0345	13.6	0.0588	18.8	0.0189
6	16.2	0.0385	16.2	0.0323	15.6	0.0476	14.3	0.0526	14.7	0.0179
7	16.2	0.0435	15.5	0.0270	14.3	0.0357	14.3	0.0526	16.1	0.0179
8	15.3	0.0400	14.9	0.0270	14.2	0.0333	14.2	0.0500	17.2	0.0208
9	14.1	0.0303	13.9	0.0256	14.2	0.0417	14.2	0.0526	18.6	0.0233
10	16.1	0.0370	16.1	0.0270	13.8	0.0357	15.2	0.0526	14.9	0.0167
11	15.9	0.0370	15.1	0.0286	13.9	0.0345	13.0	0.0455	16.5	0.0179
12	14.2	0.0357	14.4	0.0270	14.4	0.0303	13.4	0.0526	17.4	0.0196
13	14.1	0.0313	14.3	0.0256	13.9	0.0303	14.5	0.0455	18.9	0.0227
14	14.0	0.0303	13.8	0.0244	13.8	0.0294	16.3	0.0667	18.9	0.0227
20	16.8	0.0417	16.7	0.0333	14.8	0.0345	15.2	0.0588	15.4	0.0172
21	16.5	0.0385	15.9	0.0286	14.4	0.0345	12.3	0.0556	16.7	0.0175
22	15.6	0.0400	15.0	0.0294	14.5	0.0323	14.2	0.0556	17.3	0.0189
23	14.5	0.0417	14.7	0.0303	14.5	0.0294	14.3	0.0667	18.2	0.0196
24	14.4	0.0400	14.8	0.0303	14.1	0.0303	15.6	0.0625	19.5	0.0227
25	16.7	0.0417	16.4	0.0345	14.5	0.0370	14.6	0.0500	14.5	0.0167
26	15.0	0.0400	15.2	0.0303	14.6	0.0345	14.9	0.0500	15.2	0.0172
27	14.8	0.0385	14.7	0.0294	14.7	0.0370	14.0	0.0435	15.9	0.0172
28	14.4	0.0345	14.5	0.0270	14.5	0.0303	13.2	0.0556	17.4	0.0196
29	14.5	0.0333	14.6	0.0278	13.9	0.0333	15.0	0.0435	18.5	0.0233
35	20.0	0.0625	18.8	0.0323	17.8	0.0357	16.5	0.0588	16.0	0.0159
36	18.3	0.0526	18.1	0.0400	17.6	0.0476	15.6	0.0476	16.3	0.0169
37	17.5	0.0500	17.5	0.0435	16.2	0.0417	16.1	0.0500	17.1	0.0182
38	17.7	0.0526	17.6	0.0417	15.8	0.0370	15.4	0.0476	17.8	0.0200
39	16.2	0.0476	16.0	0.0370	12.4	0.0333	15.7	0.0526	19.6	0.0213

APPENDIX 4: CALIBRATION DATA SETS USED DURING THE MODIFICATION OF CERES-WHEAT VERSION 2.10 *GROSUB* ROUTINES

TABLE OF CONTENTS

Table A4.1: Mean ear densities, kernel numbers, kernel masses, field yield and yield computed from yield components (Y.C.) of the four cultivars in the sowing date x cultivar calibration data sets (*continued on pages 229 to 231*).

Data set	Trial code	Sowing date	Ears density	Kernel mass	Kernel number	Field yield	Y.C. yield
		doy	m^{-2}	mg	m^{-2}	t ha^{-1}	t ha^{-1}
W170/84							
1	WPDA8811	116	416	45.4	24068	8.85	10.93
2	WPDA8821	126	407	45.1	23528	8.82	10.60
3	WPDA8831	135	457	38.6	27676	8.77	10.68
4	WPDA8841	143	385	38.2	21659	7.25	8.26
5	WPDA8851	155	399	35.2	23248	7.50	8.18
6	WPDR8811	117	323	43.4	18919	7.78	8.21
7	WPDR8821	130	382	41.9	20994	8.27	8.80
8	WPDR8831	143	317	42.1	17544	6.73	7.38
9	WPDR8841	155	372	40.7	19387	5.57	7.89
10	WPDA8911	114	350	50.1	22368	9.26	11.21
11	WPDA8921	125	413	44.1	26111	8.85	11.51
12	WPDA8931	135	422	39.6	26625	9.02	10.55
13	WPDA8941	144	436	39.8	28980	8.86	11.54
14	WPDA8951	154	406	37.6	26866	8.61	10.11
20	WPDG8911	116	409	41.8	27726	8.14	11.60
21	WPDG8921	126	407	42.4	27174	8.69	11.53
22	WPDG8931	136	482	39.7	29920	9.41	11.89
23	WPDG8941	146	446	37.7	30636	8.25	11.55
24	WPDG8951	157	427	35.4	27240	7.34	9.63
25	WPDA9011	114	369	44.9	25855	9.92	11.61
26	WPDA9021	124	396	46.8	27295	9.56	12.78
27	WPDA9031	134	414	41.3	27472	9.44	11.35
28	WPDA9041	144	414	38.2	27385	7.33	10.47
29	WPDA9051	155	400	37.5	27490	7.45	10.32
35	WPDS9011	117	406	45.5	30545	8.18	13.90
36	WPDS9021	126	323	43.1	22542	7.72	9.70
37	WPDS9031	136	351	39.6	24038	8.13	9.51
38	WPDS9041	146	315	40.7	22061	7.26	8.98
39	WPDG9051	157	378	35.8	22350	5.37	8.00
50	WPDM9121	116	332	37.0	21837	4.94	8.08
51	WPDM9122	126	362	34.6	24565	5.49	8.50
52	WPDM9123	138	368	31.6	22928	4.68	7.25
53	WPDM9124	147	406	31.3	23656	3.53	7.41
54	WPDM9125	157	308	20.7	18235	2.37	3.78
Mean			388	39.6	24674	7.57	9.81

Table A4.1: *continued.*

Data set	Trial code	Sowing date	Ears density	Kernel mass	Kernel number	Field yield	Y.C. yield
		doy	m^{-2}	mg	m^{-2}	t ha^{-1}	t ha^{-1}
Sengwa							
1	WPDA8812	116	449	37.0	22231	6.78	8.23
2	WPDA8822	126	474	38.6	22381	7.07	8.64
3	WPDA8832	135	496	39.9	24436	5.96	9.75
4	WPDA8842	143	568	35.3	27543	7.52	9.71
5	WPDA8852	155	473	32.8	25591	8.52	8.40
6	WPDR8812	117	425	36.2	20263	6.70	7.34
7	WPDR8822	130	443	36.2	20820	7.42	7.54
8	WPDR8832	143	411	37.0	19580	6.23	7.25
9	WPDR8842	155	449	34.3	24369	6.01	8.36
10	WPDA8912	114	458	36.4	25211	8.22	9.18
11	WPDA8922	125	424	35.9	23570	8.12	8.46
12	WPDA8932	135	490	34.0	28371	8.67	9.66
13	WPDA8942	144	516	32.6	31428	8.92	10.23
14	WPDA8952	154	529	33.2	29924	8.63	9.92
20	WPDG8912	116	525	36.9	30195	7.78	11.15
21	WPDG8922	126	508	34.4	25833	8.13	8.88
22	WPDG8932	136	602	33.0	35132	8.88	11.59
23	WPDG8942	146	618	31.5	34255	8.59	10.79
24	WPDG8952	157	622	30.8	34096	7.22	10.50
25	WPDA9012	114	475	38.3	25064	7.90	9.61
26	WPDA9022	124	438	38.9	24101	8.40	9.38
27	WPDA9032	134	450	36.7	23893	8.89	8.76
28	WPDA9042	144	518	34.7	25382	7.81	8.82
29	WPDA9052	155	492	31.7	27113	7.65	8.59
35	WPDS9012	117	444	39.3	22789	6.11	8.95
36	WPDS9022	126	524	34.5	28438	7.32	9.80
37	WPDS9032	136	494	33.3	26974	7.74	8.99
38	WPDS9042	146	529	34.0	30858	7.19	10.48
39	WPDS9052	157	539	31.7	28580	5.25	9.05
50	WPDM9112	116	432	34.0	22818	5.91	7.75
51	WPDM9122	126	453	33.8	25116	5.37	8.48
52	WPDM9132	138	516	29.3	28080	4.25	8.23
53	WPDM9142	147	491	25.3	24689	3.74	6.24
54	WPDM9152	157	548	22.3	25932	2.88	5.79
Mean			495	34.2	26325	7.11	8.96

Table A4.1: *continued.*

Data set	Trial code	Sowing date	Ears density	Kernel mass	Kernel number	Field yield	Y.C. yield
		doy	m^{-2}	mg	m^{-2}	t ha^{-1}	t ha^{-1}
Rusape							
1	WPDA8813	116	355	33.7	20072	6.05	6.76
2	WPDA8823	126	425	39.8	19298	3.83	7.68
3	WPDA8833	135	466	39.3	22163	5.61	8.71
4	WPDA8843	143	380	32.4	21584	5.94	6.99
5	WPDA8853	155	391	29.1	21332	4.59	6.20
6	WPDR8813	117	345	42.8	18386	6.37	7.87
7	WPDR8823	130	395	39.3	22211	6.61	8.73
8	WPDR8833	143	339	36.1	18928	4.87	6.84
9	WPDR8843	155	321	35.2	16901	3.96	5.94
10	WPDA8913	114	433	45.7	25454	8.24	11.63
11	WPDA8923	125	440	43.5	25474	8.53	11.08
12	WPDA8933	135	427	41.0	26130	8.36	10.72
13	WPDA8943	144	458	40.3	31186	8.60	12.58
14	WPDA8953	154	460	41.0	28936	8.42	11.85
20	WPDG8913	116	446	41.7	25607	6.94	10.69
21	WPDG8923	126	449	42.2	28097	7.40	11.85
22	WPDG8933	136	486	39.5	28889	7.67	11.40
23	WPDG8943	146	454	39.7	26156	7.32	10.39
24	WPDG8953	157	423	36.4	24628	6.62	8.96
25	WPDA9013	114	419	43.0	26930	8.03	11.57
26	WPDA9023	124	399	43.8	25670	8.21	11.23
27	WPDA9033	134	419	41.8	26517	9.04	11.09
28	WPDA9043	144	440	43.0	24136	8.01	10.37
29	WPDA9053	155	405	36.9	28528	6.76	10.53
35	WPDS9013	117	372	42.4	19075	5.42	8.08
36	WPDS9023	126	367	40.3	22469	6.68	9.04
37	WPDS9033	136	391	38.7	22893	7.42	8.85
38	WPDS9043	146	418	36.4	25722	5.79	9.36
39	WPDS9053	157	384	35.2	23754	6.08	8.36
50	WPDM9131	116	350	36.6	20625	4.23	7.55
51	WPDM9132	126	373	31.5	23400	5.59	7.36
52	WPDM9133	138	406	30.5	24920	4.88	7.59
53	WPDM9134	147	418	27.0	23838	3.48	6.44
54	WPDM9135	157	389	23.4	21436	2.54	5.01
Mean			407	37.9	23863	6.41	9.10

Table A4.1: *continued.*

Data set	Trial code	Sowing date	Ears density	Kernel mass	Kernel number	Field yield	Y.C. yield
		doy	m^{-2}	mg	m^{-2}	t ha^{-1}	t ha^{-1}
Angwa							
1	WPDA8814	116	359	38.2	15500	5.33	5.91
2	WPDA8824	126	462	41.0	20387	6.83	8.35
3	WPDA8834	135	503	30.9	31040	5.71	9.59
4	WPDA8844	143	490	45.2	20056	6.50	9.06
5	WPDA8854	155	479	38.4	23870	6.27	9.17
6	WPDR8814	117	327	47.2	14106	6.00	6.65
7	WPDR8824	130	367	44.8	16206	6.94	7.26
8	WPDR8834	143	354	40.5	16794	6.18	6.80
9	WPDR8844	155	426	40.1	18244	4.67	7.31
10	WPDA8914	114	463	46.9	21882	8.41	10.26
11	WPDA8924	125	458	44.5	23959	8.01	10.67
12	WPDA8934	135	429	42.6	20747	7.65	8.84
13	WPDA8944	144	478	41.1	25047	7.70	10.30
14	WPDA8954	154	492	40.8	24915	8.02	10.16
20	WPDG8914	116	407	46.8	18807	5.87	8.80
21	WPDG8924	126	448	43.9	23187	7.16	10.18
22	WPDG8934	136	540	43.6	26657	7.96	11.62
23	WPDG8944	146	544	43.2	27028	7.59	11.68
24	WPDG8954	157	504	40.3	24333	6.89	9.79
25	WPDA9014	114	423	47.3	19526	6.18	9.23
26	WPDA9024	124	389	44.7	20551	7.49	9.19
27	WPDA9034	134	409	43.0	22362	8.23	9.61
28	WPDA9044	144	501	40.3	25109	7.20	10.11
29	WPDA9054	155	457	38.2	23224	6.37	8.86
35	WPDS9014	117	356	47.3	13258	3.25	6.28
36	WPDS9024	126	431	44.0	19756	5.67	8.70
37	WPDS9034	136	478	41.8	24292	7.38	10.16
38	WPDS9044	146	508	40.9	25248	6.61	10.32
39	WPDS9054	157	442	39.9	24608	6.32	9.82
Mean			446	42.3	21748	6.70	9.13

Table A4.2: Mean days after sowing to growth stages 31, 39, 61 and 87, and the mean ear densities, kernel numbers, kernel masses, field yield and yield computed from yield components (Y.C.) of the wheat irrigation experiment calibration data sets.

Data set	Trial code	Growth stage 31	39	61	87	Ear density	Kernel mass	Kernel number	Field yield	Y.C. yield
		das				m^{-2}	mg	m^{-2}	t ha^{-1}	t ha^{-1}
70	WITA8921	47	56	80	124	333	35.9	19329	5.66	6.93
71	WITA8922	47	56	80	127	408	35.0	24679	6.51	8.64
72	WITA8923	47	56	80	129	443	36.1	25277	6.69	9.11
73	WITA8924	47	56	80	135	508	34.3	28406	7.11	9.74
74	WITA8925	47	56	80	127	416	36.6	24305	6.37	8.89
85	WITG9021	37	50	69	115	363	35.7	19331	5.47	6.90
86	WITG9022	37	50	69	118	445	36.4	21849	6.01	7.95
87	WITG9023	37	50	69	119	426	37.0	22217	6.02	8.22
88	WITG9024	37	50	69	120	514	38.1	26022	7.14	9.90
89	WITG9025	37	50	69	116	425	34.9	24091	5.65	8.41
101	WITA9211	54	78	98	142	404	41.0	23852	8.62	9.77
102	WITA9212	54	79	98	140	375	38.8	22707	8.24	8.80
103	WITA9213	54	78	98	141	423	36.9	24342	8.41	8.99
104	WITA9214	54	79	97	139	384	38.4	22194	8.02	8.53
105	WITA9215	54	78	96	137	396	35.6	22712	7.94	8.09
106	WITA9216	54	79	97	137	380	31.9	20844	7.60	6.66
107	WITA9217	54	78	95	137	330	38.3	17680	6.98	6.78
108	WITA9218	54	79	95	135	396	35.3	21986	6.95	7.75
109	WITA9219	54	78	95	135	373	32.6	20050	6.66	6.54
110	WDDA8921	44	52	71	112	205	29.2	9052	1.71	2.65
111	WDDA8922	46	56	74	115	249	28.9	11324	2.23	3.27
112	WDDA9223	46	58	77	119	340	30.0	16108	3.50	4.83
113	WDDA8924	46	60	83	126	480	28.8	24589	5.37	7.08
114	WDDA8925	46	60	86	131	472	33.0	25270	6.79	8.34
115	WDDG8921	43	52	67	105	284	28.8	16134	2.47	4.64
116	WDDG8922	43	57	74	120	558	27.1	37671	5.08	10.22
Mean		47	63	83	127	397	34.4	22001	6.12	7.60

APPENDIX 5: RAW DATA PERTAINING TO THE VALIDATION OF WHVZIM22 UNDER WELL-WATERED AND DEFICIT-IRRIGATED CONDITIONS

TABLE OF CONTENTS

Table A5.1: Observed (O) and predicted (P) days from sowing to growth stages TS, 31, 39, 61 and 87 of four cultivars under well-watered conditions (*continued on page 235*).

Data set	Trial code	TS		31		39		61		87	
		O	P	O	P	O	P	O	P	O	P
W170/84											
15	WPDR8911	45	41	43	50	76	71	99	94	157	152
16	WPDR8921	47	47	44	55	76	75	97	99	153	151
17	WPDR8931	42	49	43	57	77	79	99	100	151	148
18	WPDR8941	49	50	46	59	80	81	100	99	150	146
19	WPDR8951	51	53	49	61	82	81	97	97	144	143
30	WPDG9011	38	39	44	45	61	62	80	83	142	144
31	WPDG9021	42	41	47	48	66	68	88	89	142	146
32	WPDG9031	41	41	44	49	65	69	86	91	137	143
33	WPDG9041	42	44	48	52	72	73	91	93	133	140
34	WPDG9051	46	46	51	55	77	75	92	93	131	136
40	WPDA9111	NR	46	47	56	79	75	103	98	160	151
41	WPDA9121	NR	50	53	57	87	81	105	100	155	151
42	WPDA9131	NR	50	58	59	92	80	105	100	156	147
43	WPDA9141	NR	52	60	62	88	82	104	98	150	145
44	WPDA9151	NR	53	61	61	89	80	101	95	147	141
45	WPDD9111	NR	37	48	45	72	65	89	89	146	146
46	WPDD9121	NR	40	52	49	71	70	94	92	145	144
47	WPDD9131	NR	46	49	55	80	78	96	98	139	144
48	WPDD9141	NR	50	52	60	82	80	94	98	134	141
49	WPDD9151	NR	52	57	60	80	79	96	96	131	136
Sengwa											
15	WPDR8912	35	31	41	38	62	60	88	81	154	148
16	WPDR8922	35	33	42	42	65	63	88	86	150	146
17	WPDR8932	38	37	43	45	65	65	89	89	145	144
18	WPDR8942	36	38	41	46	68	68	89	89	145	142
19	WPDR8952	40	39	44	48	69	70	89	89	141	139
30	WPDG9012	26	28	37	35	51	52	67	71	132	140
31	WPDG9022	32	31	38	37	51	55	72	76	132	140
32	WPDG9032	30	31	39	38	55	58	74	79	132	139
33	WPDG9042	29	32	41	41	56	61	79	82	128	136
34	WPDG9052	32	35	41	43	60	64	81	83	126	133
40	WPDA9112	NR	NR	39	42	64	64	82	87	145	147
41	WPDA9122	NR	NR	42	46	69	65	92	88	149	145
42	WPDA9132	NR	NR	50	46	73	70	93	89	144	143
43	WPDA9142	NR	NR	52	47	74	70	92	89	145	140
44	WPDA9152	NR	NR	56	49	74	69	92	86	137	137
45	WPDD9112	NR	NR	40	35	55	55	73	76	137	142
46	WPDD9122	NR	NR	41	37	60	57	78	81	141	141
47	WPDD9132	NR	NR	47	42	58	63	81	86	136	139
48	WPDD9142	NR	NR	43	46	69	69	86	89	131	137
49	WPDD9152	NR	NR	49	48	70	68	84	87	128	132

Table A5.1: *continued.*

Data set	Trial code	TS O	TS P	31 O	31 P	39 O	39 P	61 O	61 P	87 O	87 P
Rusape											
15	WPDR8913	37	34	37	41	68	63	92	85	153	146
16	WPDR8923	38	37	41	47	70	67	91	90	149	145
17	WPDR8933	39	40	41	48	71	70	92	91	145	142
18	WPDR8943	40	42	41	50	74	72	97	93	146	140
19	WPDR8953	47	43	44	53	76	77	95	91	142	138
30	WPDG9013	30	31	37	39	53	55	70	74	130	138
31	WPDG9023	30	33	37	40	54	58	75	79	133	137
32	WPDG9033	31	33	38	40	57	60	77	82	132	137
33	WPDG9043	32	34	40	43	60	63	82	84	127	134
34	WPDG9053	33	38	40	46	66	67	85	86	122	131
40	WPDA9113	NR	36	41	45	69	66	89	90	149	145
41	WPDA9123	NR	40	43	49	70	69	96	91	152	143
42	WPDA9133	NR	42	50	50	78	73	100	94	143	142
43	WPDA9143	NR	42	52	51	78	72	97	92	143	138
44	WPDA9153	NR	44	57	52	80	73	96	89	138	135
45	WPDD9113	NR	30	41	37	56	58	74	79	135	140
46	WPDD9123	NR	32	42	40	61	61	87	84	139	139
47	WPDD9133	NR	38	49	46	62	69	90	90	134	138
48	WPDD9143	NR	41	42	50	70	72	90	91	129	136
49	WPDD9153	NR	42	51	52	76	73	92	89	127	131
Angwa											
15	WPDR8914	33	28	37	35	63	57	84	77	149	140
16	WPDR8924	33	30	39	38	66	60	87	83	143	139
17	WPDR8934	34	34	39	43	66	63	87	86	142	137
18	WPDR8944	35	35	40	43	69	66	89	86	142	135
19	WPDR8954	39	36	42	45	71	68	88	86	137	132
30	WPDG9014	24	26	32	33	49	50	63	68	120	131
31	WPDG9024	25	29	34	35	50	52	69	73	126	133
32	WPDG9034	28	28	32	35	55	55	72	76	124	131
33	WPDG9044	28	29	35	37	56	57	76	79	126	130
34	WPDG9054	29	32	36	40	61	61	79	81	121	127

Table A5.2: Observed (O) and predicted (P) days from sowing to growth stages TS, 31, 39, 61 and 87 of four cultivars under deficit-irrigated conditions.

Data set	Trial code	31		39		61		87	
		O	P	O	P	O	P	O	P
75	WITG8921	43	42	57	62	77	83	122	131
76	WITG8922	43	42	58	62	76	83	128	134
77	WITG8923	43	42	57	62	77	83	128	131
78	WITG8924	43	42	58	62	78	83	132	138
79	WITG8925	43	42	58	62	75	83	125	130
80	WITA9021	47	46	58	67	78	89	120	133
81	WITA9022	47	46	58	67	78	89	125	138
82	WITA9023	47	46	58	67	77	89	125	137
83	WITA9024	47	46	58	67	78	89	128	143
84	WITA9025	47	46	58	67	78	89	124	136
95	WITB9111	44	49	60	69	79	83	114	117
96	WITB9112	43	49	59	69	78	85	119	120
97	WITB9113	44	49	60	68	77	82	120	119
98	WITB9114	44	49	60	69	81	85	118	122
99	WITB9115	44	49	60	69	80	86	122	127
100	WITA9111	59	62	82	81	99	100	136	137
101	WITA9112	58	62	82	81	98	100	137	139
102	WITA9113	58	62	81	81	99	99	137	136
103	WITA9114	59	62	82	81	98	100	135	136
104	WITA9115	58	62	84	81	102	100	142	145
105	WITA9116	58	62	84	81	101	100	142	146
122	WDDA9021	47	46	58	66	75	83	116	126
123	WDDA9022	47	46	58	67	81	89	125	134
124	WDDG9021	41	38	50	55	66	69	109	116
125	WDDG9022	41	38	50	58	71	79	116	125
128	WDDB9111	44	49	60	63	77	76	107	110
129	WDDB9112	44	49	60	67	80	82	111	114

Table A5.3: Observed (O) and predicted (P) ear densities (TPSM) and yield components for four cultivars under well-watered conditions.

Data Set	Trial code	TPSM O	TPSM P	Kernel wt. O	Kernel wt. P	Kernel no. O	Kernel no. P	Field yield O	Field yield P	Y.C. Yield O	Y.C. Yield P
		Ears m^{-2}		mg $kernel^{-1}$		kernel m^{-2}		t ha^{-1}			
W170/84											
15	WPDR8911	331	432	46.0	46.3	20203	24916	8.76	9.81	9.30	11.54
16	WPDR8921	454	454	41.4	42.0	27481	28403	8.25	10.14	11.37	11.93
17	WPDR8931	394	427	38.7	39.2	23510	26307	8.20	8.77	9.09	10.31
18	WPDR8941	465	398	36.1	39.0	30986	23871	7.55	7.91	11.17	9.31
19	WPDR8951	353	388	33.5	37.7	22876	20394	7.13	6.54	7.67	7.69
30	WPDG9011	296	366	44.8	46.1	21157	22503	7.66	8.82	9.48	10.37
31	WPDG9021	303	384	42.9	43.0	23673	25155	8.67	9.19	10.15	10.82
32	WPDG9031	381	403	42.1	39.6	26800	25852	8.78	8.70	11.28	10.24
33	WPDG9041	413	401	38.9	36.1	27033	25596	8.52	7.85	10.53	9.24
34	WPDG9051	359	395	33.2	33.1	23616	23726	6.47	6.68	7.84	7.85
40	WPDA9111	398	429	42.4	44.5	25790	26053	9.25	9.85	10.94	11.59
41	WPDA9121	360	400	39.6	42.7	21376	23712	8.95	8.61	8.47	10.13
42	WPDA9131	425	412	36.2	41.2	27729	24417	8.99	8.55	10.04	10.06
43	WPDA9141	457	383	37.5	42.2	30313	22477	9.35	8.06	11.35	9.49
44	WPDA9151	425	371	37.8	42.7	26633	20219	8.98	7.34	10.07	8.63
45	WPDD9111	332	464	50.0	42.3	21607	20602	7.02	7.41	10.80	8.71
46	WPDD9121	365	465	40.9	38.7	24331	23683	7.90	7.79	9.95	9.17
47	WPDD9131	378	440	35.8	36.0	23219	27637	6.92	8.46	8.31	9.95
48	WPDD9141	392	453	34.4	33.6	22598	25736	6.21	7.35	7.77	8.65
49	WPDD9151	397	418	31.1	34.1	24425	24355	5.83	7.06	7.60	8.31
SENGWA											
15	WPDR8912	433	446	36.7	41.0	21859	24057	7.72	8.38	8.01	9.86
16	WPDR8922	458	491	34.9	37.7	24387	25535	8.02	8.18	8.51	9.63
17	WPDR8932	415	489	34.5	35.3	22177	28404	8.20	8.52	7.65	10.03
18	WPDR8942	440	462	33.1	34.5	26019	26499	8.10	7.77	8.61	9.14
19	WPDR8952	453	439	32.5	33.2	26311	25179	8.29	7.11	8.54	8.36
30	WPDG9012	420	390	39.9	41.0	23026	20879	6.60	7.28	9.19	8.56
31	WPDG9022	392	440	38.8	38.4	21279	23221	7.63	7.58	8.25	8.92
32	WPDG9032	486	444	36.2	36.2	29130	25544	7.94	7.86	10.55	9.25
33	WPDG9042	537	497	33.1	32.5	29836	26363	7.73	7.28	9.87	8.57
34	WPDG9052	513	432	31.8	29.9	30154	24570	6.70	6.24	9.58	7.35
40	WPDA9112	415	461	40.0	39.5	21091	24403	7.97	8.19	8.43	9.64
41	WPDA9122	409	475	38.7	38.0	20325	26288	8.26	8.49	7.86	9.99
42	WPDA9132	456	426	35.5	35.8	26757	23701	9.22	7.21	9.51	8.48
43	WPDA9142	440	436	33.5	35.3	25029	23983	9.18	7.20	8.39	8.47
44	WPDA9152	486	444	32.5	36.3	26556	23252	8.22	7.17	8.62	8.44
45	WPDD9112	393	485	37.8	39.0	22282	19267	6.81	6.39	8.42	7.51
46	WPDD9122	424	510	37.3	35.6	24009	20773	7.62	6.29	8.96	7.40
47	WPDD9132	450	546	35.2	32.3	24504	27162	7.49	7.46	8.62	8.77
48	WPDD9142	496	511	31.3	29.6	26967	28207	6.89	7.10	8.45	8.35
49	WPDD9152	489	480	27.7	28.5	29700	26784	7.59	6.49	8.24	7.63
RUSAPE											
15	WPDR8913	412	415	46.6	47.0	22422	23985	8.28	9.58	10.44	11.27
16	WPDR8923	418	449	43.4	43.0	23347	26281	7.95	9.61	10.13	11.30
17	WPDR8933	433	411	41.5	40.0	24112	26974	8.13	9.17	10.00	10.79
18	WPDR8943	408	426	37.2	38.5	25273	26223	7.43	8.58	9.40	10.10
19	WPDR8953	417	403	39.0	38.4	26122	23412	7.54	7.64	10.19	8.99
30	WPDG9013	393	350	44.7	47.0	23731	20934	6.78	8.36	10.61	9.84
31	WPDG9023	385	389	43.2	43.2	23802	23699	7.39	8.70	10.29	10.24
32	WPDG9033	377	394	41.4	41.1	23256	25906	7.93	9.05	9.63	10.65
33	WPDG9043	471	420	40.2	37.4	28182	25845	7.67	8.22	11.32	9.67
34	WPDG9053	437	409	35.4	33.2	26544	24595	5.39	6.94	9.38	8.17
40	WPDA9113	392	418	42.0	45.2	21054	24718	8.41	9.50	8.84	11.17
41	WPDA9123	379	418	42.7	42.7	22715	25037	9.37	9.09	9.70	10.69
42	WPDA9133	438	389	40.8	41.4	27701	25355	9.24	8.92	11.30	10.50
43	WPDA9143	422	392	42.1	40.3	23675	24887	9.15	8.53	9.96	10.03
44	WPDA9153	423	369	41.0	41.5	27082	22311	8.91	7.87	11.11	9.26
45	WPDD9113	352	444	43.8	44.4	22913	18808	6.67	7.10	10.04	8.35
46	WPDD9123	355	464	41.0	40.4	21769	21459	7.32	7.37	8.93	8.67
47	WPDD9133	410	445	40.0	36.6	25343	26519	5.43	8.25	10.14	9.71
48	WPDD9143	401	447	36.4	34.1	23538	26530	7.03	7.69	8.57	9.05
49	WPDD9153	410	415	35.4	32.6	26047	24315	6.01	6.74	9.22	7.93
ANGWA											
15	WPDR8914	417	446	45.0	47.0	20351	20959	6.98	8.37	9.15	9.85
16	WPDR8924	408	468	43.2	45.5	20738	22547	7.39	8.72	8.96	10.26
17	WPDR8934	444	498	43.8	42.4	21005	24558	7.51	8.85	9.21	10.41
18	WPDR8944	448	493	41.0	39.8	21776	24135	7.78	8.16	8.92	9.61
19	WPDR8954	421	438	42.4	38.8	20953	22330	7.36	7.36	8.89	8.66
30	WPDG9014	400	384	49.0	47.0	18332	17570	6.04	7.02	8.98	8.26
31	WPDG9024	416	429	48.9	46.1	20733	20353	7.21	7.98	10.14	9.38
32	WPDG9034	418	423	42.8	42.4	22472	22364	7.94	8.06	9.62	9.48
33	WPDG9044	498	487	42.0	39.4	23592	23681	6.71	7.93	9.91	9.33
34	WPDG9054	523	450	38.7	35.9	26569	23059	7.03	7.04	10.28	8.28

Table A5.4: Observed (O) and predicted (P) ear densities (TPSM) and yield components for wheat grown under deficit-irrigated conditions.

Data Set	Trial code	TPSM		Kernel wt.		Kernel no.		Field yield		Y.C. Yield	
		O	P	O	P	O	P	O	P	O	P
		Ears m^{-2}		mg $kernel^{-1}$		kernel m^{-2}		t ha^{-1}			
75	WITG8921	512	420	27.8	24.4	28091	25865	5.81	5.36	7.82	6.31
76	WITG8922	583	423	29.7	31.7	34918	25922	6.51	6.98	10.36	8.22
77	WITG8923	480	388	31.2	26.9	28877	25929	6.84	5.93	9.02	6.97
78	WITG8924	589	410	30.1	33.0	34976	25791	7.79	7.23	10.53	8.51
79	WITG8925	508	375	30.6	23.5	28911	25854	6.56	5.16	8.85	6.08
80	WITA9021	369	422	36.2	20.6	19833	26340	4.91	4.61	7.18	5.43
81	WITA9022	387	456	35.2	32.3	22940	26911	5.86	7.39	8.07	8.69
82	WITA9023	444	465	34.4	29.6	25942	27021	5.80	6.80	8.92	8.00
83	WITA9024	509	468	37.2	38.6	26108	27010	6.76	8.86	9.71	10.43
84	WITA9025	450	437	34.3	25.6	25793	26963	5.68	5.87	8.85	6.90
95	WITB9111	208	197	38.2	24.5	11743	14605	3.00	3.04	4.48	3.58
96	WITB9112	268	234	40.2	27.9	14181	18072	4.02	4.29	5.70	5.04
97	WITB9113	233	245	40.3	34.1	13855	13090	3.06	3.79	5.58	4.46
98	WITB9114	262	260	41.0	31.7	14599	18527	5.01	4.99	5.99	5.87
99	WITB9115	349	308	39.2	34.0	20110	19516	6.22	5.64	7.88	6.64
100	WITA9111	357	371	35.0	23.3	19675	24398	7.22	4.83	6.89	5.68
101	WITA9112	388	374	37.4	28.5	22680	24393	7.88	5.91	8.47	6.95
102	WITA9113	341	346	37.2	24.9	19764	23186	7.17	4.91	7.35	5.77
103	WITA9114	375	391	34.5	20.0	20658	24066	6.50	4.09	7.12	4.81
104	WITA9115	442	402	32.4	40.3	25174	24404	7.43	8.36	8.15	9.83
105	WITA9116	409	408	35.9	41.2	23958	24422	8.83	8.55	8.59	10.06
122	WDDA9021	363	266	28.4	20.0	17682	6794	2.63	1.15	5.01	1.36
123	WDDA9022	566	486	29.7	21.5	33796	27020	5.40	4.94	10.02	5.81
124	WDDG9021	268	300	32.6	20.0	14871	6985	3.18	1.19	4.84	1.40
125	WDDG9022	443	476	31.2	21.5	26957	25291	5.55	4.62	8.40	5.44
128	WDDB9111	96	194	34.6	22.1	4940	4476	1.06	0.84	1.71	0.99
129	WDDB9112	236	188	26.2	20.0	12306	8914	2.02	1.52	3.22	1.78

APPENDIX 6: VARIABLE NAMES USED IN WHVZIM22 AND WIRROPT6.BAS

TABLE OF CONTENTS

Table A6.1: Description of the variables described in the thesis from WHV21 and those added to the modified CERES-Wheat model (WHVZIM22) (*continued on pages 241 and 242*).

Variable	Description
aa	Intercept of the linear regression of the ground minimum temperature on the screen air temperature, °C.
ALT	Altitude of the weather file location, m
ALTFACT	Altitude correction factor as an indicator of the frequency of frost occurrence in Zimbabwe (after Law, 1979).
AWR	Assimilate area to dry mass ratio, $cm^2\ g^{-1}$.
bb	Slope of the linear regression of the ground minimum temperature on the screen air temperature.
BIOMAS	The accumulated dry mass of above-ground plant material following seedling emergence, $g\ m^2$.
CARBO	Daily plant dry matter production, $g\ plant^{-1}$.
CUMPH	Accumulated phyllochron intervals and equivalent leaf number on main stem, unitless.
DT	Day time air temperature, °C.
DTT	Daily thermal time, °C.
DUL	Drained upper limit of plant available soil water, $m^3\ m^{-3}$.
EGFT	Zero to unity index describing the effect of air temperature on leaf extension growth.
EP1	Actual plant evaporation, $10^1\ mm\ d^{-1}$.
EXPFACT	Exposure factor as an indicator of the frequency of frost occurrence in Zimbabwe (after Law, 1979).
FROST	Factor applied to reduce kernel numbers when the ground minimum temperature declines below 0°C.
FYIELD	Field scale grain yield, $t\ ha^{-1}$.
G2R	Kernel growth rate factor used during growth phase four, mg kernel d^{-1}.
GRNWT	Dry mass of kernels, $g\ plant^{-1}$.
GROLF	Daily growth of leaves, $g\ plant^{-1}$.
GROGRN	Daily growth of the kernels, $g\ plant^{-1}$.
GROSTM	Daily stem growth, $g\ plant^{-1}$.
GROUNDT	Exposed ground minimum air temperature, °C.
GPLA	Green plant leaf area, $cm^2\ plant^{-1}$.
GPP	Kernel number per plant.
HRLT	Daylength, including civil twilight, h.
IPAR	The proportion of incident photosynthetically active radiation intercepted by a wheat canopy as a function of leaf area index, unitless.
IPAR1	The proportion of incident photosynthetically active radiation intercepted by a wheat canopy as a function of leaf area index, unitless.
IPAR2	The proportion of incident photosynthetically active radiation intercepted by a wheat canopy as a function of tiller density, unitless.
ISTAGE	Phenological stage.

Table A6.1: *continued.*

Variable	Description
LAI	Leaf area index, unitless.
LATFACT	Combined latitude and dewpoint correction factor as an indicator of the frequency of frost occurrence in Zimbabwe (after Law, 1979).
LFWT	Leaf dry mass on a plant, g $plant^{-1}$.
LL	Lower limit of plant available soil water, m^3 m^{-3}.
MAXGWT	Maximum kernel size, mg $kernel^{-1}$, dependent on the duration of the linear kernel filling stage and the kernel growth rate.
P1...5	The thermal time duration of growth phases one to five, °C d.
PAR	Photosynthetically active radiation, MJ m^{-2}.
PCARB	Daily amount of carbon fixed, g $plant^{-1}$.
PGRNWT	Predicted kernel mass, mg $kernel^{-1}$.
PHINT	The thermal time interval between leaf tip emergence of successive leaves, °C d.
PHINTLE	The thermal time requirement for leaf emergence of leaves on the main stem (leaf number dependent), °C d.
PLA	Plant leaf area, cm^2 $plant^{-1}$.
PLAG	The rate of expansion of leaf area on one plant, cm^2 $plant^{-1}$ d^{-1}.
PLAGMS	Plant leaf area growth on the main stem, cm^2 $plant^{-1}$ d^{-1}.
PLALR	Plant leaf area loss rate, g $plant^{-1}$ d^{-1}.
PLANTS	Plant density, plants m^{-2}.
PRFT	Photosynthetic reduction factor for low and high air temperatures, unitless.
PTF	Proportion of assimilate partitioned to the above-ground plant parts, unitless.
RGFILL	Kernel growth rate, mg $kernel^{-1}$ d^{-1}.
RTDEP	Depth of rooting, cm.
RTSW	Ratio of the mass of the actual stem dry mass to the potential stem dry mass, used to calculate final tiller numbers, unitless.
SENLA	Area of leaf that senesces on a given day, cm^2.
SOLRAD	Daily solar irradiance, MJ m^{-2}.
STMWT	Stem dry mass of an average plant after terminal spikelet, g $plant^{-1}$.
SUMDTT	The sum of daily thermal time (DTT) for each phenological stage, °C d.
SW(L)	Soil water content of soil layer L, m^3 m^{-3}.
SWDF1	Soil water deficit factor used to calculate the reduction in photosynthesis, unitless.
SWDF2	Soil water deficit factor used to calculate the reduction in leaf area expansion and tillering, unitless.

Table A6.1: *continued.*

Variable	Description
SWMIN	Minimum stem dry mass of a plant at after anthesis (WHV21) or at ear emergence (WHVZIM22), used to calculate the amount of reserves that can be remobilised to kernels during growth phase five, g plant^{-1}.
TBASE	Base temperature where development rate is zero, °C.
TC1	Tiller number increment per unit daily thermal time, as a function of plant density, tiller plant^{-1} (°C d)$^{-1}$.
TC2	Tiller number increment per unit solar irradiance, as a function of plant density, tiller plant^{-1} (MJ m^{-2})$^{-1}$.
TDU	Thermal development units, °C d.
TEMPMN	Minimum daily air temperature, °C.
TEMPMX	Maximum daily air temperature, °C.
TF	Total correction factor, used to estimate the frequency of frost occurrence in Zimbabwe (after Law, 1979).
TI	Fraction of phyllochron interval accumulated each day as a function of DTT, unitless.
TILN	Number of tillers per plant.
TILSW	Potential dry mass of a single tiller stem plus ear, used to calculate final tiller numbers, g tiller^{-1}.
TPSM	Tiller density, tillers m^{-2}.
TRF	Tiller reduction factor for mean daily air temperatures greater than 24°C.
TRWU	Total potential root water uptake, cm d^{-1}.
TT31	Thermal time to growth stage 31 from terminal spikelet, °C d.
TTD	Thermal time duration in a growth phase, °C d.
TTM	Thermal time to physiological maturity, °C d.
W1	Soil water deficit factor applied to leaf extension and tillering in growth phase one.
YCYIELD	The dry mass grain yield calculated from yield components, t ha^{-1}.

Table A6.2: Description of the variables used in the wheat irrigation optimization programme, WIRROPT6.BAS. Note, the new WHVZIM22 variable names are given in Table A6.1. Original WHV21 variable names remained unchanged (refer to Ritchie and Otter, 1984, for a complete list and description of WHV21 variable names.) (*continued on pages 244 and 245*).

Variable	Description
Aiha()	Amount of irrigation applied with irrigation number *Nirrha* in the maximum gross margin per unit area regime, mm
Aimm()	Amount of irrigation applied with irrigation number *Nirrmm* in the maximum gross margin per unit water regime, mm
Airr()	Irrigation amount for irrigation number *Nirr*, mm
AWD()	Profile available water depletion on day of irrigation number *Nirr*
AWDha()	Profile available water depletion on the day of irrigation number *Nirrha* in the maximum gross margin per unit area regime, mm
AWDmm()	Profile available water depletion on the day of irrigation number *Nirrmm* in the maximum gross margin per unit water regime, mm
constcost	Constant costs of wheat production, ZW$ ha^{-1}
Cultivar$	Cultivar name
DMC	Daily change in kernel water content, % d^{-1}
Dot	Counter in subroutine *DOT*
Effirr	Irrigation efficiency, %
Finish	Variable to hold the elapsed time since midnight, set at the end of the optimization process
GMha!	Gross margin per unit area, ZW$ ha^{-1}
GMmm!	Gross margin per unit water, ZW$ mm^{-1}
GMhaInt	The irrigation interval associated with the maximum gross margin per unit area regime, d
GMmmInt	The irrigation interval associated with the maximum gross margin per unit water regime, d
harvcost	Harvesting and transport costs, ZW$ t^{-1}
Iday()	Day of year for irrigation number *Nirr*
Idha()	Day of year for irrigation number *Nirrha* in the maximum gross margin per unit area regime
Idmm()	Day of year for irrigation number *Nirrmm* in the maximum gross margin per unit water regime
irrapp	Irrigation application amount, mm
irrcost1	Cost of irrigation water, ZW$ mm^{-1}
irrcost2	Cost of irrigation application, ZW$ $cycle^{-1}$
IrrInt	Irrigation interval, d
IrrIntMin	Variable to determine the minimum irrigation interval of the irrigation regime applied in the first loop to establish the potential yield
IrrReqt	Soil profile irrigation requirement, mm

Table A6.2: *continued.*

Variable	Description
LN3	Day of year of the emergence of leaf number three
LN3mm	Day of year of the emergence of leaf number three in the maximum gross margin per unit water regime
LN3ha	Day of year of the emergence of leaf number three in the maximum gross margin per unit area regime
MaxGMhaArea	The area of the maximum gross margin per unit area regime, ha
MaxGMmmArea	The area of the maximum gross margin per unit area regime, ha
MaxGMha	Maximum GMha, ZW$ ha^{-1}
MaxGMmm	Maximum GMmm, ZW$ mm^{-1}
MaxGMhaY	The field yield of the maximum gross margin per unit area regime, kg ha^{-1}
MaxGMmmY	The field yield of the maximum gross margin per unit water regime, kg ha^{-1}
MaxGMhamm	The gross margin per unit water of the maximum gross margin per unit area regime, ZW$ mm^{-1}
MaxGMmmha	The gross margin per unit area of the maximum gross margin per unit water regime, ZW$ ha^{-1}
MaxInterval	Maximum irrigation interval, d
MaxTotGM	Maximum total gross margin, ZW$
MaxYield	Maximum yield, kg ha^{-1}
MC	Kernel water content, %
MCHVST	Kernel water content at harvest maturity, %
MinInterval	Minimum irrigation interval, d
Netprice	Net price of wheat grain, ZW$ t^{-1}
Nirr	Irrigation number
Nirrha	Irrigation number in the maximum gross margin per unit area regime
Nirrmm	Irrigation number in the maximum gross margin per unit water regime
potarea	Potential area of irrigable land, ha
RunLoop	Switch to check on whether the programme is in the first or later loops
Start	Variable to hold the elapsed time since midnight, set at the start of the optimization process
SPROFILE$()	Array to hold the soil profile names from file *SPROFILE.WH2*
TOTGM	Total gross margin, ZW$
TotGMInt	The irrigation interval associated with the maximum total gross margin regime, d
Totirr	Total irrigation applied, mm
TOTCOST	The total cost of an irrigation regime, ZW$
TotCostha	The total cost of the maximum gross margin per unit area regime, ZW$

Table A6.2: *continued.*

Variable	Description
TotCostmm	The total cost of the maximum gross margin per unit water regime, ZW$
TotGMha	The total gross margin of the maximum gross margin per unit area regime, ZW$
TotGMmm	The total gross margin of the maximum gross margin per unit water regime, ZW$
Titlet$	Farm name
watres	Available water resources, ML
Z31	Day of year of Zadoks growth stage 31
Z31mm	Day of year of Zadoks growth stage 31 in the maximum gross margin per unit water regime
Z31ha	Day of year of Zadoks growth stage 31 in the maximum gross margin per unit area regime
Z39	Day of year of Zadoks growth stage 39
Z39ha	Day of year of Zadoks growth stage 39 in the maximum gross margin per unit area regime
Z39mm	Day of year of Zadoks growth stage 39 in the maximum gross margin per unit water regime
Z61	Day of year of Zadoks growth stage 61
Z61mm	Day of year of Zadoks growth stage 61 in the maximum gross margin per unit water regime
Z61ha	Day of year of Zadoks growth stage 61 in the maximum gross margin per unit area regime
Z87	Day of year of Zadoks growth stage 87
Z87ha	Day of year of Zadoks growth stage 87 in the maximum gross margin per unit area regime
Z87mm	Day of year of Zadoks growth stage 87 in the maximum gross margin per unit water regime
Z90	Day of year of Zadoks growth stage 90
Z90mm	Day of year of Zadoks growth stage 90 in the maximum gross margin per unit water regime
Z90ha	Day of year of Zadoks growth stage 90 in the maximum gross margin per unit area regime